MECHANISTIC INSIGHTS INTO THE ROLE OF METALS IN THE MAILLARD REACTION USING MASS SPECTROMETRY AND ISOTOPE LABELING TECHNIQUES

OSSANNA NASHALIAN

Department of Food Science and Agricultural Chemistry

McGill University, Montreal

June, 2016

A thesis submitted to McGill University in partial fulfilment of the requirements of the degree of Doctor in Philosophy

SUGGESTED SHORT TITLE:

The role of metals in the Maillard reaction

ABSTRACT

Trace metals are food components that can play an important role in regulating the Maillard reaction through their redox activity and high ligand binding affinity especially towards amino acids. The resulting amino acid-metal complexes are known to possess a different chemical reactivity relative to their free counterparts and are expected to behave differently during thermal treatments. Understanding how these metal complexes degrade independently or react with other food components during processing can provide important insight into their fundamental role in the context of the Maillard reaction. In the absence of sugars, studies performed through heating of different metal salts (Cu, Fe, Zn, Ca) with amino acids such as glycine and alanine under pyrolytic conditions indicated that copper (II) and iron (III), due to their high oxidation potential, were able to induce oxidative decarboxylation of amino acids and formation of aroma-active Strecker aldehydes or their derivatives as detected by GC/MS. Furthermore, studies performed with synthetic $(Ala)_2Cu$ and $(Gly)_2Cu$ complexes indicated that they constituted the critical intermediates undergoing free radical oxidative degradation followed by the loss of carbon dioxide and the generation of Strecker aldehydes. The reactivity of the amino acid-metal complexes in the Maillard reaction was further explored in the presence of various aldehydes. Using paraformaldehyde and glycine copper complexes in aqueous mixtures heated at 110^{o}C for 2 hours, the ability of the metal salts to catalyze the transformation of α-amino acids into their hydroxymethyl-derivatives through a process known as Akabori reaction was studied. The mechanism of this reaction was elucidated using ESI/qTOF/MS/MS and isotope labeling techniques providing for the first time mass spectrometric evidence for the detailed mechanism of the Akabori transformation of glycine and in particular the importance of formation of Schiff base adduct as a necessary step prior to final conversion into serine and hydroxymethyl-serine. Furthermore, the results of these studies have indicated that sugars do not interfere with the Akabori transformation. On the contrary, isotope labeling studies indicated the ability of $(Gly)_2Cu$ complexes to act as molecular scaffolds that are able to undergo multiple reactions with glucose (in the presence and absence of paraformaldehyde) to generate various copper complexes of sugar conjugates. These relatively stable intermediates allowed for the slower release of browning and aroma precursors such as Amadori products during heating as assessed by the extent of browning and total volatile release. Moreover, the oxidative degradation of various sugar conjugated copper complexes generated reactive amino-sugars such as 1-amino-1-deoxy-fructose (fructosamine), 2-

amino-2-deoxy-glucose (glucosamine) which are not easily accessible under the Maillard reaction conditions. Furthermore, the amino-sugars were found to undergo further reactions to generate important flavor compounds such as fructosazine and deoxy-fructosazine or react with other sugars and undergo dehydration reactions. Alternatively, the pyrolytic degradation of glucose under basic conditions provided by the glycine sodium salt hydrate has led to the formation of 2,5-dimethyl-4-hydroxy-tetrahydrofuran-3-one, the reduced form of furaneol®. Subsequent in-depth isotope labeling studies indicated that the 2,5-dimethyl-4-hydroxy-tetrahydrofuran-3-one was generated through dimerization/cyclization of acetol catalyzed by amino acid metal salts. On the other hand, the reactivity of other food components able to complex with metal ions such as purine and pyrimidine bases was also explored. Heating aqueous reaction mixtures containing sugars and adenine and copper salts or synthetic adenine copper complexes was found to generate for the first time di-glycated adenine adducts in addition to adenosine. Furthermore, the reaction of furanmethanol with adenine in the presence of ribose was found to generate kinetin, an important plant hormone with possible food applications, while its reaction with adenosine generated kinetin riboside as confirmed by HPLC-DAD-MS and ESI/qTOF/MS/MS analysis.

RESUMÉ

Les métaux-traces sont des composants alimentaires qui peuvent jouer un rôle important dans la régulation de la réaction de Maillard par leur activité d'oxydoréduction et leur forte affinité de liaison aux ligands, en particulier les acides aminés. Les complexes acides aminés-métal possèdent une réactivité chimique différente par rapport à leurs contreparties libres. Il est donc attendu qu'ils aient un comportement différent pendant des traitements thermiques. Comprendre comment ces complexes métalliques se dégradent de façon indépendante ou réagissent avec les autres composants alimentaires pendant la transformation peut offrir une vision importante de leur rôle fondamentale dans le contexte de la réaction de Maillard. En l'absence de sucres, les études effectuées pour chauffer les différents sels métalliques (Cu, Fe, Zn, Ca) avec les acides aminés comme la glycine et l'alanine dans des conditions pyrolytiques ont indiqué que le cuivre (II) et le fer (III) ont pu induire une décarboxylation oxydative des acides aminés et induire la formation d'aldéhydes de Strecker aromatiquement actifs ou leurs dérivés, détectés par chromatographie en phase gazeuse/spectre de masse (GC/MS), imputable à leur fort potentiel d'oxydation. De plus, les études effectuées avec les complexes synthétiques $(Ala)_2Cu$ et $(Gly)_2Cu$ indiquent qu'ils sont les intermédiaires critiques qui subissent la dégradation oxydative par radicaux libres suivi de la perte de dioxyde de carbone et la génération d'aldéhydes de Strecker. La réactivité des complexes acides aminés-métal dans la réaction de Maillard a été étudiée plus en profondeur en présence de différents aldéhydes. Utilisant le paraformaldéhyde et les complexes glycine-cuivre en mélanges aqueux chauffés à 110^{o}C pendant 2 heures, la capacité des sels métalliques à catalyser la transformation des acides aminés α en dérivés hydroxyméthyles par un processus connu sous le nom de réaction d'Akabori a été étudie. Le mécanisme de cette réaction a été élucidé au moyen de techniques de ESI/qTOF/MS/MS et de marquage d'isotopes et offre les premières preuves en spectrométrie de masse du mécanisme détaillé de la transformation d'Akabori de la glycine et, en particulier, l'importance de la formation de l'adduit de la base de Schiff comme étape nécessaire au préalable à la conversion finale en sérine et hydroxyméthyl-sérine. De plus, les résultats de ces études indiquent que les sucres n'interfèrent pas dans la transformation d'Akabori. Au contraire, les études de marquage d'isotopes indiquent que la capacité des complexes $(Gly)_2Cu$ d'agir comme échafaudage moléculaire est capable de subir de multiples réactions avec le glucose (en présence ou absence de paraformaldéhyde) pour générer les différents complexes cuivrés de conjugués de sucre. Ces intermédiaires relativement stables permettent une libération plus lente des précurseurs

du brunissement et des arômes, comme les produits d'Amadori, pendant le chauffage tel qu'évalué par l'ampleur du brunissement et la libération des produits volatils totaux. De plus, la dégradation oxydative des différents complexes cuivrés conjugués aux sucres a généré des sucres aminés réactifs comme le 1-amino-1-désoxy-fructose (fructosamine), 2-amino-2-désoxy-glucose (glucosamine) qui ne sont pas facilement accessibles sous les conditions nécessaires à la réaction de Maillard. De plus, les sucre aminés subissent des réactions subséquentes pour générer d'importants composés reliés à la saveur comme la fructosazine et la désoxy-fructosazine ou réagissent avec d'autres sucres et subissent des réactions de déshydratation. De façon alternative, la dégradation pyrolytique du glucose sous des conditions de base offertes par le complexe glycine-cuivre a mené à la formation de 2,5-diméthyl-4-hydroxy-tétrahydrofuran-3-one, la forme réduite du furaneol®. Des études approfondies subséquentes en marquage d'isotopes ont indiqué que le 2,5-diméthyl-4-hydroxy-tétrahydrofuran-3-one a été généré par la dimérisation/cyclisation de l'acétol catalysé par les sels métalliques d'acides aminés. D'autre part, la réactivité des autres composants alimentaires capables de former des complexes avec les ions métalliques, comme les bases purine et pyrimidine, a aussi été explorée. Le chauffage des mélanges réactionnels aqueux contenant des sucres et de l'adénine et des sels de cuivre ou des complexes synthétiques d'adénine-cuivre a démontré pour la première fois la génération d'adduits d'adénine diglyquée en plus de l'adénosine. De plus, la réaction du furanméthanol avec l'adénine en présence de ribose a généré la kinétine, une hormone végétale importante avec de possibles applications alimentaires, tandis que sa réaction avec l'adénosine a généré la kinétine riboside, confirmé par analyses HPLC-DAD-MS et ESI/qTOF/MS/MS.

STATEMENT FROM THE THESIS OFFICE

In accordance with the regulations of Graduate and Postdoctoral Studies of McGill University, the following statement from the Guidelines for Thesis Preparation is included:

Candidates have the option of including, as part of the thesis, the text of one or more papers submitted, or to be submitted, for publication, or the clearly-duplicated text of one or more published papers. These texts must conform to the "Guidelines for Thesis Preparation" and must be bound together as an integral part of the thesis.

The thesis must be more than a collection of manuscripts. All components must be integrated into a cohesive unit with a logical progression from one chapter to the next. In order to ensure that the thesis has continuity, connecting texts that provide logical bridges between the different papers are mandatory.

The thesis must conform to all other requirements of the "Guidelines for Thesis Preparation" in addition to the manuscripts.

As manuscripts for publication are frequently very concise documents, where appropriate, additional material must be provided in sufficient detail to allow a clear and precise judgement to be made of the importance and originality of the research reported in the thesis.

In general when co-authored papers are included in a thesis, the candidate must have made a substantial contribution to all papers included in the thesis. In addition, the candidate is required to make an explicit statement in the thesis as to who contributed to such work and to what extent. This statement should appear in a single section entitled "Contribution of Authors" as a preface of the thesis.

When previously published copyright material is presented in a thesis, the candidate must obtain, if necessary, signed waivers from the co-authors and publishers and submit these to the Thesis Office with the final deposition.

.

ACKNOWLEDGEMENTS

My deepest gratitude and appreciation is to my advisor Dr. Varoujan Yaylayan for his contributions of time, knowledge, and funding that made my Ph.D. experience possible. The passion that he has for research was extremely contagious and increased my motivation to learn and grow as a young research scientist. Dr. Yaylayan, I have been remarkably fortunate to have you as my advisor. Thank you for your constant support, wisdom, patience, ongoing guidance, modesty, advice and understanding, and for giving me the freedom to explore on my own, while at the same time guiding me through all the paths of this journey. I am forever grateful to you.

To my parents and brother, thank you for your unconditional love and support. I value all the sacrifices you have made to support me in all my pursuits. I love you. To Eric, thank you for your love, friendship, and constant support. A very special thanks goes to my dear friends Ms. Ghina Itani and Dr. Hussein Hassan. Ghina and Sous, I wouldn't be here if it weren't for you. Thank you for being a positive force in my life and for always being there for me and never letting me give up on my dreams.

My profound gratitude goes to His Excellency Bishop Anoushavan Tanielian for his constant support to me through my Ph.D. journey.

I also gratefully acknowledge the Calouste Gulbenkian Foundation (Portugal) for their generous financial support.

I would like to extend my appreciation to Dr. Alexander Wahba from the Mass Spectrometry lab at McGill Chemistry department for his friendship, prompt service and assistance to me throughout my Ph.D. work. To all my friends, lab mates, especially Paula and Anja, and the administrative support staff especially Ms. Leslie LaDuke and Ms. Diane chan, thank you for constantly assisting me in many different ways.

Last but certainly not least, I am grateful to the members of the thesis advisory committee Drs. David Kitts, Valerie Orsat, Stéphane Bayen, Ashraf Ismail, and Benjamin Simpson for their time, support and feedback on this work.

CONTRIBUTION OF AUTHORS

This thesis is presented in a manuscript format and consists of nine chapters. Chapter 1 introduces the important role of metal ions in the Maillard reaction and presents the rationale for conducting this study, research hypothesis, experimental methodology, objectives and the significance of the study. In Chapter 2 a current and in-depth literature review is presented on the various important aspects of the Maillard reaction and the rationale behind the need for controlling this reaction. Also this chapter provides a thorough and current literature review surrounding the role of metal ions in the Maillard reaction and provides an understanding of their coordination with food components. Chapters 3 through 8 are based on published manuscripts and are bridged logically and sequentially through connecting paragraphs. Chapter 9 presents a brief conclusion and the contributions of this investigation to knowledge. This dissertation is in accordance with guidelines for thesis preparation as published by the Faculty of Graduate Studies and Research of McGill University

The present author was responsible for the concepts, design of experiments, experimental work, and manuscript preparation in all the published and submitted papers. Dr. Varoujan Yaylayan, the thesis supervisor, had direct advisory input into the work as it progressed and as manuscript co-author critically edited the dissertation prior to its submission. Ms. Xi Wang also co-authored Chapter 7 "Formation of the reduced form of furaneol® (2,5-dimethyl-4-hydroxy-tetrahydrofuran-3-one) during the Maillard reaction through catalysis of amino acid metal salts" and provided partial data input through her master's thesis work.

PUBLICATIONS

Nashalian, O.; Yaylayan, V. A. (2017). Reactivity of nitrogen atoms in adenine and $(Ade)_2Cu$ complexes towards ribose and furanmethanol: Formation of adenosine and kinetin. *Food Chemistry*, 215, 463-469.

Nashalian, O.; Wang, X.; Yaylayan, V. A. (2016). Formation of the reduced form of furaneol® (2,5-dimethyl-4-hydroxy-tetrahydrofuran-3-one) during the Maillard reaction through catalysis of amino acid metal salts. *Food Chemistry*, 210, 43-48.

Nashalian, O.; Yaylayan, V. A. (2016). In situ formation of the amino sugars 1-amino-1-deoxy-fructose and 2-amino-2-deoxy-glucose under Maillard reaction conditions in the absence of ammonia. *Food Chemistry*, 197, Part A, 489-495.

Nashalian, O.; Yaylayan, V. A. (2015). Sugar-conjugated bis(glycinato)copper(II) complexes and their modulating influence on the Maillard reaction. *Journal of Agriculture and Food Chem*istry, 63, 4353-4360.

Nashalian, O.; Yaylayan, V. A. (2015). *De novo* synthesis of amino acids during the Maillard reaction: New insights to Akabori modification. *Journal of Agriculture and Food Chem*istry, 63, 328–334.

Nashalian, O.; Yaylayan, V. A. (2014). Thermally induced oxidative decarboxylation of copper complexes of amino acids and formation of Strecker aldehyde. *Journal of Agriculture and Food Chem*istry, 62, 8518–8523

Publication without a peer-review process:

Nashalian, O.; Yaylayan, V. A. (2015). The role of amino acid metal complexes in the Maillard and Akabori reactions. *IMARS Highlights*. 10, 5-10.

CONFERENCE PRESENTATIONS

- Nashalian, O.; Wang, X., and Yaylayan, V. A. Formation of a Reduced Form of Furaneol® During the Maillard Reaction. IFT, Chigaco, USA, 2016.

- Nashalian, O.; Yaylayan, V. A. The role of amino acid metal complexes in the Maillard and Akabori reactions. 12th International Symposium on the Maillard Reaction (ISMR), Tokyo, Japan, 2015.

- Nashalian, O.; Yaylayan, V. A. Formation of amino sugars in the Maillard reaction. 12th International Symposium on the Maillard Reaction (ISMR), Tokyo, Japan, 2015.

- Nashalian, O.; Yaylayan, V. A. Isotope labelling studies on the influence of copper on the mechanism of alanine interaction with glucose. 17th IUFoST World Congress of Food Science and Technology and EXPO, Montreal, Canada, 2014.

TABLE OF CONTENTS

LIST OF TABLES

LIST OF FIGURES

ABBREVIATIONS

Ade	Adenine
$(Ade)_2Cu$	*Bis*(adeninato)copper complex
AGE	Advanced glycation end product
Ala	Alanine
$(Ala)_2Cu$	*Bis*(alaninato)copper complex
amu	Atomic mass unit
AR	Amadori rearrangment
ARP	Amadori rearragment product
BCA	Bicinchoninic acid assay
Ca	Calcium
CEL	Carboxyethyllysine
Cl	Chloride
CML	Carboxymethyllysine
Cu	Copper
DAD	Diode array detector
DNA	Deoxyribonucleic acid
dAGE	Dietary advanced glycation end product
ESI	Electrospray ionization
ESR	Electron spin resonance
Fe	Iron
GC	Gas chromatography
Glc	Glucose
Gly	Glycine
$(Gly)_2Cu$	*Bis*(glycinato)copper complex
HMW	High molecular weight
IARC	International agency for research on cancer
Ile	Isoleucine
LC	Liquid chromatography
Leu	Leucine
LMW	Low molecular weigh
Mg	Magnesium
MR	Maillard reaction
MRPs	Maillard reaction product
MS	Mass spectrometry
MS/MS	Tandem mass spectrometry

m/z	Mass to charge
Na	Sodium
Ni	Nickel
NMR	Nuclear magnetic resonance
Phe	Phenylalanine
ppm	Parts per million
Py	Pyrolysis
qTOF	quadrupole time of flight
RAGE	Receptor for advanced glycation end products
Ser	Serine
$(Ser)_2Cu$	*Bis*(serinato)copper complex
TIC	Total ion chromatogram
UHPLC	Ultra high performance liquid chromatography
Val	Valine
Zn	Zinc

CHAPTER 1

INTRODUCTION

1.1 GENERAL INTRODUCTION

Ever since its discovery by Louis Camille Maillard in 1912, the Maillard reaction has become one of the most important and challenging areas of research in food chemistry and thermal processing for the production of food with desirable quality attributes. For decades, it has been studied and explored in attempts to control and regulate its different pathways particularly with regard to color and aroma development. Among the many factors that can directly control the Maillard reaction are the presence of those components in food that can react with Maillard reaction precursors, such as amino acids and sugars, to enhance or delay the formation of Amadori intermediates. Metal ions are such examples of reactive food components that have been studied for their role in regulating the Maillard reaction. Their importance surfaced from various studies that were conducted to determine their catalytic role in promoting oxidation pathways and affecting the rates of the reaction in aqueous systems (O'Brien & Morrissey, 1997; Ramonaitytė et al., 2009, Rendleman 1990). The addition of metals to sugar/amino acid model systems were reported to affect both the intensity of browning and rate of the reaction in a concentration dependent manner (Cheng *et al.*, 2012 Ramonaitytė et al., 2009, Rendleman 1990). Also, the importance of metal ions has been demonstrated through their ability to prevent the formation of certain harmful Maillard reaction products such as acrylamides, both in model systems involving asparagine and sugars and in food models (Gokman and Senyuva, 2007; Sadd et al., 2008). Moreover, the effect of metal ions on the Maillard reaction was found to depend on the type of metal ion. For example, iron and copper were found to enhance browning the most when added to different sugar-amino acid model systems (Kwak & Lim, 2004). However, the exact mechanism of how metal ions can affect the Maillard reaction or the different stages and pathways of the reaction have not been elucidated. Although both Maillard reaction precursors can react with metals, amino acids have a greater affinity to form stable coordinated complexes through their amino and carboxylate groups. However, the behavior of such amino acid metal complexes under the Maillard reaction conditions still remain unexplored today. Independently, amino acid metal complexes have been reported to undergo thermally induced intramolecular redox reactions generating Strecker aldehydes (Yablokov et al., 2014); while in the presence of Strecker aldehydes, Akabori et al., (1959) used α-amino acid metal complexes for the commercial synthesis of their corresponding β-hydroxy counterparts. Although foods contain the required precursors for such transformations, their occurrence has never been explored or reported. Furthermore, no systematic or mechanistic studies were conducted to explore

the fundamental role of metal ions in the Maillard reaction at the molecular level. Understanding how these complexes behave and react with other components in foods during thermal treatments constitutes the main rational behind this thesis. The findings from such studies can significantly contribute in providing an intervention strategy to control this reaction and consequently the generation of color and flavor during food processing. Additionally, the versatility of metal affinity towards organic compounds can be extended to other nucleophilic food components such as nucleobases and nucleotides that are also known for their high affinity towards metal ions. However, the exact chemistry of this interaction and the behaviour of nucleobase-metal complexes in the Maillard reaction have also not been studied. In general, information regarding the metal ions and their effect on the physical and chemical aspects of the Maillard reaction is still lacking. Controlling such a reaction with a wide spectrum of end products through the use of metal ions can contribute greatly towards regulating and enhancing its applications in food.

1.2 RATIONALE AND RESEARCH OBJECTIVES

Elucidating the fundamental behaviour of metal ions in the Maillard reaction requires performing a systematic and stepwise exploration of their role in the reaction. Based on the identified research gaps, the main objective of this work was to elucidate the basic mechanism and new pathways by which metal ions can influence and control the Maillard reaction using a model system approach (aqueous and non-aqueous), chemical synthesis, isotope labelling techniques and mass spectrometry tools.

The specific objectives of this study were:

1. To explore the chemistry of amino acid-metal interactions under the Maillard reaction conditions using amino acids with various metal salts and synthetic copper complexes of alanine and glycine in the absence of carbonyl electrophiles such as aldehydes or sugars.
2. To investigate the occurrence of Akabori transformation during the Maillard reaction as a possible mechanism for *de novo* synthesis of amino acids through the interaction of glycine copper complexes with a simple Strecker aldehyde.
3. To study the fundamental aspects of glycine-glucose interaction in the presence of metal ions by substituting glycine with glycine copper complexes or adding $CuCl_2$ to aqueous model systems.

4. To explore the differences in the reactivity of various *aldo* and *keto* sugars towards glycine and their corresponding copper salts in aqueous Maillard reaction mixtures.
5. To study the vital role of amino acid metal salts as reagents that can catalyze base induced enolization and fragmentation of glucose while simultaneously enhancing aldol condensation type reactions under pyrolytic and aqueous reaction conditions.
6. To explore how other food components such as purine nucleobases that are also capable of complexing with metal ions react towards sugars alone or with sugars and amino acids during the Maillard reaction.

1.3 EXPERIMENTAL APPROACH

Due to the complexity of Maillard reaction pathways in foods, model systems which can provide a more practical and direct mechanistic information, are routinely utilized for their study. Model systems are typically comprised of a limited number of reactants and studied under strictly controlled conditions. They have been used in the literature since the earliest investigation of the Maillard reaction (Beacham and Dull, 1951) and contributed significantly to our understanding of the fundamental processes, reaction and various product formation pathways. To achieve a comprehensive and in-depth understanding of the fundamental interactions of sugars with metal complexes of amino acids and nucleobases during the Maillard reaction, aqueous and non-aqueous (pyrolytic) model systems were used in this investigation. The model systems consisted of various reactants such as amino acids, sugars, various aldehydes, and metal salts in addition to synthetically prepared amino acid-metal or nucleobase-metal complexes (Figure 1.1). Both sets of model systems were subsequently analyzed using the applicable analytical tools as described in the sections below. All model systems were prepared and analyzed at least in duplicates.

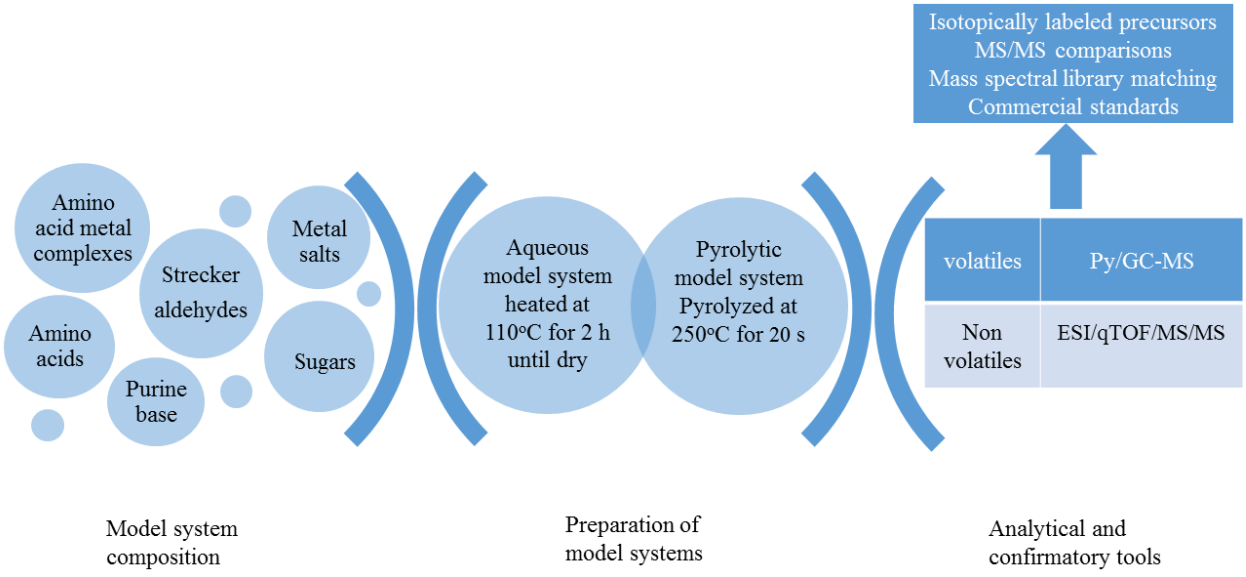

Figure 1.1. Schematic illustration of preparation of samples, analysis and confirmation.

1.3.1 Synthesis of Amino Acid–Metal Complexes

Various amino acid-metal and nucleobase-metal complexes such as $(Ala)_2Cu$, $(Gly)_2Cu$, and $(Ser)_2Cu$, and $(Ade)_2Cu$ were prepared by dissolving 1 mole of amino acid or nucleobase in methanol (10 mL) in the presence of KOH (0.05 g) followed by the addition of 0.5 mole of $CuCl_2$. The precipitates obtained were washed with methanol, filtered, and dried. The metal adducts were confirmed by obtaining their elemental composition from their accurate masses determined by ESI/qTOF/MS analysis. Isotope-labeled precursors were prepared similarly.

1.3.2 Analysis of the volatile reaction products

The analysis of the non-polar and volatile reaction products was performed using pyrolysis gas chromatography-mass spectrometry (Py/GC-MS). Pyrolysis which is the thermal decomposition of chemical compounds in an inert atmosphere, coupled to a separation and identification tool such as GC-MS (Py-GC/MS) can be a very useful method for the identification of a wide range of Maillard reaction compounds with different physical and chemical properties (Jahirul *et al.*, 2012; Yaylayan and Keyhani, 2000). This technique uses flash heating at high temperatures for very short time, which allows the thermal breaking and rearrangement of molecular bonds (Jahirul *et al.*, 2012; Kusch, 2012). Dry model systems comprising of various sugars and/or amino acids, or amino acids with metal salts, or synthetic amino acid metal complexes were homogenized and

mixed using a micro scale porcelain mortar and pestle. After thorough mixing, approximately 0.5 mg of the individual reactants or their mixtures were weighed into a quartz tube (0.3mm thickness) plugged at both ends with glass wool (Supelco, USA) and pyrolyzed at 250^{o}C for 20 s. The Py/GC-MS unit, comprised of a Varian CP-3800 gas chromatography coupled to a Saturn 2000 ion trap detector, was interfaced to a CDS Pyroprobe 2000 unit through a valved interface (CDS 1500), while the separation of analytes was performed using a fused silica DB-5MS column.

1.3.3. Analysis of the non-volatile reaction products

On the other hand, the polar profile of the heated residues and their non-volatile components were analyzed using Electrospray Ionization quadrupole Time of Fight Tandem Mass Spectrometry (ESI/qTOF/MS/MS). This type of soft ionization technique allows the analysis of intact chemical species, which makes it an ideal tool for this work to analyze both covalently and non-covalently bound molecules and metal complexes in the gas phase (Banerjee & Mazumdar, 2012). To determine the influence of metal ions on the Maillard reaction, all model systems were analyzed in the absence (control) and presence of corresponding metal salts or metal complexes. The samples were weighed, dissolved in water (2mL) and heated on a sand bath at a nominal temperature of 110^{o}C for 2 hours until dry. The ESI/qTOF/MS system comprised of a Bruker Maxis Impact quadruple-time of flight mass spectrometer (Bruker Daltonics, Bremen, Germany) was operated in positive ion mode. The dry residues were subsequently reconstituted in LC grade water to a concentration of 1 mg/mL. The samples were then diluted 10-fold in 10% methanol prior to analysis by ESI/qTOF/MS. In this study, a non-targeted approach was adopted to analyze the different model systems. Following analysis, the ESI spectrums of metal containing model systems were compared to their corresponding controls (non-metal containing) to identify ions specific to the model systems containing the metals. The additional confirmation of selected product ions was done by comparing their MS/MS fingerprints to those of commercial or synthetic standards (Figure 1.2).

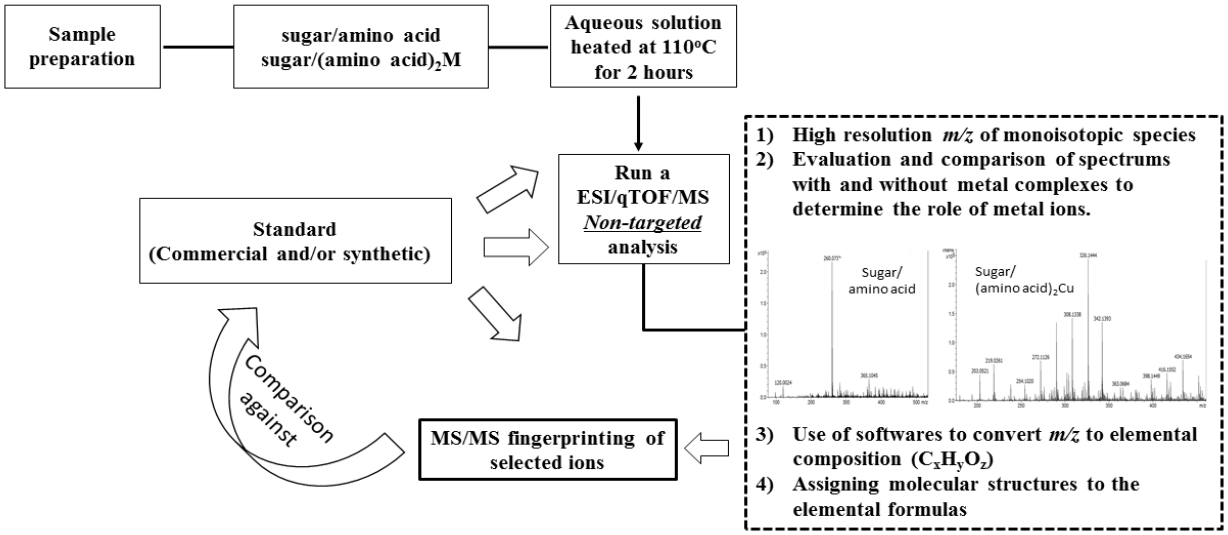

Figure 1.2. Preparation and analysis of samples using ESI/qTOF/MS/MS.

1.3.4 Structural identification and confirmatory tools

The identity of the generated products was verified by different techniques. Substituting the reactants with their corresponding isotopically labeled counterparts such as ^{13}C labeled sugars and amino acids, and ^{15}N labeled amino acids allowed us to estimate labeled atom incorporation in the products, making this approach a good confirmatory and tracking tool in mechanistic studies. Other confirmatory tools included analysis of the elemental composition of generated products from their high resolution masses, mass spectral library matches, the use of commercial or synthetic standards. Also tandem mass spectrometry was used in which the MS/MS spectra of selected product ions were compared to those of commercial standards. Additionally, the incorporation of copper in the identified complexes was confirmed by its isotopic signature through detection of M+2 peaks at 30% relative intensity.

1.4 Significance of The Proposed Research

Although the importance of metal ions as a means to control the Maillard reaction is well recognized, research conducted in this area is incomplete and there is a lack of comprehensive understanding regarding the molecular mechanism of their action. Since metals are ubiquitously present in foods as nutritionally important components, understanding their in-depth interaction and behavior with Maillard reaction reactants during thermal treatments is essential. In this study

we present, for the first time, a systematic and fundamental information about their chemical interactions in the context of the Maillard reaction. This study also generated important mechanistic information on the multifunctional role of amino acid-metal complexes in modulating the Maillard reaction, which was through their ability to promote the oxidative decarboxylation of free and sugar conjugated amino-acid metal complexes and eventually controlling the release of two of the most important intermediates of the Maillard reaction, Strecker aldehydes and Amadori products. We also provided for the first time mass spectrometric evidence for the detailed mechanism of Akabori transformation through Schiff base formation as a necessary step for the activation of the complex and the conversion of glycine into serine and hydroxymethyl-serine. We also identified for the first time the mechanisms of formation of amino sugars and Mannich bases during the Maillard reaction. Additionally, we elucidated the role of amino acid salts as basic catalysts able to enhance glucose degradation and formation of shorter chain reactive intermediates. Finally, we presented the mechanism by which the complexation of adenine with metal ions can enhance its reactivity towards sugars and furanmethanol to generate adenosine and various kinetin derivatives. Beyond its academic contribution and impact, the pathways, precursors and the products identified in this investigation can be used to control the generation and release of color, aroma and other specific thermally generated products in food.

CHAPTER 2

LITERATURE REVIEW

2.1 THE MAILLARD REACTION: A BRIEF HISTORICAL PERSPECTIVE

The Maillard reaction is a thermally accelerated, non-enzymatic browning reaction between compounds with carbonyl and amino groups (Echavarria et al., 2012; Newton et al., 2012; Nursten, 2005). Its discovery can be traced to a simple observation of color formation recorded at the beginning of the 20th century by the French scientist Louis Maillard. This reaction has since evolved into what is now considered to be an independent research area and one of the most important and challenging reactions in the field of food chemistry (Echavarria et al., 2012; Monnier, 1990). Although, the chemistry of the reaction of sugars with amino compounds has been investigated by Schiff (1866) and Fischer (1886) before 1912, it was following Maillard's initial observation that interest was initiated in studying this reaction both in food and physiological systems. Numerous studies have been published over the past century in an effort to unravel the detailed network of reactions that leads to the formation of color aroma and flavor. One of the earliest key findings was in the 1920s when Amadori identified *N*-glycosides as labile products of Schiff bases, although afterwards the term "Amadori products" were assigned to the first stable products of the Maillard reaction (Hellwig and Henle, 2014) (Figure 2.1). Years later, Heyns identified the analogue of Amadori product as "Heyns product" from ketoses. In the early 1940s, as interest grew in the production of heat-treated foods, scientists started exploring various parameters that can affect the Maillard reaction. In this context, Doob et al. (1942) was the first to propose the importance of relative humidity as a factor that can control the formation of color during the reaction (Finot, 2005). Also, the role of other components such as the metal ions copper and iron was recognized in enhancing the reaction, while those such as sulfates prevented it (Finot, 2005). On the other hand, several research groups identified aroma active aldehydes as byproducts of amino acid and sugar decomposition (Hellwig and Henle, 2014). This decomposition reaction was later, in 1948, named as "Strecker degradation". In 1953, the American scientist John Hodge (1953), presented the first complete scheme of the browning reaction, which facilitated in exploring the individual reaction pathways of the Maillard reaction under food-relevant conditions creating a plethora of research and literature. Starting early 1960s, scientists also started exploring the harmful products generated from the Maillard reaction with the discovery of glycated hemoglobin in 1968. The following years and into the 1990s marked a shift in the focus of the Maillard reaction from food and nutrition to its role in the human body. Various advanced glycation end products were identified, characterized and correlated not only to diabetes but also

to many other pathophysiological and chronic conditions such as Alzheimer's disease, aging, and atherosclerosis. Currently, the role of Maillard reaction in medicine is considered as a separate theme within the field of the Maillard reaction research (Gerrard, 2006). In the past few decades, another class of "unwanted" Maillard reaction products collectively known as process-induced toxicants have started to attract attention in heat-processed foods with the identification of heterocyclic amines and acrylamide at the beginning of this century (Finot, 2005).

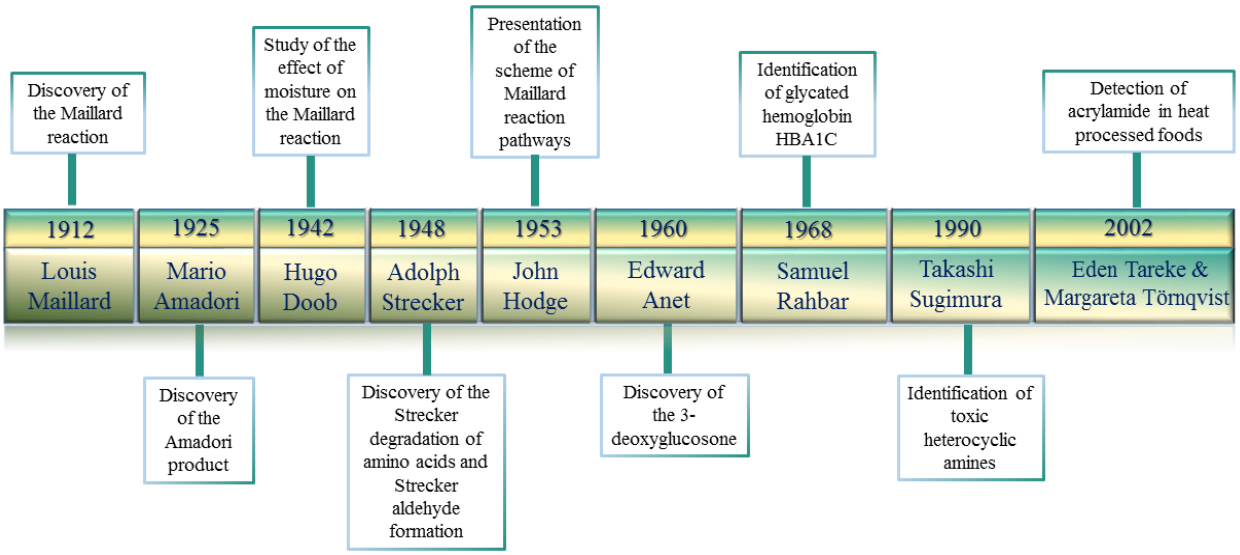

Figure 2.1. A graphic timeline for some of the key discoveries made in the Maillard reaction literature

2.2 The Chemistry of The Maillard Reaction

What makes the Maillard reaction phenomenal is that it begins with a simple nucloephilic attack by an amino compound onto an electrophilic center such as a carbonyl moiety and leads to the generation of various intermediates that are organoleptically significant in providing color, texture, taste, flavor, and aroma to foods (Luevano-Contreras & Chapman-Novakofski, 2010; Newton et al., 2012). On the other hand, potentially harmful by-products, such as heterocyclic amines, furans, acrylamide, and advanced dietary and biological glycation end-products (AGEs) are also known to result from this reaction (Troise & Fogliano, 2013; Perez Locas & Yaylayan, 2004; Yaylayan et al., 2005). Although there are various routes for the formation of different Maillard reaction products, the scheme presented by Hodge (1953) is still considered to provide a general summary

of the processes occurring during the Maillard reaction. This scheme divides the reaction into three consecutive stages (Figure 2.2). The initial phase of the reaction begins with the formation of a glycosylamine that immediately dehydrates into a Schiff base, which in turn slowly rearranges to a relatively more stable ketosamine adduct otherwise known as Amadori Rearrangement Product (ARP), if the reducing sugar is an aldose, or Heyn's rearrangement product, if the reducing sugar is a ketose (Newton et al., 2012; Hodge, 1953; Yaylayan et al., 1994) (Figure 2.3). As the reaction proceeds, earlier generated products undergo an array of transformations depending on the pH. When the pH of the system is less than 7, Amadori/Heyns rearrangement compounds are known to undergo a 1,2-enolization and then elimination to produce 3-deoxyosones. If the reacting sugar is glucose, then the 3-deoxyosone is a 3-deoxyglucosone, which upon dehydration gets converted into 5-Hydroxymethylfurfural (HMF). On the other hand, when the pH of the system is greater or equal to 7, ARP/ Heyn's products are channeled to undergo an irreversible 2,3-enolization. The 2,3-enolization can further branch out into two routes; 1-deoxyosone and 4-deoxyosone. The 2,3-enolization route generates reductones, dicarbonyls and many other products. During this stage, a sub-reaction, known as the Strecker degradation, can branch out between the generated α-dicarbonyl compounds and amines, producing aminoketones, aldehydes and carbon dioxide. The Strecker aldehyde and the condensation products of aminoketones are considered to be important aroma sources in foods. The various chemical reactions of the intermediate phase include aldol, retroaldol reactions, enolizations, decarboxylations, dehydrations and Michael additions (Nursten, 2005). These reactions are vital for the quality attributes of foods in terms of appearance, texture, color and flavor. In the final stage of the Maillard reaction, the intermediates formed during the intermediate stage undergo more dehydration and polymerize to form high molecular weight deeply colored melanoidins (Figure 2.2).

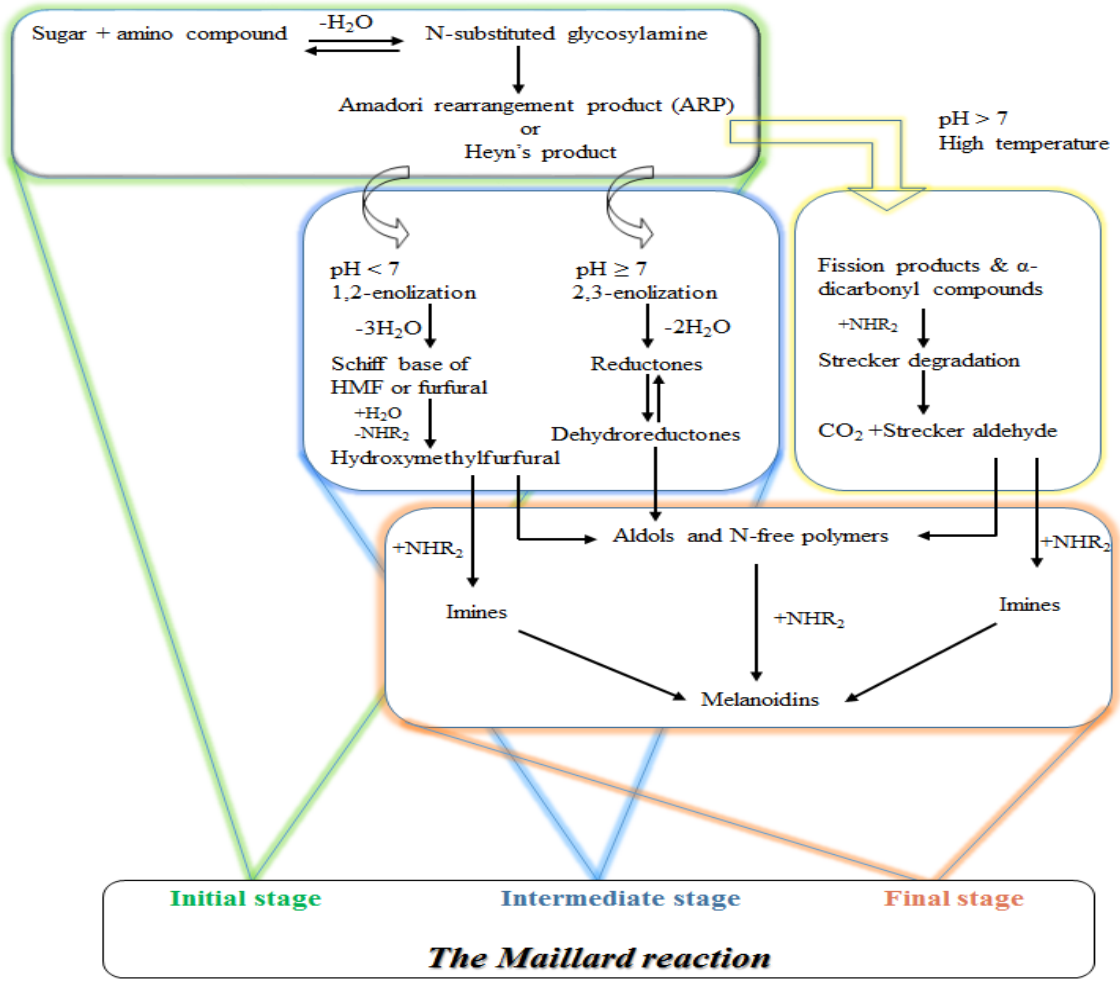

Figure 2.2. Schematic diagram of the Maillard reaction adopted from Hodge (1953) scheme.

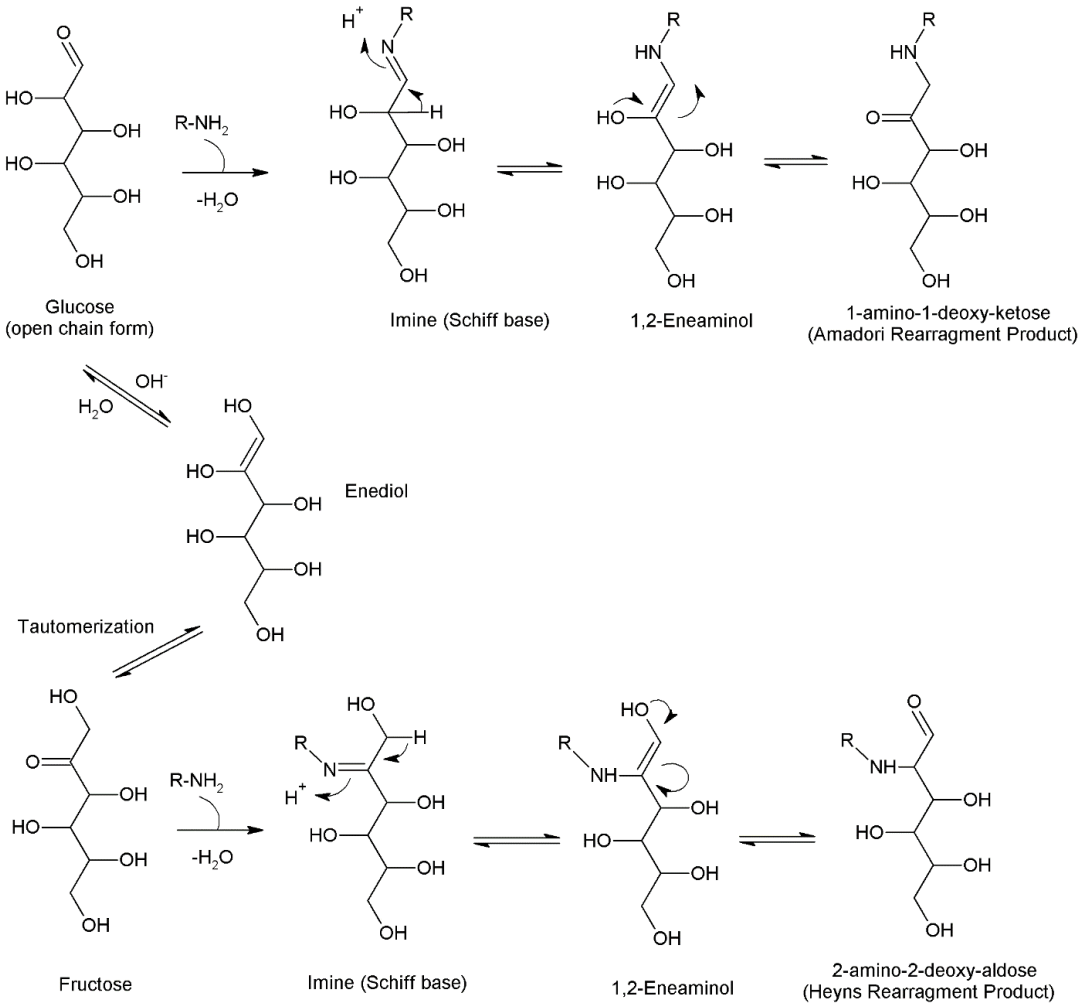

Figure 2.3. The formation of Amadori and Heyns rearrangement products from aldo and keto sugars, respectively.

2.3 SIGNIFICANCE OF THE MAILLARD REACTION: THE SWEET AND THE BITTER

The Maillard reaction is remarkably widespread, it occurs at relatively low temperatures in textiles, soils, pharmacological preparations, foodstuff and biological systems (Luevano-Contreras & Chapman-Novakofski, 2010; Nusrten, 2005; Srikanth et al., 2011; Ulrich & Cerami, 2001; Wolff, 1993). However, what is relevant to food scientists and the food industry is its occurrence during food processing and especially during roasting, baking, cooking, frying and grilling (Friedman, 1996; Newton et al., 2012). Although the Maillard reaction is needed to enhance the sensory attributes and even the functional properties of foods, it can also have undesired effects. Hence, the nutritional properties as well as the consequences associated with the Maillard reaction and its

generated products can be grouped into 2 major categories; desired and undesired (Figure 2.4). The desired effects include the distinctive organoleptic qualities (color, aroma and texture) of many foods, such as breads, cookies, cakes, meat, beer, chocolate, popcorn, and others, which develop as they undergo the Maillard reaction. On the other hand, the Maillard reaction has been correlated with undesired outcomes such as decreased protein availability, increased nutrient chelation (Seiquer et al., 2008), and production of potentially hazardous compounds, such as biological and dietary advanced glycation end products, and toxicants such as acrylamide, furans, heterocyclic amines and others (Troise & Fogliano, 2013).

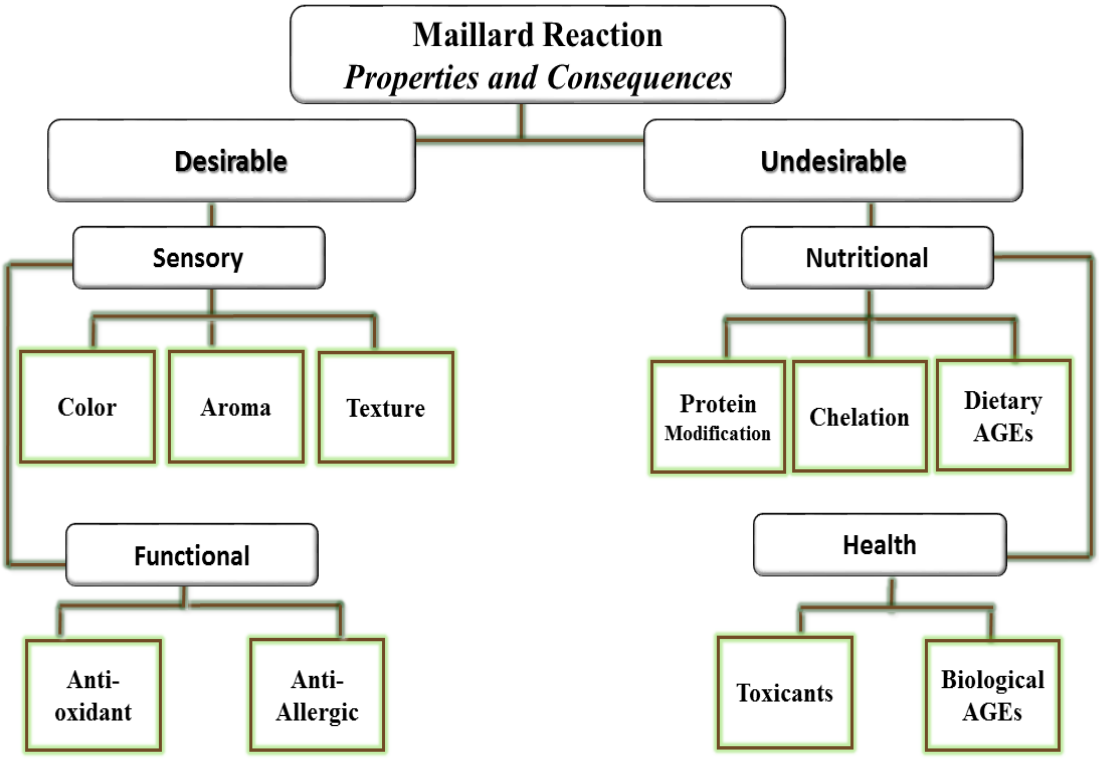

Figure 2.4. Schematic presentation of some important Maillard reaction properties and consequences.

2.4 Desirable Properties of the Maillard reaction and the Formation of Important Maillard Reaction Products (MRPs).

For decades, the Maillard reaction and its products have been the focus of not only food scientists but also the food industry to provide safe and healthy food, which is at the same time appealing to the public in its organoleptic qualities such as flavor, aroma, color and texture. During the Maillard

reaction various important intermediates and products are generated which include different amino sugars, furanones, Strecker aldehydes, pyrazines, pyrroles and many others. These various Maillard reaction products are important in determining the flavor profiles of many foods.

2.4.1 Formation of color during the Maillard reaction

The development of color is one of the most important and obvious features of the Maillard reaction. During the process of browning, a heterogeneous mixture of low molecular weight (LMW) compounds, generally comprised of 2-4 rings linked together with a double bond, and high molecular weight (HMW) polymeric melanoidins (>12 KDa) with chromophore groups are formed (Nursten, 2005; O'Brien & Morrissey, 1989). These compounds can be either nitrogenous or non-nitrogenous (mainly from furfurals and dehydroreductones) in nature and can range in color from pale yellow to dark brown depending on the type of the reactant and the extent of reaction (Ames, 1990, 1998; Morales & Van Boekel, 1998). In the 1940s, a large number of studies emerged that examined the florescence of various Maillard reaction intermediates. Chromophores, which are fluorescent compounds generated in the early stages of the reaction of amino acids with sugars, are considered to be precursors to melanoidins and indicators of reaction rate and product generation (Friedman & Kline, 1950; Knerr & Severin, 1993). Fluorescent and colored products can also be obtained from the further breakdown of Amadori products (Van Boekel, 1998). In 1999, Hayase and his co-workers identified several colored pyrole derivatives, namely two blue (Blue-M1& Blue-M2) and two red (Red-M1 & Red-M2) pigments in xylose-glycine model systems stored at 28ºC for 96 hours (Hayase et al., 1999, 2006). Hoffman et al. (1997) also investigated the production of a red colored product (l-H-Pyrrol-3(2H)-one), in a model mixture solution of furan-2-carboxaldehyde (the thermal reaction product of pentoses) and L-alanine (Hoffman et al, 1997). These pigments were found to be capable of polymerization and further integration into melanoidins. As for melanoidins, they continue to challenge Maillard reaction researchers due to their extremely complex nature. They are formed at the advanced stages of the reaction from the condensations and cyclizations of various lower molecular weight MRPs and even after decades of research into this area, little is known about the chemical structures of melanoidins. In real foods, melanoidins tend to be HMW, although in model systems relatively lower molecular weight melanoidins (<5KDa) can be detected (Wang et al., 2011). LMW and HMW melanoidins are ultimately responsible for the brown color of heated foods.

2.4.2 Generation of aroma and flavor during the Maillard reaction

Since flavor is highly influenced by the chemical senses of taste and smell, the volatile aromatic compounds generated during the reaction determine the flavor of foods. The detection and identification of volatile Maillard reaction products was greatly advanced with improvements in extraction techniques and with the development of highly sensitive gas chromatography/mass spectrometry instruments and high resolution capillary columns. More than 1000 volatile compounds have been reported to form in various foods such as meats, seafoods, and bakery products (Chuyen, 1998; Ho, 1996; Taylor & Mottram, 1996). In 1981, Nursten categorized these volatiles into 3 groups based on their primary reactants; sugars, amino acids and the interaction volatile products of the first 2 groups (Nursten, 1981). The aromatic compounds generated from sugars, which can also be found as a result of caramelization, include furans, pyrones, cyclopentenes, smaller carbonyl compounds, and organic acids. Compounds generated from amino acids include different Strecker aldehydes in addition to nitrogen and sulphur containing compounds. As for the interaction group, compounds generated include different pyrroles, pyridines, pyrazines, imidazoles, oxazoles, thiazoles, thiophenes, dithiolanes, trithiolanes, dithianes, trithianes, and furanthiols. Mottram et al. further classified the flavour compounds according to their heteroatoms (Mottram et al, 2007). The cluster of compounds with oxygen functional group included furfurals, 5-HMFs, furanones, pyranones, 2,3-butanedione, 2,3-pentanedione, methylpropanal, 3-methylbutanal, phenylacetaldehyde, with concentration in foods ranging from 1μg/kg up to 100 mg/kg. Nitrogen containing groups included products such as oxazoles, oxazolines, pyrazines, pyrroles, pyrrolines, and their concentrations in food usually range between 0.001 and 10 mg/kg. The last group of heteroatoms is the sulfur containing group which has the strongest aroma compounds and they include different thiazoles and thiazolines, dithiazines, furanthiols and sulphides (Mottram, 2007; Nursten, 2005).

Although some of the above mentioned products can be generated directly from sugars (through caramelization) or amino acids (see section 2.4.2.1), the main precursor for the generation of all of above mentioned volatiles are the Amadori rearrangement products. On the other hand, a variant of Amadori or Heyns rearrangement products are the "amino sugars" such as fructosamine or glucosamine which are the Amadori rearrangement products of sugars with ammonia. Because of the presence of a free amino group, they are considered to be more reactive than sugars

themselves (Kraehenbuehl et al., 2008; Hrynets et al., 2013) or the Amadori/Heyns rearrangement compounds. In Maillard reaction model systems glucosamine is reported to generate more reaction products relative to sugars when heated alone or reacted with amino acids (Kraehenbuehl et al., 2008; Hrynets et al., 2015). In the study by Kraehenbuehl et al. (2008) glucosamine was found to generate relatively higher browning, pyrazine and sulphur-containing flavour products compared to different acidic and basic sugars when reacted with cysteine. Also, Shu (1998) reported the formation of several volatile products, such as different pyrazine derivatives, pyrrole-2-carboxaldehyde, and furfural, after heating glucosamine in aqueous solution at 150 °C for 5 min at different pH values. A recent study (Hrynets et al., 2015) has indicated that glucosamine produces significant amounts of dicarbonyls and some pyrazines, even at 37 °C, when incubated at longer times. On the other hand, Jun et al., (2003) studied the non-volatile thermal degradation of glucosamine in aqueous solution. In their study Jun et al. reported that heating glucosamine in water at 100°C for 2 h generated several non-volatile products, such as fructosazine, deoxy-fructosazine and their acetylated derivatives. The reactivity of glucosamine was also studied in dry model systems. Compared to fructose, glucosamine was reported to generate a different flavour profile and composition of isolated volatiles when reacted with sodium acetate at 200 °C in the absence of any solvent (Chen & Ho, 1998). Two classes of flavor compounds, namely Strecker aldehydes and furanones, are specifically interesting because of diversity of their aroma profiles and low threshold values. The former is considered to be an important volatile product related commonly to amino acids, and the latter is a key odorants formed universally in many foods and mostly related to the second reactant in the Maillard reaction, sugars.

2.4.2.1 Formation of Strecker aldehydes

Strecker aldehydes are one of the earliest identified Maillard reaction products (Hellwig and Henle, 2014; Nursten, 2005; Schonberg & Moubacher,1952; Yaylayan et al., 2003). They are amino acid specific products and can be considered as the carbonyl remnants of amino acids generated following the loss of carbon dioxide and amino groups. Strecker aldehydes are known to contribute to the flavor of many foods, possessing distinct aromas specific to the amino acid that they originate from. Although Strecker aldehydes are mostly known to be generated through the Strecker degradation reaction, they can also be produced during the Maillard reaction through alternate or independent routes (Figure 2.5). In fact, in 2003 and after a thorough review of Strecker

literature, Yaylayan (2003) proposed four different pathways to generate Strecker aldehydes. One such pathway is through the independent degradation of amino acids during high temperature treatments. In 2001, Yaylayan and Keyhani detected the formation of Schiff base adducts between the Strecker aldehydes and their corresponding amines or amino acids following pyrolysis of amino acids alone at 250^{o}C. Another pathway is through α-dicarbonyl mediated decarboxylation and deamination of amino acids. In this scenario, the Amadori products can also generate their corresponding Strecker aldehydes, though an α-imino dicarbonyl intermediate and following decarboxylation and deamination, generate their corresponding Strecker aldehydes. The fourth pathway is the degradation of Amadori rearrangement products directly into Strecker aldehydes either through decarboxylation of the Schiff base of Amadori product or through using metal ions such as copper to convert the Amadori products into an eneaminol intermediate which can undergo rearrangements and decarboxylation to release Strecker aldehydes (Hofmann and Schieberle, 2000; Yaylayan, 2003). In the latter situation, the model system was studied in aqueous solutions and the role of copper was to catalyze the oxidation of Amadori products into their corresponding eneaminol moieties. On the other hand, in 2014, Yablokov et al., studied the kinetics and mechanism of thermal decomposition of amino acid copper complexes in dry mixtures at 230°C. Yablokov reported an oxidative degradation mechanism of the complexes initiated by copper followed by the loss of carbon dioxide and the generation of an ethanimine adduct (Yablokov et al., 2014). Since the focus of Yablokov's work was to study the decarboxylation of the amino acids and not their products, the potential of further hydrolysis of the generated ethanimine into Strecker aldehydes was not considered nor detected and reported. From the viewpoint of Maillard reaction chemistry, this route can and should also be considered as a possible pathway that can enhance the formation of Strecker aldehydes. Yablokov et al. (2014) also reported that the rate constants for the thermal degradation reactions of various amino acid copper complexes were highly dependent upon the nature and bulkiness of their side chains, and rates of degradation of such amino acid complexes decreased in the following order: serine > phenylalanine > leucine > isoleucine > valine > glycine > alanine.

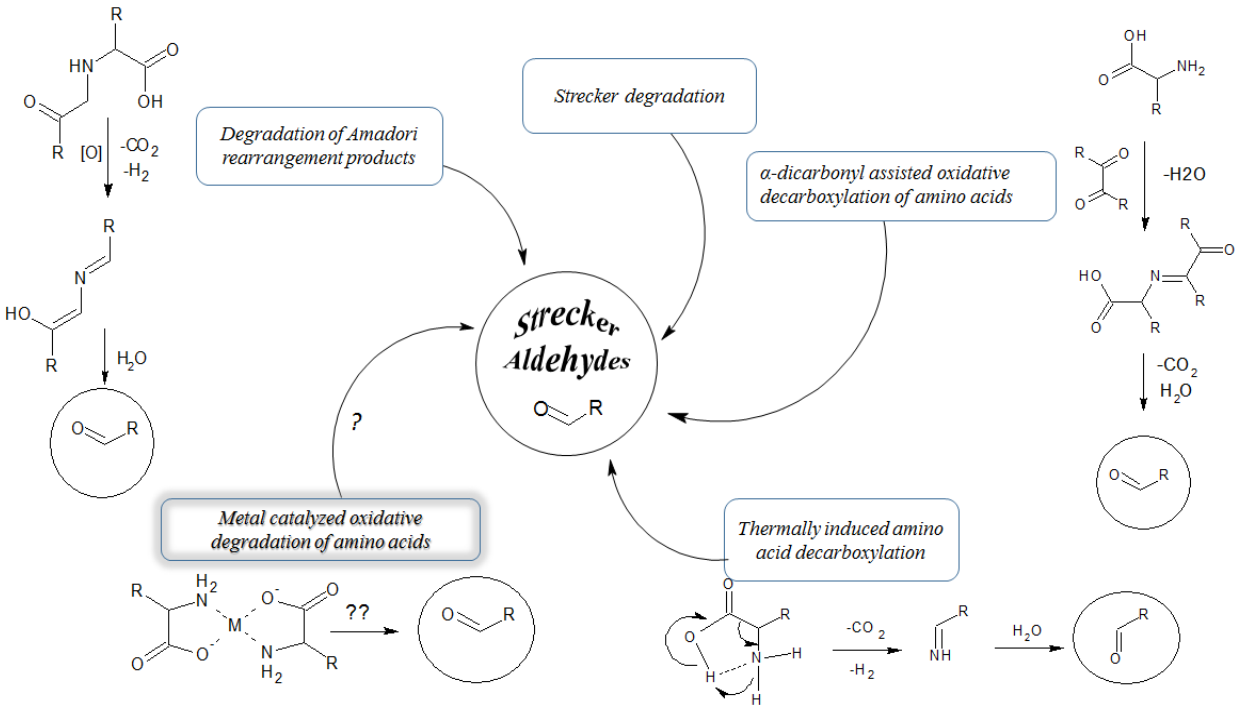

Figure 2.5. Different pathways of Strecker aldehydes formation.

2.4.2.2 Formation of aroma active furanone derivatives

One of the unique characteristics of the Maillard reaction is its ability to generate products in heated foods that can also be generated naturally. One example is the production of the aroma active furanones such as 4-hydroxy-2,5-dimethyl-3(2H)-furanone (Furaneol®) and 3-hydroxy-4,5-dimethylfuran-2(5H)-one (Sotolon), 2,5-dimethyl-4-methoxy-2H-furan-3-one, 2-ethyl-4-hydroxy-5-methyl-3(2H)-furanone, and 4-hydroxy-5-methyl-3(2H)-furanone (norfuraneol®) (Figure 2.6). These furanones are important low odor threshold odorants with common (due to their furanone structure) and yet diverse flavor profiles that can range from sweet caramel like to earthy to meat like flavors depending on their concentration (Hodge, 1967; Schwab, 2013, Zabetakis et al., 1999). They are primarily biosynthesized in fruits, plants and microorganisms through multistep enzymatic reactions (Blank & Fay, 1996; Schwab, 2013; Slaughter, 1999), but they can also be generated from thermal treatments during the Maillard reaction. Under relatively mild pH conditions, 3(2H)-furanones are known to originate either directly from intact sugars or in the presence of amino acids and 1, 2-dicarbonyl intermediates generated during the reaction (Blank, Devaud & Fay, 1996 and Blank and Fay, 1996). Additionally, similar to other Maillard reaction products, the amount and type of the thermally generated furanones have been found to

be dependent on the nature of the reactants (sugars and amino acids) and reaction conditions (temperature, time and duration) (Slaughter, 1999). In 1992, Schieberle described the formation of furnaeol in several heat treated foods and studied the effect of sugar type on furnaeol® formation. Schieberle identified fructose-1,6-diphosphate to be the major precursor for the formation of furnaeol through the dehydration of its acetylformoine intermediate (Schieberle, 1992). Yaylayan et al., also proposed the formation of furnaeol through the acetylformoine intermediate from heated glucose-6-phosphate and glycine (Yaylayan et al, 2003), or directly from 1-deoxyglucosone (Yaylayan and Keyhani, 2000), while Blank and Fay (1999) explored the formation of furaneol® during the Maillard reaction by heating xylose, ribose or arabinose with alanine and glycine (Blank and Fay, 1999). Because of their important flavor characteristics, scientists have tried to chemically synthesize furaneol® for commercial purposes. In 1981, Ross et al, patented their method of "Preparation of 2,5-dimethyl-4-hydroxy-2,3-dihydrofuran-3-one" (U.S. patent No 4,290,960, 1981). The synthesis method comprised of many steps and during this process they generated furaneol® by oxidizing it from its reduced form 2,5-dimethyl-4-hydroxy-tetrahydrofuran-3-one. Due to their significance to aroma and flavor, new pathways that can generate different and novel furanones are desirable.

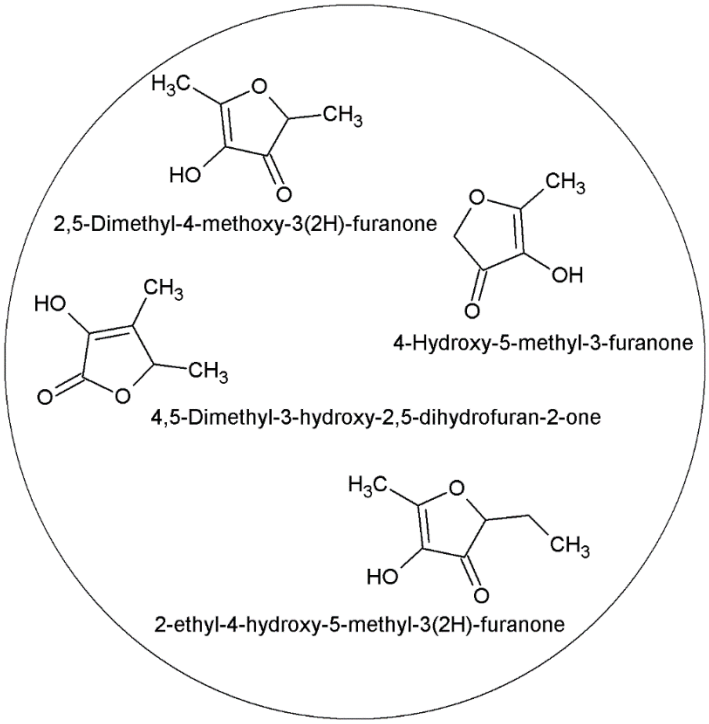

Figure 2.6. Important aroma active furanone derivatives.

2.4.3 Functional properties of the Maillard reaction products.

Beyond their contribution to flavor, color and texture; earlier generated MRPs such as Amadori products and reductones in addition to melanoidins are also known to possess health promoting benefits such as antioxidant and antibacterial properties due to their radical scavenging activity (Zeng, Zhang, Guan, & Sun, 2011) and anti-allergenic effects. However, some of these properties cannot be categorized straightforwardly as desirable. Despite the large number of studies which support that these Maillard reaction products are beneficial to health, there are many others that present contradictory findings. An example is a recently published review by Gupta et al., (2016) where he presented a very realistic review of the inconsistencies in the allergenic or anti-allergenic properties of the Maillard reaction. Although MRPs can lower allergenicity by deactivating certain epitopes through glycation, they can also shift the non-allergenic profile of food into an allergenic one by altering specific motifs in IgE epitopes and even forming neo-allergens or neo-antigens that can worsen the severity of allergic reaction in sensitive individuals. Additionally, the many advance glycation end products (AGEs) such as carboxymethyllysine (CML), pyrraline and methylglyoxal that are generated during the MR can also act as pro-oxidants and immunogens by inducing the activation and proliferation of various immune cells. Gupta et al., (2016) also raised a very important point in their review recognizing not only the ability of the Maillard reaction to be affected by the food matrix but also the variabilities and changes that happen to the food matrix as a result of the Maillard reaction.

2.5 UNDESIRED ASPECTS OF THE MAILLARD REACTION

2.5.1 Advanced glycation end products: biological and dietary

The classic pathway for the *in vivo* glycation of proteins is very similar to that of *in vitro* amino-carbonyl reactions. It usually occurs over long periods of time when excess sugar in the body (mainly glucose) reacts with proteins via the Maillard reaction. Depending on glucose concentrations, this process is reversible at the beginning of the reaction cascade. Several intermediates are formed within hours, days and weeks. Early Amadori reaction products such as HbA_{1C} are examples of the intermediates that are formed within days, but the accumulation of Amadori products forces the reaction into the more advanced stages of the Maillard reaction. Advanced glycation end products are believed to form during the last stage of the Maillard reaction

parallel with melanoidins (Nursten, 2005; Poulsen et al., 2013), and similar to melanoidins (see section 2.4.1), they also consist of HMW (protein bound) and LMW (amino acid and peptide bound) fractions. The formation of AGEs requires an oxidative pathway; either through the autoxidation of glucose (the Wolff pathway), or Schiff base (the Namiki Pathway) or Amadori products (the Hodge Pathway) (Nursten, 2005) and/or the peroxidation of lipids. It typically occurs in the presence of oxidative stress and leads to the generation of reactive dicarbonyl compounds such as glyoxal, methylglyoxal, and 3-deoxyglucosone; which in turn react with the amino acid side chains, such as arginine or lysine, of peptides or proteins. There are also various types of AGEs formed; CML being one of the most commonly known AGEs and a marker of AGEs formed in foods. In addition to CML, furosine, pentosidine, pyrraline and CEL are also commonly formed AGEs (Poulsen et al., 2013) (Figure 2.7). Once AGEs are formed for several weeks, the process becomes irreversible and new AGEs can then form cross links between different proteins, lipids and even DNA and remain in the body for years affecting cellular processes and protein functionality (Luevano-Contreras & Chapman-Novakofski, 2010). Some commonly encountered cross-linked AGEs include glyoxal lysine dimer, methyl glyoxal, lysine dimer and pentosidine (Figure 2.7).

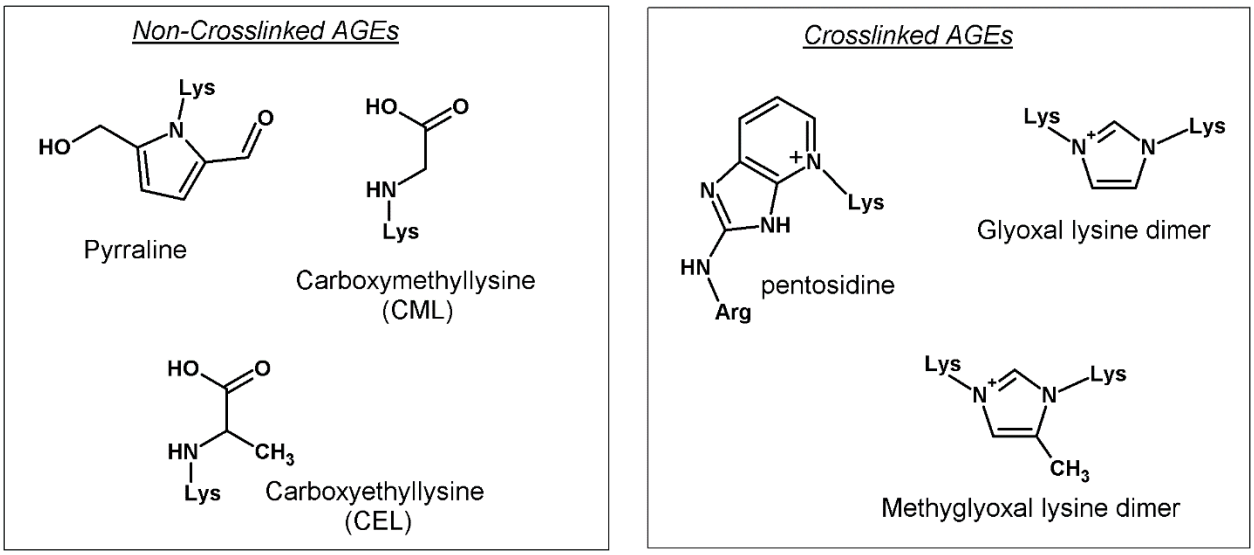

Figure 2.7. The chemical structures of important AGEs.

On the other hand, dietary AGEs or dAGEs are advanced glycation end products that are either naturally present in uncooked foods of animal origin or as part of their normal metabolism or newly generated in cooked foods via the Maillard reaction (Poulsen et al., 2013; Tessier and Birlouez-

Aragon, 2012; Uribarri et al., 2010). Until recently, the consumption of diet-derived AGEs was not regarded to pose any health risks to the consumers, some researchers remain skeptical as to whether these MRPs can actually take part in aggravating certain pathophysiological conditions. Over the past decade, the importance and consequences of consuming dAGEs has been recognized and since then the levels of dAGEs in various foods (Goldberg et al., 2004; Uribarri et al., 2010) and the efficacy of their absorption and metabolism in both animal and human studies have been determined (Poulsen et al., 2013). Other intervention studies reported that the dietary restrictions of MRP can improve oxidative stress and inflammatory signaling molecules in animals and humans (Bastos and Gugliucci. 2015). The contribution of individually consumed foods to the total dAGEs exposure is now better understood.

The recently published Interdisciplinary Comprehensive Arm Rehabilitation Evaluation (ICARE) clinical study presented the dietary exposure of adults to CML, which took into account the concentrations of CML per ingested food and dietary intake of that particular food. In this study, the cereal group (56%) comprised of bread, biscuits, breakfast cereals, and in that order, contributed the highest amount to CML intake, followed by grilled meat and fish group (16%) and dairy products (14%) (Tessier and Birlouez-Aragon, 2012). Currently, there are several reviews that have summarized and evaluated the existing literature in this area and concluded that the ingestion of dAGEs can increase the *in vivo* pool of MRPs and their contribution to the development of many chronic diseases (Clarke et al., 2016; Gupta and Uribarri, 2016; Poulsen et al., 2013; Tessier and Birlouez-Aragon, 2012; Uribarri et al., 2010). Furthermore, several cross sectional and cohort type investigations were conducted and reported a high correlation between the consumption of dierary AGEs to chronic diseases such as pancreatic cancer (Jiao et al., 2015), or Alzeihmer's disease (Perrone and Grant, 2015). The mechanisms by which AGEs lead to the development of their effects can be either receptor independent, by causing structural damage to proteins, or through cell surface receptor dependent (RAGE) process (Poulsen et al., 2013; Thornalley, 1998).

2.5.2 The adverse nutritional consequences of the Maillard reaction

Unfortunately, the Maillard reaction is also correlated with adverse nutritional consequences. One adverse effect is glycation induced partial or total loss of enzyme activity, which can also influence

their consequential effect on allergenicity (section 2.4.3). However, the most common nutritional consequence associated with the Maillard reaction is the decrease in the availability, nutritional value, and loss of biological activity of proteins as they participate in the Maillard reaction by reacting with sugars directly or with the dicarbonyls generated in the reaction. Although amino acids such as tryptophan and arginine can also be affected, the "blocking" of lysine is considered to be the most concerning consequence of the Maillard reaction (Nursten, 2005; Mehta el al, 2016). Glycation also affects the digestibility of proteins and formation of cross-links which in turn affects their susceptibility to be broken down by digestive enzymes (Ajandouz et al., 2008). In a clinical trial to evaluate the dietary protein utilization in male adolescents, Seiquer et al. (2008) reported that the consumption of a high MRP diet resulted in 47% increase in fecal nitrogen excretion indicating a significant reduction in protein absorption.

Another group of nutrients that are affected during the Maillard reaction are minerals, as they are easily chelated by MRPs (Seiquer et al., 2008). Although all minerals can be potentially affected to a certain extent, but both *in vitro* and *in vivo* experiments have consistently shown that iron is the mineral that is influenced by far the most by MRPs, while other minerals such as copper and zinc have shown inconsistent results. The *in vivo* studies carried out to determine the effect of MRP on nutrient chelation is mostly conducted in rats, and have shown that compared to diets low in MRPs feeding on those that are rich in MRPs can enhance the absorption and retention of minerals such as copper and zinc (with inconsistencies) (Delgado-Andrade et al., 2002) but mostly iron (Delgado-Andrade et al., 2015; Roncero-Ramos et al., 2016) and their bioaccumulation in organs such as liver. However, experiments performed in humans did not show any variations in results between consuming diets high and low in MRP mostly due to the short duration of these experiments (Garcia et al., 2009; Mesías et al., 2009). *In vitro* studies similarly indicated that MRPs generated from heated sugar-amino acid model systems have enhanced iron chelating properties and can lower iron solubility in gastrointestinal digestion simulated experiments (Delgado-Andrade et al., 2004). A similar effect can also be seen on other elements such as magnesium. As for calcium bioavailability, although the findings are inconclusive, deoxy-pyridinoline, a bone resorption marker, was found to decrease with the intake of diets high in MRP, indicating a possibly less efficient bone turnover rate (Mesías et al., 2009). The coupling of MRP with metals was also found to be pH sensitive and dependent on the type of the metal. Iron was found to

complex with Arginine-xylose model at both pH 5 and 8 (Einarsson, 1987), while zinc complexed with high molecular weight products arising from corn products only at pH 5 (Johnson et al., 1983). In a later study, Migo et al. (1993) reported that complexes formed between Al, Ca and Fe and MRP were optimum at pH values between 2 to 4 and these complexes became destabilized and dissociated when pH levels were raised above 4 (Migo et al., 1993).

2.5.3. The toxicological aspects of the Maillard reaction

During the Maillard reaction, the formation of toxic products proceeds in parallel to the formation of color and aroma. These Maillard reaction toxicants include compounds such as acrylamide, heterocyclic amines, 4-methylimidazoles, HMF, furans and many others (Figure 2.8). Which toxicant is generated from the Maillard reaction during heating depends on factors such as cooking/heating temperature, time and also on the type of heat treated food (i.e. food components). The two major food groups that are considered as important sources for the formation of these MRPs are; first carbohydrate-rich foods that can generate compounds such as acrylamides and HMF, and second, meat and fish groups that are known to be the main source of heterocyclic amines (Meurillon and Engel, 2016). The presence of these Maillard reaction products in foods is considered to be extremely undesirable due to their mutagenic and/or genotoxic properties that, in addition to their possible carcinogenic effects, can alter cellular functions or even damage DNA (Hellwig and Henle, 2014). In fact, in October 2015 the International Agency for Research on Cancer (IARC) held an assembly to evaluate the carcinogenicity of red and processed meats and after considerations of the amount of toxicants that meats can have and/or generate upon thermal treatments, in addition to the data linking consumption of red or processed meat and colorectal or stomach cancers, two classifications were made. Consuming red meat was classified as probably carcinogenic to humans (group 2B) and processed meat as "carcinogenic to humans" (Group 1) (Bouvarda et al., 2015; Meurillon and Engel, 2016). Previously the **IARC had also classified acrylamide "***probably carcinogenic to humans*" **class 2A** (IARC, 1994). In 2002, after it was detected in relatively high amounts in various foods (Stadler et al., 2002), considerable efforts were made to lower the acrylamide content of processed foods via several mitigation strategies that used either physical processes (optimization of processing temperature and time) or biological (fermentation by yeasts) or chemical (use of enzymes or metal ions) to restrict its formation (Hellwig and Henle, 2014; Wen et al., 2016).

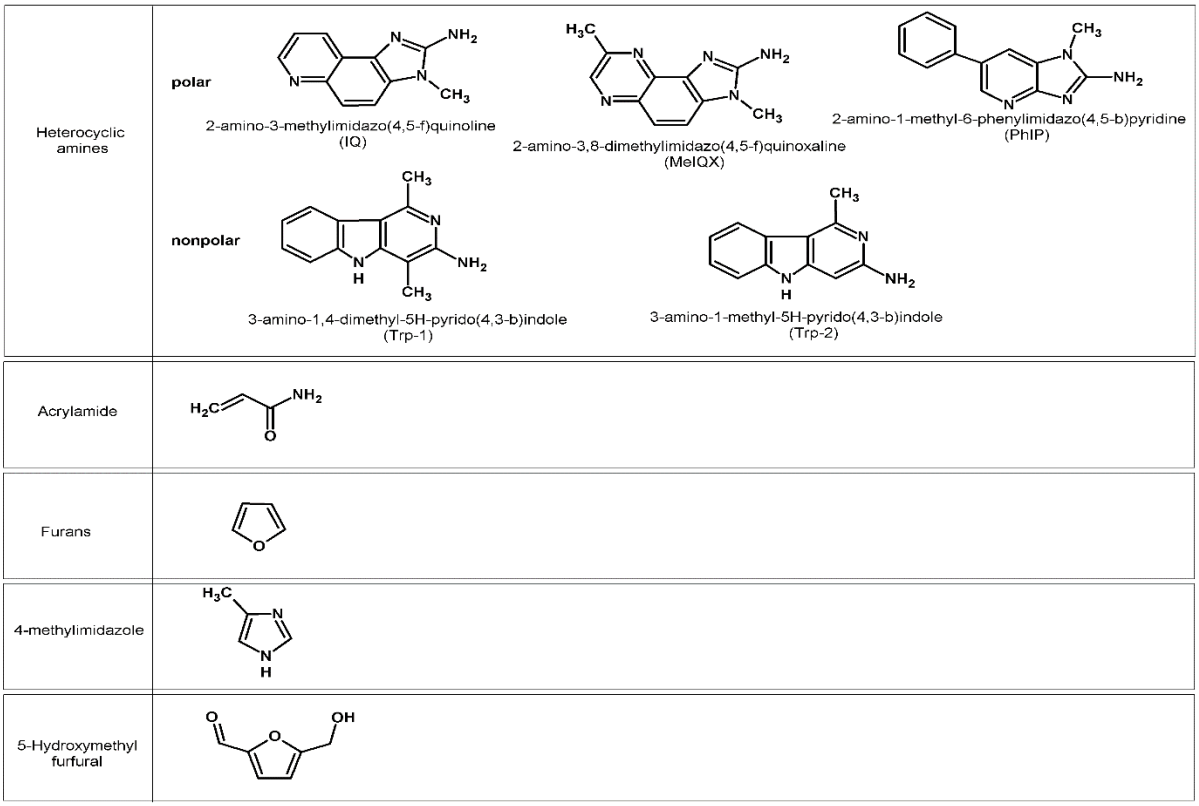

Figure 2.8. Chemical structure of harmful Maillard reaction products

2.6 IMPORTANCE OF CONTROLLING THE MAILLARD REACTION

Although the nature of the desired and undesired Maillard reaction products is relatively well recognised, controlling the various factors that generate these products and their formation pathways have been extremely challenging (Ames, 1990; Mottram, 2010; Jaeger, 2010). Various factors are extensively modulated and studied in order to find optimum conditions to either enhance or suppress the formation of different Maillard reaction products. Some of these factors are related to processing conditions such as pH, temperature and water activity, while others are related to the contribution of various food components and their concentrations to the development of different MRPs.

2.7 PHYSICAL FACTORS THAT REGULATE THE MAILLARD REACTION

2.7.1 Effect of pH

The initial rate of the Maillard reaction and the generation of the reactive intermediates are highly influenced by the pH of the system. In fact, pH is one of the earliest and most studied factor for its

role in controlling and channeling the Maillard reaction. Initially, pH affects the degradation of the Amadori/Heyns rearrangement compounds and their progression into the 1,2 or 2,3 enolization routes. Also, it has been shown that the rate of browning in general is optimum at pH ranges extending from 6 to 10. In aqueous systems, pH is usually controlled through the use of acidic or basic buffer solutions, the development of browning is usually low at acidic pH and tends to increase with increasing pH to a maximum value of pH 9-10 (Nursten, 2005). The browning of sugar-amino acid mixtures and their polymerization were found to be enhanced at pH values between 8 and 10 (Ajandouz & Puigserver, 1999; Ajandouz et al., 2001), while glucose degradation has been shown to increase up to 50% as the pH of the system increases from 4.6 to 8 (Martins & Van Boekel, 2005a). This is probably because the reactive forms of the sugar (enhanced mutarotation and open chain form) and the amino acid (un-protonated amino groups) are ideal under alkaline conditions (Newton et al., 2012). On the other hand, in non-aqueous reaction mediums, the acidity or the basicity of reaction mixtures can be controlled by substituting neutral sugars and amino acids with their charged counterparts. This can be particularly practical when studying non-aqueous model systems such as in pyrolytic experiments. In 2008, Kraehenbuehl et al., studied the effect of using acidic and basic sugars in altering the profiles of the Maillard reaction in monosaccharide-cysteine model system. Kraehenbuehl et al., reported the formation of more complex MR profile and more volatiles in the charged sugar models than with neutral monosaccharides.

2.7.2 Effect of Temperature

Temperature is probably the most influential factor in the browning reaction and, like the pH, it is considered to direct the course of the Maillard reaction (Martins & Van Boekel, 2005a). Louis Maillard himself studied how the rate of the reaction increased with increasing temperature and reaction duration. The optimum temperature for browning is considered to be between 125 and 160°C (Coghe et al., 2006). It is speculated that the depletion of reactants and the formation of end products in the system increases with increasing temperature. Kinetic studies rely on the use of Arrhenius equation to study the mechanism and the influence of temperature on the rate of the reaction (Martins & Van Boekel, 2005b; Morales & van Boekel, 1998). An increase of 10°C in temperature can double the rate of the reaction. However, temperature can be a “two edged knife”; on one hand it can speed up the browning process; on the other hand, it can lead to the formation

of potentially harmful products. Acrylamide, for example, is produced by the reaction between asparagine and a reactive carbonyl compound at temperatures above 120°C (Stadler et al., 2002).

2.7.3 Effect of Water Activity

The Maillard reaction, which proceeds through dehydration and loss of water, can progress in both aqueous and non-aqueous systems, but the rate of the reaction decreases at both low and high moisture levels because of either "increased diffusion resistance" or increased dilution of reactants (Ames, 1990; Baltes, 1982). A water activity (a_w) range of 0.4-0.8 has been reported to be optimum for the reaction (Shilton, 2003). Many studies have tried to stabilize or control the Maillard reaction by manipulating the water activity of the system. In a recent study, Bassama et al. (2011) demonstrated that acrylamide formation/elimination reactions were enhanced by decreasing water activity from 0.972 to 0.43 (Bassama et al., 2011). A way to influence a_w is to add humectants either as solid (for example sorbitol) or liquid (for example glycerol and alcohols), which are known to exert significantly higher amount of browning compared to the solid forms for the same amount of reactants (Mustapha et al., 1998).

2.8 The Role of Different Food Components in Controlling the Maillard Reaction

The initiation and progression of the Maillard reaction is highly dependent on the type, chemical form and the relative concentration of the primary reactants. Similar to the physical factors, Maillard reactants are continuously studied for their role to influence the reaction. Among these components reducing sugars and amino acids are relatively well explored. Recently, efforts have been directed towards understanding the role of other food components on the Maillard reaction. In the past few years, lipids have been extensively studied not only for their ability to contribute to flavor and aroma formation, but also for their ability to degrade in the presence of amino acids into toxic by-products such as biogenic amines during heating (Zamora & Hidalgo, 2011). Carboxylic acids and polyphenols have also been reported to play an important role in inhibiting glycation (Gao et al., 2010; Kokkinidou and Peterson, 2013). Also, metal ions have been studied for their potential role in controlling the Maillard reaction by various ways; accelerating reaction rates and color formation; complexing with generated Maillard reaction products (section 2.5.2) and even in mitigation strategies to lower the formation of specific undesired MRPs. However, the fundamental mechanisms of interaction of metal ions with sugars and amino acids at the molecular

level have not been explored, and how metal ions can influence the reaction or the generation of specific products is not well understood or elucidated. Given the ubiquitous nature of metal ions in various foods and their natural tendency to complex with organic molecules and by doing so altering their chemistry, understanding how they can influence the Maillard reaction can provide important insights into their role in regulating different Maillard reaction pathways and products.

2.8.1 Metal ions and their coordination with food components

Metals are either naturally found in food or added for various reasons and their intake is nutritionally important to provide normal growth and maintenance of the body and the regulation of different physiological processes and biochemical reactions (Nabrzyski, 2007; Prashanth et al., 2015) (Figure 2.9). However, the daily intake of metals depends on many factors such as the quantity of food consumed containing metals, the chemical form and their interaction with other food components (Nabrzyski, 2007). Divalent and trivalent metal ions such as iron (Fe), Copper (Cu), and Zinc (Zn) are specifically interesting due to their ability to form complexes with other organic ligands (such as proteins, porphyrins, flavines, and others) both *in vitro* and *in vivo*. What is relevant to food processing is their ability to form complexes with sugars, amino acids and other food components such as nucleobases all known for their ability to participate in the Maillard reaction by affecting aroma and color of heated foods (Cambero et al., 2000; Chen, Chin & Ho, 2004).

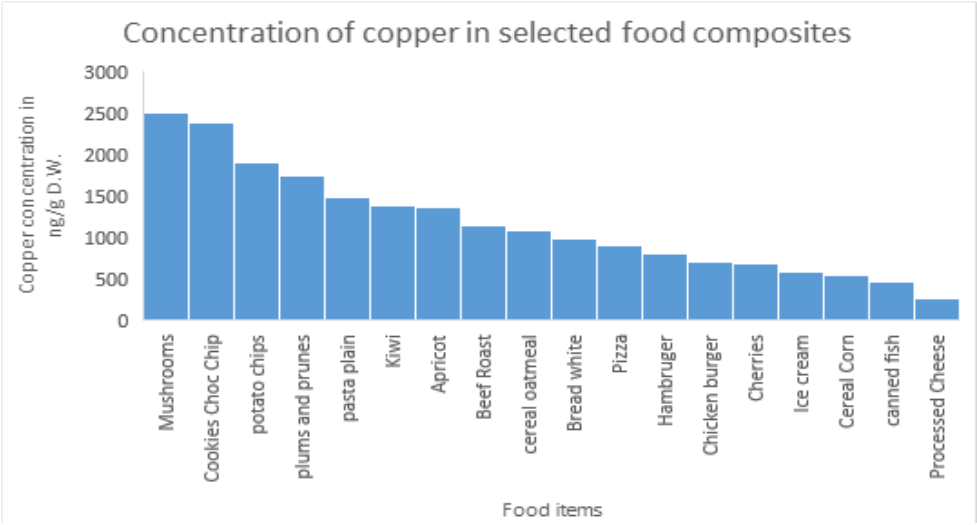

Figure 2.9. Average concentration of copper in selected food composites adopted from the Canadian Total Diet Study (2003-2007). The highest concentration was that of organ meats (not shown in the figure) with an average of 103 mg of copper/kg of food composite (reproduced from http://www.hc-sc.gc.ca).

2.8.1.1 Metal complexation with amino compounds: amino acids and nucleosides

An amino moiety in the Maillard reaction context most commonly refers to amino acids, although it can also include peptides and proteins (polymers of amino acids), and other primary or secondary amine containing molecules such as nucleosides and nucleobases. In addition to their reactivity towards carbonyl electrophiles, amino group containing molecules can also complex with metal ions to form coordinated ligands. For amino acids, metal coordination commonly occurs via N or O-chelation through their amine and carboxylate electron donor groups (Figure 2.10). The formed metal complexes are typically comprised of a central metal ion that is bonded via coordinate covalent bonds to the donor atoms, but the structure of the metal complexes can vary depending on the amino acid and the metal ion type. Simple amino acids such as glycine can easily form stable five membered chelate rings with various metals; while larger amino acids that possess additional metal binding sites in their structures, or those that contain aromatic or imidazole rings such as histidine can form complexes of diverse structures (Beck, 2009, 2011; Shimazaki et al., 2009) (Figure 2.10). On the other hand, nucleoside- and nucleobase-metal coordination chemistry is more complicated and much different from that of amino acids. Nucleobases do not have carboxylate groups, thus the complexation with the metal ion occurs via the nitrogen atoms on the purine or pyrimidine ring. In nucleobase-metal coordination literature a variety of complexation modes have been proposed, and due to the inconsistencies among different studies, various ligands have been reported throughout the past decades. For example, adenine is reported to coordinate with copper at N^9 or N^6 or N^7 nitrogen to form monodentate ligand or to N^3/N^9 or N^7/N^9 groups in bi- or poly-dentate ligands (Bugella-Altamirano et al., 2002; Ilavarasi et al., 1997; Mishra et al., 2008). Moreover, in nucleosides, metals can also coordinate with the sugar moiety. For example, copper can complex with guanosine-2'-monophosphate, via an axial Cu-O^5 bond with the ribose (Sigel, 1993). The complexation of amino acids and nucleobases with metals also depend on metal type. For example, amino acids form very weak complexes with alkali metal ions and with Mg and Ca, but much stronger complexes with transition metal ions such as copper and zinc (Shimazaki et al., 2009). Similarly, nucleobases complex with transition metals such as Ni and Cu through their N^7 atom, while Mn preferably binds to N^1 and Zinc to N^1 and N^7 atoms (Sigel, 1993).

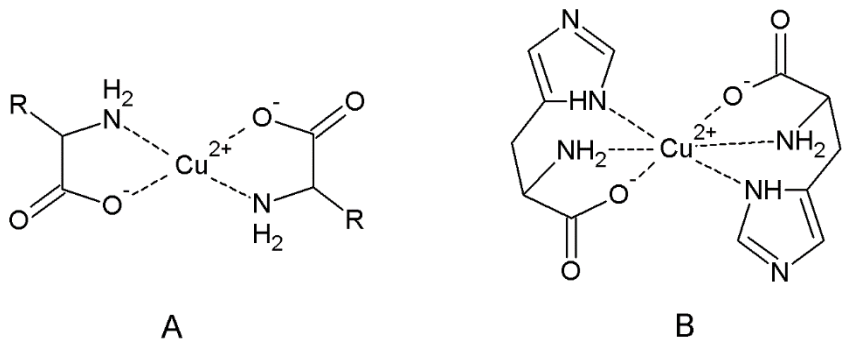

Figure 2.10. Binary complexes of metals such as copper with (A) simple amino acids and (B) histidine.

In addition to structural changes, the coordination of amino acids with metals can change the chemical reactivity of the ligand; consequently, affecting its interactions with other molecules through hydrogen bonding, π–π stacking, and hydrophobic interactions (Beck, 2009, Girnth-Weller and Beck, 1982). For example, the complexation of amino acids with metals is known to enhance the acidity of the α-CHR group of metal coordinated amino acids allowing it to undergo aldol reaction with small aldehydes in the Akabori transformation (Figure 2.11). Williams and Busch (1965) demonstrated through NMR studies,that the enhanced acidity and lability of α-methylene hydrogens in such complexes are due to the electron-withdrawing action of the metal ions. Under alkaline conditions, the developing carbanion can serve as a nucleophile that can condense with a carbonyl moiety such as formaldehyde or acetaldehyde. However, it is also proposed that the amino acid-metal complexes first enhance the nucleophilicity of the nitrogen groups towards the aldehydes to first form Schiff bases which is then followed by the subsequent activation of the α-carbon to generate the carbanion (Belikov et al., 1969). Taking advantage of such altered reactivities, Akabori et al. (1959) was the first to report the chemical synthesis of serine or threonine from glycine in the presence of two common Strecker aldehydes, formaldehyde and acetaldehyde, respectively. This transformation of one amino acid into another was catalyzed by metal salts such as copper and iron. The generality of this reaction was later extended to different amino acids (serine, glycine, and alanine) and different metal complexes (Ni, Co, and Cu) and using various aldehydes (acetaldehyde, formaldehyde, pyruvic acid, and benzaldehyde) (Ichikawa et al., 1970; Girnth-Weller and Beck, 1982).

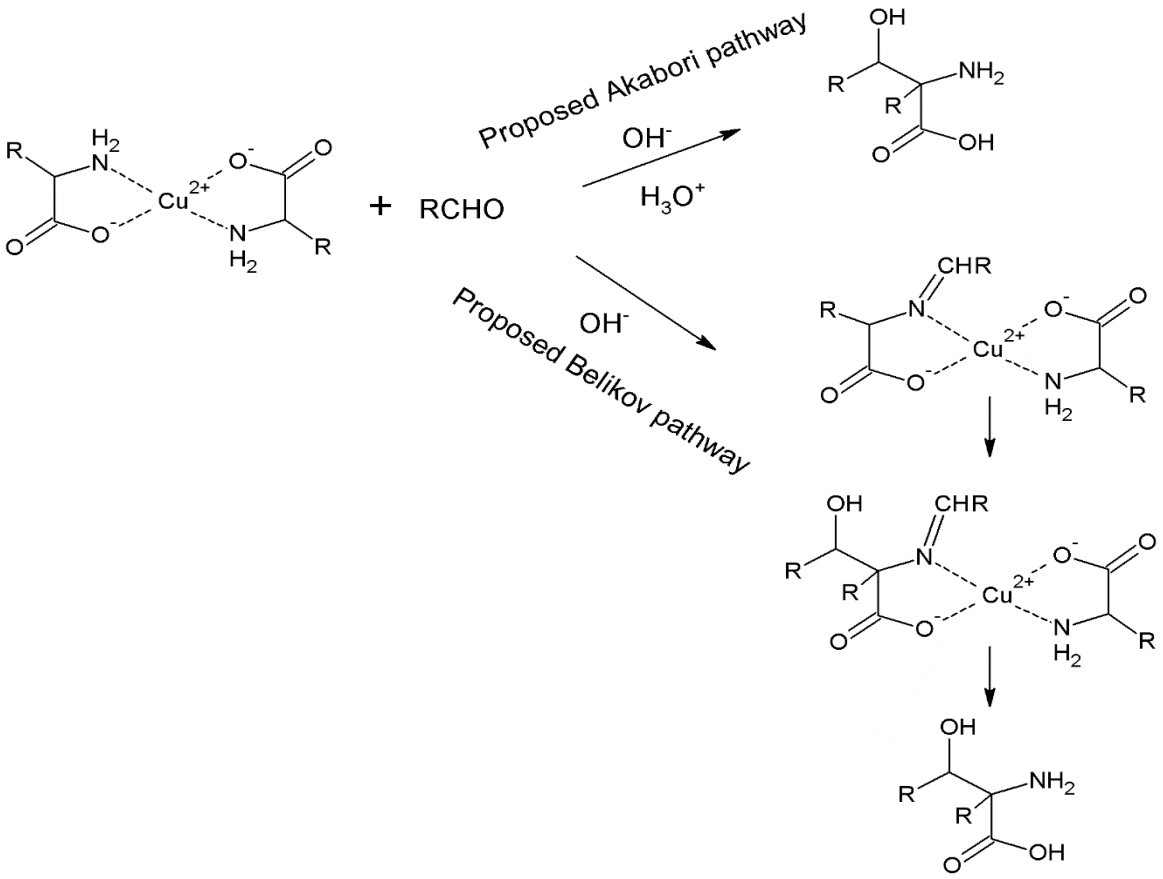

Figure 2.11. The two proposed pathways [original Akabori pathway (Akabori et al., 1959) vs Belikov (Belikov et al., 1969) pathway] for the conversion of α-amino acids into β-OH derivatives via the Akabori reaction.

Another outcome of the enhanced reactivity of amino acid metal complexes is their ability to undergo thermal decomposition and decarboxylation through an intramolecular redox reaction to generate Strecker aldehydes. Yablokov et al. (2014) reported the kinetics of thermal degradation of copper complexes of several amino acids at 230°C. Yablokov indicated that oxidative degradation mechanism of the complex is initiated with the formation of carboxylamine free radical, followed by the loss of carbon dioxide and the generation of alkylamine radicals and its recombination products.

2.8.1.2 Complexation with sugars and amino-sugar derivatives

Reducing sugars are the second crucial components required for the Maillard reaction. Similar to amino acids they can also form complexes with metal ions. However, due to the presence of

polyhydroxy groups in sugars, the formed complexes can have multiple structures depending on the synthesis conditions such as solution pH, solvent and metal types, and the steric arrangement of the OH functional groups (Hricovíniová, 2015). Sugar-metal complexes are easily formed under strongly alkaline solutions. Under neutral or acidic aqueous conditions, such as in foods, alcohol or diol functional groups of sugars are not properly solvated resulting in unstable complexes (Gyurcsik and Nagy, 2000). Many sugar-metal complexes have been synthesized in the literature for various uses in biology and bioorganic chemistry. With transition metals such as copper, iron and cobalt, sugars form mostly either monovalent or divalent complexes (Gyurcsik and Nagy, 2000). Bandwar et al., (1997) synthesized the various salts of several *aldo* and *keto* sugar complexes with metals such as manganese, nickel and cobalt. The complexes were reported to be di-nuclear when synthesized from ethanolic solutions and di- or tetra-nuclear in aqueous solutions. They also reported that the stability of the sugar-metal complexes in aqueous solutions to be sugar dependent with ribose being the most stable followed by maltose, glucose, xylose and fructose (Bandwar et al., 1997). Geetha et al (1996) also synthesized the iron complexes of various sugars from a methanol solution of stoichiometric mixtures of sugar and metal. The generated ligands were either mononuclear or dinuclear species coordinated through hydroxo-bridges. Alternatively, Cerchiaro et al., (2005) reported a higher stability of fructose-copper complex compared to glucose-copper complex due to the furanose isomeric form that the former assumes when complexed with copper. Also, they reported that the complexation of copper with fructose occurs at 1-CH_2OH and the anomeric OH, while the complexation with glucose occurs through the anomeric OH and O-5 atom (Figure 2.12).

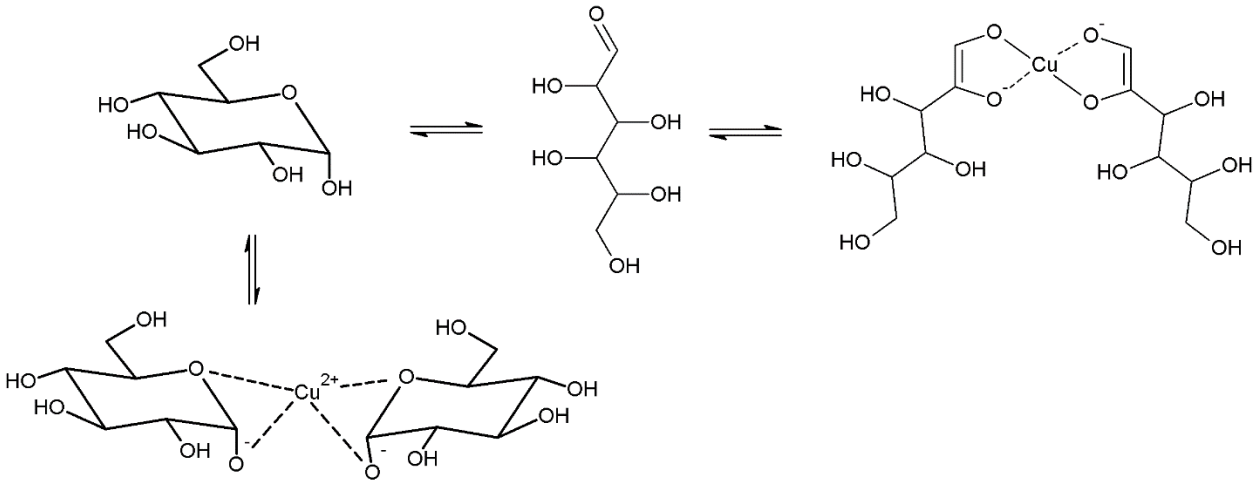

Figure 2.12. The complexation of glucose with copper adapted from Cerchiaro et al. (2005)

On the other hand, various research groups were interested in preparing complexes of Amadori products. Tonkovic et al. (1997) and Gyurcsik et al. (1993) synthesized various complexes Amadori compounds with iron, copper, and nickel and characterized them using various analytical techniques such as X-ray spectroscopy, nuclear magnetic resonance (NMR), and circular dichroism (CD) spectroscopy. In 2002, Horikawa et al., (2002) synthesized and studied the thermal degradation of copper complexes of Amadori compounds. They reported that such complexes undergo oxidative degradation and generate hydroxyl radicals and various dicarbonyl products faster than their free counterpart. Similarly, Cheng and Kawakishi (1994) reported several copper-catalyzed oxidative decomposition products of Amadori compounds of tripeptides. In addition to ARP, copper complexation to glucosamine has also been investigated using potentiometry and ESR spectroscopy (Whitfield et al., 1993). Micera et al (1985) proposed that the glucosamine copper complexes have a dimeric structure with a central copper ion (Figure 2.13).

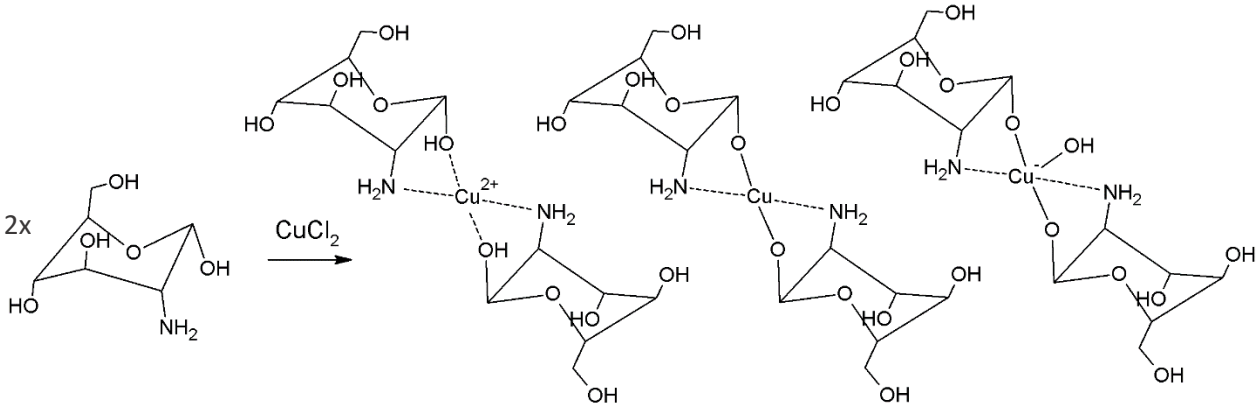

Figure 2.13. proposed structures of glucosamine copper complexes (adapted from Micera et al., 1985).

2.8.2 The role of metal ions in enhancing desirable Maillard reaction properties.

The current knowledge regarding the effect of metal ions on the Maillard reaction is mainly based on studies that explore the catalytic role of metal salts in promoting reaction rates and oxidation pathways (Cheng et al., 2012; Kwak and Lim, 2004; O'Brien & Morrissey, 1997; Rendleman and Inglett, 1990; Rizzi, 2008; Ramonaityte et al. 2009; Yamaguchi et al., 2009). Rendleman et al. (1990) reported that the addition of cupric (Cu^{+2}) ions in a glucose-glycine reaction mixture, causes the rate of the reaction to be enhanced and color development to be accelerated (Rendleman and Inglett, 1990). In a recent study, Cheng et al. (2012) also reported an enhancing effect of metal

ions such as copper and zinc on the Maillard reaction in an ascorbic acid/glycine model system. The presence of metals in the reaction mixture affected both the intensity of browning of the intermediate products and increased the rate of the reaction in a concentration dependent manner (Cheng et al., 2012). Ramonaityte et al. (2009) similarly reported a clear catalytic role of the trace elements Cu, Zn, and Fe as accelerators of browning (Ramonaitytė et al., 2009). Additionally, metal ions have also be been documented for their role in enhancing oxidation products such as dicarbonyls. Fallico and Ames (1999) observed that $FeCl_3$ can promote the formation of 3-deoxyglucosone in an aqueous glucose/phenylalanine model system but only when heated at pH 5 (Fallico and Ames, 1999). While Horikawa et al. (2002), also reported the formation of hydroxyl radicals and various dicarbonyl products in solutions containing copper complexed Amadori rearrangement products, such as the *n*-butylamine/glucose Amadori copper complex. Similarly, Cheng and Kawakishi (1994) reported several copper-catalyzed oxidative decomposition products of Amadori compounds of tripeptides. Recently Weiser et al. (2012) reported that simple sugar derivatives, particularly, α-hydroxy ketones can also influence the reduction of copper. They studied the effect of the α-hydroxy ketones in bicinchoninic acid assays (BCA) that depends on the reduction of cupric (Cu^{+2}) to cuprous (Cu^{+}) under alkaline conditions, and reported the ability of this class of derivatives to form an enediol intermediates and lead to positive BCA analysis. This ability α-hydroxy ketones to behave like a reducing sugar can actually be extended to the role of the sugars in reducing copper from cupric to cuprous forms (Weiser et al., 2012).

2.8.3 The influence of metal ions on the mechanism of the Maillard reaction.

Although the exact mechanism of how metal ions can affect the Maillard reaction is still not clear, it has been proposed that metals increase the rate of the reaction because of their ability to oxidize Amadori compounds, accelerating the formation of melanoidins (Ramonaitytė et al., 2009). It has been proposed that iron, for example, can combine with carbonyl and hydroxyl groups of the Maillard intermediates such as 2-hydroxy-3,5-dihydroxy-1-4-pyridone acetic acid to form complexes. High-molecular-weight reductones have also been reported to form complexes with metal ions through polynuclear ligands. Their ability to complex with amino acids and sugars, change the structural configurations of proteins and catalyze redox reactions has also been reported (O'Brien & Morrissey, 1997; Ramonaitytė et al., 2009). The type of the metal ion, heating time and the type of amino acid involved are the major factors that affect the browning reaction (Kwak

& Lim, 2004). A similar assumption was proposed by O'Brien & Morrissey (1997) who classified the metal ions according to their strength of binding to Maillard reaction products with Mg^{+2} having the strongest capacity, followed by Cu^{+2}, Ca^{+2} and Zn^{+2}. Moreover, cupric ions can stimulate the oxidation of glycosylated proteins formed at the beginning of the reaction and regenerate free primary amino groups (O'Brien & Morrissey, 1997). Rizzi (2008) similarly observed that heating aqueous solutions of amino acids/pentose sugars at 100^{o}C in the presence of Ca^{+2} and Mg^{+2} ions (divalent cations) resulted in enhanced browning development, compared to Li^{+}, Na^{+}, K^{+}, Rb^{+} and Cs^{+} (monovalent cations). Also, many trace elements can serve as Lewis acids catalysts in the Maillard reaction by forming coordination or metal complexes with sugars or amino acids in dry or, as reported by Kobayashi et al. (2002), in aqueous media. By forming Lewis adducts, metals can be involved in acid-catalyzed reactions such as aldol reactions, which are very important in the formation of Maillard reaction products.

2.8.4 Metal ions used in mitigation strategies to reduce undesired Maillard reaction products: the example of acrylamide

As mentioned previously (see section 2.5.3), the generation of acrylamide and HMF during the Maillard reaction is considered to be highly undesirable. Metal ions have been considered as an important means to control and restrict their formation during thermal treatments. On one hand, metal ions have been found to contribute to the formation of acrylamides via imination pathway of the glycosylamine of asparagine (Granvogl & Schieberle, 2006), while on the other hand, a vast number of publications discuss the use of cations or the salts of various metals in lowering or preventing the formation of acrylamide both in model systems involving asparagine and sugars, and in food models. Studies show that adding monovalent and divalent cations such as Na^{+}, Ca^{+2} or Mg^{+2} to bakery doughs prior to baking, or dipping potatoes in $CaCl_2$ or NaCl prior to frying can cause a significant drop in the formation of acrylamides (Elder et al., 2004; Gokmen et al., 2007a; Sadd et al., 2008). Fortunately, these cations are widely used in bakery products as ways of preservation and fortification. For example, calcium fortification in doughs is achieved by the addition of $CaCl_2$ or calcium propionate. Furthermore, the addition of these metals as suppression strategies to acrylamide formation does not seem to affect the sensory properties or the appearance of the foods in terms of color and aroma development after cooking. Sadd et al. (2008) reported that the 0.3% obligatory calcium fortification of dough in the U.K. significantly lowered

acrylamide formation while additional calcium fortification caused an even further drop in acrylamides (Sadd et al., 2008). Furthermore, the effect of metal ions on acrylamide are observed to be dependent on cation type. In investigating the effects of several monovalent, divalent, and trivalent cations of Na^{+}, K^{+}, Ca^{+2}, Mg^{+2}, Zn^{+2}, and Fe^{+3}, in a glucose–asparagine model system, Gokmen & Senyuva (2007b) observed that the addition of all these cations in equimolar amounts to the Maillard reactants led to a significant reduction (97% or more) in the amounts of generated acrylamide, but also enhanced the formation of hydroxymethyl furfural and furfural generation. Similar results were obtained in a separate fructose-asparagine model by Gokmen & Senyuva (2007a). A significant drop in the acrylamide formation was also observed in a potato model treated with Fe^{+3} and Ca^{+2} (Gokmen & Senyuva, 2007a). The addition of Ca and Mg salts ($CaCl_2$ and $MgCl_2$) to potato powder models significantly lowered the acrylamide produced during cooking (Mestdagh et al., 2008). In 2009, Levine et al. reported an acrylamide reduction of 35% and 60% upon the addition 1% and 2% $CaCl_2$ to bread and cracker dough, respectively (Levine & Ryan, 2009). The ratio of cation to asparagine is an important variable on the acrylamides reducing capacity of the metal ions. Elder et al. (2004) proposed that the optimum ratio of cation to asparagine is 1:3 or 1:2 or 1:1, and that for some metals such as magnesium, a higher ratio of 2:1 is required for effectiveness (Elder et al., 2004). The type of metal salt is also considered important in influencing acrylamide formation. For example, calcium chloride is considered to be much more efficient to reduce acrylamide compared to $CaCO_3$, although the latter is the most commonly used source of calcium for the fortification of various foods (Keramat et al., 2011).

One of the several proposed mechanisms for the effect of metal ions on lowering acrylamide formation is their direct influence on the acrylamide generating reactants. In the presence of metal ions, hexoses such as glucose, undergo a triple dehydration pathway and form hydroxymethylfurfural as a key end products, lowering the amount of the Schiff base formed that leads to acrylamide formation (Figure 2.14). Cations also affect the rate of thermal degradation of these reactants. In a reaction mixture containing asparagine, sugar(glucose), and cations, the thermal decomposition of glucose is faster compared to asparagine, the rate of degradation of which is only inversely proportional to the increasing concentration of cations in the mixture (Gokmen & Senyuva**,** 2007b; Wen et al., 2016). Moreover, metal ions have been reported to reduce the pH of the system in which they are added (Tareke et al., 2002; Vadlamani & Seib,

1999). The pH lowering capacity of the metal ions is due to their ability to compete with and displace protons in molecules with functional groups that contain oxygen, nitrogen, or sulfur atoms (such as carboxylic or amino groups). This is usually permitted at pH levels that can allow such a competitive transformation between cations and protons to take place. Also, the addition of divalent metals causes inhibition of the carbonyl groups to form acrylamide from Asparagine by forming stable polymers with the Asparagine (Sadd et al., 2008). It has been postulated that cations also complex with acrylamide.

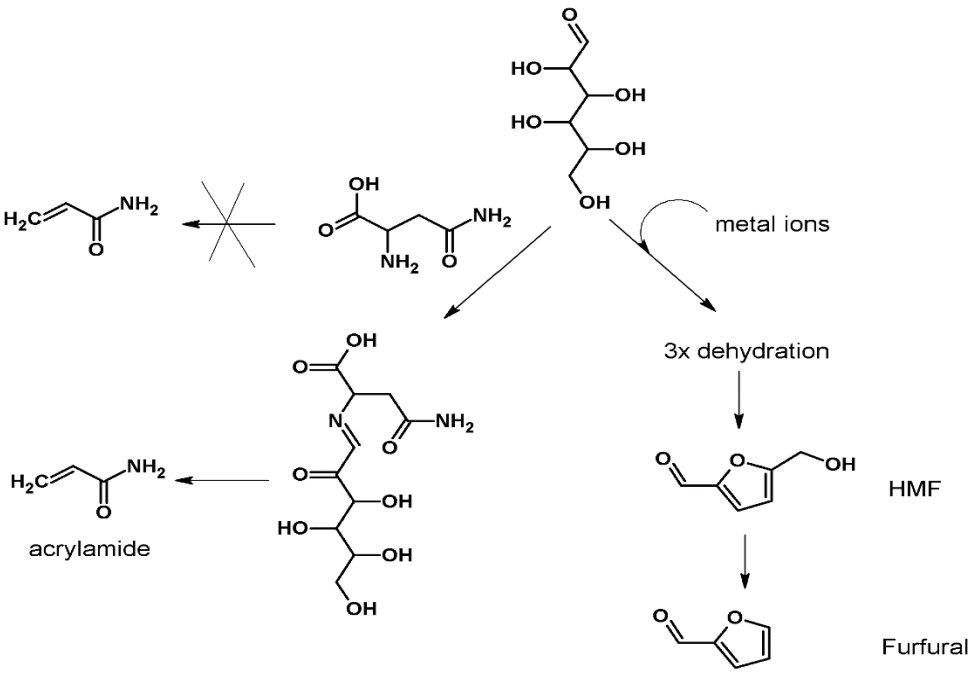

Figure 2.14. The formation of acrylamide and HMF in the presence and absence of metal ions.

2.9 A Synopsis of the Current Approaches and their Limitations in Understanding and Controlling the Maillard Reaction

Although it has been over one hundred years since its discovery, the Maillard reaction is still considered a hot topic in the field of Food Science. Lack of understanding on how the complex food matrices influence the reaction rates and profile of the products are considered important factors that drive the current research.

2.9.1 Advances made in studying the Maillard Reaction:

The influence and control of the Maillard reaction pathways in real foods can be extremely challenging. Food matrices are not only exceedingly dynamic and complex mixtures of monomeric

and polymeric compounds with diverse physical and chemical properties, but also the analysis of the multitude of Maillard reaction products generated in food mixtures can be very difficult to achieve. The main advances made over the past years in studying the Maillard reaction are highlighted below.

2.9.1.1 The dry and aqueous model system approach

To minimize the complexity of food systems and to establish the fundamental chemistry of the Maillard reaction, researchers have resorted to studying this reaction in simplified model systems typically comprised of a limited number of reactants under controlled conditions. The advantage of using model systems is that they provide practical and mechanistic information about the specific sugar and amino acid interaction (Mottram and Taylor, 2010). They also allow researchers to investigate the fundamental processes, the kinetics and rate of formation of various Maillard reaction products. Model systems can be either dry or aqueous and can contain multiple reactants in mediums where influencing factors such as water activity, temperature, and pH can be strictly controlled and manipulated. There is a wide range of model systems reported in the literature designed for investigation of various aspects of the reaction, such as color and aroma generation (Fogliano *et al.*, 1999; Hwang et al. 2011; Monti *et al.*,1998). More importantly, model systems are utilized to predict specific precursors and for elucidation of mechanistic pathways of specific reaction products through isotope labelling technique (Limacher *et al.*, 2008; Perez Locas & Yaylayan, 2004). However, the greatest disadvantage of model systems is that they do not represent real food matrices. Even the most complex and multicomponent model systems cannot remotely reflect processes occurring within food matrices; where the mobility, availability, the complexity of components (with various states of polymerization), in addition to the interaction of generated reaction products with a vast array of other food components can be overwhelming.

2.9.1.2 Emulsions as complex model system.

To simulate actual food systems, additional layers of complexity such as emulsions can be added to model systems in a controlled manner. Hence, various simple emulsion or microemulsion model systems can be designed to explore the Maillard reaction. One emulsion based technique is encapsulation. The idea of using encapsulation in the context of the Maillard reaction was introduced recently as a means to control the formation of undesirable Maillard reaction products

such as acrylamides and HMF (Fiore et al., 2012; Troise & Fogliano 2013). Encapsulation is a powerful technique that involves encasing the encapsulated material in a microenvironment to deliver and release its contents at a controlled rate. Also, the careful selection of the appropriate coating material can help the encapsulated compound to easily flow through various mediums or phases (hydrophobic or hydrophilic) and survive various environmental conditions such as pH and temperature. This approach was recently used by Fiore et al. (2012), to microencapsulate NaCl during the baking of cookies. Fiore et al., (2012) reported a reduction of HMF formation of around 10% at the highest NaCl concentration (Fiore et al., 2012) without affecting the sensory properties of the prepared cookies. Also, Troise et al., (2016) recently reported that milk heated with encapsulated ascorbic acid resulted in an up to 50% reduction in several MRPs including Amadori products, Carboxymethyllysine (CML) and Carboxyethyllysine (CEL), compared to non encapsulated mixtures. However, the disadvantages of this technique should also be considered. Encapsulation might not be applicable for all types of molecules and the synthesized microcapsules might not be resistant to relatively harsh processing conditions such as very high temperatures and pressure. Also, the process might be considered too costly especially when the outcome only reflects modest change in results.

On the other hand, even more complex model systems have been designed by spiking actual food samples, green coffee beans, with labeled and unlabeled Maillard reaction precursors in "biomimetic in-bean system" experiments. (Poisson et al., 2009). Such a technique uses coffee beans as microreactors that can provide realistic information about the actual processes happening in green coffee beans during roasting compared to simple model systems. The extension of this technique to other foods such as different types of cereals or legumes (lentils, beans, peas) which vary in nutrient composision can help provide a better information about the Maillard reaction occuring in each of these matrices during cooking.

2.9.1.3 Using advanced analytical techniques to study the Maillard reaction: The Proteomic approach

Proteomics is a highly complex omic approach that aims to study the complete protein composition of physiological samples in order to gain a thorough understanding of the metabolic processes that occur within biological systems (Pischetsrieder and Baeuerlein, 2009). In this approach, various analytical techniques such as two-dimensional gel electrophoresis (2-DE), nuclear magnetic

resonance spectroscopy, isotope labeling technique and mass spectrometry are used not only to detect and identify proteins, but also to understand the changes that proteins might undergo (such as post transitional modifications) in a food product. Recently the notion of using the proteomic approach to understand the changes that occur to proteins during thermal processing has become more recognized among Maillard reaction researchers (Ames, 2005; Pischetsrieder & Baeuerlein, 2009). Several protein bound MRPs in heated foods such as milk have been identified using proteomic tools. The main advantage of using this approach is that it can provide information on a wide spectrum of products in a sensitive and timely manner, without requiring tedious experimental preparations. Additionally, this approach might only provide information on specific analytes such as those that are water soluble, non-volatile and easily ionisable. However, the amount of data generated through non-targeted analyses can be immense and the extraction of useful information can be considered too time consuming.

2.9.2 The future of Maillard reaction research

Despite the many advances made in the understanding of the Maillard reaction, there is still a wide gap in our knowledge-base that must be filled in order to truly control and manipulate this reaction in real foods. Bridging this gap is a challenging task and relies on using comprehensive and complete approaches coupled with advanced analytical techniques to truly understand the effect of food matricies on the Maillard reaction and the consequences of ingesting MRPs on health and well-being. To achieve such a comprehensive overview, it is not enough only to consider the changes that individual components (such as proteins) undergo during food processing, but to have a broad understanding of all the constituents that come together to determine the organoleptic, physiological, and toxicological aspects of the Maillard reaction. Such a concept can be considered as part of a relatively new omics approach called foodomics (Herrero, 2012; Ibanez et al, 2012), which takes into consideration the combination of proteomics, genomics, lipidomics, glycomics, transcriptomics and metabolomics approaches to explore the various aspects of changes in food during processing with the ultimate aim of improving human nutrition. Adoption of the foodomics approach to study the effect of thermal processing on the Maillard reaction cannot be viewed as just utilizing a new analytical method to acquire new chemical information but it extends beyond that in understanding the implications of the consumption of MRPs, their metabolism, and overall effect on human health.

CONNECTING PARAGRAPH

Chapter 2 provided an overview of the important aspects of the Maillard reaction related to the quality of foods and presented a thorough review of the recent literature pertaining to the role of metal ions in the Maillard reaction, in addition to the current knowledge gaps and limitations in this area. It also provided the rationale for investigating the fundamental chemistry of their interaction with different Maillard reaction precursors and intermediates. Chapter 3 presents a systematic investigation of the chemistry of amino acid-metal interactions under the Maillard reaction conditions using different amino acids and metal salts and synthetic copper complexes of alanine and glycine in the absence of carbonyl electrophiles. Chapter 3 was published in the *Journal of Agriculture and Food Chem*istry: Nashalian, O.; Yaylayan, V. A. (2014). Thermally induced oxidative decarboxylation of copper complexes of amino acids and formation of Strecker aldehyde, 62, 8518–8523.

CHAPTER 3

THERMALLY INDUCED OXIDATIVE DECARBOXYLATION OF COPPER COMPLEXES OF AMINO ACIDS AND FORMATION OF STRECKER ALDEHYDE

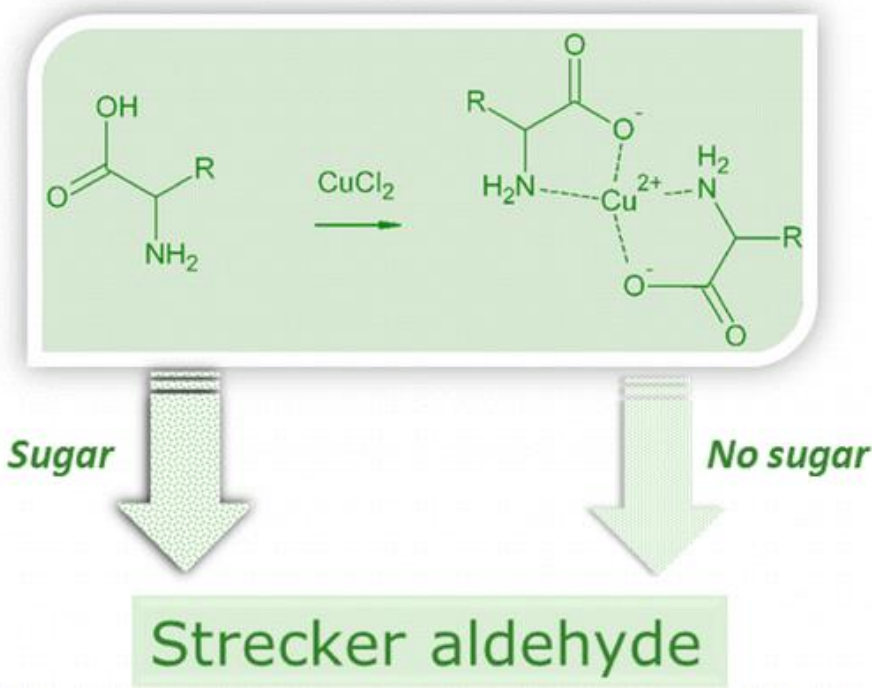

3.1 ABSTRACT

In the Maillard reaction, independent degradations of amino acids play an important role in the generation of amino acid specific products such as Strecker aldehydes or their Schiff bases. Such oxidative decarboxylation reactions are expected to be enhanced in the presence of metals. Preliminary studies performed through heating of alanine and various metal salts (Cu, Fe, Zn, Ca) under pyrolytic conditions indicated that copper (II) and iron (III) due to their high oxidation potentials were the only metals able to induce oxidative decarboxylation of amino acids and formation of Strecker aldehyde or its derivatives as detected by GC/MS. Furthermore, studies performed with synthetic alanine and glycine copper complexes indicated that they constituted the critical intermediates undergoing free radical oxidative degradation followed by the loss of carbon dioxide and the generation of Strecker aldehydes which were detected either as stable Schiff base adducts or incorporated in moieties such as pyrazine or pyridine derivatives.

3.2 INTRODUCTION

Metal salts, such as copper sulfate, are commonly found or added to foods for a variety of reasons. The corresponding metal complexes formed during processing with amino acids and sugars (Figure 3.1) or other Maillard reaction productsmay alter their chemical reactivity during thermal treatment (O'Brien and Morrissey, 1997), generating or enhancing specific reaction products, such as those of oxidation or decomposition. Understanding how these independent complexes thermally degrade provides important insight into their fundamental behavior in the context of the Maillard reaction. Over the past few decades, the role of metal salts and their potential to affect the Maillard reaction has been studied by several researchers (Kwak and Lim, 2004, O'Brien and Morrissey, 1997; Ramonaitytė et al., 2009; Rendleman,1990). Considerable efforts have been expended to study the catalytic role of metal salts in promoting oxidation pathways and affecting the rates of the reaction in aqueous systems. Moreover, recently, it has been demonstrated that metal ions can accelerate the formation of specific Maillard reaction products, such as advanced glycosylation end product (AGE)-modified peptides (Frolov et al., 2014). On the other hand, the use of cations and their salts were explored in mitigation strategies in lowering or preventing the formation of certain Maillard reaction products, such as acrylamide, in both model systems involving asparagine and sugars and food models (Gokmen and Senyuva,2007a; Sadd et al., 2008). Although the exact mechanism of how metal ions can affect the Maillard reaction is still not clear,

it has been proposed that metals increase the rate of the reaction because of their ability to oxidize Amadori compounds, accelerating the formation of melanoidins (Ramonaitytė et al., 2009). High-molecular-weight reductones have also been reported to form complexes with metal ions through polynuclear ligands (O'Brien and Morrissey, 1997; Ramonaitytė et al., 2009). Their ability to complex with amino acids, change the structural configurations of proteins, catalyze redox reactions, and act as Lewis acid catalysts by forming metal coordination complexes with sugars has also been reported (Choudhary et al., 2013). Amino acids could be considered as prime targets for metal complex formation, and although the role of such complexes in the Maillard reaction has not been studied, enhancements in the Strecker aldehyde formation were reported in the presence of copper ions by Hofmann and Schieberle (2000). Furthermore, copper was found to catalyze the oxidative decarboxylation of a synthetic amino dioic acid in aqueous solution, converting it into an amino monocarboxylic acid (Fitzpatrick and Hopgood,1974). Recently, Yablokov et al. reported the kinetics of thermal degradation of copper complexes of several amino acids at 230°C (Yablokov et al., 2014), indicating an oxidative degradation mechanism of the complex initiated with the formation of carboxylamine free radical, followed by the loss of carbon dioxide and the generation of alkylamine radicals and its recombination products. Furthermore, the rate constants for the thermal degradation reactions of various amino acid copper complexes were highly dependent upon the nature and bulkiness of their side chains, and rates of degradation of such amino acid complexes decreased in the following order: Ser > Phe > Leu > Ile > Val > Gly > Ala. The objective of this study was to explore the thermal degradation of synthetic copper complexes of various amino acids, particularly alanine and glycine, and their degradations in the presence of various metal salts {iron(II) or iron(III) chlorides, zinc chloride, calcium chloride [two generally recognized as safe (GRAS) metal chloride salts], and copper(I) and (II) chlorides}. The chloride salts of metals were selected because of their ability to form more volatile chlorinated reaction products (Troise et al., 2013). In this study, we explore the role of metal salts and amino acid metal complexes in the decomposition reactions of amino acids.

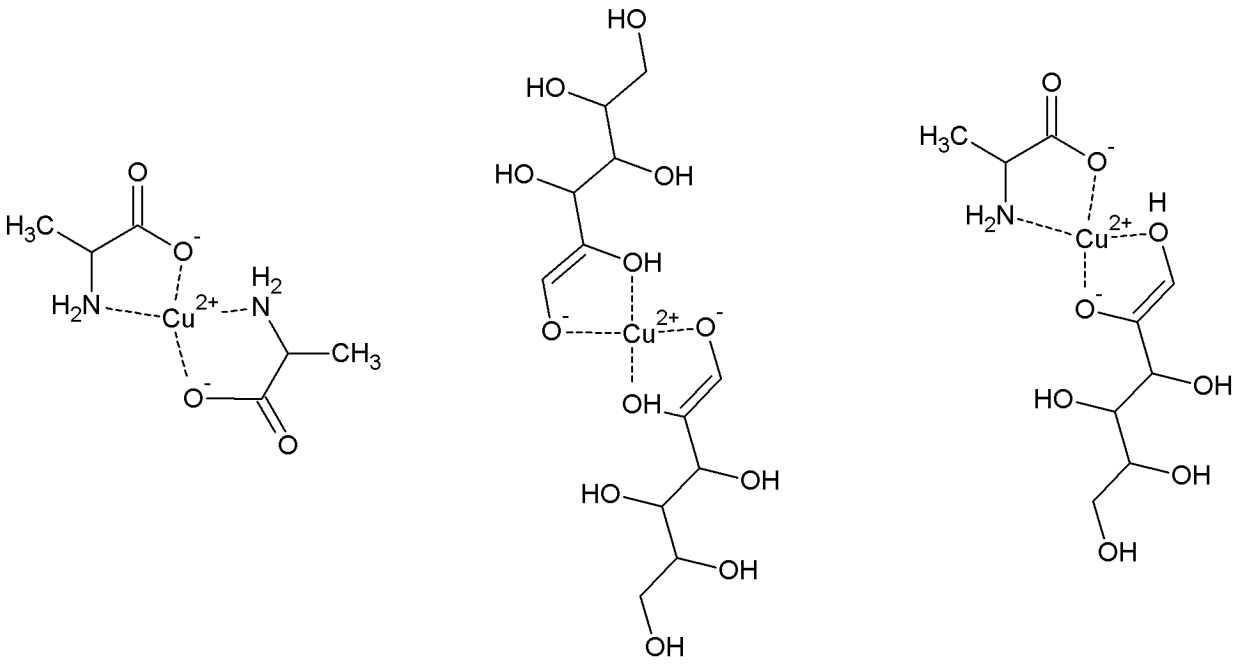

Figure 3.1. Possible complexes of copper with glucose and alanine.

3.3 MATERIALS AND METHODS

3.3.1 Materials and Reagents

L-alanine (99%), L-methionine (99%), L-leucine (99%), L-glycine (98%), copper (II) chloride ($CuCl_2$) (99.9%), copper (I) chloride (CuCl) (97%), calcium chloride ($CaCl_2$), zinc chloride ($ZnCl_2$) (98%), chloral hydrate (98%), 2-methylpyridine (98%), potassium hydroxide, D-glucose and acetaldehyde (99.5%) were purchased from Sigma-Aldrich Chemical Co. (Oakville, ON, Canada). The [^{13}C-1]alanine (98%), [^{13}C-2]alanine (98%), [^{13}C-3]alanine (98%), [^{15}N]alanine, [^{13}C-1,^{13}C-2]glycine (98%) were purchased from Cambridge Isotope Laboratories (Andover, MI).

3.3.2 Preparation of model Systems

Model systems comprising of amino acids alone, amino acids with metal salts (in a 2:1 relative molar ratio) or synthetic amino acid metal complexes (see Table 3.1) were homogenized and mixed using a microscale porcelain mortar and pestle. After thorough homogenization, approximately 0.5 mg of the individual reactants or their mixtures were weighed into a quartz tube (0.3mm thickness) plugged at both ends with glass wool (Supelco, Bellefonte, PA), inserted inside the coil

probe, and pyrolyzed at 250°C for 20 s under a helium atmosphere, as described below. All samples were analyzed in duplicate

Table 3.1. Composition of the reactants in the model systems.

Amino acids[a]	Metal salts	Synthetic metal complexes
alanine	$CuCl_2$/CuCl	$(Gly)_2Cu$
glycine	$FeCl_2$/$FeCl_3$	$(Ala)_2Cu$
leucine	$ZnCl_2$	(Gly)Cu(Ala)
methionine	$CaCl_2$	

[a] All of the listed amino acids were studied in the presence and absence of metal ions. The amino acids alanine and glycine were studied with all of the metal salts listed in the table and as synthetic metal complexes. Leucine and methionine were studied only with $CuCl_2$.

3.3.3 Synthesis of amino acid-metal adducts

Alanine-copper and glycine-copper complexes or mixed complexes were prepared by dissolving alanine (0.89g), glycine (0.75g), [^{13}C-1,^{13}C-2]glycine, or an equimolar mixture of alanine and glycine at room temperature in methanol (10 mL) in the presence of KOH (0.05g) and stirred until all completely dissolved followed by the addition of 0.5 mol of $CuCl_2$. The dark blue (with $CuCl_2$) precipitates were filtered washed with methanol and dried.

3.3.4 Pyrolysis Gas Chromatography−Mass Spectrometry (Py-GC/MS)

A Varian CP-3800 gas chromatograph coupled to a Saturn 2000 ion trap detector interfaced to a CDS Pyroprobe 2000 unit through a valved interface (CDS 1500) was used for Py-GC/MS analysis of model systems shown in Table 3.1. The samples were packed in the quartz tube inserted inside the coil probe and pyrolyzed at 250 °C for 20 s under a helium atmosphere. The separation was performed using a fused silica DB-5MS column (50-m length x 0.2mm i.d. x 33 µm film thickness). The GC method used for the analysis of the volatiles was as follows: GC column flow rate was regulated by an electronic flow controller (EFC) and set at a pressure pulse of 55 psi for first 3 minutes then decreased to 32 psi at the rate of 300 psi/min and finally increased to 70 psi at a rate of 1.23psi/min for the rest of the run. The GC oven temperature was set at −5 °C for first 5 min using CO_2 as the cryogenic cooling source and then increased to 50 °C at a rate of 50 °C/min.

Then, the oven temperature was again increased to 270 °C at a rate of 8 °C/min and kept at 270 °C for 5 min. The samples were detected by using an ion-trap mass spectrometer. The MS transfer-line temperature was set at 250 °C, manifold temperature was set at 50 °C, and the ion-trap temperature was set at 175 °C. The ionization voltage of 70 eV was used, and EMV was set at 2000 V. The generated data was analyzed using the AMDIS_32 version 2.69 computer software and peak identification done using the NIST version 2.0 mass spectral research program.

3.3.5 Liquid Chromatograph-Mass spectrometric (LC-MS) analysis of the amino acid-copper synthetic adducts

The dry samples were dissolved in deionized water (Millipore, Billerica, MA) to a concentration of 1 mg/mL. The sample was then diluted 10 folds in 10% methanol prior to analysis by LC-MS. The LC-ESI-MS analysis comprised of a Dionex Ultimate 3000 RS liquid chromatograph (Dionex, Germering, Germany) coupled to a Bruker Maxis Impact quadruple-time of flight mass spectrometer (Bruker Daltonics, Bremen, Germany) in positive mode. 1 µl of the sample was injected directly into the LC-MS. The electrospray interphase settings were the following: nebulizer pressure 0.6 bar, drying gas 8 L/min, 180°C, capillary voltage 4500 V. Scan range was from 100 to 1000 m/z. The data was analyzed using Bruker Compass DataAnalysis software version 4.1.

3.3.6 Structural identification

Specific reaction products (listed in Table 3.2) were identified by comparison of their retention times and mass spectra with commercial or *in situ* generated standards in addition to NIST library matches and stable Isotope labelling data (Table 3.2). Elemental composition of selected metal complexes were based on their accurate mass determination by ESI-qTOF analysis (alanine-copper complex at *m*/*z* 261.9985 [M + Na] (calculated for $C_6H_{12}CuN_2NaO_4$ with an error of -1.4ppm, and glycine copper complex at m/z 233.9665 [M + Na] (calculated for $C_4H_8N_2O_4CuNa$ with an error of 5.443 ppm).

3.4 Results and Discussion

Under the Maillard reaction conditions, independent degradation reactions of amino acids play an important role in the generation of amino-acid-specific products that result from thermal

decarboxylation or oxidative decarboxylation (Figure 3.2), leading to the formation of amines (Moldoveanu, 2010) and Strecker aldehydes captured as imines by the amino acid or its corresponding amine (Yaylayan, 2003; Yaylayan and Keyhani, 2001). Such oxidative decarboxylation reactions are expected to be enhanced in the presence of oxidizing species, such as copper and contribute to the pool of aroma-active aldehydes (Fitzpatrick and Hopgood, 1974). On the other hand, oxidative decomposition of sugars leads to the formation of α-dicarbonyl compounds, such as glucosone and deoxyglucosone that can trigger the Strecker reaction of amino acids, producing even more Strecker aldehydes along with 2-aminocarbonyl compounds, the precursors of pyrazines. Currently, the relative contribution of the two pathways of generating Strecker aldehydes is not known in food products. Because of the importance of these aldehydes, enhancement of the pathways generating them could be a critical factor in flavor production and control. Because of the oxidative capacity of some metal salts, such as copper salts, it was predicted that, in their presence, the oxidative decarboxylation reactions could be encouraged. To understand metal–amino acid interactions and their influence on the production of specific reaction products, such as Strecker aldehydes, model systems containing amino acids were studied in the presence and absence of metal ions as both their free salts or synthesized amino acid–copper complexes (see Table 3.1). The purpose of the latter was to eliminate the effect of counterions, such as chlorides, and assess its importance as an intermediate.

Table 3.2. Decomposition products observed in alanine-copper complex and alanine $CuCl_2$ mixtures.

model system	structure	retention time[a] (min)	isotope incorporation
Alanine-$CuCl_2$	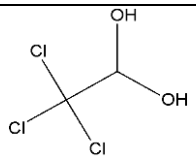 chloral hydrate	10.2 (10.2)	1 x C-2 1 x C-3 0 x N
Alanine-$CuCl_2$ Alanine-CuCl	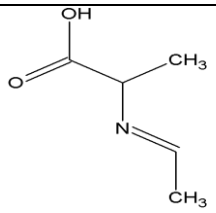 2-ethylideneamino propanoic acid [b]	13.2 (13.2)	1 x C-1 2 x C-2 2 x C-3 1 x N
Alanine-$CuCl_2$	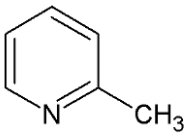 2-methylpyridine	12.2 (12.2)	3 x C-2 3 x C-3 1 x N
Alanine-$CuCl_2$	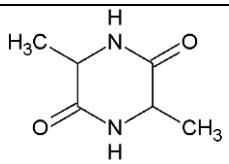 3,6-dimethyl piperazine-2,5-dione	25.9 (25.9)	2 x C-2 2 x C-3 2 x N

[a] Values in parenthesis represents those of the commercial or synthesized standards
[b] The *in situ* preparation of 2-ethylideneamino propanoic acid comprised of 0.5 mg alanine and 1µL acetaldehyde- mixed and pyrolyzed under standard pyrolytic conditions.

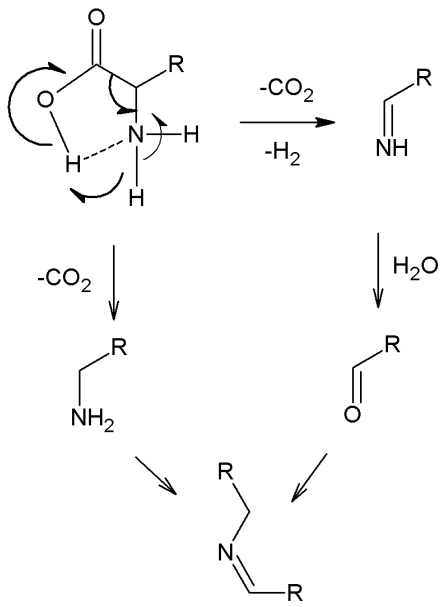

Figure 3.2. Proposed mechanism of thermally induced oxidative auto-decarboxylation of amino acids.

Unlike other amino acids with longer side chains, such as leucine and methionine (Yaylayan and Keyhani, 2001), alanine when pyrolyzed in the absence of metal salts did not generate any significant amount of degradation products that could be observed under the experimental conditions. However, when the synthetic copper salt $(Ala)_2Cu$ of alanine was pyrolyzed, a single major peak was observed that was characterized, resulting from the Schiff base formation between the intact alanine and its Strecker aldehyde (see Table 3.2). The same peak was also observed in the various copper and iron(III) salt/alanine mixtures along with other products. On the other hand, leucine and methionine in the absence of metal salts generated under pyrolytic conditions Schiff bases of Strecker aldehydes with their corresponding decarboxylated amino acids (Yaylayan and Keyhani, 2001), (see Figure 3.2). Similarly, the formation of these Schiff bases was increased in the presence of copper salts. These observations clearly indicated that, although some amino acids can undergo thermally induced oxidative decarboxylation on their own and generate Strecker aldehydes, however, in the presence of copper or iron(III) salts, this ability is greatly facilitated or even accelerated by the formation of copper complexes.

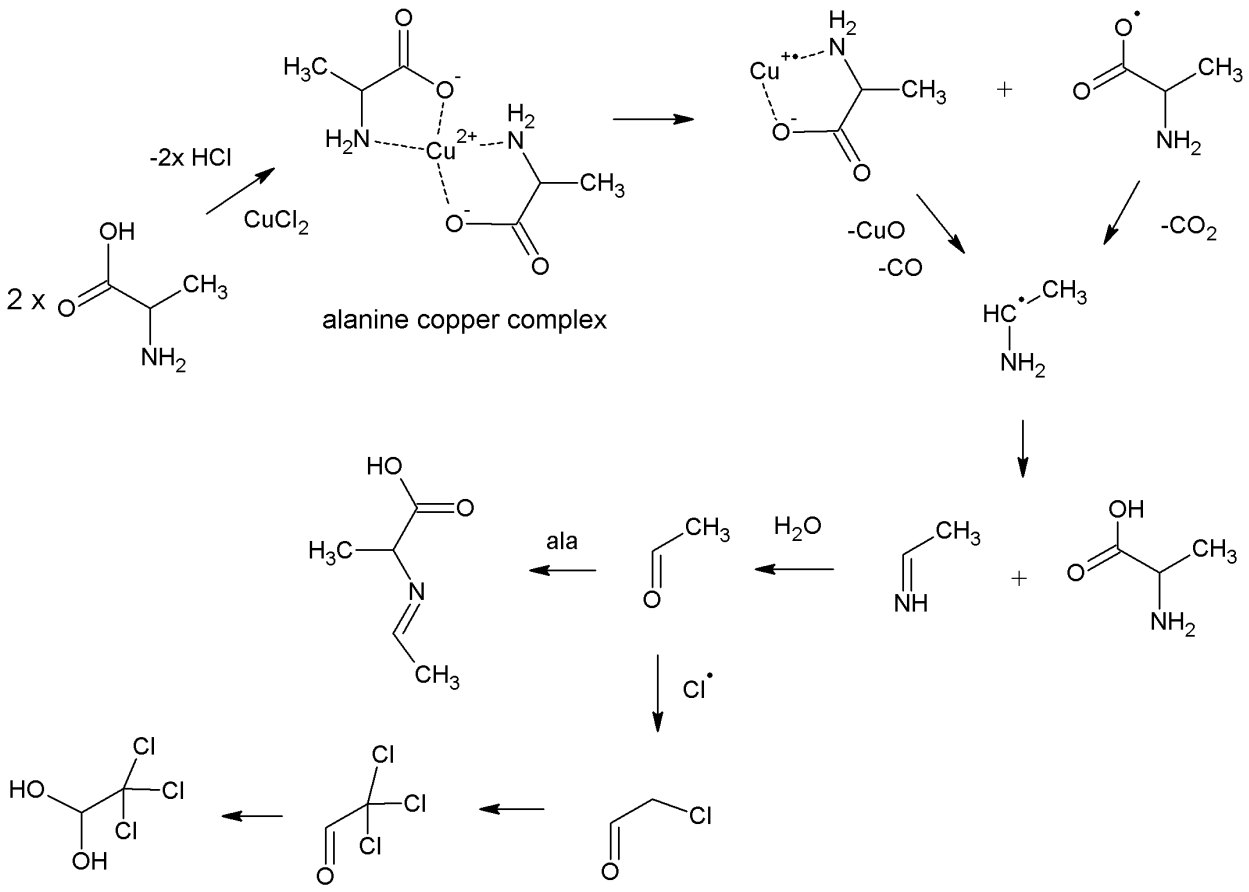

Figure 3.3. Proposed mechanism of copper-assisted thermal decarboxylation of alanine and acetaldehyde formation.

To confirm the generality of this observation, another amino acid glycine was chosen that behaves similar to alanine and does not undergo oxidative decarboxylation on its own. However, when glycine was pyrolyzed in the presence of copper salts or as its copper complex, it generated various Strecker aldehyde derivatives, such as pyrazines (Guerra and Yaylayan, 2010), that were verified through NIST library searches and isotope-labeling studies using synthetic [^{13}C-1, ^{13}C-2]glycine–copper complex, which generated pyrazine and two of its derivatives methyl- and 2,6-dimethyl pyrazines, incorporating four, five, and six glycine atoms, respectively. This label incorporation pattern was consistent with those reported by Guerra and Yaylayan (2010). Pyrazine and alkyl-substituted pyrazines can be formed through dimerization of azomethine ylides, which, in turn, can be formed from the Schiff base adducts of glycine and formaldehyde, the Strecker aldehyde of glycine. The same complex also generated 4-hydroxybutanal, the aldol product of two acetaldehyde molecules. Guerra and Yaylayan (2010) also demonstrated that acetaldehyde can be

generated from glycine and formaldehyde through a chain elongation reaction (Guerra and Yaylayan, 2010).

Although other metals, such as calcium and zinc, can also complex with amino acids, however, when copper or iron (III) chloride was replaced with calcium or zinc chlorides in the reaction mixtures, they did not promote Strecker aldehyde formation. This observation underlines the significance of the nature and reactivity of the metal ions in these complexes, considering that copper in its oxidation sate +2 and iron in its oxidation state +3 are known to have higher redox potentials compared to the other metals studied. The high redox potential enhances the electron affinity of copper, which, in turn, affects its reactivity and how easily it can accept and donate electrons (Bishop, 1976). In addition, the Lewis acid character of the metal ions also influences the stability of the complexes by forming metal–amino acid bonds with differing bond strengths depending upon the metal type, which, in turn, would affect their thermal dissociation capacity. On the other hand, when alanine was replaced with other amino acids, such as leucine and methionine, in the $CuCl_2$ reaction mixtures, similar enhancements in their corresponding Strecker aldehyde concentrations were observed relative to the model systems lacking $CuCl_2$ salts. Interestingly, when the mixed glycine/alanine copper complex (AlaCuGly) was analyzed, a significant enhancement in the formation of pyrroles, pyridines, and pyrazines relative to single amino acid complexes was observed. Furthermore, ethylamine and acetic acid were observed in iron (III) chloride/alanine model systems, in addition to the Schiff base adducts of Strecker aldehyde, indicating the ability of the iron to oxidize acetaldehyde and generate nitrogen-centered free radicals.

3.4.1 Proposed Mechanism of Copper-Assisted Oxidative Decarboxylation of Alanine and Acetaldehyde Formation

The analysis of the metal salt–alanine reaction products indicated that the influence of the metal ions on the thermal degradation profile of alanine was highly dependent upon the type of metal ion. Among the metal chloride salts investigated, CuCl, $CuCl_2$, and $FeCl_3$ were found to be the only salts that induced significant changes to the thermal degradation profile of alanine that could be observed under the experimental conditions, causing the generation of new products (see Table 3.2). The results pointed to the role of copper to be stoichiometric rather than catalytic, as supported by the generated products and their formation mechanism (see Figure 3.3). $CuCl_2$ can form stable complexes with 2 mol of alanine with the release of HCl, as shown in Figure 3.3, and

the resulting complex can undergo thermal decomposition through an intramolecular redox reaction to generate a copper-centered radical cation and a carboxylamine radical (Shelkovnikov and Yeroshkin, 1985; Yablokov et al., 2014). Both products can be converted into the ethylamine radical, the former through the loss of CuO and CO and the latter through the thermal decarboxylation mechanism. A subsequent disproportionation reaction between the carboxylamine radical and ethylamine radical generates free alanine and ethanimine molecules. The hydrolysis of imine can lead to the formation of the Strecker aldehyde, which can immediately form a Schiff base adduct with the released free alanine, as shown in Figure 3.3. This identified adduct, which confirms the formation of both acetaldehyde and alanine, as predicted in the proposed mechanism, was the main product observed when the synthetic copper complex of alanine was pyrolyzed. The identity of this adduct was verified through comparison of its retention time to that of pyrolytically generated standard from alanine and acetaldehyde and through isotope-labeling experiments with [^{13}C-1]alanine, [^{13}C-2]alanine, [^{13}C-3]alanine, and [^{15}N]alanine (see Table 3.2), in addition to its mass spectral fragmentation pattern, which was consistent with the proposed structure (see Figure 3.4).

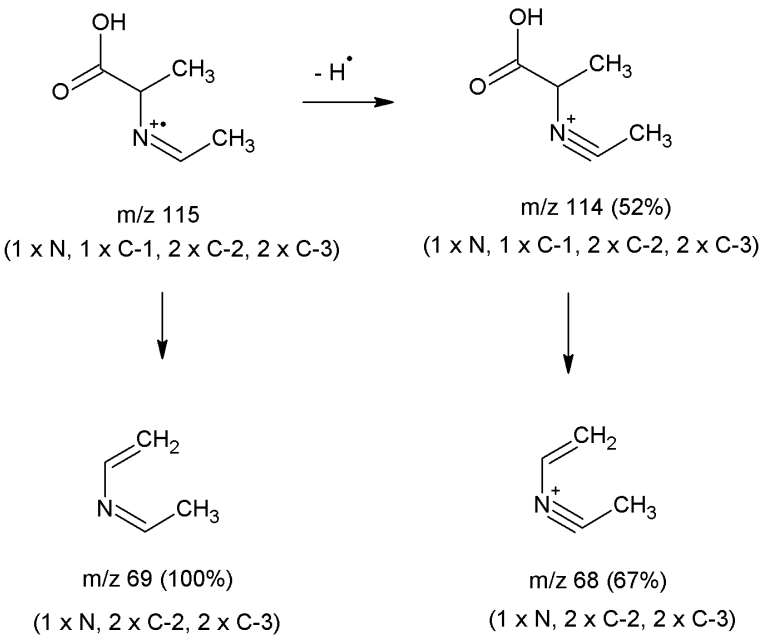

Figure 3.4. Mass spectral fragmentation patterns of 2-ethylidineamino propionic acid (values in parenthesis represent the observed alanine atom incorporations).

Further evidence for the release of free alanine was the detection of 3,6-dimethyl piperazine-2,5-

dione, as shown in Table 3.2. The same diketopiperazine was also observed in the alanine copper complexes analyzed at 270 °C by Yablokov et al. (Yablokov et al., 2014) On the other hand, the model systems containing chloride salts, such as $CuCl_2$, that can release HCl provided additional evidence for the formation of acetaldehyde because of the ability of HCl to chlorinate acetaldehyde and form chloral hydrate (Figure 3.3). The structure of chloral hydrate was confirmed by comparison of its mass spectrum and retention time to a commercially available standard (Table 3.2). Additionally, the labeling studies confirmed that chloral hydrate contains ^{13}C-2 and ^{13}C-3 atoms of alanine, while the number of chlorine atom incorporation was confirmed through its natural isotope abundance pattern. In addition to chloral hydrate, several chlorinated and non-chlorinated methylpyridines were also detected in $CuCl_2$–alanine model systems. Isotope-labeling studies have indicated that 2-methylpyridine incorporated three ^{13}C-2, three ^{13}C-3 atoms, and one nitrogen atom from alanine, implying an aldol-type condensation involving acetaldehyde and ethanimine, followed by cyclization (Figure 3.5). The mass spectra and retention time of 2-methylpyridine were further confirmed using a commercially available standard.

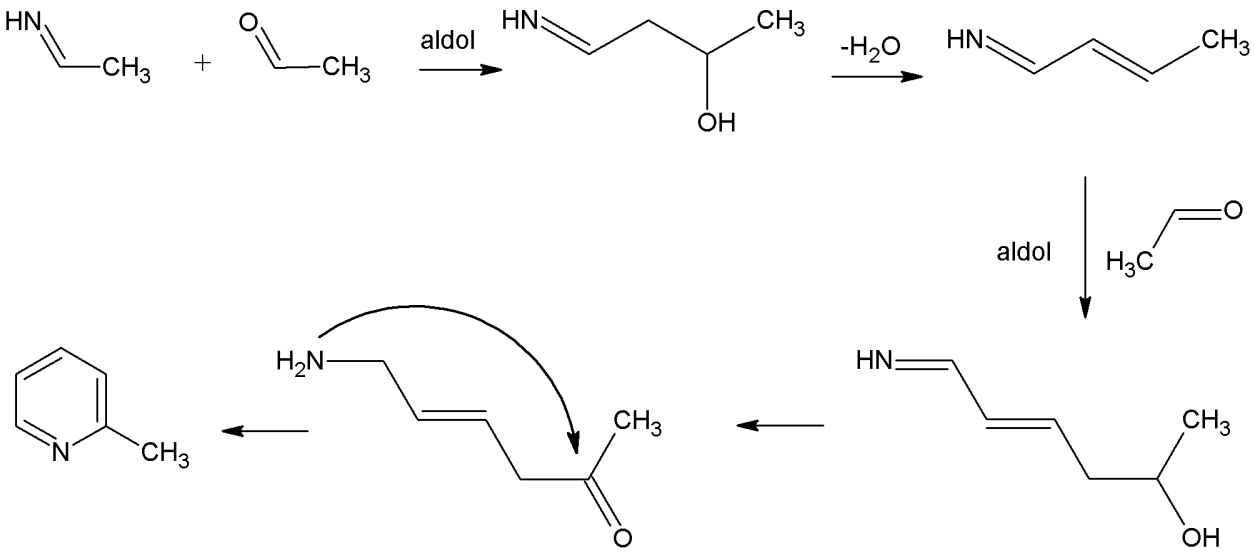

Figure 3.5. Proposed mechanism of 2-methylpyridine formation from acetaldehyde.

Copper(II) and iron(III) were found to be the most reactive metals that are able to complex with amino acids, promote their oxidative decarboxylation in a thermally induced free-radical pathway,

and enhance the formation of important Strecker aldehydes. This ability was demonstrated when the amino acid was replaced with the alanine copper complex in a Maillard model system consisting of glucose and alanine. In this reaction system, the total intensity of ethyl-substituted pyrazines that incorporated ^{13}C-2 atoms of alanine was increased by 10-fold compared to the total intensity of corresponding ethyl-substituted pyrazines in the glucose alanine model system, indicating enhanced production of the Strecker aldehyde acetaldehyde and its subsequent reaction with dihydropyrazines to generate various ethyl-substituted derivatives. With the absence of any toxicological evidence to prohibit their use as flavor-potentiating additives, these amino acid–metal complexes might provide a cost-effective way to enhance the flavor of heated foods. This pathway of generating Strecker aldehydes through thermal degradation of easily available metal–amino acid complexes in the absence of sugar-derived α-dicarbonyl compounds can be considered a convenient strategy to introduce such aroma-active volatiles in foods lacking carbohydrates or a sugar source.

CONNECTING PARAGRAPH

The results obtained in chapter 3 indicated that heating glycine and alanine with copper (II) and iron (III) complexes induces the oxidative decarboxylation of amino acids and formation of their respective Strecker aldehydes. Due to their high oxidation potentials Cu (II) and Fe(III) were the only metals able to do so. Furthermore, the results also indicated that the formation of the amino acid-metal complex itself constitutes the critical intermediate in initiating the oxidative decarboxylation mechanism and generation of Strecker aldehydes. In chapter 4, we further explore the role of glycine-copper complexes since in the presence of Strecker aldehydes they are known to transform α-amino acids into their hydroxymethyl derivatives in a process commonly known as the Akabori reaction. The occurrence of this transformation was investigated in the presence of formaldehyde, the Strecker aldehyde of glycine. Chapter 4 was published in the *Journal of Agriculture and Food Chem*istry: Nashalian, O.; Yaylayan, V. A. (2015). *De novo* synthesis of amino acids during the Maillard reaction: New insights to Akabori modification. *Journal of Agriculture and. Food Chem*istry, 63, 328–334.

CHAPTER 4

DE NOVO SYNTHESIS OF AMINO ACIDS DURING THE MAILLARD REACTION: NEW INSIGHT INTO THE MECHANISM OF AKABORI TRANSFORMATION

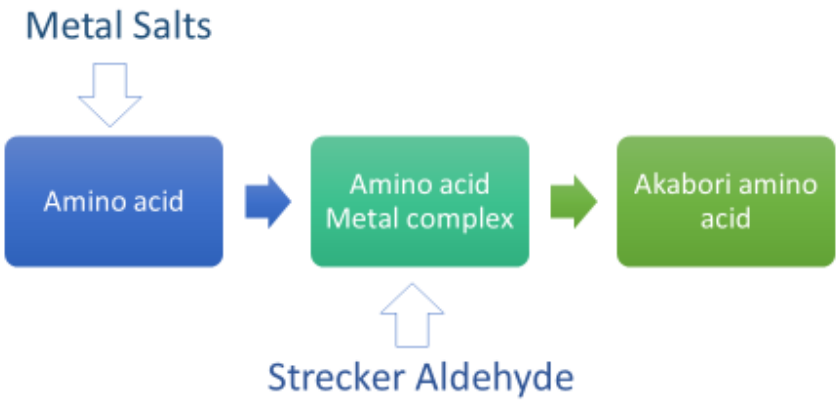

4.1 ABSTRACT

The transformation of α-amino acids into their hydroxymethyl derivatives during the Maillard reaction is an intriguing possibility for catalysis by metal salts in the presence of Strecker aldehydes; the process is commonly known as the Akabori reaction. The mechanism of this reaction was studied in the presence of glucose, using glycine copper complex and paraformaldehyde as Akabori model system in aqueous mixtures heated at 110 °C for 2 h and subsequently analyzed by qTOF/ESI/MS. Isotope-labeling studies of the various products identified have provided for the first time mass spectrometric evidence for the detailed mechanism of Akabori transformation, particularly the formation of Schiff base adducts prior to the final conversion into serine and hydroxymethyl-serine. Furthermore, the results have indicated that sugars do not interfere with such transformations and, on the contrary, the presence of glycine–copper complexes in the Maillard model systems can enhance the production of Maillard reaction intermediates.

4.2 INTRODUCTION

Contrary to the reaction of α-amino groups of amino acids with carbonyl moieties, which has been studied for over a century, the interaction of α-carbons of α-amino acids with aldehydes such as Strecker aldehyde has not been examined in detail in the context of the Maillard reaction. Akabori et al. first reported the chemical synthesis of serine or threonine from glycine in the presence of two common Strecker aldehydes, formaldehyde and acetaldehyde (Akabori et al., 1959). This transformation of one amino acid into another was catalyzed by metal salts such as copper and iron and is commonly referred to as the Akabori reaction (Beck, 2009). The generality of this reaction was later extended to different amino acids (serine, glycine, and alanine) and different metal complexes (Ni, Co, and Cu) and using various aldehydes (acetaldehyde, formaldehyde, pyruvic acid, and benzaldehyde) (Ichikawa et al., 1970; Sato et al.,1957). The transformation of the α-amino acids into their corresponding β-hydroxy amino acids required relatively mild conditions; heating at 100 °C for 1 h in water generated both serine and threonine with average yields of 30% (Akabori et al., 1959) and 32–80% (Ichikawa et al., 1970; Ikutani,1959; Sato et al.,1957), respectively. The initial mechanism proposed by Akabori et al. attributed the activation of the α-carbon to the formation of the amino acid metal complexes (Akabori et al., 1959). Williams and Busch demonstrated through NMR studies the enhanced acidity and lability of α-

methylene hydrogens in such complexes due to the electron-withdrawing action of the metal ions (Williams and Busch, 1965). Under alkaline conditions, the formed carbanion would serve as a nucleophile that can condense with a carbonyl moiety such as formaldehyde or acetaldehyde (Akabori et al., 1959; Sato et al., 1957). However, it was later proposed that the amino acid metal complexes first undergo Schiff base formation with the aldehyde followed by the subsequent activation of the α-carbon to generate carbanion (Belikov et al., 1969; Ichikawa et al., 1970). The formation of the Schiff base adducts was assumed to enhance even more the acidity of the α-carbon, allowing the reaction to proceed at milder pH conditions and with higher yields (Ichikawa et al., 1970). The formation of Schiff base intermediates was further confirmed in polarimetric studies involving serine–copper complexes and formaldehyde (Teo and O'Connor,1984), and glycine–copper complex and acetaldehyde through observation of their subsequent intramolecular cyclization products initiated by the newly formed serine hydroxyl groups to generate 1,3-oxazolidine moieties as reported by the two research groups of Aune et al. (Aune et al., 1970) and Teo and O'Connor (Teo and O'Connor,1984).

Although the Akabori reaction was initially intended for chemical synthesis to generate β-hydroxy amino acids, the conditions needed for its formation are readily available in food. Many foods are heated under conditions similar to those of the Akabori reaction, and the needed precursors the amino acids, Strecker aldehydes, and metals are either present or generated during processing. In fact, a variant of this reaction has been observed under pyrolytic conditions (Yayalyan and Keyhani, 1999), where the α-carbons of amino acids were activated toward nucleophilic addition with aldehydes. However, such activation was initiated through decarboxylation (Figure 4.1, pathway A) rather than through metal catalysis as in the case of the Akabori reaction, and consequently the resulting adduct after deamination step constituted a chain elongation process of the aldehyde rather than the formation of a new amino acid as in the case of Akabori reaction (Figure 4.1, pathway B). If Akabori transformation can be demonstrated to be a feasible pathway in the Maillard reaction, it can generate hitherto unknown amino acid structures or enhance the concentration of serine and threonine levels that are known to generate sugar-like reactive intermediates upon thermal degradation (Shu, 1999). Considering the fact that the occurrence of this reaction could influence the aroma profile and may even generate potentially unknown amino acid structures, we have studied its role in Maillard model systems using glucose, glycine, and

paraformaldehyde aqueous mixtures heated at 110 °C for 2 h and subsequently analyzed by qTOF/ESI/MS.

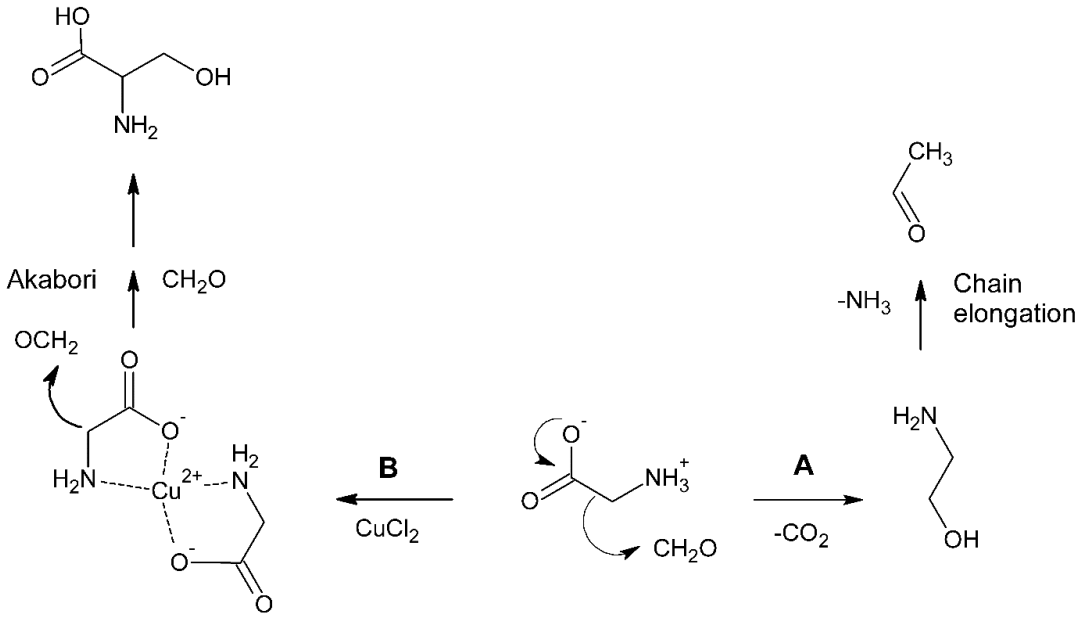

Figure 4.1. Activation of the α-carbon of glycine as nucleophile (A) through thermal decarboxylation with subsequent chain elongation of formaldehyde and (B) through metal complex formation (Akabori reaction) in the presence of formaldehyde (see Figure 4.2 for details).

4.3 MATERIALS AND METHODS

4.3.1 Materials and Reagents

L-Glycine (98%), L-alanine (99%), L-serine (99%), D-glucose, paraformaldehyde, potassium hydroxide (KOH), and copper(II) chloride ($CuCl_2$) (99.9%) were purchased from Sigma-Aldrich Chemical Co. (Oakville, ON, Canada). [^{13}C-1,^{13}C-2,^{15}N]glycine (98%) and [U_6-^{13}C]glucose (99%) were purchased from Cambridge Isotope Laboratories (Andover, MA, USA). LC-MS grade water and methanol (OmniSolv, >99%) were obtained from VWR International (Mississauga, ON, Canada).

4.3.2 Synthesis of Amino Acid–Metal Complexes

$(Ala)_2Cu$, $(Gly)_2Cu$, and $(Ser)_2Cu$ complexes were prepared by dissolving alanine (0.89 g), glycine (0.75 g), and serine (1.05 g) in methanol (10 mL) in the presence of KOH (0.05 g) followed by the

addition of 0.5 mol of $CuCl_2$. The dark blue precipitates were washed with methanol, filtered, and dried. The amino acid adducts were confirmed by obtaining their elemental composition from their accurate masses determined by qTOF/ESI/MS analysis (alanine–copper complex at *m*/*z* 261.9985 $[M + Na]^+$ (calculated for $C_6H_{12}CuN_2NaO_4$ with an error of −1.4 ppm, glycine–copper complex at *m*/*z* 233.9665 $[M + Na]^+$ (calculated for $C_4H_8CuN_2NaO_4$ with an error of 5.4 ppm), and serine–copper complex at *m*/*z* 272.0059 $[M + H]^+$ (calculated for $C_6H_{13}CuN_2O_6$ with an error of 3.9 ppm). Isotope-labeled precursors were prepared similarly.

4.3.3 Sample Preparation

Model systems (6.0 mg) consisting of amino acid metal complexes were mixed with glucose (equimolar amounts) and excess paraformaldehyde (20 mg), dissolved in water (2 mL), and heated on a sand bath in an open vial (5 mL capacity) at 110 °C for 2 h until dry. Controls such as serine and $(Ser)_2Cu$ were also similarly heated and analyzed generating ions at *m*/*z* 106.0492 and 272.0059, respectively. To generate some of the observed intermediates, mixtures comprising $(Ser)_2Cu$/glycine and $(Gly)_2Cu$/excess serine were similarly heated and analyzed, generating the ions at *m*/*z* 241.9956 and 272.0045, respectively (see Figure 4.2). In addition, $(Ser)_2Cu$ was heated in the presence of excess paraformaldehyde and analyzed as control (see Table 4.1). Selected dry residues were then analyzed for their volatile components using pyrolysis gas chromatography–mass spectrometry (Py-GC/MS), and for their nonvolatile components using electrospray ionization mass spectrometry (qTOF/ESI/MS). All samples were analyzed in duplicates.

Table 4.1. Composition of the model systems

Control model systems [a]	*Model systems* [a]
Paraformaldehyde/$CuCl_2$	$(Gly)_2Cu$/paraformaldehyde
Glycine/paraformaldehyde	(^{13}C-1 Gly)$_2$Cu/paraformaldehyde
$(Gly)_2Cu$*	(^{13}C-2 Gly)$_2$Cu/paraformaldehyde
$(Gly)_2Cu$/Serine*	(^{15}N Gly)$_2$Cu/paraformaldehyde
Glycine/Serine*	$(Gly)_2Cu$/Glucose-paraformaldehyde
Glycine/Serine/Paraformaldehyde	$(Gly)_2Cu/U_6$-^{13}C Glucose-paraformaldehyde
Glycine	$(Ala)_2Cu$/paraformaldehyde
Serine	$(Ser)_2Cu$
	$(Ser)_2Cu$/Glycine

[a]Heated (110^{o}C for 2 hours in water) and dried model systems were first analyzed by qTOF/ESI/MS for non-volatiles and some model systems (indicated by asterix) were also thermally desorbed by Py-GC/MS for volatile analysis.

4.3.4 Quadrupole Time of Flight/Electrospray Ionization/Mass Spectrometric (qTOF/ESI/MS) Analysis

The dry reaction residues or synthetic samples were dissolved in water to a concentration of 1 mg/mL. The sample was then diluted 10-fold in 10% methanol prior to analysis by qTOF/ESI/MS. The qTOF/ESI/MS system was composed of a Bruker Maxis Impact quadrupole time-of-flight mass spectrometer (Bruker Daltonics, Bremen, Germany) operated in positive ion mode. Samples (1 μL) were injected directly into the ESI/qTOF/MS. Instrument calibration was done using sodium formate clusters. The electrospray interface settings were the following: nebulizer pressure, 1.0 bar; drying gas, 8 L/min, 200 °C; capillary voltage, 4500 V. Scan range was from *m*/*z* 100 to 1000. The data were analyzed using Bruker Compass Data Analysis software version 4.1. Tandem mass spectrometry (MS/MS) was carried out in MRM mode using 20.0 eV collision energy for the ion at *m*/*z* 272.

4.3.5 Thermal Desorption by Pyrolysis Gas Chromatography–Mass Spectrometry (Py-GC-MS)

A Varian CP-3800 gas chromatograph coupled to a Saturn 2000 ion trap detector interfaced to a CDS Pyroprobe 2000 unit through a valved interface (CDS 1500) was used for the desorption of the volatiles from the dried residues. The residues from selected dry and heated model systems

shown in Table 4.1 were weighed (0.5 mg) into quartz tubes (0.3 mm thickness), plugged at both ends with glass wool (Supelco, Bellefonte, PA, USA) inserted inside a coil probe and pyrolyzed at 250 °C for 20 s under a helium atmosphere (Table 4.1). The separation was performed using a fused silica DB-5MS column (50 m length × 0.2 mm i.d. × 33 μm film thickness). The GC method used for the analysis of the volatiles was as follows: GC column flow rate was regulated by an electronic flow controller (EFC) and set at a pressure pulse of 55 psi for first 3 min and then decreased to 32 psi at the rate of 300 psi/min and finally increased to 70 psi at a rate of 1.23 psi/min for the rest of the run. The GC oven temperature was set at −5 °C for the first 5 min using CO_2 as the cryogenic cooling source and then increased to 50 °C at a rate of 50 °C/min. Then, the oven temperature was again increased to 270 °C at a rate of 8 °C/min and kept at 270 °C for 5 min. The samples were detected by using an ion trap mass spectrometer. The MS transfer line temperature was set at 250 °C, manifold temperature was set at 50 °C, and ion trap temperature was set at 175 °C. The ionization voltage of 70 eV was used, and EMV was set at 1600 V. The generated data were analyzed using the AMDIS_32 version 2.69 computer software, and peak identification was done using the NIST version 2.0 mass spectral research program.

4.3.6 Structural Identification

Evidence for the proposed structures of nonvolatile reaction intermediates were provided through qTOF/ESI MS analysis of their elemental composition and isotope-labeling studies or by the use of synthetic intermediates or standards. Furthermore, the incorporation of copper in the identified complexes was confirmed by the isotopic signature of copper through detection of M + 2 peaks at 30% relative intensity. Volatile reaction products were identified by comparison of their retention times and mass spectra with commercial or in situ generated standards in addition to NIST library matches and stable isotope labeling data.

4.4 Results and Discussion

Amino acids are one of the primary reactants required for the Maillard reaction. The type and distribution of various amino acids contribute significantly to the nutritive value and aroma profile of foods (Friedman, 1996; Wong et al., 2008). Although free amino acids are usually formed in processed food through hydrolysis of proteins, the notion that some amino acids may be also

generated *de novo* during processing from already existing precursors has not been explored in the context of the Maillard reaction. The chemical transformation known as the Akabori reaction provides this opportunity because it requires precursors that are generally found in food and reaction parameters encountered under food-processing conditions. As detailed above, the Akabori reaction transforms existing amino acids into their β-hydroxyl counterparts (Figure 4.1, pathway B), of which only two amino acids, serine and threonine, are naturally found in food proteins. The Akabori modification of amino acids has not been explored within the context of the Maillard reaction or in the presence of reducing sugars. Detailed understanding of the role of Akabori transformation within the Maillard reaction system can reveal not only the possible formation of new amino acid structures but also its possible influence on the mechanism and the general outcome of the Maillard reaction itself. Isotope-labeling studies were performed to confirm the formation of serine, the Akabori amino acid in heated (110 °C) aqueous model systems of glucose, glycine–copper complex [$(Gly)_2Cu$], and formaldehyde, and to investigate the role of glycine copper complex in modifying the Maillard reaction profile.

The various model systems listed in Table 4.1 were heated at 110 °C for 2 h, and the resulting dry residues were analyzed by qTOF/ESI/MS for nonvolatiles, and selected model systems were also analyzed by Py-GC/MS to thermally desorb and characterize the volatile reaction products already formed under aqueous heating conditions. Heating $(Gly)_2Cu$ alone mainly causes oxidative decarboxylation of glycine and formation of its corresponding Strecker aldehyde (Nashalian and Yaylayan, 2014; Yablokov et al., 2014); however, when heated in the presence of excess formaldehyde with or without glucose, the reaction mixtures generated many products and intermediates that supported the proposed formation of serine, the Akabori amino acid of glycine observed at *m*/*z* 106.0500 (see Table 4.2 and Figure 4.2) and α-hydroxymethyl-serine at *m*/*z* 136.0603, which was predicted to be formed through two consecutive Akarbori transformations of glycine and can be considered as the Akabori amino acid of serine under the Maillard reaction conditions (Otani and Winitz,1960). Furthermore, as shown in Figures 4.2 and 4.3 and Tables 4.2 and 4.3, many of the copper-containing intermediate complexes identified in the reaction medium provided, for the first time, high-resolution mass spectral evidence (qTOF/ESI/MS) for their formation supported by the presence of isotopic peaks of copper and the isotopic incorporation patterns from the specifically labeled precursors, thus further confirming the mechanistic details

of Akabori transformation of glycine. Furthermore, the model system that included glucose also showed, in addition to the above-mentioned ions, additional major ions at *m/z* 238.0930, 325.1369, and 342.1392, which were absent when the glycine–copper complex was replaced with glycine. The first two ions incorporated 6 carbon atoms from U_6-^{13}C-glucose, and their elemental compositions indicated sugar amino acid(s) adducts, whereas the third ion incorporated 12 carbon atoms from U_6-^{13}C-glucose that can be assigned to a diglycosylated ammonia. (The details of the role of glucose during the Akabori reaction will be published elsewhere).

Table 4.2. Elemental composition [a] of the common products generated in $(Gly)_2Cu$/Paraformaldehyde model system without[b] and with[c] glucose and shown in Figures 4.2 and 4.3.

$[M+H]^+$ (*m/z*)	Elemental composition	Error (ppm)
106.0500	$C_3H_8NO_3$	3.9
136.0603	$C_4H_{10}NO_4$	5.0
235.9840/237.9830[b]	$C_6H_9CuN_2O_4$	7.8
241.9943/243.9924[b]	$C_5H_{11}CuN_2O_5$	8.7
265.9949/267.9934[b]	$C_7H_{11}CuN_2O_5$	5.6
272.0044/274.0033	$C_6H_{13}CuN_2O_6$	9.4
296.0054/298.0050[b]	$C_8H_{13}CuN_2O_6$	5.3
238.0930[c]	$C_8H_{16}NO_7$	1.3
325.1369[c]	$C_{11}H_{21}N_2O_9$	37.0
342.1407[c]	$C_{12}H_{24}NO_{10}$	1.9

[a]The two masses shown represent copper isotopes ^{63}Cu/^{65}Cu.
[b]Ions observed only in $(Gly)_2Cu$ /paraformaldehyde model system.
[c]Ions observed only in $(Gly)_2Cu$/paraformaldehyde/glucose model system.

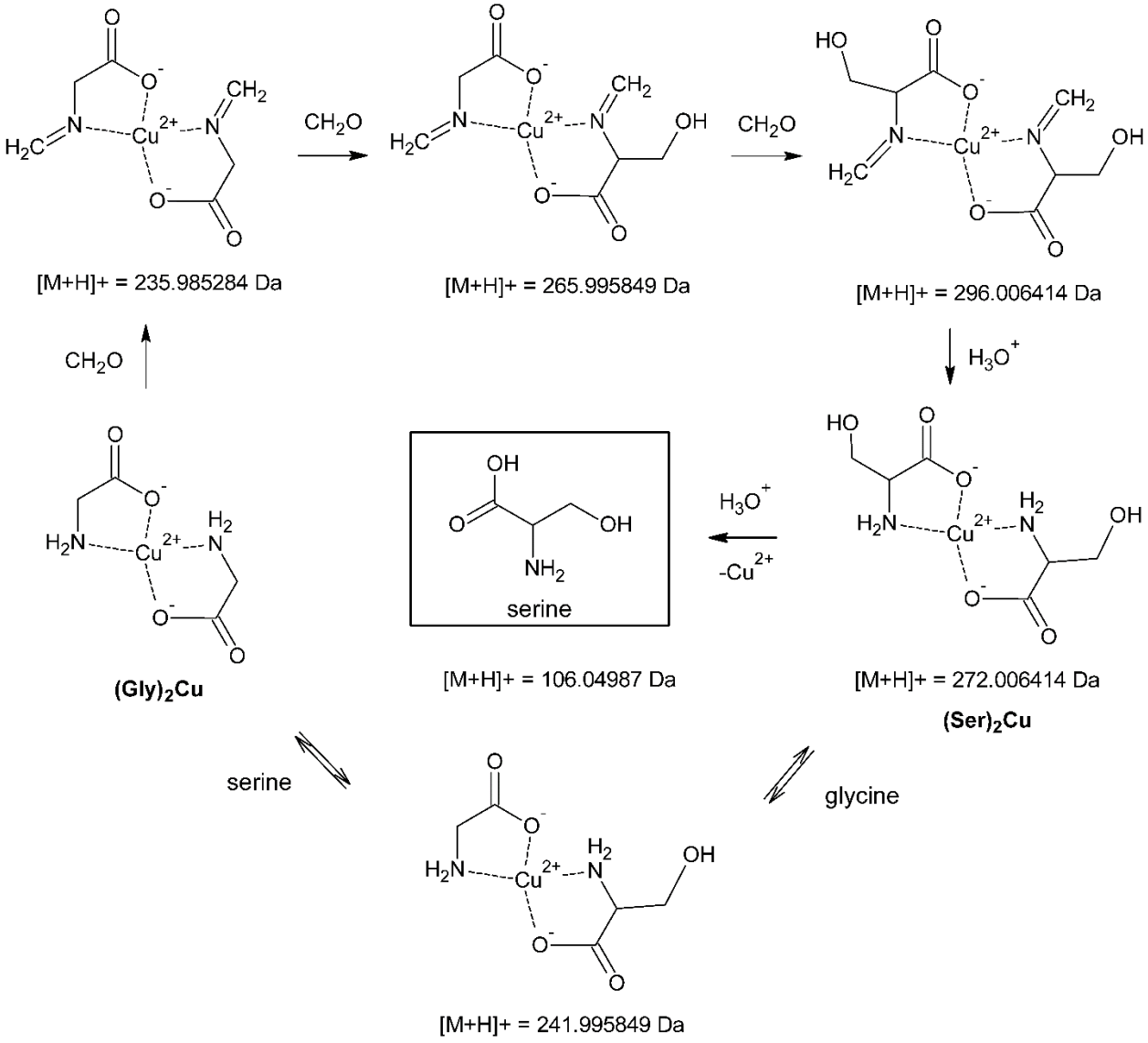

Figure 4.2. Mechanism of Akabori reaction in the presence of formaldehyde and generation of serine. $[M+1]^+$ values represent theoretical masses (corresponding observed masses are shown in Table 4.2).

Table 4.3 Elemental composition of copper containing intermediates in $(Ser)_2Cu$/paraformaldehyde model system shown in Figure 4.3.

$[M+H]^{+a}$ (*m/z*)	Elemental composition	Error(ppm)
296.0038/298.0048	$C_8H_{13}CuN_2O_6$	10.7
272.0056/274.0088	$C_6H_{13}CuN_2O_6$	5.0
284.0056/286.0035	$C_7H_{13}CuN_2O_6$	4.8
296.0038/298.0048	$C_8H_{13}CuN_2O_6$	10.7
314.0157/316.0144	$C_8H_{15}CuN_2O_7$	5.8
326.0153/328.0149	$C_9H_{15}CuN_2O_7$	6.8
356.0273/358.0323	$C_{10}H_{17}CuN_2O_8$	2.2
136.0607	$C_4H_{10}NO_4$	2.1
106.0500	$C_3H_8NO_3$	3.9

[a]The two masses shown represent copper isotopes $^{63}Cu/^{65}Cu$.

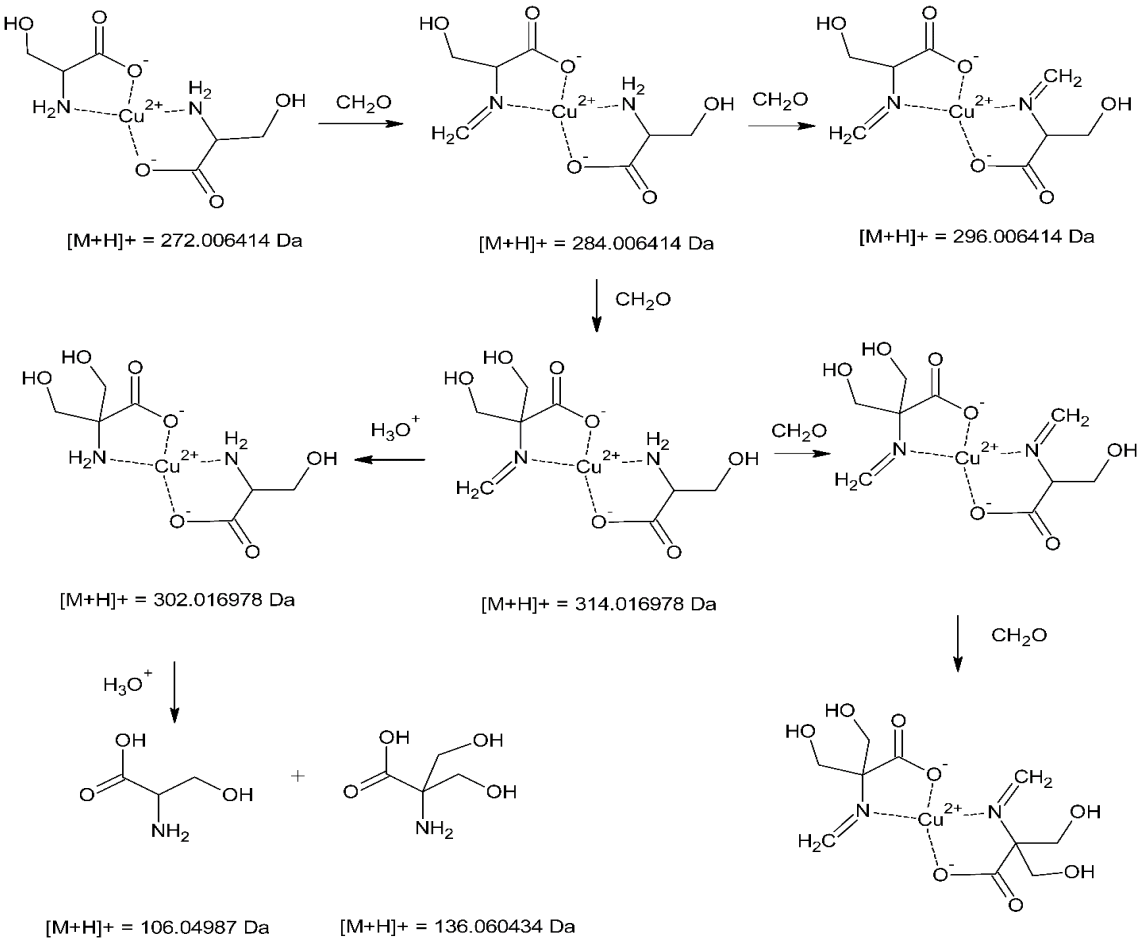

Figure 4.3. Intermediates identified in the reaction model of $(Ser)_2Cu/CH_2O$ heated in water at 110ºC for 2h. $[M+1]^+$ values represent theoretical masses (corresponding observed masses are shown in Table 4.3).

4.4.1 Mass Spectrometric and Isotope-Labeling Evidence for the Formation of Schiff Bases of Amino Acid–Metal Complexes with Aldehydes Prior to Akabori Transformation

The Akabori modification of amino acids is a stepwise transformation involving several consecutive reactions. Much like the Maillard reaction, a key initial step proposed in the Akabori reaction is the formation of imine between the amino groups of the metal complex and the excess aldehyde in the reaction mixture (Beck, 2009). This step is considered critical for the activation of the α-carbon. Although there is indirect evidence for the formation of this intermediate, no mass spectrometric evidence is presented so far. Analysis of the heated reaction mixture of $(Gly)_2Cu$ and formaldehyde indicated the formation of several copper complexes and the free serine as shown in Figure 4.2 and listed in Table 4.2. According to the intermediates identified in Figure 4.2, the glycine–copper complex undergoes double Schiff base formation with formaldehyde to generate the ion at *m*/*z* 235.9840. The activated complex then can react with two formaldehyde molecules to generate the ion at *m*/*z* 296.0054 followed by hydrolysis of the Schiff bases resulting in the formation of a $(Ser)_2Cu$ complex at *m*/*z* 272.0044. Depending on the pH, the amino acid–metal complexes can either undergo ligand exchange (Pearson and Lanier,1964) in the presence of free amino acids to generate the mixed complex (Gly)Cu(Ser) at *m*/*z* 241.9943 or decompose at lower pH values to release free amino acid serine at *m*/*z* 106.0500. As shown in Table 4.4, all of the listed intermediates display the expected isotope label incorporation patterns from C-1, C-2, and the nitrogen atom of glycine. Furthermore, each of the intermediate copper complexes also exhibited the isotopic signature of copper through detection of its M + 2 peaks at 30% relative intensity (Table 4.2). To confirm the formation of serine complex at *m*/*z* 272.0044 in the reaction mixture of $(Gly)_2Cu$ and formaldehyde, MS/MS analysis of synthetic $(Ser)_2Cu$ was performed and the product ions were compared with the daughter ions of *m*/*z* 272.0044 detected in the reaction mixture. The MS/MS fragments of this adduct matched exactly that of the synthetic standard (see Table 4.5). Furthermore, the synthetic $(Ser)_2Cu$ complex was reacted with formaldehyde to identify many of the other copper-containing complexes observed in the original reaction mixture of $(Gly)_2Cu$ and formaldehyde, which were thought to arise from the in situ formed $(Ser)_2Cu$ complex and the already present formaldehyde. Table 4.3 and Figure 4.3 show the observed and predicted complexes of copper that could be formed by the interaction of formaldehyde with serine–copper complex. These ions were also detected in the original reaction mixture of $(Gly)_2Cu$ and formaldehyde. The serine–copper complex, similar to the glycine–copper complex, can undergo Akabori transformation as shown in Figure 4.3 through Schiff base formation and

similarly generate its corresponding Akabori amino acid hydroxymethyl-serine observed at *m*/*z* 136.0603, which was originally identified by Akabori et al. (Akabori et al., 1959) as an unknown compound but later characterized as α-hydroxymethyl-serine by Otani and Winitz (Otani and Winitz,1960). The two key intermediates identified at *m*/*z* 314.0143 and 302.0151 (Figure 4.3) not only support the formation of α-hydroxymethyl-serine but provide further evidence for the importance of formation of Schiff base–metal complexes in the Akabori reaction. None of the above products were detected in the absence of copper complex of glycine or when free glycine was reacted with formaldehyde. The formation of α-hydroxymethyl-serine in this model system is noteworthy because it indicates the possibility of formation of unusual amino acids during the Maillard reaction. In addition, the reaction of alanine–copper complex with formaldehyde similarly generated the Schiff base adduct observed at *m*/*z* 264.0144, further supporting the importance and generality of Schiff base formation in the mechanism of Akabori reaction (see Figure 4.4; Table 4.6). These observations are not surprising and are consistent with the theoretical considerations regarding the ease of Schiff base formation on the amino groups of metal complexes due to the extra stabilization gained through hyperconjugation of its π-system with the metal (Belikov et al., 1969), and consequently, further enhancing the acidity of the α-carbon due to additional delocalization of the negative charge over the newly formed imminium moiety (Crugeiras et al., 2011), giving rise to a more reactive α-carbanion intermediate capable of being alkylated more readily by formaldehyde.

Table 4.4. Incorporation of labeled glycine atoms into the products of heated $(Gly)_2Cu/CH_2O$ model system (See Figure 4.2).

$[M+H]^+$ (*m/z*)	Elemental composition	Label incorporation from glycine[a]
106.0500	$C_3H_8NO_3$	1x C-1, 1x C-2, 1x N-15
136.0603	$C_4H_{10}NO_4$	1x C-1, 1x C-2, 1x N-15
235.9840	$C_6H_9CuN_2O_4$	2x C-1*, 2x C-2, 2x N-15
241.9943	$C_5H_{11}CuN_2O_5$	2x C-1, 2x C-2, 2x N-15
265.9949	$C_7H_{11}CuN_2O_5$	2x C-1, 2x C-2*, 2x N-15
272.0044	$C_6H_{13}CuN_2O_6$	2x C-1, 2x C-2, 2x N-15
296.0054	$C_8H_{13}CuN_2O_6$	2x C-1, 2x C-2, 2x N-15*

[a] The calculated error (in ppm) in all the reported ions ranged between 0.23 to 15.5 ppm except ions indicated by asterix where the error ranged between 17.3 to 28 ppm.

Table 4.5. Comparison of elemental composition[a] and accurate masses of product ions at m/z 272.0059 [generated from synthetic $(Ser)_2Cu$] and that of ion at *m/z* 272.0044 generated in the $(Gly)_2Cu/CH_2O$ reaction mixture.

Product ions of m/z 272.0059 $[M+H]^+$	Product ions of *m/z* 272.0044 $[M+H]^+$
241.9947 ($C_5H_{11}CuN_2O_5$)	241.9956 ($C_5H_{11}CuN_2O_5$)
210.0053($C_5H_{11}CuN_2O_{3)}$	210.0061 ($C_5H_{11}CuN_2O_3$)
185.9814 (C_3H_9CuNO4)	185.9826 (C_3H_9CuNO4)
123.9809 (C_2H_7CuNO)	123.9843 (C_2H_7CuNO)
106.0530 ($C_3H_8NO_3$)	106.0532 ($C_3H_8NO_3$)

[a] The calculated error (in ppm) in all the reported ions ranged between 3 and 26 ppm.

Table 4.6. Elemental composition of the reaction products[a] in the $(Ala)_2Cu$/paraformaldehyde model system shown in Figure 4.4.

$[M+H]^+$ (*m/z*)	Elemental composition	Error (ppm)
120.0650	$C_4H_{10}NO_3$	8.9
132.0645	$C_5H_{10}NO_3$	11.9
264.0144/266.0120[a]	$C_8H_{13}CuN_2O_4$	10.3

[a]The two masses shown represent copper isotopes $^{63}Cu/^{65}Cu$.

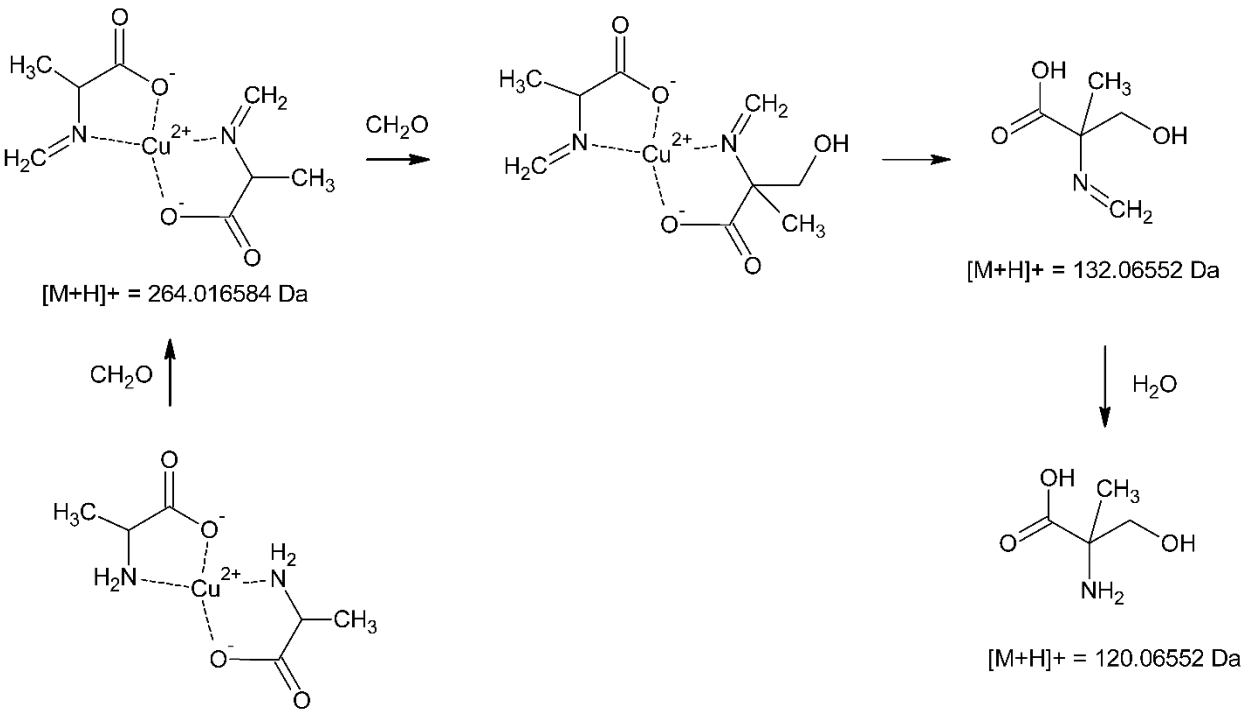

Figure 4.4. Formation of Akabori amino acid from $(Ala)_2Cu$ and CH_2O. $[M+1]^+$ values represent theoretical masses (corresponding observed masses are shown in Table 4.6).

4.4.2 Implications of the Akabori Transformation to the Volatile Profile of the Maillard Reaction

Considering that $(Gly)_2Cu$ when heated will generate serine in the presence of formaldehyde, it was expected that volatiles generated in this model system should resemble the volatiles generated in a glycine/serine system. Indeed, when the dried residues of the above heated model systems (unheated samples when pyrolyzed did not generate any volatiles) were thermally desorbed, five of the six major peaks shown in Figure 4.5 were found to be in common. Similarly, the $(Gly)_2Cu$/serine model system also shared these common peaks as shown in Figure 4.5. More importantly, the intensities of these peaks in the Akabori model system of $(Gly)_2Cu$/formaldehyde were significantly enhanced, indicating the ability of $(Gly)_2Cu$ to sustain the transformation of glycine into serine through stabilization of the important precursors shown in Figures 4.2 and 4.3 that can act as a reservoir for the continuous generation of volatiles.

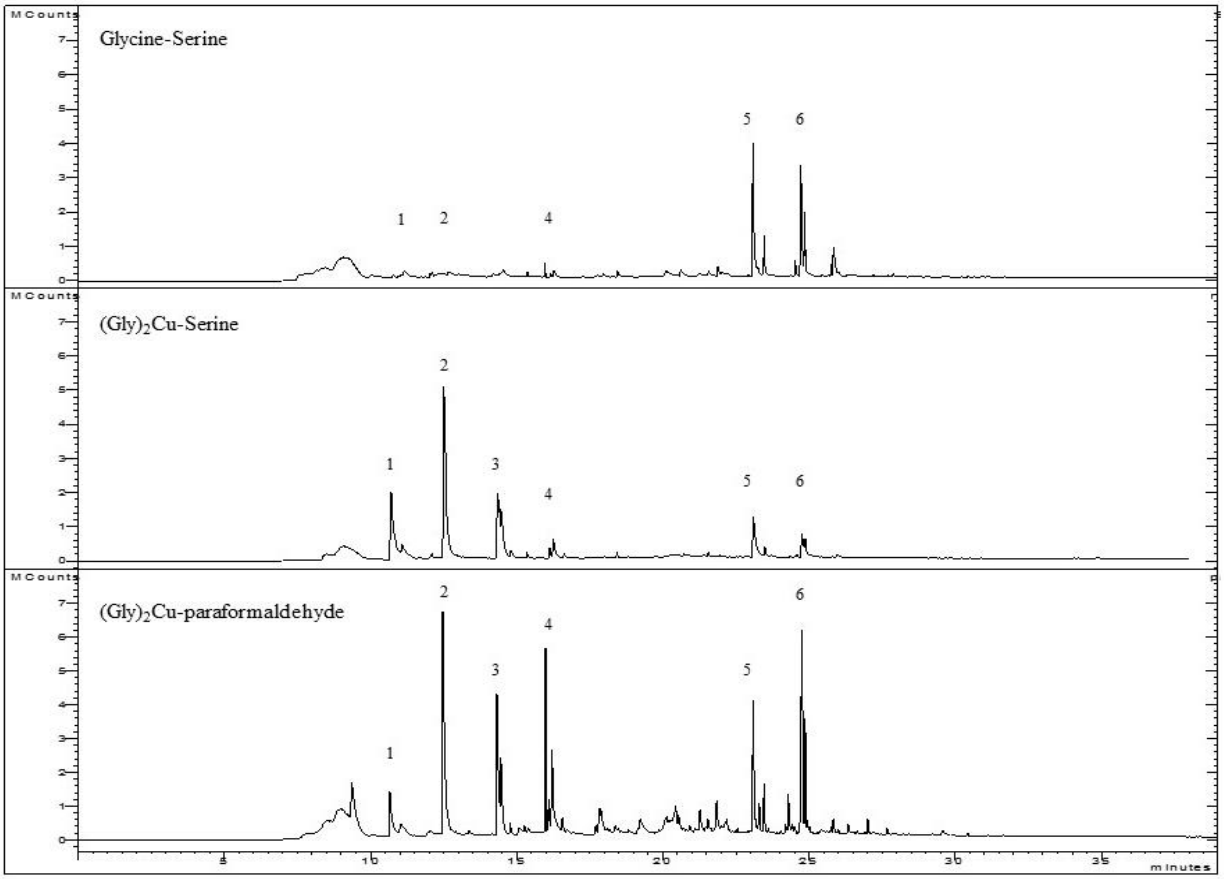

Figure 4.5. Comparison of the major volatile compounds thermally desorbed from the heated (in water at 110°C) residues of glycine/serine, $(Gly)_2Cu$/Serine and $(Gly)_2Cu$/paraformaldehyde model systems. (1) 2-methyl-(1*H*)-pyrrole, (2) 2-methylpyrazine, (3) 2,6-dimethylpyrazine, (4) 1,3,5-trimethyl hexahydrotriazine, (5) 1,5-dimethyl-2(1*H*)-pyrazinone, (6) 1,5,6-trimethyl-2(1*H*)-pyrazinone.

CONNECTING PARAGRAPH

Chapter 4 provided for the first time mass spectrometric evidence for the detailed mechanism of Akabori transformation of glycine into serine through the Schiff base intermediate of glycine-copper complex with formaldehyde. In chapter 5, we explore further the reactivity of glycine-copper complex towards larger aldehydes such as glucose in the presence and absence of smaller Strecker aldehydes. The presence of sugars in the Maillard reaction mixtures containing copper complexes of glycine and alanine was found not to interfere with Akabori transformation and on the contrary the sugars were also able to form stable amino acid metal complexes through covalent attachment as Schiff bases and were found to enhance the production Maillard reaction products. Chapter 5 was published in the Journal of Agriculture and Food Chemistry: Nashalian, O.; Yaylayan, V. A. (2015). Sugar-conjugated bis(glycinato)copper(II) complexes and their modulating influence on the Maillard reaction. *Journal of Agriculture and. Food Chem*istry, 63, 4353-4360.

CHAPTER 5

SUGAR CONJUGATED BIS(GLYCINATO) COPPER(II) COMPLEXES AND THEIR MODULATING INFLUENCE ON THE MAILLARD REACTION

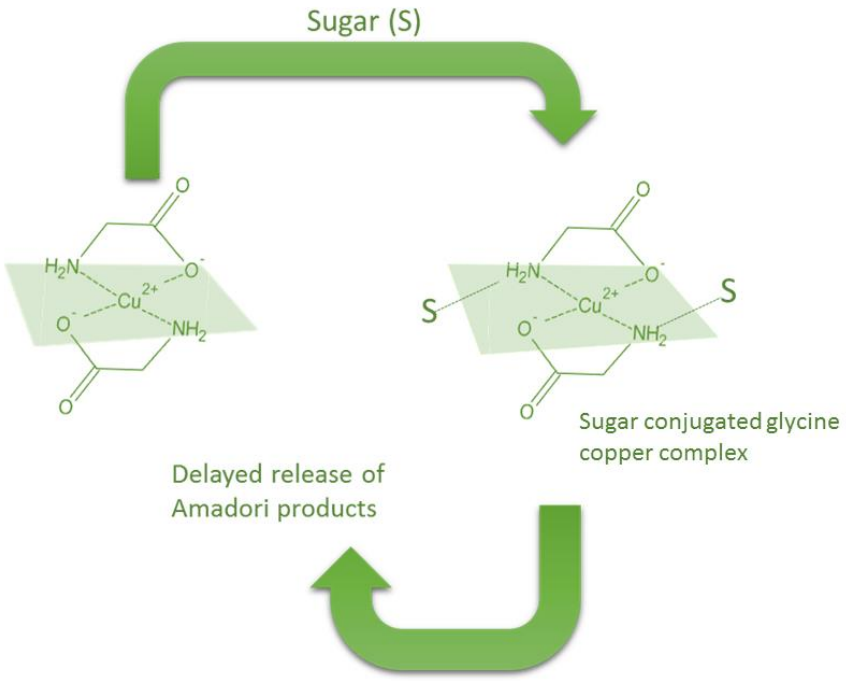

5.1 ABSTRACT

Transition metal ions are known to play an important role in the Maillard reaction in catalyzing redox reactions. They can also form strong binary complexes with amino acids with increased reactivity toward smaller aldehydes. To take advantage of this enhanced reactivity and to demonstrate the ability of glucose to conjugate with glycine copper complexes, model systems containing $(Gly)_2Cu$ and glucose or their isotopically enriched counterparts were heated in aqueous solutions in the presence and absence of paraformaldehyde at 110 °C for 2 h and the residues were analyzed by electrospray ionization/quadrupole time-of-flight/mass spectrometry (ESI/qTOF/MS). Isotope-labeling studies have indicated the ability of $(Gly)_2Cu$ complexes to act as molecular scaffolds and undergo multiple reactions with glucose to generate various complexes of sugar conjugates. These relatively stable intermediates allowed for the slower release of aroma and browning precursors, such as Amadori products, during heating, as assessed by the extent of browning and total volatile release.

5.2 INTRODUCTION

Thermally induced chemical transformations of sugars and amino acids during the Maillard reaction are generally regulated by the reaction conditions, such time, temperature, concentration, pH, solvent, and most importantly, nature of the initial reactants and composition of the reaction medium. Transition metals, for example, are one such component that are known to play an important role in regulating the Maillard reaction through their high ligand binding affinity toward sugars and amino acids and because of their redox activity, leading to enhanced reaction rates and color development in aqueous systems (Kwak and Lim, 2004; O'Brien Morrissey,1997; Ramonaitytė et al., 2009; Rizzi,1997). Among the Maillard reaction components, amino acids are the ideal ligands for complexation, especially with copper, leading to binary complexes (Beck, 2009, 2011) in which the metal ion is bound to the amino acid through amino and carboxylate groups (see Figure 5.1). Through such complexations, the amino acid–metal complexes have demonstrated to play a multifunctional role, such as enhanced Strecker aldehyde formation, oxidative decarboxylation (Nashalian and Yaylayan,2014; Yablokov et al., 2014) and conversion of one amino acid into another through Akabori reaction (Akabori et al., 1959; Nashalian and Yaylayan et al., 2015a). In addition to amino acids, copper has also been found to form stable

complexes with Amadori rearrangement products, such as the *n*-butylamine/glucose Amadori copper complex synthesized by Horikawa et al. (2002), which was found to undergo oxidative degradation to generate hydroxyl radicals and various dicarbonyl products faster than its free counterpart (Horikawa et al, 2002). Similarly, Cheng and Kawakishi (1994) reported several copper-catalyzed oxidative decomposition products of Amadori compounds of tripeptides (Cheng and Kawakishi, 1994). Tonkovicc et al. (1997) and Gyurcsik et al. (1993) also prepared synthetic complexes of different Amadori compounds with iron, copper, and nickel and characterized them using various analytical techniques such as X-ray spectroscopy, nuclear magnetic resonance (NMR), and circular dichroism (CD) spectroscopy (Gyurcsik et al., 1993; Tonkovicc et al., 1997). Currently, there is no clear understanding of the relative importance of metal ions as catalysts for oxidation or as complexing agents forming stable amino acid complexes. It is predicted that such complexes can serve as molecular scaffolds upon which different sugar moieties can be assembled, accumulated, and released over time. This fact can create the opportunity for controlling the generation of color and flavor from their precursors over a longer period of time. In this study, we explore the consequences of replacing amino acids with their copper complexes in heated aqueous (110 °C for 2 h) Maillard model systems.

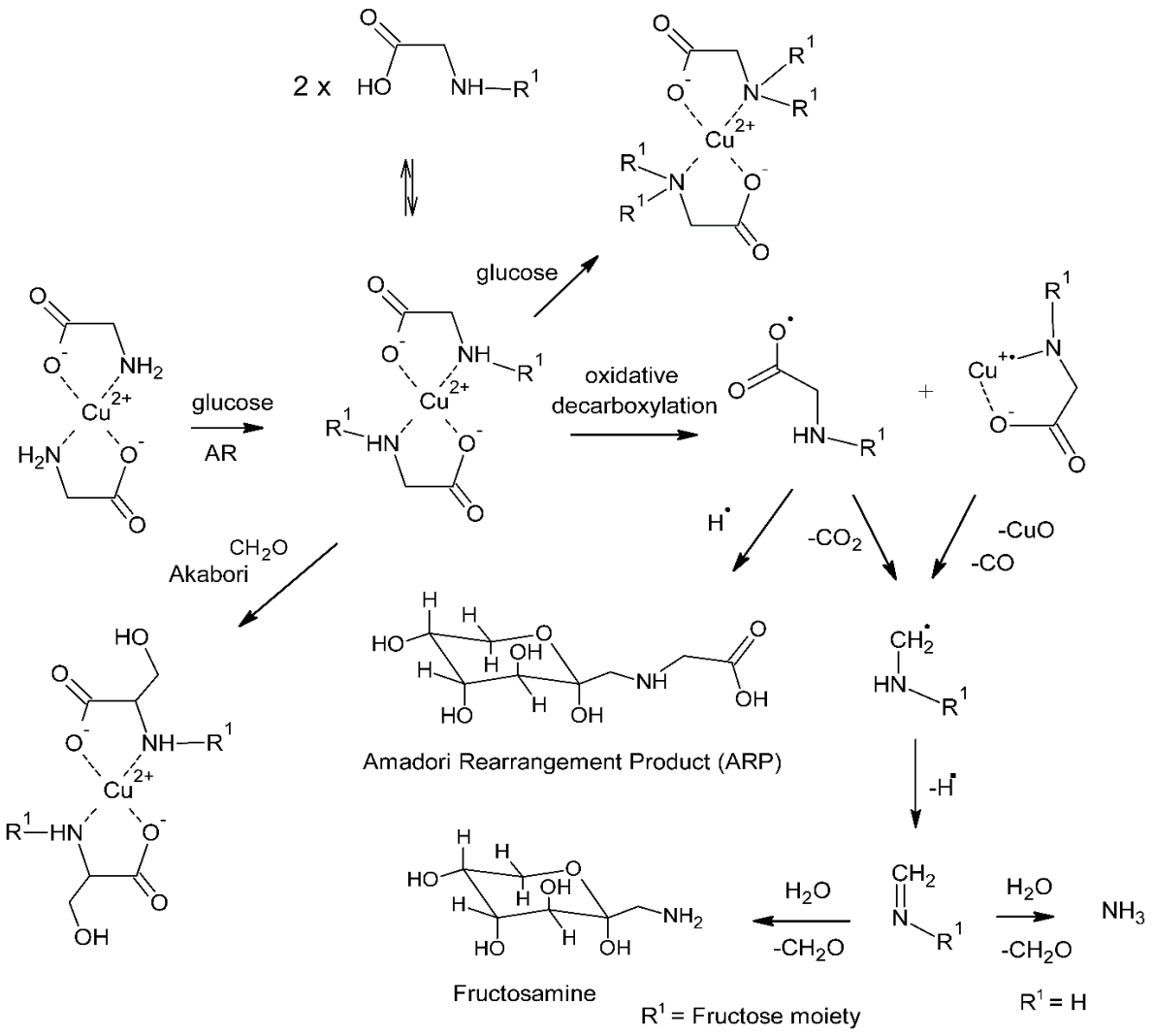

Figure 5.1. Mechanism of oxidative decarboxylation of free or sugar-conjugated amino acid copper complexes based on Nashalian and Yaylayan, 2014.
ARP Amadori Rearrangement Product
AR Amadori Rearrangement
R^1 = H or sugar moiety

5.3 MATERIALS AND METHODS

5.3.1 Materials and Reagents

L-Glycine (98%), D-glucose, paraformaldehyde, potassium hydroxide (KOH), copper(II) chloride ($CuCl_2$) (99.9%), 1-amino-1-deoxy-β-D-glucose, and ninhydrin reagent [2% in dimethyl sulfoxide (DMSO) and lithium acetate buffer] were purchased from Sigma-Aldrich Chemical Co. (Oakville, Ontario, Canada). *N*-(1-Deoxy-β-D-fructopyranos-1-yl)glycine (fructosylglycine) was purchased

from Toronto Research Chemicals (Toronto, Ontario, Canada). [^{13}C-1,^{13}C-2,^{15}N]Glycine (98%) and [U_6-^{13}C]glucose (99%) were purchased from Cambridge Isotope Laboratories (Andover, MI). Liquid chromatography–mass spectrometry (LC–MS)-grade water and methanol (OmniSolv, >99%) were obtained from VWR International (Mississauga, Ontario, Canada).

5.3.2 Synthesis of Amino Acid–Metal Complexes

$(Gly)_2Cu$ complexes were prepared by dissolving glycine (0.75 g) in methanol (10 mL) in the presence of KOH (0.05 g), followed by the addition of half a mole of $CuCl_2$ (0.67 g). The dark blue precipitate was washed with methanol, filtered, and dried. The glycine–copper complex was confirmed by obtaining its elemental composition from their accurate masses determined by electrospray ionization/quadrupole time-of-flight/mass spectrometry (ESI/qTOF/MS) analysis at *m*/*z* 233.9665 $[M + Na]^+$ (calculated for $C_4H_8CuN_2NaO_4$ with an error of 5.4 ppm). Isotope-labeled precursors were prepared similarly.

5.3.3 Sample Preparation

Model systems (10 mg) consisting of glycine/glucose (in a 2:1 relative molar ratio), glycine/glucose/$CuCl_2$ (in a 2:1:1 relative molar ratio), and $(Gly)_2Cu$/glucose (in a 1:1 relative molar ratio) with or without excess paraformaldehyde (20 mg) were dissolved in water (2 mL) and heated on a sand bath in an open vial (5 mL capacity) at 110 °C for 2 h until dry. During the reaction, the water evaporated and the sample was completely dried during the last 20 min of heating. To confirm the formation of some of the observed intermediates, commercial standards, such as glycine Amadori compound and 1-amino-1-deoxy-β-D-glucose, were used in appropriate model systems, as shown in Table 5.1. The reaction mixtures were subsequently analyzed by ESI/qTOF/MS, and some were analyzed by pyrolysis–gas chromatography/mass spectrometry (Py–GC/MS) for their volatile content. All of the samples were analyzed in duplicates.

Table 5.1. Composition of the model systems.

Model systems prepared under Akabori reaction conditions
Glycine/glucose/paraformaldehyde[a,b] (2-1)
$(Gly)_2Cu$/glucose/paraformaldehyde[b]
Model systems prepared under Maillard reaction conditions
Glycine/glucose[a,c] (2-1)
Glycine/glucose/$CuCl_2$[a] (2-1-1)
$(Gly)_2Cu$/glucose[c]
N-(1-deoxy-D-fructos-1-yl)glycine[d] (glycine Amadori compound)
N-(1-deoxy-D-fructos-1-yl)glycine/$CuCl_2$
1-Amino-1-deoxy-β-D-glucose[d]
Glucose/1-amino-1-deoxy-β-D-glucose
Glucose/1-amino-1-deoxy-β-D-glucose/$CuCl_2$

[a] Model systems that were prepared and analyzed in a 2:1 molar ratio. All other model systems in the table were prepared and analyzed in a 1:1 molar ratio.
[b] Paraformaldehyde was added in excess in the Akabori reaction model systems.
[c] Analyzed by Py/GC-MS in addition to ESI/qTOF/MS analysis.
[d] Analyzed before and after heating at 110°C for 2h

5.3.4 Ninhydrin Test

Amino acid loss (glycine) was determined using the "ninhydrin reagent solution" test method by Sigma-Aldrich, Inc., using ninhydrin reagent (2% in DMSO and lithium acetate buffer). Model systems comprising glycine/glucose and $(Gly)_2Cu$/glucose, both containing 0.05 μmol/mL (50 μM) glycine in the final concentration, were dissolved in water (2 mL) and heated at 110 °C for 2 h in a sand bath until completely dry. After heating, the residues were dissolved in water (0.5 L) and 1 mL aliquots were pipetted into test tubes. To each aliquot, ninhydrin (1 mL) reagent was added, and the test tubes were placed in a sand bath at 100 °C for 10 min. After cooling to room temperature, 95% ethanol (5 mL) was added to each test tube. The absorbance was measured at 570 nm using distilled water as a blank on an Evolution 300 ultraviolet–visible (UV–vis) spectrophotometer (Thermo Fisher Scientific, Waltham, MA).

5.3.5 Spectrophotometric Measurements

Absorbance at 420 and 550 nm was used to estimate browning of the model systems heated on a sand bath in an open vial at 110 °C for 2 h until dry. Samples (10 mg) comprising glycine/glucose (in a 2:1 relative molar ratio), glycine/glucose/$CuCl_2$ (in a 2:1:1 relative molar ratio), and

$(Gly)_2Cu$/glucose (in a 1:1 relative molar ratio) were dissolved in water (2 mL), and their absorbance was measured before and after heating, as indicated above. In both cases, the samples were diluted in distilled water (0.5 L) and 1 mL of each solution was used for the measurements. Absorbance of the samples were measured on an Evolution 300 UV–vis spectrophotometer (Thermo Fisher Scientific, Waltham, MA) using distilled water as a blank.

5.3.6 ESI/qTOF/MS Analysis

The dry reaction mixtures were dissolved in liquid chromatography (LC)-grade water to a concentration of 1 mg/mL. The samples were then diluted 10-fold in 10% methanol prior to analysis by ESI/qTOF/MS. The ESI/qTOF/MS system was comprised of a Bruker Maxis Impact quadrupole-time-of-flight mass spectrometer (Bruker Daltonics, Bremen, Germany) operated in positive-ion mode. Samples (1 μL) were injected directly into ESI/qTOF/MS. Instrument calibration was performed using sodium formate clusters. The electrospray interface settings were the following: nebulizer pressure, 0.6 bar; drying gas, 4 L/min; temperature, 180 °C; and capillary voltage, 4500 V. The scan range was from *m*/*z* 100 to 1000. The data were analyzed using Bruker Compass DataAnalysis software, version 4.1. Tandem mass spectrometry (MS/MS) was carried out in multiple reaction monitoring (MRM) mode using 20.0 eV collision energy for the ions at *m*/*z* 180 and 342.

5.3.7 Thermal Desorption by Py–GC/MS

A Varian CP-3800 gas chromatograph coupled to a Saturn 2000 ion-trap detector interfaced to a CDS Pyroprobe 2000 unit through a valved interface (CDS 1500) was used for the desorption of the volatiles from glycine/glucose and $(Gly)_2Cu$/glucose model systems before and after heating in water (2 mL) at 110 °C for 2 h. For each analysis, approximately 0.5 mg of sample was weighed into a quartz tube, sealed with glass wool, inserted into the pyroprobe, and pyrolyzed for 20 s at 250 °C. The separation was performed using a fused silica DB-5MS column (50 m length × 0.2 mm inner diameter × 33 μm film thickness). The GC method used for the analysis of the volatiles was as follows: GC column flow rate was regulated by an electronic flow controller (EFC) and set at a pressure pulse of 55 psi for the first 3 min, then decreased to 32 psi at the rate of 300 psi/min, and finally, increased to 70 psi at a rate of 1.23 psi/min for the rest of the run. The GC oven temperature was set at −5 °C for the first 5 min using CO_2 as the cryogenic cooling source and

then increased to 50 °C at a rate of 50 °C/min. Then, the oven temperature was again increased to 270 °C at a rate of 8 °C/min and kept at 270 °C for 5 min. The samples were detected using an ion-trap mass spectrometer. The MS transfer-line temperature was set at 250 °C; the manifold temperature was set at 50 °C; and the ion-trap temperature was set at 175 °C. The ionization voltage of 70 eV was used, and the electron multiplier voltage (EMV) was set at 1600 V. The generated data were analyzed using the AMDIS 32, version 2.69, computer software, and peak identification will be performed using the National Institute of Standards and Technology (NIST), version 2.0, mass spectral research program.

5.3.8 Structural Identification

Evidence for the proposed structures of non-volatile reaction intermediates was provided through ESI/qTOF/MS analysis of their elemental composition and the use of commercial or synthetic intermediates and isotope-labeling studies. Furthermore, MS/MS spectra of selected product ions were compared to those of commercial standards. The incorporation of copper in the identified complexes was confirmed by the isotopic signature of copper through detection of M + 2 peaks at 30% relative intensity.

5.4 Results and Discussion

The development of color and aromas during the Maillard reaction is highly dependent upon the nature of amino acids and sugars used and the stability of the resultant Amadori products, in addition to other environmental factors that can either promote or hinder the reactivity of Amadori compounds, such as the transition metal ions. Such ions in their free form can accelerate oxidative degradation of sugars and Amadori products and enhance browning. On the other hand, amino acids can serve as potent ligands for metal ions not only to form strong complexes but also to provide stable backbones that can act as molecular scaffolds upon which up to four sugar molecules can be conjugated as Schiff bases or Amadori rearrangement products (see Figure 5.1). The buildup of such relatively stable intermediates can serve as a vehicle for their slow and steady release over the course of the reaction that in theory can affect the overall reaction profile. There are three possible pathways that allow for the release of the amino acids or their conjugates from the complexes; dissociation of the complex and ligand exchange (Nashalian and Yaylayan,2015a;

Pearson and Lanier,1964) are considered as non-destructive mechanisms of release, and the third is through oxidative decarboxylation (Nashalian and Yaylayan,2014), where one of the amino acid moieties in the complex is decomposed and the other is released intact, as shown in Figure 5.1. Previous experiments with glycine copper complexes have demonstrated the enhanced ability of the amino groups in the complexes to undergo Schiff base formation with small aldehydes (Nashalian and Yaylayan, 2015a) and their subsequent Akabori reaction and/or oxidative decarboxylation (Nashalian and Yaylayan,2014) (see Figure 5.1). To take advantage of this enhanced reactivity of the amino groups of copper complexes of amino acids toward carbonyl compounds and to demonstrate the ability of glucose to conjugate with glycine copper complexes, model systems containing $(Gly)_2Cu$ and glucose were heated in aqueous solutions in the presence and absence of paraformaldehyde at 110 °C for 2 h and the dry residues were analyzed by ESI/qTOF/MS, with the major ions observed listed in Table 5.2. Control reactions conducted between free glycine and glucose indicated that the ions listed in Table 5.2 were not generated in the absence of the copper complexes. However, in the presence of free $CuCl_2$, the glycine/glucose mixture also generated the same peaks, although to a lesser extent. A logical sequence of reaction steps between $(Gly)_2Cu$ and glucose using the identified ions is shown in Figure 5.2. This figure also shows all of the corresponding ions generated through Akabori reaction (Nashalian and Yaylayan,2015a) in the presence of formaldehyde. Interestingly, in the presence of glucose, formaldehyde Schiff bases of $(Gly)_2Cu$ complexes were not observed.

Table 5.2. Elemental composition[a] and isotope incorporation in the products originating from $(Gly)_2Cu$/Glc model system in the absence and presence of paraformaldehyde (Akabori reaction conditions) and shown in Figure 5.2.

$[M+H]^+$ (*m/z*)[b]	Elemental composition	[^{13}C-U$_6$]Glc	[^{13}C-1]Gly	[^{13}C-2]Gly	[^{15}N]Gly
180.0872	$C_6H_{14}NO_5$	6	0	0	1
192.0856	$C_7H_{14}NO_5$	6	0	1	1
202.0709	$C_8H_{12}NO_5$	6	1	1	1
220.0816	$C_8H_{14}NO_6$	6	1	1	1
238.0930	$C_8H_{16}NO_7$	6	1	1	1
268.1038[c]	$C_9H_{18}NO_8$	6	na[d]	na	na
299.0038/301.0028	$C_8H_{14}CuNO_7$	6	1	1	1
300.0079/302.0059	$C_8H_{15}CuNO_7$	6	1	1	1
324.1268	$C_{12}H_{22}NO_9$	12	0	0	1
329.0173/331.0163[c]	$C_9H_{16}CuNO_8$	6	na	na	na
330.0228/332.0281[c]	$C_9H_{17}CuNO_8$	6	na	na	na
342.1405	$C_{12}H_{24}NO_{10}$	12	0	0	1
374.0355/376.0313	$C_{10}H_{19}CuN_2O_9$	6	2	2	2
404.0508/406.0511[c]	$C_{11}H_{21}CuN_2O_{10}$	6	na	na	na
434.0611/436.0599[c]	$C_{12}H_{23}CuN_2O_{11}$	6	na	na	na
536.0925/538.0912	$C_{16}H_{29}CuN_2O_{14}$	12	2	2	2
566.1019/568.1027[c]	$C_{17}H_{31}CuN_2O_{15}$	12	na	na	na

[a] All of the ions listed in Figure 5.2 are included in this table.
[b] The calculated error (in ppm) in all the reported ions ranged between 0.02-22ppm and the two masses shown represent copper isotopes $^{63}Cu/^{65}Cu$
[c] Products formed only in the model system containing CH_2O.
[d] na =not analyzed.

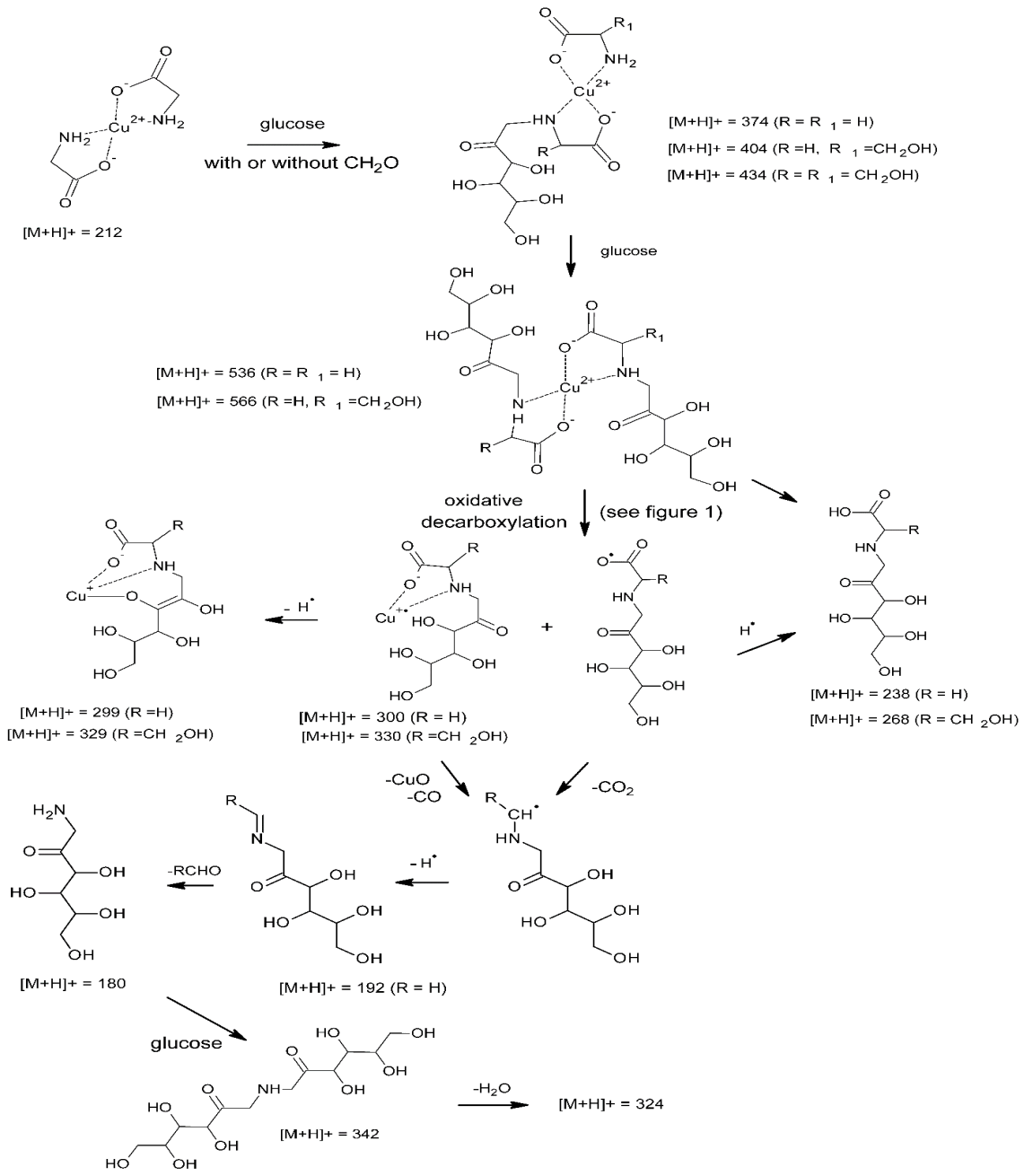

Figure 5.2. Proposed interaction of $(Gly)_2Cu$ with glucose in the presence or absence of formaldehyde

5.4.1 Glucose Conjugation with the Glycine Copper Complex

Much like the initial phase of the Maillard reaction, $(Gly)_2Cu$ can react with glucose via one of its amino groups to form Schiff bases or its Amadori rearrangement products. Theoretically, up to four sugar molecules can be conjugated with the complex. Mono- and diconjugated complexes

were observed in the $(Gly)_2Cu$/glucose model system at *m*/*z* 374.0355 and 536.0925, respectively (see Figure 5.2). In the presence of formaldehyde, the Akabori reaction will transform glycine into a serine moiety (Nashalian and Yaylayan, 2015a); consequently, in a $(Gly)_2Cu$/glucose/paraformaldehyde model system, monoconjugated complexes with either mixed amino acids observed at *m*/*z* 404.0508 or only serine at *m*/*z* 434.0611 and diconjugated complexes with mixed amino acids at *m*/*z* 566.1019 (Table 5.2 and Figure 5.2) were also detected. In Figure 5.2, diconjugated complexes are depicted as one of the two possible isomeric structures. Both mono- and diconjugated complexes can dissociate or undergo ligand exchange to release the sugar-conjugated amino acids at *m*/*z* 238.0930 (as glycine) or *m*/*z* 268.1038 (as serine). Furthermore, these complexes also underwent an oxidative decarboxylation reaction similar to the unreacted $(Gly)_2Cu$ complex (Nashalian and Yaylayan,2014), as confirmed through observation of a series of ions consistent with the process shown in Figure 5.1. This process is capable of generating free (*m*/*z* 238.0930) and a monomeric copper complex of Amadori compound (*m*/*z* 300.0079) in addition to fructosamine (*m*/*z* 180.0872) through hydrolysis of the Schiff base observed at *m*/*z* 192.0856. Furthermore, the formation of a monomeric Amadori copper complex at *m*/*z* 300.0079 was further confirmed by observing the formation of the same ion in a control experiment, where the synthetic glycine Amadori compound and $CuCl_2$ mixtures were reacted under the same conditions. The detection of the Amadori copper complex at *m*/*z* 300.0079 represents the first evidence for the *in situ* formation of the complex from glucose and a $(Gly)_2Cu$ complex.

5.4.2 Release of Amadori Products

The conjugated Amadori products could be released from the mono- or dimeric complexes observed at *m*/*z* 374.0355 and 536.0925, respectively, through either dissociation or their oxidative decarboxylation and formation of the Amadori carboxyl radical, which can combine with a hydrogen radical to form the free Amadori compound. Ions associated with the free glycine Amadori product at *m*/*z* 238.0930 along with its dehydrated derivatives were observed at *m*/*z* 220.0816 and 202.0709 in the $(Gly)_2Cu$/glucose mixtures. The Amadori product incorporated six carbon atoms from glucose and two carbon atoms (C-1 and C-2) and one nitrogen atom from glycine. The serine Amadori compound observed at *m*/*z* 268.1038 was similarly identified in the $(Gly)_2Cu$/glucose/formaldehyde mixture incorporating six carbon atoms from glucose and two carbon and one nitrogen atom from glycine (see Table 5.2).

5.4.3 Formation of Fructosamine and Deoxy-fructosamine

In the process of oxidative decarboxylation of $(Gly)_2Cu$ complexes shown in Figures 5.1 and 5.2, two free radical species can be formed: one is the Amadori carboxyl radical, and the other is the copper-centered radical in the Amadori monocopper complex at *m*/*z* 300.0079. The former can decarboxylate, and the latter can lose CO and CuO molecules to form the same decarboxylated Amadori free radical, which can immediately lose a hydrogen atom to form the Schiff base observed at *m*/*z* 192.0856 (see Figure 5.2). In this reaction mixture, an ion at *m*/*z* 180.0872 was also observed that was assigned to the fructosamine structure, the hydrolysis product of the above Schiff base through the loss of the Strecker aldehyde. This structure is expected to be formed from oxidative decarboxylation reactions of $(Gly)_2Cu$ complexes (Nashalian and Yaylayan, 2014; Yablokov et al.,2014). The tentative assignment of the fructosamine structure was based on its proposed mechanism of formation shown in Figure 5.2. In addition, the ion had a consistent elemental composition ($[M + H]^+$ $C_6H_{14}NO_5$) to that of fructosamine and showed incorporation of six carbon atoms from glucose and only one atom (nitrogen) from glycine (Table 5.2 and Figure 5.2). The structural information regarding the ion at *m*/*z* 180.0872 can also apply to its corresponding Schiff base, glycosylamine, which is typically synthesized by reacting glucose with highly reactive ammonia (Isbell and Frush, 1958; Linek et al., 1993). To further confirm the structure of the ion observed at *m*/*z* 180.0872, the commercially available Schiff base precursor (1-amino-1-deoxy-glucose or glycosylamine) was heated alone or in the presence of glucose and $CuCl_2$ in water at 110 °C for 2 h and the MS/MS spectra of the ions at *m*/*z* 180 generated in the model systems were recorded (Table 5.3). The observed MS/MS fragmentation pattern of *m*/*z* 180.0865 in the heated standard matched exactly the ions generated from the ion at 180.0872 in the heated $(Gly)_2Cu$/glucose mixture and was different from the ions in the unheated sample of 1-amino-1-deoxy-glucose, indicating that, during heating in an aqueous solution, the standard Schiff base was rearranged into its observed Amadori form. Fructosamine and the associated ions at *m*/*z* 180.0872, 192.0856, and 330.0228 were similarly generated in the formaldehyde-containing model system. The assigned fructosamine structure was further supported by the observation of its glucose adduct observed at *m*/*z* 342.1405 and its further dehydration product at *m*/*z* 324.1268. The MS/MS fragmentation of *m*/*z* 342.1405 in the reaction mixture and that generated from the heated mixtures of glucose in the presence of 1-amino-1-deoxy-glucose was also compared and found to match (Table 5.4). To our knowledge, fructosamine thus far has not been identified in any Maillard

model systems, except in synthetic preparations (Mossine and Mawhinney, 2010). An ion related to fructosamine was also identified in the reaction mixture at *m*/*z* 164.0924; this ion, similar to fructosamine, consisted of six carbon atoms derived from glucose and one nitrogen and no carbon atoms from glycine and was predicted to originate from fructosamine (*m*/*z* 180.0872) through the loss of an oxygen atom (see Figure 5.3). Such a loss could be envisaged to occur through copper-catalyzed carbon–oxygen bond cleavage with a simultaneous hydride transfer, as suggested by Rao and Rao (Rao and Rao, 2015). A proposed mechanism based on this suggestion is presented in Figure 5.3. In this proposal, the copper-centered free radical complex that forms as a result of oxidative decarboxylation of $(Gly)_2Cu$ shown in Figure 5.1 can either scavenge a hydrogen radical formed during oxidative decarboxylation and form copper hydride observed at *m*/*z* 138.9689 (pathway A) or combine with the oxygen-centered free radical on fructosamine (see Figure 5.3) and generate a new copper complex at *m*/*z* 316 (not observed, pathway B). In pathway A, fructosamine can undergo copper-catalyzed carbon–oxygen bond cleavage, preferably at the α position to carbonyl, with simultaneous hydride transfer (Rao and Rao, 2015) to from deoxy-fructosamine and the amino acid copper hydroxide complex observed at *m*/*z* 154.9627. Alternatively, the hypothetical ion at *m*/*z* 316 in pathway B can degrade into a 3-deoxy-fructosamine radical and an amino acid carboxyl radical with the loss of CuO. Both radicals can combine with hydrogen radicals formed during the process to generate glycine and the ion observed at *m*/*z* 164.0924. Similar to fructosamine, deoxy-fructosamine was also observed to react with glucose and form the ion at *m*/*z* 326.1426, shown in Figure 5.3. These ions at *m*/*z* 326.1426 and 342.1405, shown in Figure 5.2, along with their subsequent dehydration products (see Table 5.5 and Figure 5.3) constituted the major ions observed in the reaction mixture. All of the observed ions above had incorporated the expected number of labeled glucose atoms and labeled nitrogen atoms from glycine and, as expected, none of the labeled glycine carbon atoms (see Table 5.5). The above findings further support the importance of metal-catalyzed oxidative decarboxylation reactions of not only $(Gly)_2Cu$ complexes but also their corresponding sugar conjugates, generating simultaneously Amadori products, Strecker aldehydes, and fructosamine.

Table 5.3. The MS/MS fragmentation and the elemental composition of the ions observed at *m/z* 180 generated in the heated model systems

1-amino-1-deoxy-β-D-glucose[a] $[M+H]^+$ (*m/z*)	Glucose/1-amino-1-deoxy-β-D-glucose $[M+H]^+$ (*m/z*)	Glucose/1-amino-1-deoxy-β-D-glucose/$CuCl_2$ $[M+H]^+$ (*m/z*)	$(Gly)_2Cu$/glucose $[M+H]^+$ (*m/z*)
180.0863 ($C_6H_{14}NO_5$)	180.0865 ($C_6H_{14}NO_5$)	180.0861 ($C_6H_{14}NO_5$)	180.0866 ($C_6H_{14}NO_5$)
162.0756[b] ($C_6H_{12}NO_4$)	162.0766[b] ($C_6H_{12}NO_4$)	162.0768[b] ($C_6H_{12}NO_4$)	162.0762[b] ($C_6H_{12}NO_4$)
145.0430[c] ($C_6H_9O_4$)	144.0670 ($C_6H_{10}NO_3$)	144.0664 ($C_6H_{10}NO_3$)	144.0645 ($C_6H_{10}NO_3$)
144.0660 ($C_6H_{10}NO_3$)			
127.0428[c] ($C_6H_7O_3$)			
109.0257[c] ($C_6H_5O_2$)			
85.0247[c] ($C_4H_5O_2$)			

[a] Non heated commercial standard
[b] Base peak
[c] The calculated error (in ppm) for the specified ions in the commercial standard were between 25-50ppm. For all other ions, the calculated error (in ppm) ranged between 1 and 10 ppm

Table 5.4. The MS/MS fragmentation and the elemental composition of the ion observed at *m/z* 342.1405 in the heated mixtures of glucose/1-amino-1-deoxy-β-D-glucose/$CuCl_2$ and $(Gly)_2Cu$/glucose model systems.

Glucose/1-amino-1-deoxy-β-D-glucose/$CuCl_2$ $[M+H]^+$ (*m/z*)[a]	$(Gly)_2Cu$/glucose $[M+H]^+$ (m/z)[a]
342.1402 ($C_{12}H_{24}NO_{10}$)	342.1391 ($C_{12}H_{24}NO_{10}$)
324.1294 ($C_{12}H_{22}NO_9$)	324.1303 ($C_{12}H_{22}NO_9$)
306.1195[b] ($C_{12}H_{20}NO_8$)	306.1196[b] ($C_{12}H_{20}NO_8$)
288.1092 ($C_{12}H_{18}NO_7$)	288.1083 ($C_{12}H_{18}NO_7$)
240.0870 ($C_{11}H_{14}NO_5$)	240.0870 ($C_{11}H_{14}NO_5$)
204.0861 ($C_8H_{14}NO_5$)	204.0866 ($C_8H_{14}NO_5$)
174.0760 ($C_7H_{12}NO_4$)	174.0754 ($C_7H_{12}NO_4$)
162.0763 ($C_6H_{12}NO_4$)	162.0756 ($C_6H_{12}NO_4$)
144.0663 ($C_6H_{10}NO_3$)	144.0656 ($C_6H_{10}NO_3$)
127.0404 ($C_6H_7O_3$)	127.0401 ($C_6H_7O_3$)
109.0274 ($C_6H_5O_2$)	109.0282 ($C_6H_5O_2$)
97.0297 ($C_5H_5O_2$)	97.0299 ($C_5H_5O_2$)

[a] The calculated error (in ppm) in all the reported ions ranged between 0.5 and 15 ppm.
[b] Base peak

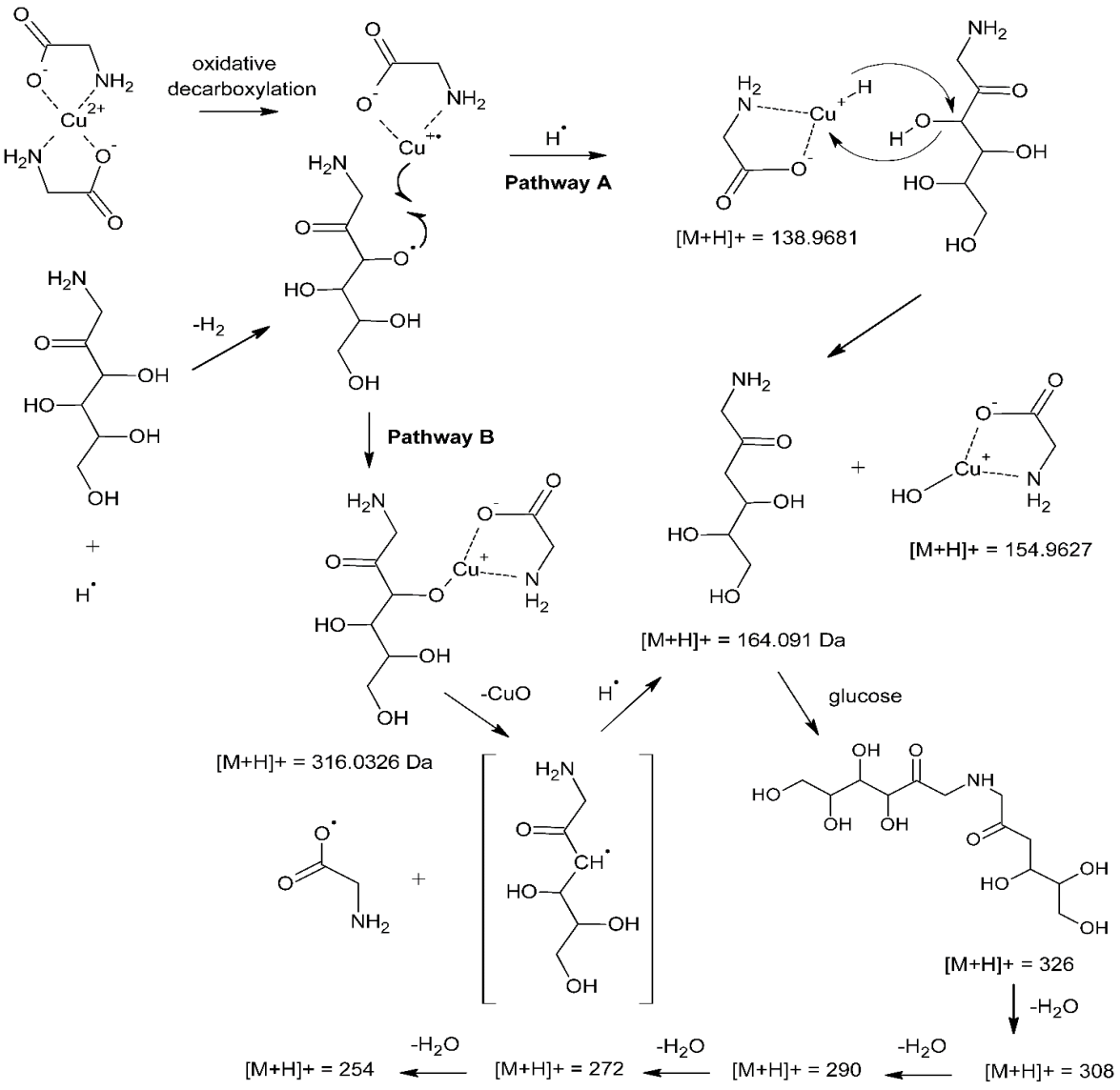

Figure 5.3. Proposed mechanism of carbon-oxygen bond cleavage in *m/z* 180. Pathway A is based on Rao and Rao (2014).

Table 5.5. Elemental composition and isotope incorporation in the reaction products originating from $(Gly)_2Cu$/Glc and associated with the ion observed at *m/z* 164.0924 shown in Figure 5.3.

$[M+H]^+$ (*m/z*)[a]	Elemental composition	[^{13}C-U$_6$]Glu	[^{13}C-1]Gly	[^{13}C-2]Gly	[^{15}N]Gly
138.9681	$C_2H_6CuNO_2$	na[b]	na	na	na
154.9627	$C_2H_6CuNO_3$	na	na	na	na
164.0924	**$C_6H_{14}NO_4$**	**6**	**0**	**0**	**1**
254.1026	$C_{12}H_{16}NO_5$	12	0	0	1
272.1112	$C_{12}H_{18}NO_6$	12	0	0	1
290.1217	$C_{12}H_{20}NO_7$	12	0	0	1
308.1321	$C_{12}H_{22}NO_8$	12	0	0	1
326.1426	$C_{12}H_{24}NO_9$	12	0	0	1

[a] The calculated error (in ppm) in all the reported ions ranged between 0.7 and 11 ppm.
[b] na=not analyzed

5.4.4 Consequences of Sugar Conjugation with Bis(glycinato)copper(II) Complexes to Browning and Total Volatile Formation

As demonstrated above, glucose tends to form various conjugates with bis(glycinato)Cu(II) complexes, which can eventually undergo oxidative decarboxylation or dissociation to release the amino acid conjugates as Amadori products. It is expected that such complexes can serve as molecular scaffolds upon which different sugar moieties can accumulate and eventually be released over time, generating colors and aromas. This fact can create the opportunity for controlled release of aroma and flavor precursors. To demonstrate the role of amino acid metal complexes in aroma formation, the total volatiles generated from model systems of glycine/glucose and $(Gly)_2Cu$/glucose were analyzed using Py–GC/MS before and after heating in aqueous solutions at 100 °C for 2 h in open vials. Heating in open vials can lead to loss of volatiles but not loss of conjugated aroma precursors. The quantitation of the volatiles was performed through comparison of their total ion abundances after thermal desorption. As expected, the total ion current of both model systems decreased after heating in open vials (see Table 5.6). The glucose/glycine model system exhibited a ∼6-fold decrease in intensity, while the heated $(Gly)_2Cu$/glucose model system showed only a ∼1.5-fold decrease relative to the unheated samples. These results indicated that, although heating in an open vial can lead to the loss of volatiles, however, as predicted, the $(Gly)_2Cu$ complex was able to retain the aroma precursors in the reaction medium and generate ∼1.6-fold more volatiles upon reheating relative to the

glucose/glycine model system. These results were also consistent with the measurement of the total content of ninhydrin-active (Tomita et al., 1964) amino acid moieties (free amino acid, amino acid–metal complex, Amadori, and Amadori–metal complex) in glycine/glucose and $(Gly)_2Cu$/glucose model systems before and after heating (100 °C for 2 h) in aqueous solutions. Table 5.6 indicates that, at the end of the reaction, the $(Gly)_2Cu$/glucose model system retained almost 94% of its total ninhydrin-active amino acid content, whereas the glucose/glycine model showed only 55.2% retention. These changes in ninhydrin-active moieties indicate that, after 2 h of heating at 100 °C, the mixture containing $(Gly)_2Cu$ was still rich in aroma precursors, such as Amadori and Amadori–metal complexes, relative to the glycine/glucose sample, consistent with ESI/qTOF/MS studies reported above and shown in Figure 5.2. Furthermore, the role of metal ions in their free forms ($CuCl_2$/glycine) and as amino acid complexes, such as $(Gly)_2Cu$, in generating browning (heating at 100 °C for 2 h) in the presence of glucose was also investigated. Using the measurements from two different wavelengths (λ = 420 and 550 nm), the obtained data have indicated that the presence of free $CuCl_2$ in the glucose/glycine model system did not change the browning of the solution, whereas the $(Gly)_2Cu$ complex reduced the browning of the reaction mixture by 15% relative to the model system lacking a source of metal (see Table 5.6), indicating the dual role that metals can play as either free ions enhancing browning or part of complexes of amino acids inhibiting the browning.

Table 5.6. Comparison of total volatiles, browning and ninhydrin active amino acid content of glycine/glucose and $(Gly)_2Cu$/glucose model systems before and after heating for 2 h at 110°C.

Total ion current (TIC) × 10^3			
Model system[a]	Before heating	After heating	Relative decrease in volatiles
Glycine/glucose	46.1±10%	7.9±10%	5.8
$(Gly)_2Cu$/glucose	20.6±10%	12.9±10%	1.6

Ninhydrin assay			
	Absorbance (λ=570nm)		
Model system	Before heating	After heating	Glycine loss (%)
Glycine/glucose	0.275 ± 0.007	0.153 ± 0.005	44.85 ± 0.636
$(Gly)_2Cu$/glucose	0.239 ± 0.001	0.224 ± 0.001	5.9 ± 0.141

Browning measurement				
Model system	Absorbance[b] (λ=420nm)	Relative extent of browning[c]	Absorbance (λ= 550nm)	Relative extent of browning[c]
Glycine/glucose	0.166 ± 0.006	1	0.142 ± 0.006	1
$(Gly)_2Cu$/glucose	0.140 ± 0.001	0.84	0.130 ± 0.001	0.91
Gly/Glc/$CuCl_2$	0.182 ± 0.001	1.1	0.157 ± 0.002	1.11

[a] Samples were pyrolyzed (250 °C, 20s) before and after heating.
[b] The absorbance of the unheated model systems was the same as that of the blank.
[c] The relative extent of browning is compared to glycine/glucose model system.

CONNECTING PARAGRAPH

In chapter 5, we demonstrated the enhanced reactivity of glycine-copper complexes towards glucose and the formation of sugar conjugated copper complexes. Furthermore, we demonstrated that these amino acid sugar conjugates allowed for the slower release of aroma and browning precursors such as Amadori products during heating as assessed by the extent of browning and total volatile release relative to reactions conducted in the absence of metal complexes. In chapter 6, we explore the generality of this observation using different sugars and the ability of their corresponding copper complexes with amino acids to undergo oxidative decarboxylation similar to their free amino acid counterparts (see Chapter 3) and generate the corresponding amino sugars such as fructosamine from glucose and glucosamine from fructose. Chapter 6 was published in *Food Chemistry*: Nashalian, O.; Yaylayan, V. A. (2016). In situ formation of the amino sugars 1-amino-1-deoxy-fructose and 2-amino-2-deoxy-glucose under Maillard reaction conditions in the absence of ammonia. *Food Chemistry,* 197, Part A, 489-495.

CHAPTER 6

IN SITU FORMATION OF THE AMINO SUGARS 1-AMINO-1-DEOXY-FRUCTOSE AND 2-AMINO-2-DEOXY-GLUCOSE UNDER MAILLARD REACTION CONDITION IN THE ABSENCE OF AMMONIA

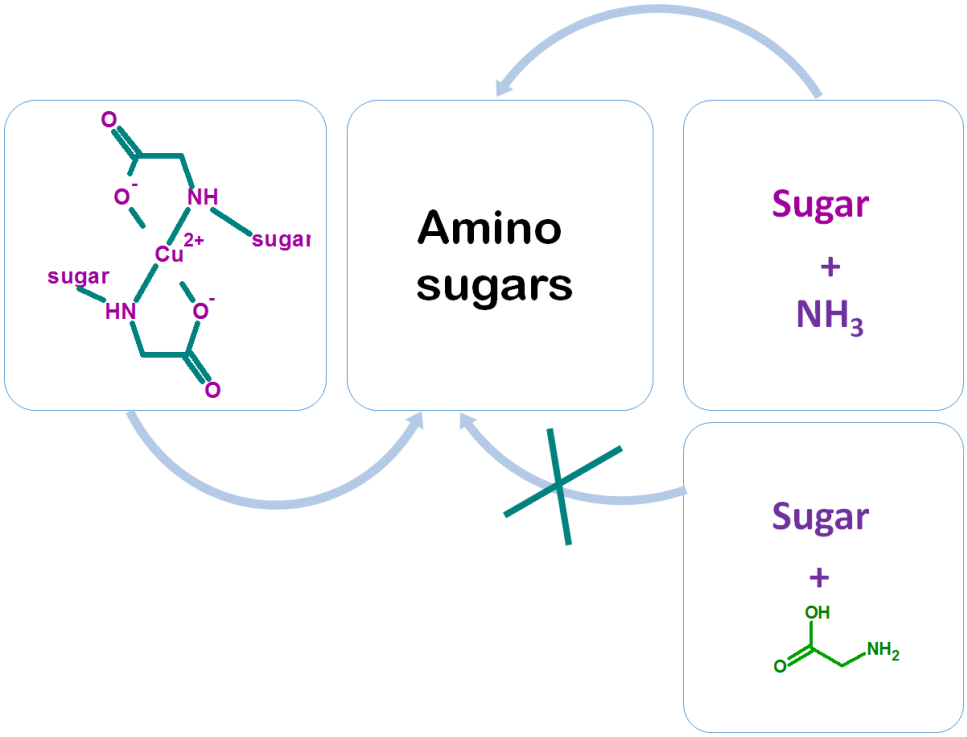

6.1 ABSTRACT

Replacing amino acids with their binary metal complexes during the Maillard reaction can initiate various processes including the oxidative degradation of their glucose conjugates generating 1-amino-1-deoxy-fructose and its derivatives. These reactive amino sugars are not easily accessible under the Maillard reaction conditions and are only formed in the presence of ammonia. To explore the generality of this observation and to study in particular the ability of fructose to generate glucosamine, the amino acid-metal complexes were heated in aqueous solutions with three aldohexoses and two ketohexoses at 110^{o}C for 2 hours and the dry residues were analyzed by ESI/qTOF/MS/MS. All the sugars generated relatively intense ions at $[M+H]^+$ 180 ($C_6H_{14}NO_5$); those ions originating from ketohexoses exhibited MS/MS fragmentations identical to glucosamine and those originating form aldohexoses showed ions identical to fructosamine. Furthermore, the amino sugars were found to from fructosazine, react with other sugars and undergo dehydration reactions.

6.2 INTRODUCTION

Although the term "amino sugars" refers to the Amadori or Heyns rearrangement products of reducing sugars with ammonia, such as glucosamine or fructosamine, in the context of the Maillard reaction it is most often used interchangeably to denote their amino acid derivatives (Mossine & Mawhinney, 2010). Because of the presence of a free amino group, they are considered to be more reactive than sugars themselves (Kraehenbuehl et al., 2008; Hrynets, et al., 2013) or more reactive than their corresponding amino acid derivatives. In Maillard reaction model systems glucosamine is reported to generate more reaction products relative to sugars when heated alone or reacted with amino acids (Kraehenbuehl et al., 2008; Hrynets et al., 2015). In the study by Kraehenbuehl et al. (2008) glucosamine was found to generate relatively higher browning, pyrazine and sulphur-containing flavour products compared to different acidic and basic sugars when reacted with cysteine. Also, Hrynets et al. (2013) reported a faster glycation rate of actomyosin with glucosamine compared to glucose. The glycated actomyosin with glucosamine also exhibited enhanced protein functional properties, such as solubility, particularly in the pH range of 8–12, and emulsifying activity and stability. A similar enhancement in chitosan/glucosamine solubility relative to that of chitosan/glucose was reported by Chung et al. (2006). Moreover, the thermal degradation of glucosamine in aqueous solutions has been studied by several research groups. Shu

(1998) reported the formation of several volatile products, such as different pyrazine derivatives, pyrrole-2-carboxaldehyde, and furfural, after heating glucosamine in aqueous solution at 150 °C for 5 min at different pH values. A recent study (Hrynets et al., 2015) has indicated that glucosamine produces significant amounts of dicarbonyls and some pyrazines, even at 37 °C, when incubated at longer times. On the other hand, Jun et al. (2003) studied the non-volatile thermal degradation of glucosamine in aqueous solution. In their study Jun et al. reported that heating glucosamine in water at 100 °C for 2 h generated several non-volatile products, such as fructosazine, deoxy-fructosazine and their acetylated derivatives. The reactivity of glucosamine was also studied in dry model systems. Compared to fructose, glucosamine was reported to generate a different flavour profile and composition of isolated volatiles when reacted with sodium acetate at 200 °C in the absence of any solvent (Chen & Ho, 1998). Despite the vast evidence on the reactivity of glucosamine in the Maillard reaction, the in situ generation of glucosamine or fructosamine as reaction intermediates or products from sugars and amino acids has not been reported except in the case of deoxy-ribosamine as a precursor of furfurylamine (Nikolov & Yaylayan, 2012). Amino sugars are usually obtained from natural sources, such as chitin or through synthetic preparations (Mossine et al., 2009). Theoretically, amino sugars can be formed through the reaction of ammonia with glucose or fructose to generate 1-amino-1-deoxy-fructose or 2-amino-2-deoxy-glucose in low yields (Heyns and Koch, 1952 and Hrynets et al., 2015). However, replacing ammonia with glycine–copper complex was found to form a product consistent with fructosamine through an oxidative decarboxylation pathway (Nashalian & Yaylayan, 2015b). Therefore, in this study we explore the in situ formation of other amino sugars and related adducts from *aldo* or *keto* sugars and glycine–copper complex in heated (110 °C for 2 h) aqueous Maillard model systems.

6.3 Materials and Methods

6.3.1 Materials and reagents

L-Glycine (98%), L-alanine (99%), L-serine (99%), D-glucose, D-mannose, D-galactose (97%), D-fructose, D-sorbose, D-glyceraldehyde, D-ribose, potassium hydroxide (KOH), copper (II) chloride ($CuCl_2$) (99.9%), β-D-glucopyranosylamine (1-amino-1-deoxy-β-D-glucose), and glucosamine hydrochloride were purchased from Sigma–Aldrich Chemical Co. (Oakville, ON, Canada). The [^{13}C-1, ^{13}C-2, ^{15}N]glycine (98%), and [U_6-^{13}C]glucose (99%) were purchased from Cambridge

Isotope Laboratories (Andover, MI). LC–MS grade water and methanol (OmniSolv, >99%) were obtained from VWR International (Mississauga, ON, Canada).

6.3.2 Synthesis of amino acid–metal complexes

$(Gly)_2Cu$ complexes were prepared by dissolving glycine (0.75 g) in methanol (10 mL) in the presence of KOH (0.05 g) followed by the addition of half a mole of $CuCl_2$ (0.67 g). The dark blue precipitate was washed with methanol, filtered and dried. Glycine–copper complex was confirmed by obtaining its elemental composition from accurate masses determined by ESI/qTOF/MS analysis at *m/z* 233.9665 $[M+Na]^+$ (calculated for $C_4H_8CuN_2NaO_4$ with an error of 5.4 ppm). Isotope labelled precursors were prepared similarly.

6.3.3 Sample preparation

Model systems (10 mg) consisting of glycine/aldohexose (glucose, mannose, or galactose) or glycine/ketohexose (fructose or sorbose) in a 2:1 relative molar ratio, and $(Gly)_2Cu$/aldohexose (glucose, mannose, or galactose) or $(Gly)_2Cu$/ketohexose (fructose or sorbose) in a 1:1 relative molar ratio, were dissolved in water (2 mL) and heated on a sand bath in an open vial (5 mL capacity) at 110 °C for 2 h until dry (Supplementary Table S6.1). The reaction mixtures were subsequently analysed by ESI/qTOF/MS. All the samples were analysed in duplicates.

6.3.4 Electrospray ionisation/quadrupole time of flight/mass spectrometry (ESI/qTOF/MS) analysis

The dry reaction mixtures were dissolved in LC grade water to a concentration of 1 mg/mL. The samples were then diluted 10-fold in 10% methanol prior to analysis by ESI/qTOF/MS. The ESI/qTOF/MS system was comprised of a Bruker Maxis Impact quadrupole-time of flight mass spectrometer (Bruker Daltonics, Bremen, Germany) operated in positive ion mode. Samples (1 μL) were injected directly into the ESI/qTOF/MS. Instrument calibration was performed using sodium formate clusters. The electrospray interface settings were the following: nebuliser pressure 0.6 bar, drying gas 4 L/min, 180 °C, capillary voltage 4500 V. Scan range was from *m/z* 100 to 1000. The data was analysed using Bruker Compass Data Analysis software version 4.1. Tandem mass spectrometry (MS/MS) was carried out in MRM mode using 10.0 eV collision energy for the ions at $[M+H]^+$ 180 and $[M+H]^+$ 268.

6.3.5 Structural identification

Evidence for the proposed structures of non-volatile reaction intermediates was provided through qTOF/ESI MS analysis of their elemental composition, and by the use of commercial or synthetic intermediates and by isotope labelling studies. Furthermore, MS/MS spectra of selected product ions were compared to those of commercial standards. The incorporation of copper in the identified complexes was confirmed by the isotopic signature of copper through detection of M+2 peaks at 30% relative intensity.

6.4 RESULTS AND DISCUSSION

One of the unique features of the Maillard reaction is its ability to generate a large array of products with different molecular diversities and chemical properties from fewer and simpler structures. Controlling such a reaction with a wide spectrum of end products can contribute towards regulating and enhancing its applications in food. The observation that amino acid–metal complexes can play a multifunctional role (Figure 6.1) in the Maillard reaction (Nashalian & Yaylayan, 2015b) can provide such an opportunity in enhancing Strecker aldehyde formation (Yablokov et al.,2014; Nashalian & Yaylayan, 2014), or transformation of amino acids into their α-hydroxymethyl derivatives (for example glycine into serine) through Akabori reaction (Akabori et al., 1959; Nashalian & Yaylayan, 2015a), or even modulating the Maillard reaction by controlling and delaying the release of Amadori products (Nashalian & Yaylayan, 2015b), and finally enhancing oxidative degradation of sugar conjugated amino acid metal complexes to generate products such as 1-amino-1-deoxy-fructose (fructosamine), the Amadori product of ammonia (Nashalian & Yaylayan, 2015b), and other amino sugars which are not easily accessible under Maillard reaction conditions and are only formed in the presence of ammonia in small amounts. In model systems incorporating glucose, glycine–copper complex was found to provide stable scaffolds upon which glucose molecules can be conjugated as Schiff bases or Amadori rearrangement products (Nashalian & Yaylayan, 2015b). This form of conjugation provided an effective way to control the release of volatiles from Amadori products. Moreover, it was found that the Amadori conjugates were able to undergo thermally induced oxidative decarboxylation, similar to glycine–copper complexes alone (Nashalian and Yaylayan, 2014 and Yablokov et al., 2014), to generate products such as Amadori–copper complexes, free Amadori products, fructosamine, deoxyfructosamine and their glucose adducts (Nashalian & Yaylayan, 2015b). To explore the

generality of this observation and to study in particular the ability of fructose to generate glucosamine in the presence of amino acid–copper complexes, the influence of sugar type on the formation of amino sugars was studied. Amino acid metal complexes were heated in aqueous solutions with three aldohexoses (glucose, mannose, or galactose) and two ketohexoses (fructose and sorbose) in addition to ribose and glyceraldehyde at 110 °C for 2 h and the dry residues were analysed by ESI/qTOF/MS. It was predicted that due to the steric differences between *aldo* and *keto* sugars in carbonyl–amine reactions, $(Gly)_2Cu$ complex may demonstrate selective conjugation with one class of sugar over the other.

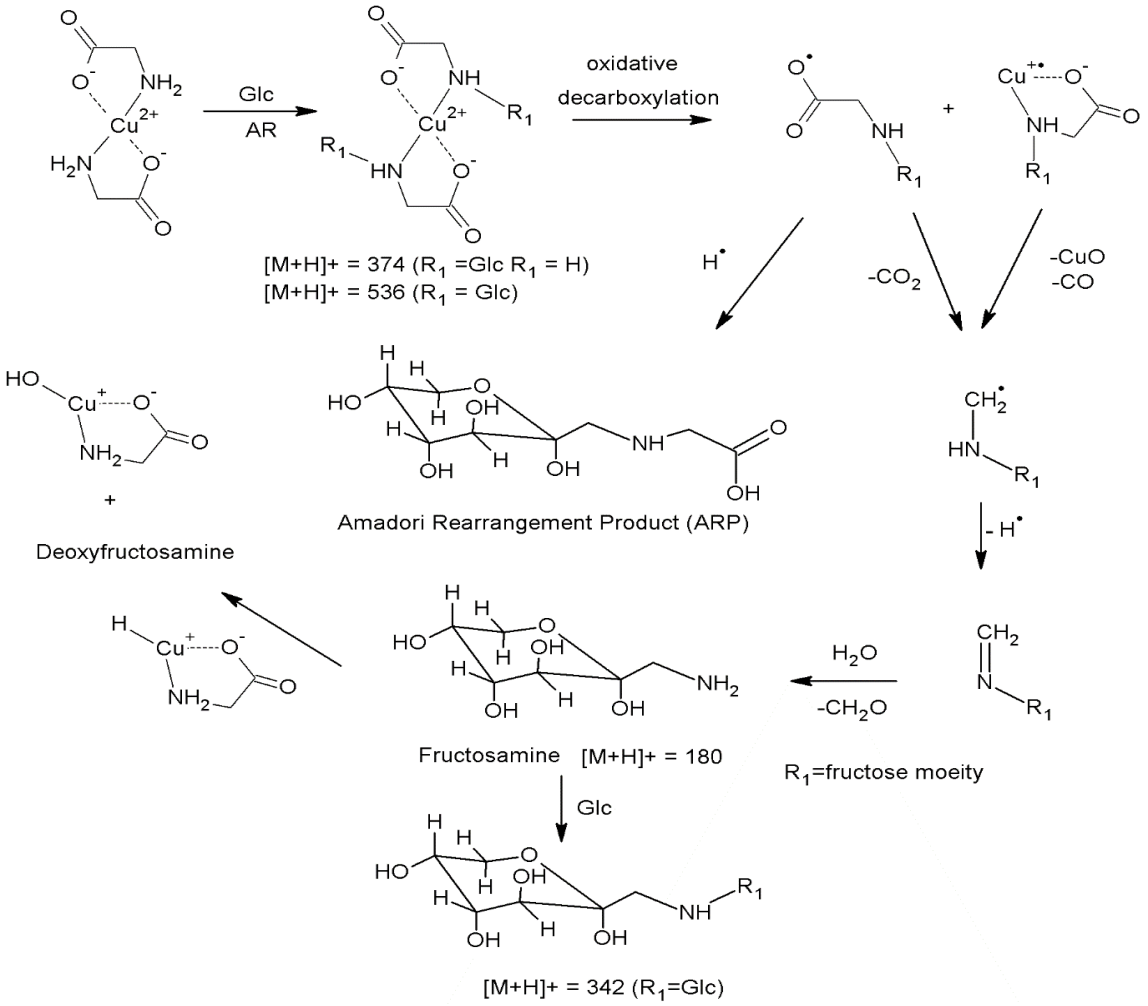

Figure 6.1. Mechanism of oxidative decarboxylation of sugar-conjugated amino acid copper complexes (see Nashalian and Yaylayan (2014) and the mechanism of deoxy-amino sugar formation (for details see Nashalian and Yaylayan (2015b).
ARP = Amadori rearrangement product AR = Amadori rearrangement R_1 = H or sugar moiety

6.4.1 Effect of sugar type on the formation of amino sugars ($C_6H_{14}NO_5$ at $[M+H]^+$ 180)

To study the ability of different hexoses to generate amino sugars with $(Gly)_2Cu$, three aldohexoses (glucose, mannose, galactose) and two ketohexoses (fructose and sorbose) were heated either with $(Gly)_2Cu$ or free glycine in aqueous solutions at 110 °C for 2 h and their ESI/qTOF/MS spectra were acquired (Supplementary Figures S6.1 and S6.2). With free glycine, *aldo* and *keto* sugars generated ESI profiles that are similar to each other (not shown), where the main peaks corresponded to the Amadori or Heyns compounds and their dehydration products. However, the substitution of glycine with $(Gly)_2Cu$ resulted in a quite different ESI profile (Supplementary Figures S6.1 and S6.2). Mannose and galactose behaved similarly to glucose (Supplementary Figure S6.1), while sorbose displayed a similar profile to fructose (Supplementary Figure S6.2). The similarity of the ESI profiles between *aldo* and *keto* sugars may be attributed to the ease of isomerisation between the sugars in the presence of free amino acids, whereas in the presence of amino acid–copper complexes the isomerisation is prevented due to the conjugation of the free sugars. The major products observed in the three *aldo* sugars can be considered mostly originating from the degradation of the initially formed mono or di-conjugated $(Gly)_2Cu$ complexes in the form of Schiff bases or Amadori rearrangement products appearing at $[M+H]^+$ 374.0355 and 536.0925, respectively (Figure 6.1). Their oxidative degradation also generated the ion at $[M+H]^+$ 180 attributed to fructosamine and several associated products at $[M+H]^+$ 342, 326, 276, 290 (Nashalian & Yaylayan, 2015b), constituting the major ions in the ESI/qTOF/MS spectra (Table 6.1). On the other hand, the spectra of the *keto* sugars, sorbose and fructose, displayed a substantial reduction in the intensity of the $[M+H]^+$ 180 and its associated ions with the predominance of the unreacted sugar at $[M + K]^+$ 219 (Supplementary Figure S6.2). The suppression in the generation of non-volatile conjugated products with the *keto* sugars could be related to the steric hindrance associated with the reaction of amino acids with the ketone moiety, compounded by the increased size of the amino acid due to its complexation with the copper. Both of these factors make the *keto* sugars less favourable to conjugate with $(Gly)_2Cu$ and thus eventually generate less amino sugars. Furthermore, the dissimilarities in the configuration of the hydroxyl groups on the sugar molecules (Laroque et al., 2008), and the forms that they adopt in solution as Amadori and Heyns products (furanose and pyranose tautomeric forms for Amadori and only pyranose for Heyns) (Mossine, Glinsky, & Feather, 1994) could also regulate their stability and reactivity in solution and affect the rate of their formation.

Table 6.1. Elemental composition[a] and isotope incorporation[b] of the major products originating from $(Gly)_2Cu$/glucose[c] (see Supplementary Figure S6.1).

$[M+H]^+$ (m/z)	Elemental composition[c]	[^{13}C-U$_6$]Glu	[^{13}C-1]Gly	[^{13}C-2]Gly	[^{15}N]Gly
164.0914	$C_6H_{14}NO_4$	6	0	0	1
180.0872	$C_6H_{14}NO_5$	6	0	0	1
203.0518	$C_6H_{12}O_6Na$	6	0	0	0
219.0264	$C_6H_{12}O_6K$	6	0	0	0
238.0930	$C_8H_{16}NO_7$	6	1	1	1
276.0478	$C_8H_{15}NO_7K$	6	1	1	1
254.1026	$C_{12}H_{16}NO_5$	12	0	0	1
272.1112	$C_{12}H_{18}NO_6$	12	0	0	1
290.1217	$C_{12}H_{20}NO_7$	12	0	0	1
299.0038/301.0028	$C_8H_{14}CuNO_7$	6	1	1	1
308.1321	$C_{12}H_{22}NO_8$	12	0	0	1
300.0079/302.0059	$C_8H_{15}CuNO_7$	6	1	1	1
324.1268	$C_{12}H_{22}NO_9$	12	0	0	1
326.1447	$C_{12}H_{24}NO_9$	12	0	0	1
342.1405	$C_{12}H_{24}NO_{10}$	12	0	0	1
374.0355/376.0313	$C_{10}H_{19}CuN_2O_9$	6	2	2	2
536.0925/538.0912	$C_{16}H_{29}CuN_2O_{14}$	12	2	2	2

[a] The two masses shown represent copper isotopes ^{63}Cu/^{65}Cu.
[b] The isotope labeling data was generated only from the labeled $(Gly)_2Cu$/glucose model system, $(Gly)_2Cu$/aldose and $(Gly)_2Cu$/ketose model systems also generated corresponding ions with identical elemental composition.
[c] The calculated error (in ppm) in all the reported ions ranged between 0.02 and 22ppm.

Oxidative decarboxylation of sugar conjugated *bis*(glycinato)copper complexes constitute the key pathway for the generation of the major products observed in the $(Gly)_2Cu$/sugar mixtures as shown in Figure 6.1 (Nashalian & Yaylayan, 2015b). In glucose or aldose models, one of the direct products of this reaction was an ion at $[M+H]^+$ 180.0872, which was confirmed to be fructosamine, the Amadori product of ammonia with glucose (Nashalian & Yaylayan, 2015b). It was hypothesised that the oxidative decarboxylation of fructose or sorbose conjugated $(Gly)_2Cu$ complexes would similarly generate glucosamine or gulosamine, the Heyns products of ammonia with fructose or sorbose. To verify this assumption, the ion at $[M+H]^+$ 180.0873 originating from

$(Gly)_2Cu$/fructose was compared with the unheated commercial standard of glucosamine hydrochloride. The MS/MS fragmentation pattern of the standard glucosamine matched exactly the ions generated from $[M+H]^+$ 180.0873 generated in the heated $(Gly)_2Cu$/fructose model system (Table 6.2). Similar to previously observed fructosamine (Nashalian & Yaylayan, 2015b), glucosamine was also found to undergo a subsequent reaction with the sugar in the reaction mixture, in this case Heyns rearrangement with fructose to generate (although to a lesser extent compared to fructosamine), the corresponding adduct at $[M+H]^+$ 342 and its dehydration product at $[M+H]^+$ 324 (Figures 6.1 and 6.2, Table 6.1). Furthermore, to demonstrate the generality of amino sugar formation with other amino acid metal complexes, $(Ala)_2Cu$ was also heated with glucose at 110 °C for 2 h and analysed as similar to $(Gly)_2Cu$/glucose. Supplementary Table S6.2 presents a comparison of the ions generated from the ESI/qTOF/MS analysis of $(Ala)_2Cu$/glucose that are equivalent to those generated in the $(Gly)_2Cu$ model systems and presented in Table 6.1. The *in situ* formation of the amino sugars highlighted the vital role of metal ions in the Maillard reaction in catalysing oxidative decarboxylation reactions to generate products that are otherwise not easily formed in the reaction. Moreover, they provided an important way to generate different varieties of amino sugars specific to the type of conjugated sugar

Table 6.2. Comparison of the MS/MS fragmentation and the elemental composition[a] of the ions observed at $[M+H]^+$180 ($C_6H_{13}NO_5$) generated in the heated model system and the commercial glucosamine·HCl salt.

Glucosamine[b] $[M+H]^+$ (*m/z*)	$[M+H]^+$ = 180 in $(Gly)_2Cu$/fructose $[M+H]^+$ (*m/z*)
162.0759[c] ($C_6H_{12}NO_4$)	162.0761[c] ($C_6H_{12}NO_4$)
144.0652 ($C_6H_{10}NO_3$)	144.0651 ($C_6H_{10}NO_3$)
126.0545 ($C_6H_8NO_2$)	126.0554 ($C_6H_8NO_2$)
114.0549 ($C_5H_8NO_2$)	114.0549 ($C_5H_8NO_2$)
102.0546 ($C_4H_8NO_2$)	102.0521 ($C_4H_8NO_2$)
98.0600 (C_5H_8NO)	98.0606 (C_5H_8NO)
85.0283 ($C_4H_5O_2$)	85.0282 ($C_4H_5O_2$)

[a] The calculated error was less than 10 ppm.
[b] Unheated commercial standard.
[c] Base peak.

6.4.2 Further reactions of amino hexoses and formation of fructosazine derivatives

Amino sugars are known to be highly reactive components (Jun et al., 2003). Once formed *in situ* from $(Gly)_2Cu$/sugar model systems, fructosamine or glucosamine and their deoxy derivatives were found to undergo subsequent reactions to generate a multitude of products. No rearrangement products of glucosamine or fructosamine with free glycine were detected in the mixture. However, both amino sugars displayed a preference to react with free sugars to generate the corresponding Amadori or Heyns products. Such adducts underwent subsequent dehydration reactions to generate ions at $[M+H]^+$ 342, 324, 326, 308, 290, and 272. The newly formed amino sugar–sugar adducts have two carbonyl functional groups that can migrate down the carbon backbones through enolisation reactions and can condense at various sites with free glycine released from its dimeric complex through dissociation or oxidative decarboxylation (Nashalian & Yaylayan, 2014). The reaction of the adduct at $[M+H]^+$ 342.0872 with glycine followed by its decarboxylation and dehydration reactions generated the ions at $[M+H]^+$ 319.1504 and $[M+H]^+$ 301.1407 (Table 6.3 and Figure 6.2). Similarly, its deoxy-derivative ($[M+H]^+$ 326.1448) generated ions at $[M+H]^+$ 303.1546 and $[M+H]^+$ 285.1444. Furthermore, amino sugars or their deoxy-derivatives are known to dimerise and after an oxidation step generate fructosazines or deoxy-fructosazine (Jun et al., 2003; Tsuchida et al., 1973; Tsuchida et al., 1976). In fact both of the above pyrazines were detected in the reaction mixtures at $[M+H]^+$ 321 and $[M+H]^+$ 305 (see Figure 6.2). Isotope labelling studies have indicated that all the ions identified above were consistent with their proposed structure and their pathways of formation (Table 6.3). In addition, alanine model system similarly generated its corresponding adducts (Supplementary Table S6.2), again indicating the generality of this observation. Furthermore, replacing hexoses with ribose or glyceraldehyde in the reaction mixtures similarly generated ions with elemental composition corresponding to amino sugars and their deoxy-derivatives and their subsequent dimerisation products, the pyrazines (see Supplementary Table S6.3).

Table 6.3. Elemental composition[a] and isotope incorporation of the ions with double nitrogen incorporation shown in Figure 6.2.

$[M+H]^+$ (m/z)[b]	Elemental composition	$[^{13}C\text{-}U_6]$Glc	$[^{13}C\text{-}1]$Gly	$[^{13}C\text{-}2]$Gly	$[^{15}N]$Gly
285.1444	$C_{13}H_{21}N_2O_5$	12	0	1	2
301.1407	$C_{13}H_{21}N_2O_6$	12	0	1	2
305.1360[c]	$C_{12}H_{21}N_2O_7$	12	0	0	2
303.1546	$C_{13}H_{23}N_2O_6$	12	0	1	2
319.1504	$C_{13}H_{23}N_2O_7$	12	0	1	2
321.1333[c]	$C_{12}H_{21}N_2O_8$	12	0	0	2

[a] The ions presented in the table were common in all $(Gly)_2Cu$/sugar model systems with calculated errors less than 10ppm.
[b] The calculated error for ions was between 0.4 and 11ppm.
[c] Ions that were also generated in the $(Ala)_2Cu$/Glc model system.

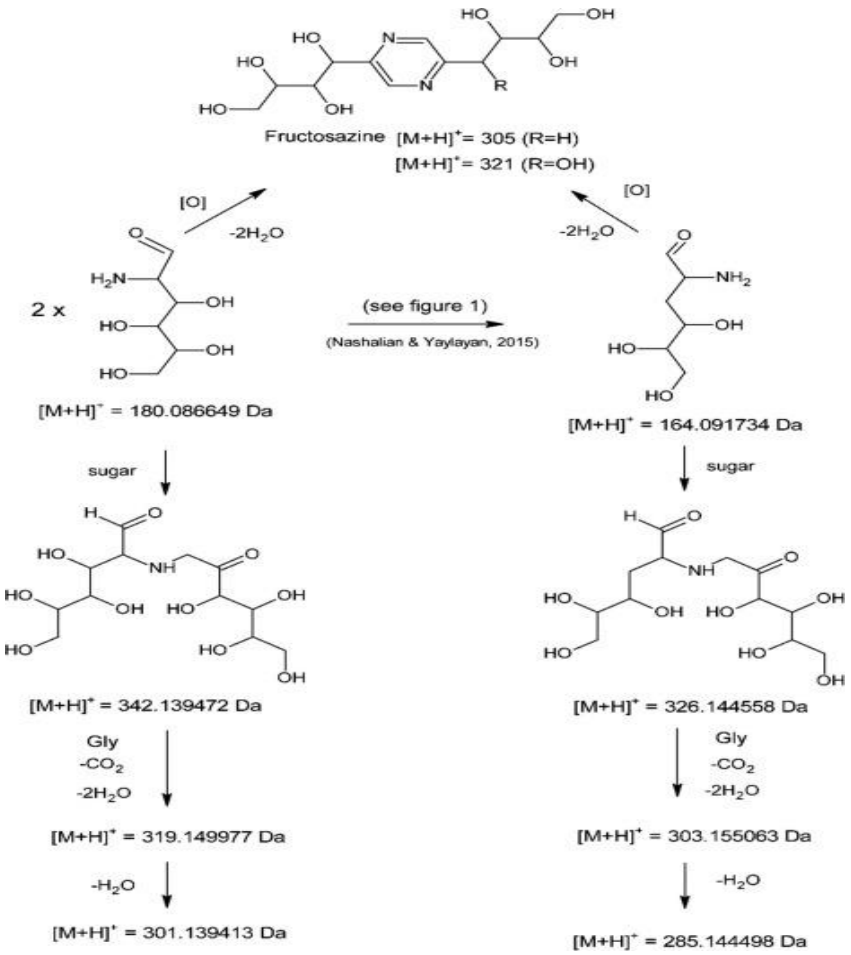

Figure 6.2. Fructosazine formation and further reactions of glucosamine. Corresponding structures with fructosamine are not shown.

6.4.3 Discovery of Mannich bases as unconventional amino acid sugar conjugates in the Maillard reaction

In our efforts to investigate the formation of other amino acid sugar conjugates in $(Gly)_2Cu$/glucose/paraformaldehyde model system (Akabori conditions), an ion was identified that incorporated a single nitrogen atom at $[M+H]^+$ 268.1038 which had an elemental composition of $C_9H_{18}NO_8$ with 6 carbon atoms originating from glucose and one from each of ^{13}C-1,^{13}C-2 in addition to one nitrogen atom from ^{15}N glycine consistent with the Amadori product of the *de novo* formed serine through Akabori reaction. An isomeric ion at $[M+H]^+$ 268.1027 was also generated in the model system lacking copper (i.e. glycine/glucose/paraformaldehyde). Since in the absence of copper Akabori transformation cannot take place, the ion at $[M+H]^+$ 268.1027 was assumed to have a different structure than that of serine Amadori and when MS/MS fragmentations from both ions were compared they were found to generate different fragment ions (see Supplementary Table S6.4) confirming the initial assumption. One such possible isomeric structure could be attributed to a Mannich base. Mannich bases can be generated through the Mannich reaction which is a three component condensation of an amino acid, formaldehyde, and an enolisable carbonyl compound with an active hydrogen atom such as the α-carbons of sugar carbonyls. In fact, the formation of Mannich bases from sugars and amino acids have been proposed previously (Marshall, 1980), and in the glycine/glucose/paraformaldehyde model systems the conditions needed for its formation are readily available. According to the Mannich reaction mechanism, formaldehyde can react first with glycine to form the corresponding Schiff base at $[M+H]^+$88.0397. This intermediate ion was detected in the reaction mixture and was found to incorporate only one C-1, one C-2, and one nitrogen atom from glycine and no carbon atoms from sugar, consistent with the expected reaction of glycine with unlabelled formaldehyde (added as paraformaldehyde) (Figure 6.3, Supplementary Table S6.5). The electrophilic addition of the imine to the C-2 atom of glucose would then yield the Mannich base at $[M+H]^+$ 268.1027. Similarly, replacing free glycine with $(Gly)_2Cu$, formaldehyde can react with glycine–copper complex to first form a single or double Schiff bases at $[M+H]^+$ 223.9787 and $[M+H]^+$ 235.9840, respectively. The addition reaction of the iminium derivative(s) with glucose can generate a hybrid Schiff base/Mannich base adduct at $[M+H]^+$ 416, a single Mannich base/glycine–copper complex at $[M+H]^+$ 404 or a double Mannich base–copper complex at $[M+H]^+$ 596 as shown in Figure 6.3. Some of the above intermediates such as ions at $[M+H]^+$ 404, 464 and 596 can generate the Mannich base at $[M+H]^+$ 268 after their dissociation. Since in the presence of $(Gly)_2Cu$ serine can

be generated through Akabori process, it was not surprising to observe the serine counterpart of the Mannich base at $[M+H]^+$ 298.1123 and its precursor ion at $[M+H]^+$ 434 (see Figure 6.3, and Table S6.5) in these model systems. As shown in Figure 6.3 more than one pathway can lead to the formation of the ion at $[M+H]^+$ 268.1038.

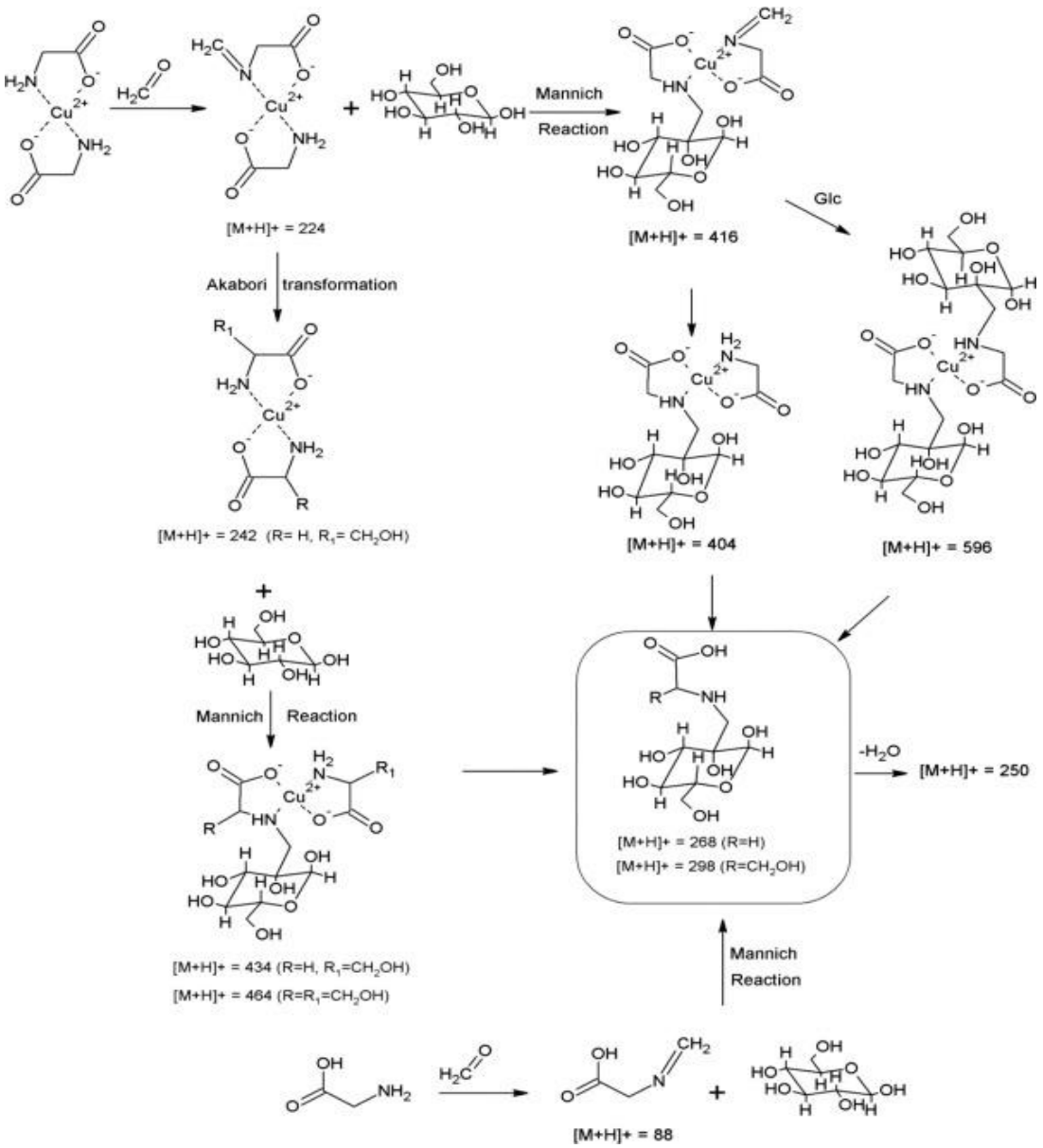

Figure 6.3. Mechanism of Mannich base formation in the presence and absence of copper (see Table S6.6).

Although the amino sugars such as glucosamine or fructosamine are known to be reactive intermediates, it has not been demonstrated yet that they can be readily formed in food or model

systems from commonly known Maillard precursors. This study provides a possible pathway for their generation in the absence of ammonia.

6.5 SUPPLEMENTARY DATA

Supplementary Table S6.1. The composition and relative molar ratios of the model systems.

Composition of the model systems[a]	Relative molar ratios
Glycine/glucose, glycine/mannose, glycine/galactose	2-1
$(Gly)_2Cu$/glucose, $(Gly)_2Cu$/mannose, $(Gly)_2Cu$/galactose	1-1
Glycine/fructose, glycine/sorbose	2-1
$(Gly)_2Cu$/fructose, $(Gly)_2Cu$/sorbose	1-1
Glycine/glucose/paraformaldehyde(excess)	2-1
$(Gly)_2Cu$/glucose/paraformaldehyde(excess)	1-1
1-amino-1-deoxy-β-D-glucose[b]	-
1-amino-1-deoxy-β-D-glucose/glucose	1-1
Glucosamine hydrochloride[c]	-

[a] All the model systems presented in the table were heated (unless specified) at 110°C for 2 hours.
[b] Analyzed before and after heating at 110°C for 2 hours.
[c] unheated commercial standard.

Supplementary Table S6.2. Elemental composition[a] of the ions identified in $(Gly)_2Cu/Glc$ and $(Ala)_2Cu/Glc$[b] model systems

$(Gly)_2Cu/Glc$ $[M+H]^+$ (*m/z*)	Corresponding $(Ala)_2Cu/Glc$ $[M+H]^+$ (*m/z*)
180.0872 $C_6H_{14}NO_5$	180.0870 $C_6H_{14}NO_5$
342.1405 $C_{12}H_{24}NO_{10}$	342.1396 $C_{12}H_{24}NO_{10}$
319.1504 $C_{13}H_{23}N_2O_7$	333.1668 $C_{14}H_{25}N_2O_7$
301.1407 $C_{13}H_{21}N_2O_6$	315.1541 $C_{14}H_{23}N_2O_6$
164.0915 $C_6H_{14}NO_4$	164.0910 $C_6H_{14}NO_4$
326.1448 $C_{12}H_{24}NO_9$	326.1436 $C_{12}H_{24}NO_9$
303.1546 $C_{13}H_{23}N_2O_6$	Not found
285.1444 $C_{13}H_{21}N_2O_5$	299.1625 $C_{14}H_{23}N_2O_5$

[a] The calculated error (in ppm) for all ions were less than 20ppm.
[b] In $(Ala)_2Cu/Glc$ model system the intact alanine adduct ($[M+H]^+$ 413.1741 $C_{15}H_{29}N_2O_{11}$) was also observed.

Supplementary Table S6.3. Elemental composition[a] of amino and deoxy amino sugars and their derivatives generated in $(Gly)_2Cu$/ribose and $(Gly)_2Cu$/glyceraldehyde model systems.

$(Gly)_2Cu$/ribose [M+H]+ m/z	Corresponding structure	$(Gly)_2Cu$/glyceraldehyde [M+H]+ m/z	Corresponding structure
229.1179 $C_{10}H_{17}N_2O_4$	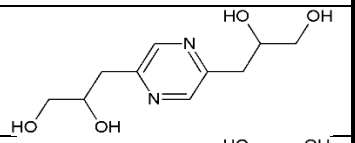	109.0761 $C_6H_9N_2$	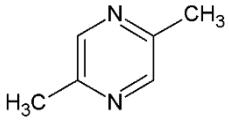
245.1126 $C_{10}H_{17}N_2O_5$	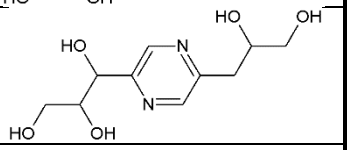	125.0705 $C_6H_9N_2O$	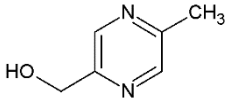
Not found	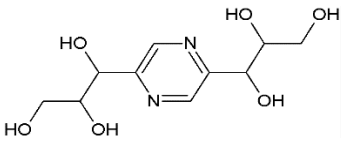	141.0655 $C_6H_9N_2O_2$	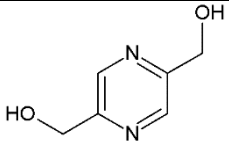
150.0760 $C_5H_{12}NO_4$	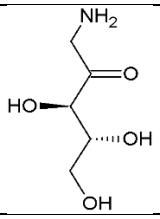	90.0557 $C_3H_8NO_2$	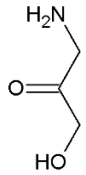
134.0809 $C_5H_{12}NO_3$	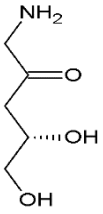		

[a] The calculated error (in ppm) for all the reported ions was less than 10ppm.

Supplementary Table S6.4. The MS/MS fragments[a] and isotope label incorporation of $[M+H]^+$ 268 generated in glycine/Glc/CH_2O and $(Gly)_2Cu$/Glc/CH_2O model systems.
[a] The calculated error (in ppm) for all ions were less than 15ppm.

Glycine/Glc/CH_2O $[M+H]^+$ *m/z*	**$(Gly)_2Cu$/Glc/CH_2O** $[M+H]^+$ *m/z*
268.1011 $C_9H_{18}NO_8$	268.1012 $C_9H_{18}NO_8$ (1xC'-1, 1xC'-2, 1x N, 1x U_6-C)
250.0907 $C_9H_{16}NO_7$	250.0922 $C_9H_{16}NO_7$ (1xC'-1, 1xC'-2, 1x N, 1x U_6-C)
232.0794 $C_9H_{14}NO_6$	88.0387 $C_3H_6NO_2$ (1xC'-1, 1xC'-2, 1x N, 0x U_6-C)
202.0700 $C_8H_{12}NO_5$	60.0445 C_2H_6NO (0xC'-1, 1xC'-2, 1x N, 0x U_6-C)
172.0585 $C_7H_{10}NO_4$	
142.0485 $C_6H_8NO_3$	
118.0494 $C_4H_8NO_3$	
106.0487 $C_3H_8NO_3$	
84.0446 C_4H_6NO	

[b] C'-1,C'-2 ,and N represent ^{13}C-1, ^{13}C-2 and ^{15}N labeled glycine, while U_6-C represents ^{13}C all carbons labeled glucose.

Supplementary Table S6.5. Elemental composition and the number of isotopically labelled atom incorporation of intermediates associated with the Mannich base in the $(Gly)_2Cu$/paraformaldehyde/glucose model system (see Figure 6.3).

$[M+H]^+$ (*m/z*)[a]	Elemental composition	[^{13}C-U$_6$]Glc	[^{13}C-1]Gly	[^{13}C-2]Gly	[^{15}N]Gly
88.0398	$C_3H_6NO_2$	0	1	1	1
223.9840/225.9875	$C_5H_9CuN_2O_4$	0	2	2	2
241.9937/243.9988	$C_5H_{11}CuN_2O_5$	0	2	2	2
250.0932	$C_9H_{16}NO_7$	6	1	1	1
268.1038	$C_9H_{18}NO_8$	6	1	1	1
268.1027[b]	$C_9H_{18}NO_8$	6	1	1	1
298.1123	$C_{10}H_{20}NO_9$	6	1	1	1
404.0513/406.0501	$C_{11}H_{21}CuN_2O_{10}$	6	2	2	2
416.0530/418.0559	$C_{12}H_{21}CuN_2O_{10}$	6	2	2	2
434.0597/436.0561	$C_{12}H_{23}CuN_2O_{11}$	6	2	2	2
464.0693/466.0710	$C_{13}H_{25}CuN_2O_{12}$	6	2	2	2
596.1150/598.1172	$C_{18}H_{33}CuN_2O_{16}$	12	2	2	2

[a]The calculated error (in ppm) for all ions were less than 20ppm.
[b]The ion at $[M+H]^+$ 268 generated in the glycine/glucose/paraformaldehyde model system.

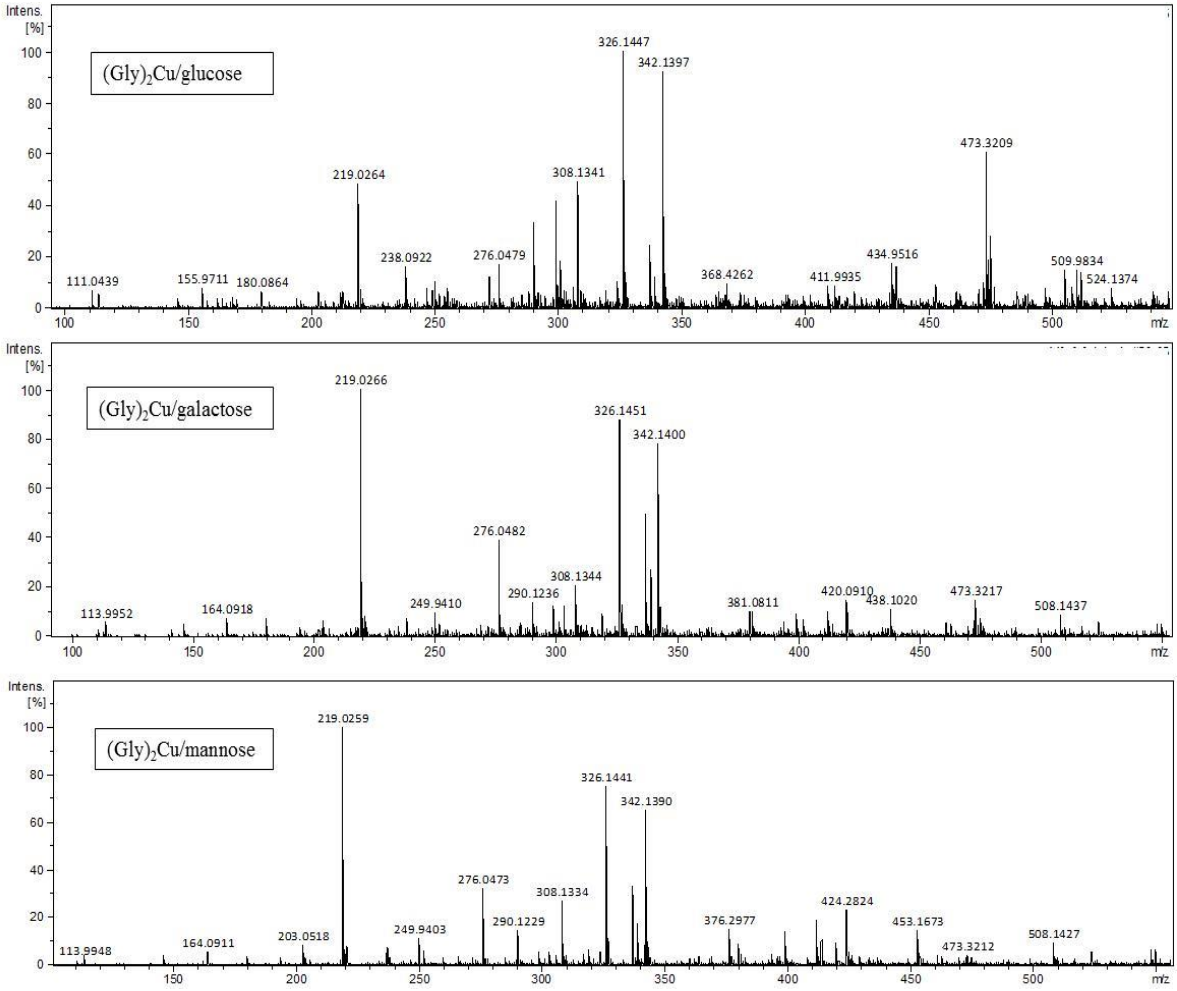

Supplementary Figure S6.1. ESI/qTOF/MS spectra of glycine copper complexes with glucose, galactose and mannose.

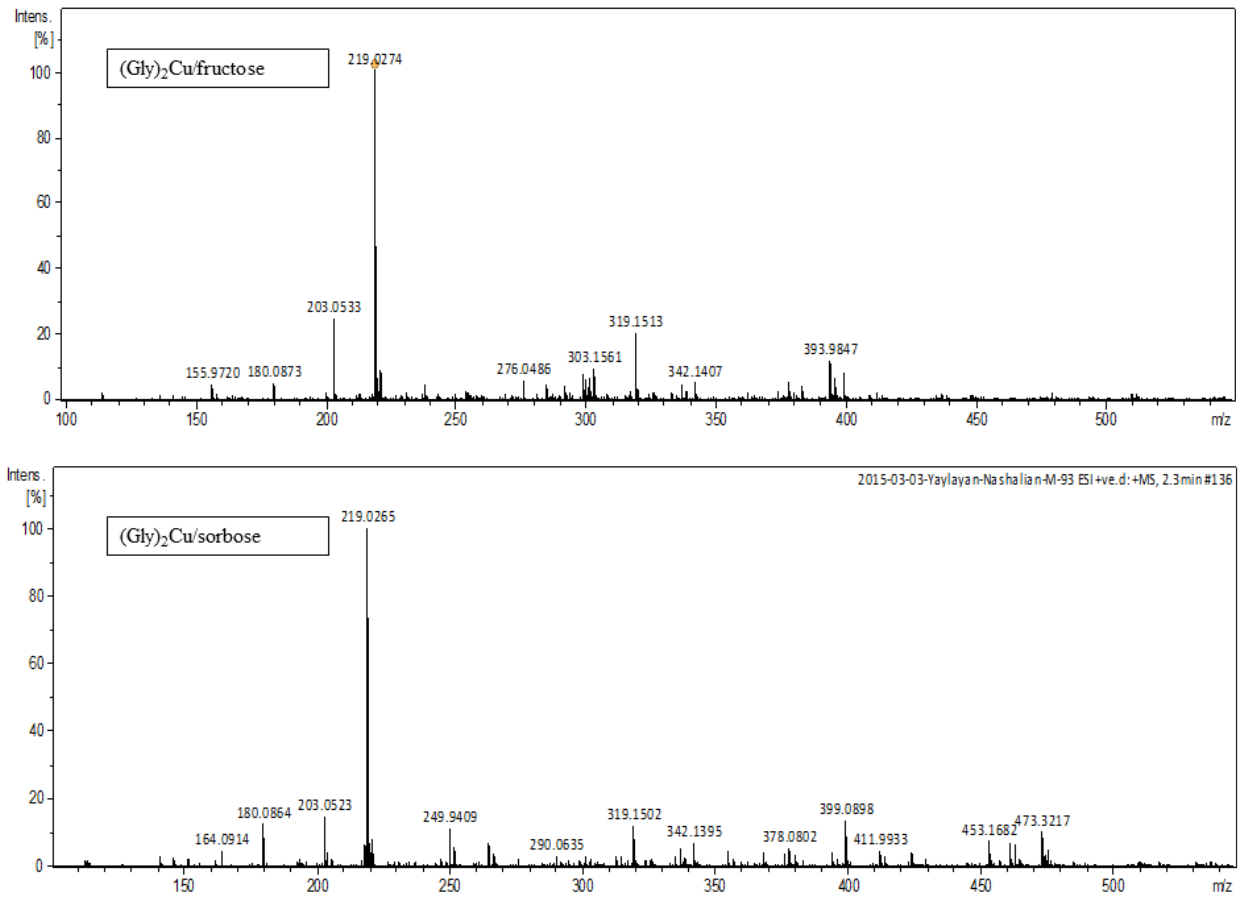

Supplementary Figure S6.2. ESI/qTOF/MS spectra of glycine copper complex with fructose or sorbose

CONNECTING PARAGRAPH

In the previous chapters, amino acid transition metal complexes were used to investigate the effect of transition metal ions on the Maillard reaction. Since sodium glycinate is a commonly used reagent that can also modify the acid/base properties of the reaction medium, it was predicted that such amino acid salts that are unable to form binary complexes can behave differently than the binary complexes and induce base catalyzed sugar fragmentations and formation of reactive carbonyl intermediates and volatile sugar fragments. In chapter 7, we explored the pyrolytic degradation of glucose in the presence of sodium glycinate and other metal complexes and observed as expected increased formation of sugar degradation products. Chapter 7 was published in *Food Chemistry:* Formation of the reduced form of furaneol® (2,5-dimethyl-4-hydroxy-tetrahydrofuran-3-one) during the Maillard reaction through catalysis of amino acid metal salts. *Food Chemistry*, 210, 43-48.

CHAPTER 7

FORMATION OF THE REDUCED FORM OF FURANEOL® (2,5-DIMETHYL-4-HYDROXY-TETRAHYDROFURAN-3-ONE) DURING THE MAILLARD REACTION THROUGH THE CATALYSIS OF AMINO ACID METAL SALTS

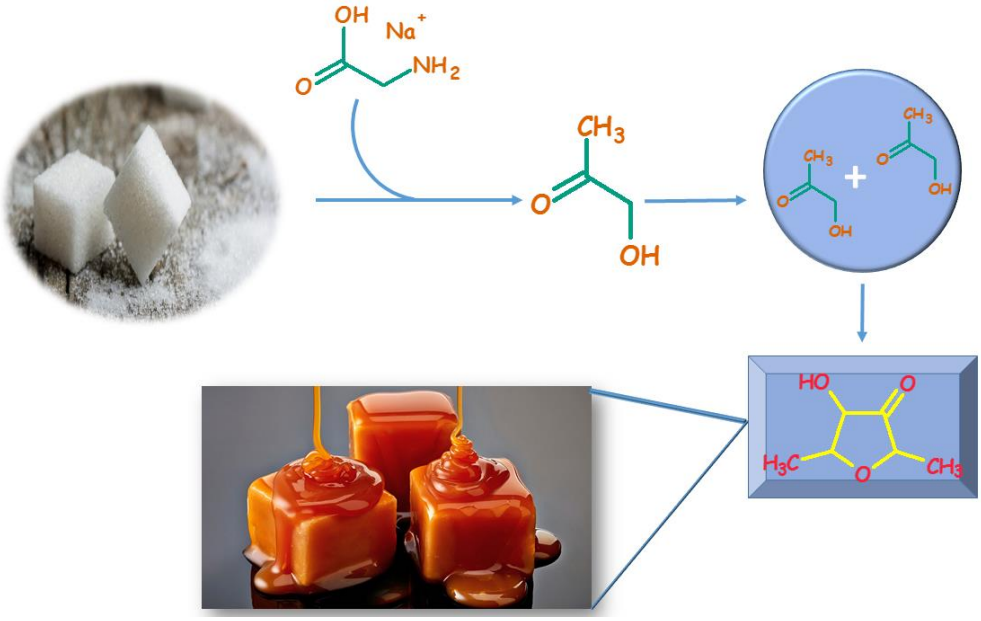

7.1 ABSTRACT

Under pyrolytic conditions the acidity/basicity of Maillard reaction mixtures can be controlled through the use of hydrochloride or sodium salts of amino acids to generate a diversity of products. When the degradation of glucose was studied under pyrolytic conditions using excess sodium glycinate the reaction was found to generate a major unknown peak having a molecular ion at *m*/*z* 130. Subsequent in-depth isotope labelling studies indicated that acetol was an important precursor of this compound under pyrolytic and aqueous heating conditions. The dimerisation and cyclisation of acetol into 2,5-dimethyl-4-hydroxy-tetrahydrofuran-3-one was found to be catalysed by amino acid metal salts. Also, ESI/qTOF/MS studies indicated that the unknown peak has expected molecular formula of $C_6H_{10}O_3$. Finally, a peak having the same retention time and mass spectrum was also generated pyrolytically when furaneol® was reduced with $NaBH_4$ confirming the initial hypothesis regarding the unknown peak to be the reduced form of furaneol®.

7.2 INTRODUCTION

Thermally generated 3(2*H*)-furanone derivatives such as 4-hydroxy-2,5-dimethyl-3(2*H*)-furanone (furaneol)®, 2-ethyl-4-hydroxy-5-methyl-3(2*H*)-furanone (homofuraneol), and 4-hydroxy-5-methyl-3(2*H*)-furanone (norfuraneol®) are considered to be important flavour compounds because of their low odour threshold values and diverse flavour profiles. Although naturally biosynthesised in fruits, plants and microorganisms through multistep enzymatic reactions (Blank and Fay, 1996; Schwab, 2013; Slaughter, 1999), these furanones have also been reported to form in varying concentrations in a number of thermally processed foods and in Maillard model systems. Under relatively mild pH conditions, 3(2*H*)-furanones are known to originate either directly from intact sugars or in the presence of amino acids and 1,2-dicarbonyl intermediates generated during the Maillard reaction (Blank et al., 1996; Blank and Fay, 1996). Additionally, similar to other Maillard reaction products, the amount and type of the thermally generated furanones have been found to be dependent on the nature of the reactants (sugars and amino acids) and reaction conditions (temperature, time and duration) (Slaughter, 1999). Interestingly, in a recent investigation (Wang, 2014) of thermal degradation of glucose in the presence of amino acid salts, a major and unique product was observed when glucose was pyrolysed in the presence of sodium glycinate. This unknown product exhibited a molecular ion at *m*/*z* 130 and based on the initial data obtained it was hypothesised to be the reduced form of furaneol® (2,5-dimethyl-4-hydroxy-tetrahydrofuran-3-

one). This hypothetical structure, however, was not reported in the literature except in the patent document of Ross Karl-Heinz et al. (1981) titled "Preparation of 2,5-Dimethyl-4-hydroxy-2,3-dihydrofuran-3-one" (U.S. Patent No 4,290,960, 1981). In their efforts to chemically synthesise furaneol®, Ross Karl-Heinz et al. (1981) generated the "novel" 2,5-dimethyl-4-hydroxy-tetrahydrofuran-3-one in a three-step reaction starting with the epoxidation of hex-3-ene-2,5-diol into 3,4-epoxy-hexane-2,5-diol, followed by the cyclisation of the latter into 2,5-dimethyl-3,4-dihydroxytetrahydrofuran, which after oxidation over a silver catalyst generated the 2,5-dimethyl-4-hydroxytetrahydrofuran-3-one (IUPAC name 4-hydroxy-2,5-dimethyloxolan-3-one also known as 2,5-anhydro-1,6-dideoxy-3-hexulose). Ross Karl-Heinz et al. (1981) also reported that the "novel" 2,5-dimethyl-4-hydroxytetrahydrofuran-3-one had a boiling point of 61–65 °C at 1 mbar. In the final step of the furaneol® synthesis, the 2,5-dimethyl-4-hydroxytetrahydrofuran-3-one was oxidised to directly generate furaneol® in 75–80% recovery yield. Unfortunately, no information about the sensory properties of the reduced furaneol® (2,5-dimethyl-4-hydroxy-tetrahydrofuran-3-one) was reported. However, furanone derivatives are known to possess common flavour characteristics related to their chemical structure. In fact, their caramel-like aroma note is attributed to their molecular structure and ability to form a hydrogen bond between the 4-hydroxy group and the adjacent keto group in a planar configuration (Hodge, 1967; Schwab, 2013); hence, the reduced furaneol® can be expected to have flavour notes similar to that of furaneol®.

Considering the knowledge gap in this particular 3(2*H*)-furanone derivative, the present study aimed at using sugar and amino acid model systems in addition to isotope labelling techniques to investigate the origin and the mechanism of its formation from Maillard reaction precursors under pyrolytic and aqueous heating conditions.

7.3 Materials and Methods

7.3.1 Reagents and chemicals

Glucose, acetol (90%), DL-lactaldehyde solution (⩾95%), glycine (98%), alanine (99%), glycine sodium salt hydrate (98%), calcium chloride, copper (II) chloride (99.9%), zinc chloride (⩾98%), potassium hydroxide, 2,5-dimethyl-4-hydroxy-3(2*H*)-furanone (98%), and sodium borohydride (99%) were purchased from Sigma–Aldrich Chemical Co. (Oakville, ON, Canada). Labelled [^{13}C-1]glucose (99%), [^{13}C-2]glucose (99%), [^{13}C-3]glucose (99%), [^{13}C-4]glucose (99%), [^{13}C-

5]glucose (99%), [^{13}C-6]glucose (99%), [U6-^{13}C]glucose (99%), [^{13}C-1]glycine (98%), [^{13}C-2]glycine (99%), and [^{15}N]glycine (98%) were purchased from Cambridge Isotope Laboratories (Andover, MI).

7.3.2 Synthesis of metal–amino acid salts

Copper glycinate, zinc glycinate, calcium glycinate and copper alaninate were prepared according to a previously published procedure (Nashalian & Yaylayan, 2015a) by dissolving glycine (0.75 g) or alanine (0.89 g) in methanol (10 mL) in the presence of KOH (0.05 g), followed by the addition of half a mole of $CuCl_2$ (0.67 g) or $ZnCl_2$ (0.68 g) or $CaCl_2$ (0.56 g). The precipitates were washed with methanol, filtered and dried. The metal–amino acid complexes were confirmed by obtaining their elemental composition from their accurate masses determined by ESI/qTOF/MS.

7.3.3 Preparation of the model systems for pyrolysis

Homogenised mixtures (0.5 mg) containing 2:1 ratio of glycine to sugar, 2:1 glycine sodium salt hydrate to sugar, or 1:2 ratio of sugar to KOH were packed inside a quartz tube (0.3 mm thickness), plugged with quartz wool, and inserted inside a coil probe and pyrolysed at 200 °C for 20 s under helium atmosphere. Isotopically labelled precursors were analysed similarly except model systems containing labelled glycine where pyrolysis was performed in the presence of KOH (Supplementary Table S7.1). All samples were analysed in duplicate.

7.3.4 Preparation of aqueous model systems for ESI/qTOF/MS analysis

Acetol and sodium glycinate hydrate (in a 1:2 relative molar ratio) were dissolved in water (2 mL) and heated on a sand bath in an open vial (5 mL capacity) at 150 °C for 1 h until dry. The reaction mixture was then analysed by ESI/qTOF/MS. All samples were analysed in duplicate.

7.3.5 Pyrolysis–gas chromatography–mass spectrometry (Py–GC–MS)

Samples were analysed according to previously published procedures (Guerra and Yaylayan, 2010; Nashalian and Yaylayan, 2015a); in summary a Varian CP-3800 GC coupled to a Varian Saturn 2000 mass spectrometry detector (Varian, Walnut Creek, CA) was used for the analysis of the model systems. The pyrolysis unit included a valved interface (CDS 1500), which was installed onto the GC injection port and connected to a CDS Pyroprobe 2000 unit (CDS Analytical, Oxford,

PA). The samples were analysed on a DB-5MS column (5% diphenyl, 95% dimethylpolysiloxane) with column dimensions of 50 m length × 0.2 mm internal diameter × 33 μm film thickness (J & W Scientific, Folsom, CA) using helium as the carrier gas. The GC column flow rate was regulated by an electronic flow controller (EFC) and set at a delayed (30 s) pressure pulse of 70 psi for the first 4 min and maintained with a constant flow of 1.5 mL/min for the rest of the run. The GC oven temperature was set at −5 °C for the first 5 min using CO_2 as the cryogenic cooling source and then increased to 50 °C at a rate of 50 °C/min. Then, the oven temperature was again increased to 270 °C at a rate of 8 °C/min and kept at 270 °C for 5 min. The MS transfer line temperature was set at 250 °C, the manifold temperature was set at 50 °C, and the ion trap temperature was set at 175 °C. An ionisation voltage of 70 eV was used, and EMV was set at 1850 V.

7.3.6 Electrospray ionisation/quadrupole time of flight/mass spectrometry (ESI/qTOF/MS) analysis

Samples were analysed according to a previously published procedure (Nashalian & Yaylayan, 2015a); in summary, the dry reaction mixtures were dissolved in LC-grade water to a concentration of 1 mg/mL. The samples were then diluted 10-fold in 10% methanol prior to analysis by ESI/qTOF/MS. The ESI/qTOF/MS system was comprised of a Bruker Maxis Impact quadrupole-time of flight mass spectrometer (Bruker Daltonics, Bremen, Germany) operated in positive ion mode. Samples (1 μl) were injected directly into the ESI/qTOF/MS. Instrument calibration was performed using sodium formate clusters. The electrospray interface settings were the following: nebuliser pressure 0.6 bar, drying gas 4 L/min, 180 °C, capillary voltage 4500 V. Scan range was from *m/z* 100 to 1000. The data was analysed using Bruker Compass Data Analysis software version 4.1.

7.3.7 Structural identification of the 2,5-dimethyl-4-hydroxytetrahydrofuran-3-one (reduced furaneol®)

The proposed structure of the reduced furaneol® (2,5-dimethyl-4-hydroxy-tetrahydrofuran-3-one) was confirmed based on the *in situ* formation from commercial standards, mass spectral fragmentation (presented in Figure 7.1), elemental composition obtained from high resolution ESI/MS data, and isotope labelling. The isotope labelling experiments were carried out using individually labelled [^{13}C-1] to [^{13}C-6]glucose, individually labelled [^{13}C-1], [^{13}C-2], [^{15}N]glycine,

and [U_6-^{13}C]glucose precursors. The reported percent label incorporation values (corrected for natural abundance and for percent enrichment) are the average of duplicate analyses and are rounded off to the nearest multiple of 5%.

7.4 RESULTS AND DISCUSSION

The Maillard reaction can be considered as a natural manifestation of combinatorial chemistry of sugars, amino acids and their degradation products, generating a variety of chemical structures. The series of subsequent reactions such as dehydrations, eliminations, aldolisation, retro-aldolisation and cyclisations that follow the initial carbonyl–amine reaction can generate a myriad of products depending on different reaction conditions, such as reactant type, concentration, and pH of the system (Van Boekel, 2006).

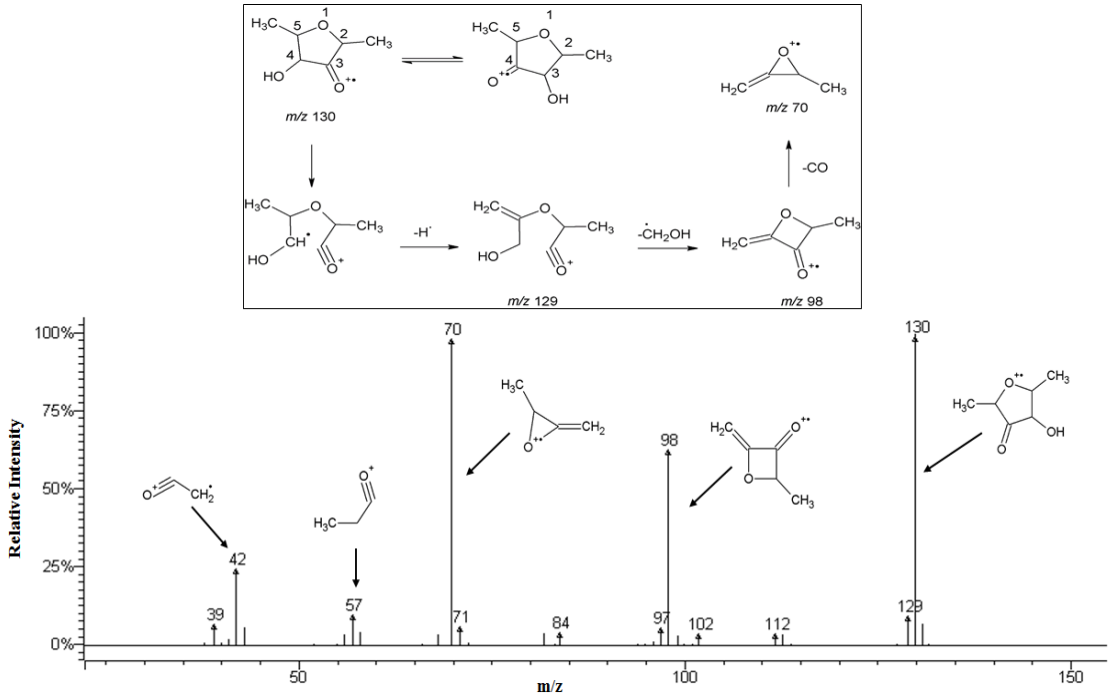

Figure 7.1. Proposed mechanism of electron impact mass spectral fragmentations of 2,5-dimethyl-4-hydroxytetrahydrofuran-3-one. For isotope incorporation data see Table 7.3 and Supplementary Table S7.3.

Under pyrolytic conditions the acidity/basicity of the reaction mixtures can be modulated through the use of sodium or hydrochloride salts of amino acids. When the degradation of glucose was being investigated under pyrolytic conditions using excess sodium glycinate the reaction was found to result in an overall altered reaction profile relative to glycine and was found to generate a major and distinctive peak having a molecular ion at *m*/*z* 130. Additionally, when glucose and glycine were replaced with labelled counterparts as presented under the experimental section, the subsequent isotope labelling studies indicated that the unknown peak incorporated six carbon atoms from glucose but no carbon or nitrogen atoms from glycine. Based on its nominal molecular weight and isotope incorporation pattern, it was hypothesised that the observed product having a molecular ion at *m*/*z* 130 may be derived from one of the known C_6 sugar degradation products such as HMF (*m*/*z* 126), 5-methylfurfural (*m*/*z*110), furaneol® (*m*/*z* 128) etc. but most likely it corresponded to the reduced form of furaneol® (2,5-dimethyl-4-hydroxytetrahydrofuran-3-one). To confirm this hypothesis, commercially available furaneol® was pyrolysed in the absence and presence of sodium borohydride under basic conditions. Indeed in the presence of sodium borohydride, furaneol® was found to generate a chromatographic peak having the same retention time and mass spectral fragmentation pattern (Figure 7.1) as that of the peak generated from the reaction of glucose with sodium glycinate, thus confirming the proposed structure. On the other hand, the glucose/sodium glycinate model system, which generated the unknown product as a prominent peak did not generate furaneol®, indicating that the product in question was most likely not formed through the reduction of furaneol®, but through an alternate route. Hence, to investigate further the origin of the unknown product, variously labelled glucose with ^{13}C at individual carbon atoms was reacted with sodium glycinate under pyrolytic conditions. The label incorporation pattern in *m/z* 130 was investigated using Py–GC/MS and the percent label incorporation from each glucose carbon atom in the unknown peak is listed in Table 7.1. Analysis of the isotope labelling pattern indicated that the unknown compound at *m/z* 130 in fact did not originate through the reduction of *in-situ* formed furaneol®, but on the contrary it required the cyclisation of two 3-carbon fragments generated from sugar due to the presence of doubly labelled carbon atoms in the unknown product (Table 7.1) consistent with the absence of furaneol® in the reaction mixture. As for the nature of the 3-carbon sugar-generated fragments, they are most likely limited to either acetol/lactaldehyde or glyceraldehyde/dihydroxyacetone fragments in addition to pyruvaldehyde. Among the possible fragments, acetol/lactaldehyde pair can generate the target compound through

known chemical reactions with minimum energy expenditure, first undergoing aldol addition, followed by cyclisation and dehydration steps (Novotny et al., 2007), without the need for oxidation or reduction steps as shown in Figure 7.2. In fact, the pyrolysis of glucose in the presence of sodium glycinate generated, in addition to the unknown peak, relatively high amounts of acetol (see Supplementary Table S7.2), suggesting a possible link between the two products. It is a well-known fact that sugar fragmentations are accelerated under alkaline conditions, generating enhanced amounts of degradation products such as acetol and various other 1,2-dicarbonyls (Novotny et al., 2007; Weenen, 1998). Subsequently, when commercially available acetol or acetol/lactaldehyde mixtures were pyrolysed alone and in the presence of sodium glycinate, both model systems generated the unknown peak although in the presence of sodium glycinate the peak intensity was significantly enhanced particularly in the model system containing acetol and lactaldehyde, where the intensity showed an increase by an order of magnitude (see Supplementary Table S7.2), highlighting the important role that acetol and its enolised form (lactaldehyde) play as precursors of this compound. Additionally, the model system containing acetol/sodium glycinate was heated at 150 °C for 1 h in 2 mL aqueous solution and the dry residue was analysed by ESI/qTOF/MS. The analysis revealed the formation of an ion at [M + Na] = 153.0523 corresponding to the sodiated ion of the unknown peak with the expected molecular formula of $C_6H_{10}O_3Na$ (with a 3 ppm error), indicating the ability of glucose/sodium glycinate model to generate 2,5-dimethyl-4-hydroxytetrahydrofuran-3-one under aqueous heating conditions.

Table 7.1. Percent ^{13}C-label distribution[a] in *m/z* 130

	M	M+1	M+2
C1	50	40	10
C2	40	50	10
C3	20	50	30
C4	10	50	40
C5	20	40	40
C6	40	50	10

[a] Generated from variously labeled glucoses in glucose/sodium glycinate hydrate model systems. The % standard error was different for each labelled glucose however it varied between 5 to 25%.

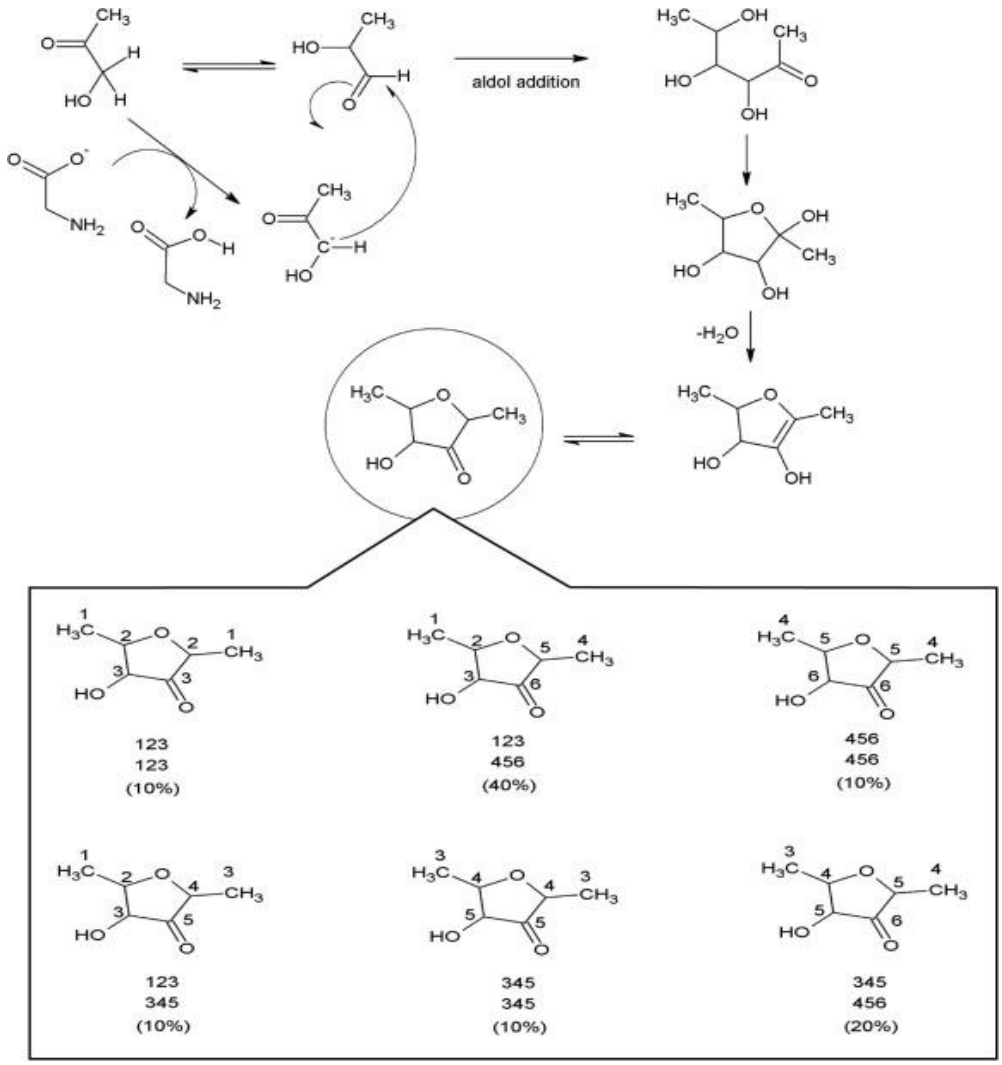

Figure 7.2. Proposed mechanism of formation of 2,5-dimethyl-4-hydroxytetrahydrofuran-3-one through dimerisation of two 3-carbon sugar fragments (acetol and lactaldehyde) and the origin of its various isotopomers. The numbers indicate glucose carbon atom positions.

7.4.1 Proposed mechanism of formation of acetol and its dimerisation to generate 2,5-dimethyl-4-hydroxy-tetrahydrofuran-3-one (reduced furaneol®)

The above studies have indicated that the reduced form of furaneol® of *m*/*z* 130 can be generated under both aqueous alkaline conditions and pyrolytically using amino acid sodium salts. Furthermore, its precursor has been identified as acetol, which can isomerise into lactaldehyde and undergo aldol addition followed by cyclisation and dehydration as shown in Figure 7.2. In this reaction, sodium glycinate plays a dual role, first as an isomerisation catalyst (proton donor/proton acceptor) and second as a base for aldolisation. If the proposed formation mechanism is correct, the isotope incorporation patterns of acetol (Table 7.2) should be reflected in the unknown peak, since it arises from the dimerisation of two acetol molecules. According to the isotope

incorporation data presented in Table 7.2 three distinct isotopomers of acetol can be generated from the degradation of glucose in the presence of sodium glycinate having C1–C2–C3 (40%), C3–C4–C5 (20%), and C4–C5–C6 (40%) sequences (Table 7.2 and Figure 7.3). The most abundant two sequences (40% each) were found to originate from the retro-aldol reaction of 1-deoxyglucosone and 4-deoxy-5-ketohexose as shown in Figure 7.3. These two pathways have been previously reported by Yaylayan and Keyani (2000) when glucose was degraded in the presence of free glycine. Additionally, it seems that sodium glycinate can initiate a third but minor pathway (20%) generating acetol with C3–C4–C5 carbon sequence. This isotopomer is proposed to arise through a 3-deoxy-4-ketohexose intermediate which can undergo two consecutive retro-aldol reactions to generate the observed acetol (see Figure 7.3). As expected, the above identified isotope labelling pattern of acetol (Table 7.2) was reflected in the isotope incorporation pattern of the unknown peak (Table 7.1) generated by the combination of two acetol molecules (Figure 7.2) to produce the compound at *m*/*z* 130 as shown in Figure 7.2. The random combinations of any two acetol molecules out of the three isotopomers should statistically generate a distribution pattern of the adducts consistent with the initial concentrations of the starting isotopomers, such as the two most abundant isotopomers of acetol with sequences of C1–C2–C3 and C4–C5–C6 generating the most abundant (40%) isotopomer of *m*/*z* 130 as shown in Figure 7.2. The validity of the proposed mechanism was further confirmed when commercially available acetol and lactaldehyde were separately added to the [$^{13}U_6$] glucose/glycine sodium hydrate model system. As a result, the compound at *m*/*z* 130 exhibited mixed isotope incorporation pattern which included unlabelled product (*m*/*z* 130), partially labelled with three atoms (*m*/*z* 133), and completely labelled (*m*/*z* 136) product, further confirming the role of acetol and lactaldehyde as the three carbon precursors of the compound (Supplementary Table S7.3).

Table 7.2. Percent ^{13}C-label distribution in acetol[a] (*m*/*z* 74)

m/z 74	M	M+1
C1	60	40
C2	60	40
C3	40	60
C4	40	60
C5	40	60
C6	60	40

[a] Generated from variously labeled glucoses in glucose/sodium glycinate hydrate model system. The % standard error was different for each labelled glucose however it varied between 5 to 25%.

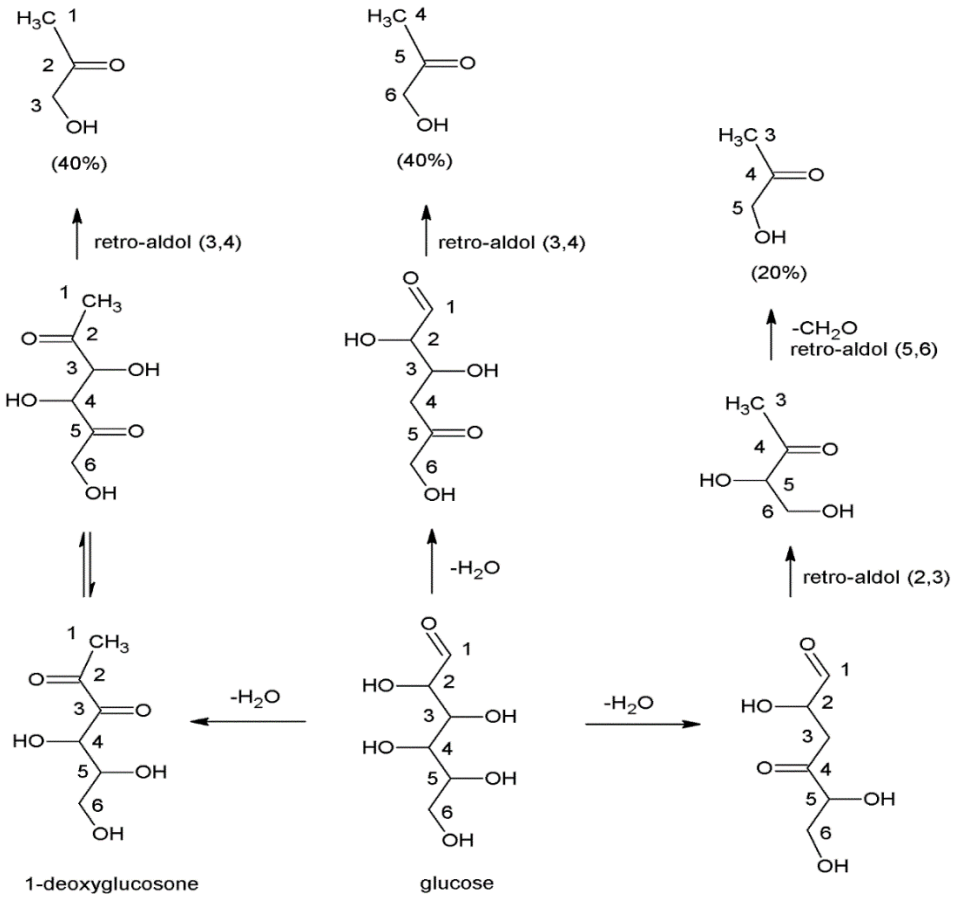

Figure 7.3. Glucose fragmentation pathways and formation of three isotopomers of acetol (see also Table 7.2).

7.4.2 Electron impact mass spectral fragmentation pattern of 2,5-dimethyl-4-hydroxy-tetrahydrofuran-3-one (reduced furaneol®)

The electron impact mass spectral fragmentation pattern of 2,5-dimethyl-4-hydroxytetrahydrofuran-3-one is shown in Figure 7.1. The molecular ion at *m*/*z* 130 generated four fragment ions at *m*/*z* 98, 72, 57 and 42. The major fragment at *m*/*z* 98 can arise from the molecular ion by a neutral loss of CH_3OH losing carbon atoms either from ring position 3 or 4 as indicated in Figure 7.1 and followed by subsequent neutral loss of CO from *m*/*z* 98 losing again carbon atoms either from ring position 3 or 4 to give rise to *m*/*z* 70. The ring positions 3 and 4 are populated by glucose carbon atoms 3, 5 or 6 according to Figure 7.2 (see Figure 7.2 inset). Consequently, these fragment ions should display increased relative intensities of unlabelled ions (M) and decreased intensities of M + 1 and M + 2 ions when ^{13}C-3, or ^{13}C-5 or ^{13}C-6 labelled glucose is used in the model systems, as shown in Table 7.3. However, unlike the ion at *m*/*z* 98,

the ion at *m*/*z* 70 can also arise from an alternate pathway giving rise to an isomeric structure incorporating ring atoms 2, 3 and 4 and a methyl group instead of ring atoms 2, 5 and two methyl groups; as a result the expected changes in the isotope incorporation pattern will be effected for the ion at *m*/*z* 70 and consequently will not follow the same profile changes as that of the ion at *m*/*z* 98.

Table 7.3. Percent ^{13}C incorporation from individually[a] labelled ^{13}C-glucoses indicated below in the molecular ion at *m*/*z* 130 and in its major mass spectral fragments.

m/*z*		C1	C2	C3	C4	C5	C6
130	M	50	40	20	10	20	40
	M + 1	40	50	50	50	40	50
	M + 2	10	10	30	40	40	10
98	M	50	40	40	10	30	45
	M + 1	40	50	60	50	50	55
	M + 2	10	10	10	40	20	0
70	M	50	40	50	40	40	50
	M + 1	40	50	40	50	50	50
	M + 2	10	10	10	10	10	0

[a] For uniformly labelled ^{13}C-U_6 glucose containing model systems see Supplementary Table S7.3.

7.4.3 Catalytic role of amino acid metal salts in enolisation/aldolisation reactions

Enolisation and aldol-type reactions occurring during the Maillard reaction are essential for generating new compounds from simple degradation products such as acetol. Such reactions require proton donor/acceptors to initiate enolisations and relatively strong bases to abstract α-hydrogens from carbonyl compounds for aldolisation reactions to occur. A crucial step in the generation of the compound at *m*/*z* 130 is the enolisation of acetol into lactaldehyde followed by their dimerisation through aldol reactions (Figure 7.2). These transformations do not happen efficiently in the absence of sodium glycinate even when KOH was used, which highlights the important role that amino acid metal salts play in catalysing both enolisations and aldol condensation reactions. Furthermore, this observation was generalised using different metal salts (copper glycinate, calcium glycinate, zinc glycinate) and a different amino acid (copper alaninate). When pyrolysed with acetol, all of the above mentioned model systems were found to generate the compound at *m*/*z* 130 (Supplementary Table S7.2), although the metal salts with a relatively higher

redox potential such as copper and zinc were found to catalyse the formation of the compound at *m*/*z* 130 more efficiently compared to calcium and sodium salts.

Due to the general availability of the precursors required for the generation of 2,5-dimethyl-4-hydroxytetrahydrofuran-3-one, it can be expected that sugar degradation reactions occurring in the presence of amino acid metal salts can potentially generate this compound in aqueous solutions. Furthermore, the specific formation pathways and the precursors identified in this work, can provide further opportunities for their generation in flavour formulations designed for specialty applications in food products.

7.5 SUPPLEMENTARY DATA

Supplementary Table S7.1. The composition of the model systems

Model systems[a]	**Model systems with isotopically labeled precursors**	**Control model systems**
Glucose/sodium glycinate hydrate	[U_6-^{13}C]glucose/sodium glycinate hydrate	Acetol
Glucose/KOH	[U_6-^{13}C]glucose/acetol/sodium glycinate hydrate[b]	Acetol/KOH
Acetol/copper glycinate	[U_6-^{13}C]glucose/ lactaldehyde/sodium glycinate	Acetol/sodium glycinate.hydrate[c]
Acetol/zinc glycinate	[^{13}C-1] to [^{13}C-6]glucose/sodium glycinate hydrate	Furaneol®/KOH
Acetol/calcium glycinate	Glucose/[^{13}C-1]glycine/KOH	Furaneol®/$NaBH_4$/KOH
Acetol/copper alaninate	Glucose/[^{13}C-2] glycine/KOH	Acetol/lactadehyde/sodium glycinate hydrate
	Glucose/[^{15}N] glycine/KOH	

[a] The model systems were analyzed in a 1-2 molar ratio of sugar or acetol to amino acid. Individually labelled glucose, glycine or ^{13}C-[U_6]glucose models were analyzed similarly.
[b] The model system comprised of [U_6-^{13}C]glucose/acetol or lactaldehyde/sodium glycinate hydrate was analyzied in a (1-1-2 molar ratio).
[c] Acetol/sodium glycinate hydrate was analyzed by pyrolysis and by ESI-QTOF-MS analysis following heating at 150^{o}C for 1 hr.

Supplementary Table S7.2. Efficiency[a] of formation of acetol and/or 2,5-dimethyl-4-hydroxy-tetrahydrofuran-3-one in different model systems.

Model system	Acetol	2,5-dimethyl-4-hydroxy-tetrahydrofuran-3-one
Glucose	2.1×10^9	0
Glucose/ sodium glycinate hydrate	4.4×10^9	3.1×10^9
Glucose/KOH	6.1×10^9	0
Acetol	-	1.6×10^8
Acetol/sodium glycinate hydrate	-	3.3×10^9
Acetol/calcium glycinate	-	3.5×10^9
Acetol/zinc glycinate	-	6.6×10^9
Acetol/copper glycinate	-	7.1×10^9
Acetol/copper alaninate	-	6.7×10^9
Acetol/lactaldehyde/sodium glycinate hydrate	-	4.6×10^{10}
Acetol/KOH	-	4.0×10^8

[a] The values are expressed as the chromatographic peak area of 2,5-dimethyl-4-hydroxy-tetrahydrofuran-3-one per mole of glucose or acetol in the presented model systems.

Supplementary Table S7.3. Number of ^{13}C labeled atoms incorporated in the major mass spectral fragments of *m/z* 130 generated from uniformly labeled ^{13}C glucose/sodium glycinate and from ^{13}C glucose/sodium glycinate/acetol mixtures[a]

m/z	^{13}C-U_6	^{13}C-U_6/acetol[a]
130	6	0, 3, 6
98	5	0, 3, 5
70	4	0, 2, 4

[a] acetol is equimolar with ^{13}C-U_6 glucose in the mixture of ^{13}C glucose/sodium glycinate/acetol.

CONNECTING PARAGRAPH

Since in the previous chapters we demonstrated that the ability of amino acids to complex with metals influenced the outcome of the Maillard reaction, in chapter 8 we investigate the reactivity of other food components such as purine bases towards metal ions and their behaviour with sugars and amino acids during the Maillard reaction. In this chapter we explore the interaction of nucleosides and nucleobases alone or in adenine-copper complexes during the Maillard reaction. In the absence of metals, ribose selectively formed mono ribosylated N^6 adenine, but in the presence of $(Ade)_2Cu$ complex they also generated di-ribosylated $N^{6,9}$ adenine. On the other hand, the reaction of furanmethanol with adenine in the presence of ribose generated kinetin and its isomer, while its reaction with adenosine generated kinetin riboside. Chapter 8 was submitted for publication: Reactivity of nitrogen atoms in adenine and $(Ade)_2Cu$ complexes towards ribose and furanmethanol: formation of adenosine and kinetin.

CHAPTER 8

REACTIVITY OF NITROGEN ATOMS IN ADENINE AND $(ADE)_2CU$ COMPLEXES TOWARDS RIBOSE AND FURANMETHANOL: FORMATION OF ADENOSINE AND KINETIN

8.1 ABSTRACT

To explore the interaction of nucleosides and nucleobases in the context of the Maillard reaction and to identify the selectivity of purine nitrogen atoms towards various electrophiles, model systems composed of adenine or adenosine, glycine, ribose and/or furanmethanol (with and without copper) were studied in aqueous solutions heated at 110^{o}C for 2 hours and subsequently analyzed by ESI/qTOF/MS/MS in addition to isotope labeling techniques. The results indicated that ribose selectively formed mono ribosylated N^6 adenine, but in the presence of $(Ade)_2Cu$ complex the reaction mixture generated mono-, di- and tri- substituted sugar complexes and their hydrolysis products of mono ribosylated N^6 and N^9 adenine adducts and di-ribosylated $N^{6,9}$ adenine. Furthermore, the reaction of furanmethanol with adenine in the presence of ribose generated kinetin and its isomer, while its reaction with adenosine generated kinetin riboside as confirmed by comparing the MS/MS profiles of these adducts to those of commercial standards.

8.2 INTRODUCTION

Investigation of the chemistry of interaction of reducing sugars with nucleobases may contribute to our understanding of the role of the Maillard reaction in transforming purine and pyrimidine bases into various Maillard modified products. Due to the spontaneous nature of the Maillard reaction such studies may also help elucidate how small molecules in the prebiotic world could assemble into complex structures forming nucleosides, nucleotides and DNA. Nucleosides for example can be viewed as N^9-Schiff bases of ribose and under relatively mild temperatures (37^{o}C-100^{o}C) various groups have indeed reported the formation of Amadori/Schiff base adducts in sugar/nucleobase mixtures (Dutta et al., 2006; Dutta et al., 2005; Knerr et al., 1994; Nissl et al., 1996). When ribose was reacted with adenine at 100^{o}C in dry state, it generated two products, a N^6-ribosyladenine (Schiff base or Amadori adduct) as the major product and around 2% adenosine as a minor product (Fuller et al., 1972) indicating the preference of sugars to undergo carbonyl amine reaction with adenine at nitrogen atom other than N^9. Unlike the behavior of amino acids in the Maillard reaction which has been extensively studied over the past century, such reactions with nucleobases have been relatively less explored in detail. Many foods contain nucleic acid material that can generate free purine and pyrimidine bases upon thermal hydrolysis (Cambero et al., 2000; Wondrak et al., 1997), and their addition or substitution with conventional Maillard reactants can

consequently lead to the generation of a variety of new Maillard reaction intermediates or products. In food mimicking model systems, the thermal hydrolysis of ATP and nucleic acids was reported to contribute to the Maillard reaction by enhancing the flavour perception of certain foods such as meats (Cambero et al., 2000; Chen et al., 2004). However, the exact chemistry of this interaction was not reported, and the behaviour of these components under cooking conditions is currently unknown. In 1997, Wondrak et al., (1997) reported that heating herring sperm DNA at 160^{o}C in aqueous solution and/or incubating it (free acid) without any sugars resulted in the hydrolysis of DNA and the formation of several furanone derivatives including 5-methyl-3(2*H*)-furanone, a known Maillard reaction product (Cerny & Davidek, 2003) and N^6-furfuryladenine, a furan derivative of adenine commonly known as kinetin. Kinetin is considered to be a highly bioactive plant hormone (Amasino, 2005) that is known to possess several desirable properties for human applications including anti-carcinogenic activity (Voller, et al., 2010). Although the presence of kinetin has not been reported to the best of our knowledge in the Maillard reaction mixtures containing free adenine and ribose, the conditions needed for its formation are available in foods. Therefore, in this study we explore the possible interactions of adenine with sugars (ribose, glucose and fructose) and furanmethanol in the presence and absence of copper and glycine in aqueous model systems heated at 110^{o}C for 2 hours.

8.3 MATERIALS AND METHODS

8.3.1 Materials and Reagents

Glucose, fructose, ribose, glycine (98%), copper (II) chloride ($CuCl_2$) (99.9%), potassium hydroxide, kinetin (99%), Kinetin riboside, adenine (≥99%), adenosine (≥99%), 2′-deoxyadenosine-5′-monophosphate (98-100%), and furanmethanol (98%) were purchased from Sigma-Aldrich Chemical Co. (Oakville, ON, Canada). Labeled [U_5-^{13}C]ribose (99%) were purchased from Cambridge Isotope Laboratories (Andover, MI).

8.3.2 Preparation of the adenine containing model systems

Model systems (10mg) comprising of 2′-deoxyadenosine-5′-monophosphate, adenine, or adenosine alone or with sugars (glucose or fructose or ribose and/or furanmethanol), and/or glycine

were dissolved in water (2 mL) and heated on a sand bath in an open vial (5 mL capacity) at 110°C for 2 hours until dry. The detailed composition of model systems and their relative ratios are presented in Supplementary Table S8.1. All the samples were analyzed in duplicates. Although ribose, glucose and fructose were used in all the experiments, the results were mainly discussed using ribose as a representative sugar due to its intrinsic presence in nucleotides.

8.3.3 Synthesis of bis(adeninato)copper(II) complex

The *bis*(adeninato)copper(II) or $(Ade)_2Cu$ complexes were prepared by dissolving adenine (1.35g) in methanol (10 mL) in the presence of KOH (0.05g) followed by the addition of half a mole of $CuCl_2$ (0.67g). The precipitate was washed with methanol, filtered and dried. $(Ade)_2Cu$ complex was confirmed by obtaining its elemental composition from its accurate mass determined by ESI/qTOF/MS analysis at $[M+H]^+ = 332.0102$ (calculated for $C_{10}H_9CuN_{10}$ with an error of 1.9 ppm).

8.3.4 Electrospray Ionization/Quadrupole time of flight/Mass spectrometry (ESI/qTOF/MS) analysis

The dry reaction mixtures were dissolved in LC grade water to a concentration of 1 mg/mL. The samples were then diluted 10-fold in 10% methanol prior to analysis by ESI/qTOF/MS. The ESI/qTOF/MS system was comprised of a Bruker Maxis Impact quadruple-time of flight mass spectrometer (Bruker Daltonics, Bremen, Germany) operated in positive ion mode. Samples (1µl) were injected directly into the ESI/qTOF/MS. Instrument calibration was performed using sodium formate clusters. The electrospray interface settings were the following: nebulizer pressure 0.6 bar, drying gas 4 L/min, 180°C, capillary voltage 4500 V. Scan range was from 100 to 1000 *m/z*. The data was analyzed using Bruker Compass Data Analysis software version 4.1. Tandem mass spectrometry (MS/MS) was carried out in MRM mode using 20.0 eV collision energy for selected ions.

8.3.5 Liquid Chromatography-Diode Array Detector-Mass spectrometry (LC-DAD-MS) analysis

Selected samples in Supplementary Table S8.1 were analyzed by LC-DAD-MS using a Dionex Ultimate 3000 UHPLC with a DAD detector (200nm-600nm) coupled to a Bruker Maxis Impact QTOF in positive ESI mode. Samples were separated on a Phenomenex Luna C18(2) column (5

μM 100A 2.2 x 50 mm) using a gradient of 98% mobile phase A (0.1% formic acid in H_2O) and 2% mobile phase B (0.1% formic acid in Acetonitrile) to 100 % mobile phase B in 8 minutes. The data was processed and using Bruker data analysis software version 4.1.

8.3.6 Structural identification

Evidence for the proposed structures of non-volatile reaction intermediates were provided through ESI/qTOF/MS analysis of their elemental composition, and by the use of commercial or synthetic intermediates and by isotope labeling studies. Furthermore, retention times, UV spectrum and MS/MS spectra of selected product ions were compared to those of commercial standards. The incorporation of copper in the identified complexes was confirmed by the isotopic signature of copper through detection of M+2 peaks at 30% relative intensity.

8.4 Results and Discussion

Although the reaction of nucleobases with sugars has been studied in the past; however, no information is available on the selectivity of the purine base nitrogen atoms towards various electrophiles. The glycation of adenine with sugars such as ribose have been shown to generate mainly N^6- substituted ribosyladenine in addition to negligible amounts of adenosine, (Fuller et al., 1972; Maurel and Convert, 1990). Additionally, the generation of adenosine has been shown to be enhanced in the presence of metal ions, which in turn, are known to coordinate with adenine at various locations generating stable complexes (Harkins & Freiser, 1958; Ilavarasi et al., 1997; Lippert, 2000). Currently, the pathways of generation of Maillard-type reaction products from nucleobases such as adenine under cooking conditions are not known. To understand the nature of such interactions under the Maillard reaction conditions, adenine/sugar model systems were chosen to investigate the role of added amino acids and metal salts or metal bound adenine such as *bis*(adeninato)copper on the selectivity and the profile of their interaction in aqueous systems heated at 110^{o}C for 2 hours and subsequently analyzed by electrospray ionization tandem mass spectrometry (ESI/qTOF/MS/MS). Although ribose, glucose and fructose were used in all the experiments, the results were mainly discussed using ribose as a representative sugar due to its intrinsic presence in nucleotides.

8.4.1 Interaction of adenine with ribose or glucose and formation of monoglycated adducts

To confirm the literature information (Dutta, 2006; Maurel and Convert, 1990) that adenine sugar mixtures generate only N^6 monoglycated products, adenine/ribose or glucose aqueous model systems were heated at 110^{o}C for 2 hours. The ESI/qTOF/MS analysis indicated that the reaction indeed generated only mono-ribosylated or mono-glucosylated adenine adducts at [M+H]=268 and [M+H]=298, respectively, which were detected as major ions in the ESI/qTOF/MS spectrum of these mixtures (Table 8.1 and Figure 8.1). These adducts can be formed through the known carbonyl-amine reaction between the sugars and adenine or nucleosides such as guanosine (Kner et al., 1994; Nissl et al., 1996), followed by condensation to generate their corresponding Schiff bases or Amadori rearrangement products (Table 8.1 and Figure 8.1). To verify that these interactions can also occur under Maillard reaction conditions and in model systems containing amino acids, glycine was added to the adenine/glucose and adenine/ribose aqueous model systems and heated similarly at 110 ^{o}C for 2 h. In the presence of the added glycine, the above mentioned glycated adenine at [M+H] = 268 and [M+H] = 298 were indeed generated along with free glycine Amadori adducts with both sugars and their dehydration products (see Table 8.1 and Figure 8.1). Moreover, the generated Amadori products of glycine were also found to further react with adenine, similar to free sugars to generate their corresponding Heyns rearrangement products at [M+H]=355 and [M+H]=324 from glucose and ribose Amadori products, respectively (Table 8.1 and Figure 8.1). All of the ribose containing adducts were found to incorporate predicted number of labeled carbon atoms from ribose when isotopically labeled $^{13}U_5$-ribose was used as reactant (Table 8.1).

The interaction of sugars with adenine can generate mainly two positional isomers at N^6 and N^9 as in adenosine. However, literature studies (Fuller at al., 1972) have indicated that N^6-isomer is the major adduct under the experimental conditions. Consequently, when the MS/MS profiles of sodiated adenosine standard and the ion at [M+Na]=290 were compared, they were found to be different (see Supplementary Figure S8.1). Similarly, the protonated ions also showed similar differences. In adenosine the purine ring is β-N-glycosidically linked to the anomeric carbon of ribose and stabilized as cyclized Schiff base, whereas the ribose moiety in the ion [M+Na]=290 is most probably stabilized as Amadori rearrangement product, especially since its MS/MS pattern displays characteristic losses of two water molecules as shown in the supplementary Figure S8.1. Furthermore, one of the interesting adducts of adenine with Maillard generated reaction products

from ribose is known as kinetin (N^6-furfuryladenine) which in theory could be formed in such mixtures at N^6 position through dehydrations and reduction of the mono-ribosylated adduct. However, the examination of the adenine/ribose reaction mixture indicated that neither kinetin (N^6-furfuryladenine) nor its riboside (N^6-furfuryladenosine) were formed in these model systems.

Table 8.1. Elemental composition and isotope incorporation (for ribose) of sugar adducts with adenine and presented in Figure 8.1.

Sugars	Monoisotopic mass	Elemental composition	Error (ppm)	[U_5-^{13}C] ribose
Glucose	238.0908	$C_8H_{16}NO_7$	7.8	-
	262.0951	$C_{11}H_{12}N_5O_3$	4.1	-
	280.1061	$C_{11}H_{14}N_5O_4$	5.4	-
	298.1152	$C_{11}H_{16}N_5O_5$	0.2	-
	320.0954	$C_{11}H_{15}N_5O_5Na$	5.3	-
	355.1368	$C_{13}H_{19}N_6O_6$	0.5	-
Ribose	208.0826	$C_7H_{14}NO_6$	2.3	5
	232.0853	$C_{10}H_{10}N_5O_2$	7.9	5
	250.0932	$C_{10}H_{12}N_5O_3$	3.2	5
	268.1031	$C_{10}H_{14}N_5O_4$	5.5	5
	290.0852	$C_{10}H_{13}N_5O_4Na$	4.5	5
	325.1234	$C_{12}H_{17}N_6O_5$	8.1	5
Fructose	298.1147	$C_{11}H_{16}N_5O_5$	1.5	-

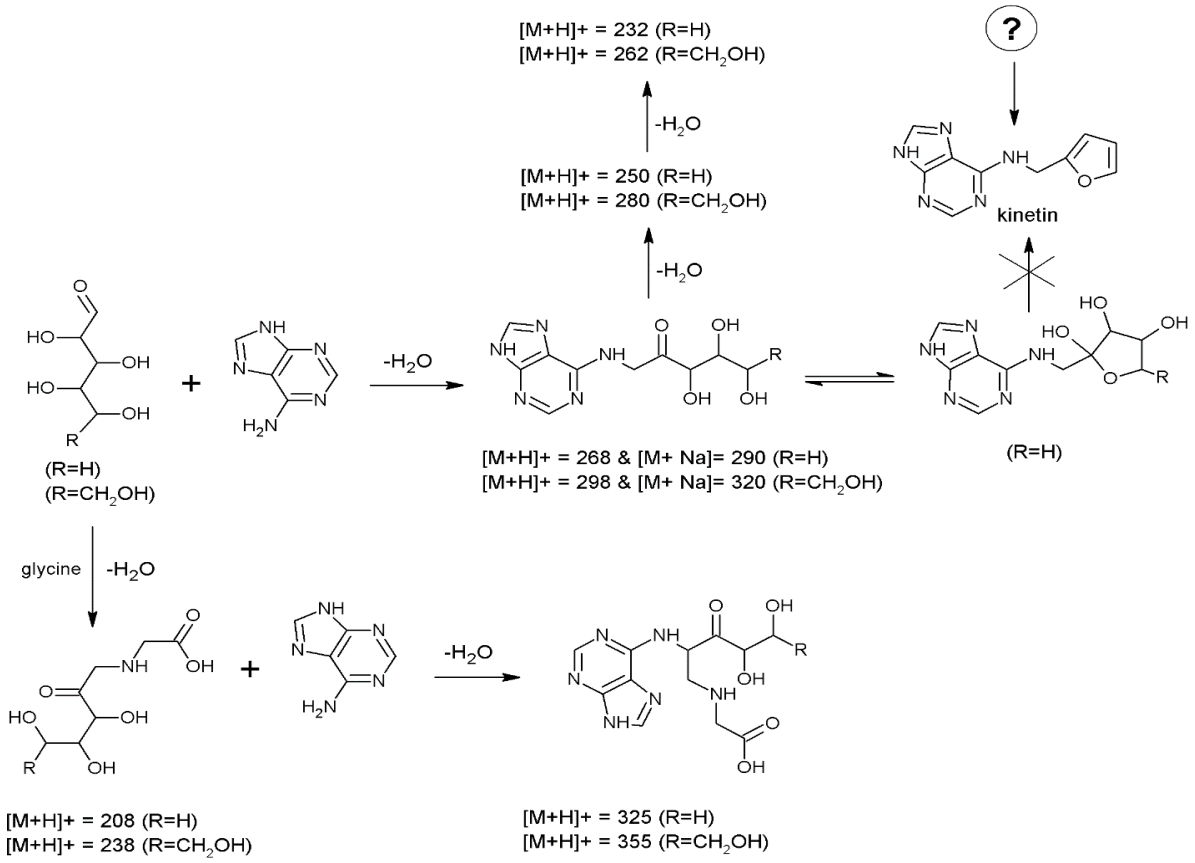

Figure 8.1. Proposed pathways of formation of sugar-adenine and Amadori-adenine adducts.

8.4.2 Interaction of adenine with ribose (or glucose) and formation of diglycated adducts in the presence of copper salts.

Studies conducted by Fuller at al. (1972) indicated that heating free ribose and adenine also generated very small amounts of adenosine, and that its formation was enhanced by the addition of metal ions. Similarly, recent studies have indicated that addition of copper salts to Maillard model systems also enhances selected Maillard reaction products such as the formation of amino sugars (Nashalian & Yaylayan, 2016). To explore this possibility, aqueous model systems consisting of $(Ade)_2Cu$/glucose, $(Ade)_2Cu$/ribose, or $CuCl_2$/adenine/ribose were prepared and heated (110 ^oC for 2 h). The ESI/qTOF/MS analysis indicated that the reaction profile was different from that of free adenine/sugar reaction shown in Figure 8.1. In addition to the monoglycated adenine and adenine Amadori adducts reported in Table 8.1, mono-, di- and tri- substituted sugar complexes of $(Ade)_2Cu$ were also observed at [M+H]=464, 596 and 728 respectively in addition to their hydrolysis products of di-glycated and di-ribosylated adenine adducts at [M+H]=460 and

[M+H]=400, respectively (see Table 8.2). To the best of our knowledge this is the first time di-glycated adenine adducts are reported. In the absence of copper, mainly mono-glycation of adenine is known to occur as was demonstrated from NMR studies (Maurel and Convert, 1990) and confirmed above and this can be best explained by the presence of only one reactive primary amino group in adenine able to react with sugars at position N^6. However, the complexation of adenine with copper not only can enhance the reactivity of the N^6 but also that of N^7 and N^9 due to the polarization of the Cu-N bonds and the increased electron density on these nitrogen atoms (see the structure of $(Ade)_2Cu$ in Figure 8.2). This altered reactivity of adenine allows multiple sugar additions to occur. When $CuCl_2$/adenine mixture was heated alone both monomeric and dimeric forms of the complex were detected at [M+H]=233 and [M+H]=332. On the other hand when $(Ade)_2Cu$ was heated alone only the ion at [M+H]=332 was observed (see Figure 8.2 and Table 8.2). In nucleobase-metal binding chemistry, there is a controversy as to which are the preferred sites of copper complexation on the adenine molecule (Bugella-Altamirano et al., 2002; Lippert, 2000), however, due to enhanced reactivity of the adenine ring towards sugars and the observed mass of the complex we propose the *bis* adduct shown in Figure 8.2 in which the two N^6 atoms are covalently attached and the two N^7 are coordinated with the copper atom. The N^7 is generally considered as preferred site of complexation (Bugella-Altamirano et al., 2002; Lippert, 2000; Mishra et al., 2008). According to Figure 8.2, when $(Ade)_2Cu$ first interacts with a sugar, the two most reactive N^6 atoms generate mono- and diglycted $(Ade)_2Cu$ complexes at [M+H] = 464 and 596, respectively. Due to enhanced reactivity of N^9 in the $(Ade)_2Cu$ complex the sugars can further conjugate at these sites and generate tri-glycated $(Ade)_2Cu$ complexes at [M+H] = 728 (see Figure 8.2 and Table 8.2). During the reaction and upon hydrolysis multi-glycated $(Ade)_2Cu$ complexes can release various isomers of mono- and diglycted adenines as detected at [M+H]=268 (ribose), [M+H]=400 (for ribose) and [M+H]=460 (for glucose) (See Supplementary Figure S8.2). If this hypothesis is true, and if N^9 is the second major site of glycation, then in the case of ribose the formed di-ribosylated adduct at [M+H]=400 will be equivalent to ribosylated adenosine which already has an inherent ribose molecule on N^9. To prove this hypothesis, adenosine was reacted with ribose or $^{13}U_5$-ribose and the MS/MS of the adduct at [M+H]=400 in the adenosine/ribose model system was compared to that of the di-ribosylated adenine at [M+]=400. As shown in Figure 8.2, the MS/MS profiles of the two adducts were found to be identical confirming the proposed mechanism of copper activation. Moreover, isotope labeling studies showed that under 20eV

collision energy the daughter ion at [M+H] = 268 (see supplementary Figures S8.2 and S8.3) mainly arises (86%) from the loss of the inherent ribose moiety (Schiff base) in adenosine rather than the more stable Amadori moiety formed by the reaction of adenosine with added ribose. These observations provide additional evidence that copper complexation on N^7 can enhance the formation of adenosine. Additionally, the formation of adenosine was found not to be affected when glycine was added to the model systems. Also, the presence of ribose in all ribose containing adducts was verified by its isotopic signature when $^{13}U_5$-[ribose] was used. To extend the generality of the above observations to *keto* sugars (Amadori adducts), fructose/adenine and fructose/$(Ade)_2Cu$ were similarly prepared and analyzed and were found to generate consistent results as that of glucose and ribose (Tables 8.2 and 8.3).

Table 8.2. Elemental composition and isotope incorporation (for ribose) of sugar[a] conjugates of $(Ade)_2Cu$ complex and presented in Figure 8.2.

Monoisotopic mass[b]	Elemental composition	Error (ppm)	[U_5-^{13}C] ribose
232.9519/234.9500	$C_5H_5CuClN_5$	4.5	0
268.1031	$C_{10}H_{14}N_5O_4$	5.5	5
290.0855	$C_{10}H_{13}N_5O_4Na$	3.5	5
332.0301/334.0298	$C_{10}H_9CuN_{10}$	1.9	0
332.0299/334.0297[c]	$C_{10}H_9CuN_{10}$	2.6	0
400.1468	$C_{15}H_{22}N_5O_8$	0.8	10
460.1668[d]	$C_{17}H_{26}N_5O_{10}$	2.5	-
464.0753/466.0773	$C_{15}H_{17}CuN_{10}O_4$	4.9	5
494.0828/496.0818[d]	$C_{16}H_{19}CuN_{10}O_5$	1.6	-
596.1166/598.1169	$C_{20}H_{25}CuN_{10}O_8$	2.2	10
728.1554/730.1590	$C_{25}H_{33}CuN_{10}O_{12}$	2.9	15

[a] Glucose and fructose generated corresponding conjugated adducts with $(Ade)_2Cu$ complex.
[b] The two masses shown represent copper isotopes $^{63}Cu/^{65}Cu$.
[c] Ion generated in the synthetic $(Ade)_2Cu$
[d] Ions generated in the $(Ade)_2Cu$/glucose model syste

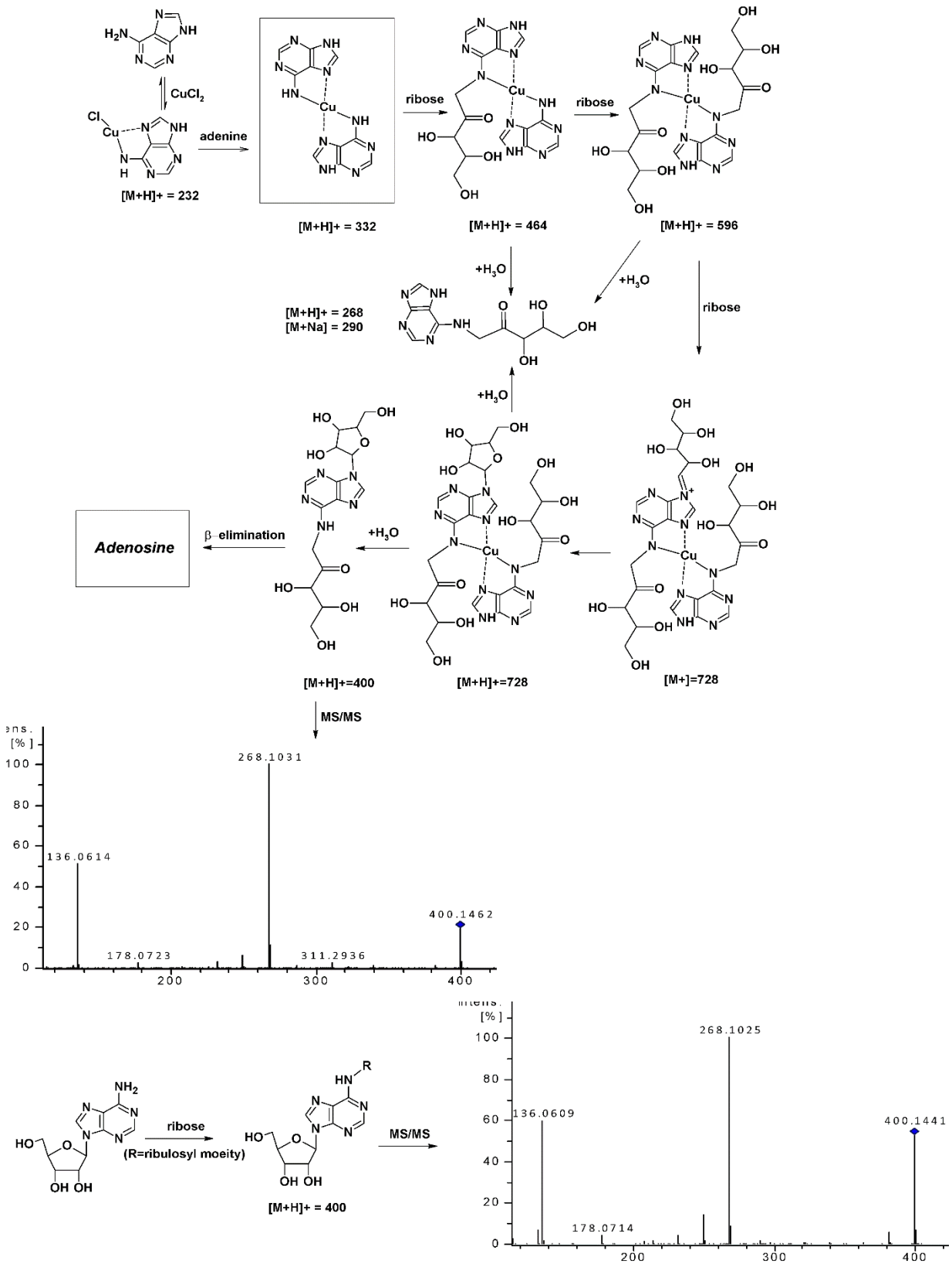

Figure 8.2. Proposed mechanism of formation of *bis*(adeninato)Cu complex and its catalysis of di-ribosylation of adenine.

8.4.3 Formation of kinetin and its riboside in ribose/furanmethanol/adenine model system

The occurrence and formation of kinetin during the Maillard reaction has never been reported in model systems with adenine, although it can be formed from DNA at Maillard reaction conditions (160^{o}C) (Wondrak, Tressl and Rewiki, 1997). As has been indicated above the reaction of adenine with ribose in the absence of copper salts generated only mono-ribosylated N^6 adduct at [M+H] = 268, however, the reaction mixture did not generate kinetin (N^6-furfuryladenine). Furanmethanol which is a known thermal degradation product of ribose during the Maillard reaction (Cerny & Davidek, 2003; Meynier, & Mottram, 1995) was considered to be an important precursor that should theoretically enhance the formation of kinetin when reacted with adenine. Subsequently, model systems consisting of adenine, ribose and furanmethanol were heated in aqueous solutions at 110^{o}C for 2 hours. The ESI/qTOF/MS analysis of the reaction mixture indicated the formation of adducts at [M+H]=216 and [M+H]=348 in addition to ribosylated adenine at [M+H]=268 (see Table 3 and Figure 3). The ion at [M+H]=216 had the same elemental composition as that of kinetin (see Table 3 and Figure 3). However, when the MS/MS profile of the ion at [M+H]=216 was compared to that of kinetin standard (base peak at [M+H] = 148]), it was found to be a possible mixture of kinetin and its isomers (N^6 or N^9-isomers) based on the observation of two base peaks at [M+H]= 173 and [M+H] = 148] in its MS/MS profile (see Figure 3 and Supplementary Table S2). The N^9 and N^6 isomers of kinetin can be formed through nucleophilic reaction at C-2 or C-6 positions of furylium ion generated after dehydration of furanmethanol as shown in Figure 3. One such kinetin isomer at [M+H] = 216, was generated from heated commercially available dAMP whose MS/MS spectrum showed a base peak at [M+H] = 173. This dehydrated and de-phosphorylated dAMP product was the only major peak in the heated sample of dAMP. The ion at [M+H] = 148 in the MS/MS spectrum could be tentatively considered as a marker ion for kinetin and the ion at [M+H] = 173 as a marker for its isomers.

The second ion observed in the reaction mixture of adenine/ribose/furanmethanol at [M+H]=348 had elemental composition consistent with that of commercial kinetin riboside ($C_{15}H_{18}N_5O_5$) and incorporated five carbon atoms from $^{13}U_5$-ribose. The comparison of the MS/MS spectrum of the ion at [M+H] = 348 to that of the MS/MS spectra of commercially available kinetin riboside and that generated *in situ* from furanmethanol reaction with adenosine (see Supplementary Figure S4) indicated that all the three model systems shared the ion at [M+H] = 216 representing kinetin as

their base peaks, however, the MS/MS spectrum of the ion at [M+H] = 348 generated from adenine, ribose and furanmethanol model system also generated the marker ions at [M+H] = 173 and 148 indicating the possible formation of two isomeric ribose adducts generating isomeric kinetins (see Supplementary Table S2 and Figure 3).

To further confirm that the furanmethanol/adenine/ribose model system generated kinetin and its isomers, the sample was further separated on a UHPLC column coupled to a diode array detector and compared to that of commercial kinetin. The commercial Kinetin standard eluted at 3.4 min as a single large peak and showed two λ_{max} at 211 nm and 274 nm (Supplementary Figure S5). On the other hand, the furanmethanol/adenine/ribose chromatogram showed the generation of several peaks among them were the two distinct peaks matching the mass of kinetin at m/z 216 (Supplementary Figure S6). The first peak eluted at 2.7 min and had λ_{max} values at 210 nm and 269 nm while the second peak eluted at exactly the same retention time as that of standard kinetin (3.4 min) and had the same λ_{max} values at 211 nm and 274 nm as the kinetin standard, providing irrefutable evidence for its formation (Supplementary Figure S6).

According to Figure 3, adenine reacts with furanmethanol at N^6 and N^9 positions forming kinetin and its possible isomers at [M+H] = 216 and at the same time reacting with ribose to form ribosylated adenine at N^6 ([M+H] = 268), the latter can further react with furanmethanol at N^6 and N^9 positions to form two isomers of ribose adducts of kinetin at [M+H] = 348 as shown in Figure 3. The β-elimination of ribose moieties from the kinetin riboside isomers can enhance the kinetin formation in the reaction mixture on the expense of its isomer, since ribose can react back much faster with the primary amino group of the kinetin isomer than the secondary amines in the kinetin molecule, converting the kinetin isomer to its riboside. Analysis of kinetin/ribose reaction mixtures heated at 110ºC for 2 hours did not indicate the formation of any adducts supporting the above statement.

Table 8.3. Elemental composition and isotope incorporation (for ribose) of the ions [M+H] = 216 and [M+H] = 348 generated in various model systems presented below and in Figure 8.3.

Model system	Monoisotopic mass	Elemental composition	Error (ppm)	[U_5-^{13}C] ribose
Furanmethanol/ribose/adenine	216.0869	$C_{10}H_{10}N_5O$	7.5	-
	348.1273	$C_{15}H_{18}N_5O_5$	10	5
	370.1115	$C_{15}H_{17}N_5O_5Na$	3.3	5
dAMP[a]	216.0875	$C_{10}H_{10}N_5O$	4.8	-
Kinetin[b]	216.0864	$C_{10}H_{10}N_5O$	9.9	-

[a] 2′-deoxyadenosine-5′-monophosphate
[b] Commercial standard

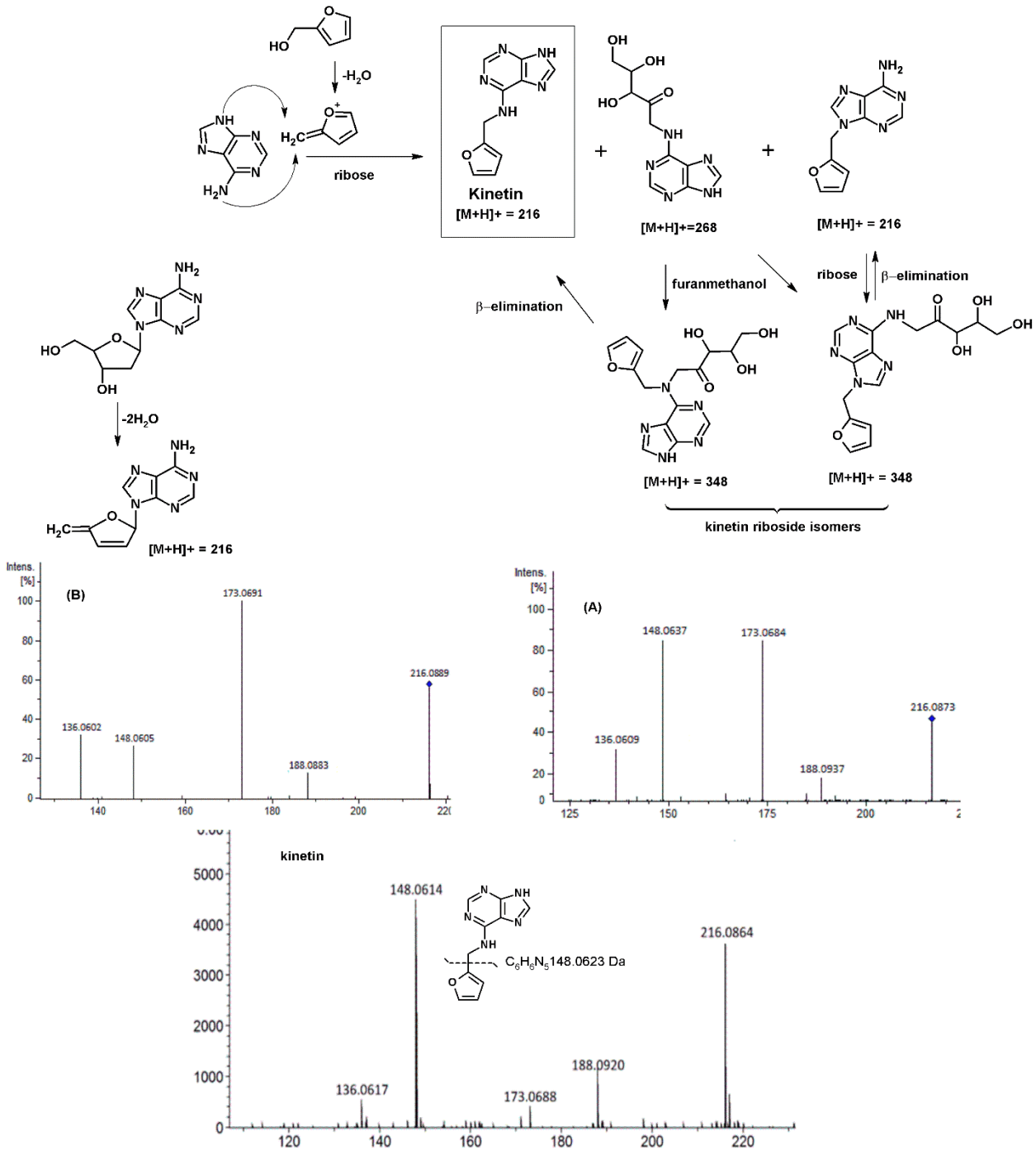

Figure 8.3. Proposed pathway of formation of Kinetin and its isomer during the Maillard reaction. Also see Supplementary Figure S8.4.

A) The MS/MS fragmentation pattern of the ion at [M+H] = 216 generated in the adenine/ribose/furanmethanol reaction mixture.

B) The MS/MS fragmentation pattern of the ion at [M+H] = 216 generated in heated dAMP model system at 110^{o}C for 2h.

8.5 CONCLUSIONS

This study indicated that adenine exhibits inherent selectivity to sugars mainly forming single Amadori adduct at the primary N^6-amino position whereas binary adenine copper complexes are activated to react with both N^6 and N^9 positions. Furthermore, furanmethanol through its reactive furylium ion can also form both N^6 and N^9 adducts of adenine to generate kinetin and kinetin isomer. The ability of adenine Amadori adducts to undergo β-elimination can further enhance their potential to generate kinetin and adenosine in Maillard reaction mixtures.

8.6 SUPPLEMENTARY DATA

Supplementary Table S8.1. The composition and relative ratio of the model systems

Model system	Relative molar ratio
Adenine/ribose	1-1, 1-4
Adenine/[U_5-^{13}C]ribose	1-1
Adenine/glucose	1-1
Adenine/fructose	1-1
Adenine/ribose/furanmethanol	2-1-1
Adenine/glucose/glycine	1-1-1
Adenine/ribose/glycine	1-1-1
Adenine/ribose/furanmethanol/glycine	2-1-1-1
Adenine/$CuCl_2$	1-0.5
Adenine/$CuCl_2$/ribose	1-0.5-1
$(Ade)_2Cu$[a]	-
$(Ade)_2Cu$ /ribose	1-1
$(Ade)_2Cu$ /glucose	1-1
$(Ade)_2Cu$/[U_5-^{13}C]ribose	1-1
$(Ade)_2Cu$ /ribose/glycine	1-1-2
Adenosine/ribose	1-1
Adenosine/furanmethanol	1-1
Deoxyadenosine monophosphate dAMP[a]	-
Kinetin[a]	-
Kinetin riboside	-

[a]The selected commercial and synthetic standards were analyzed before and after heating at 110°C for 2 h.

Supplementary Table S8.2. MS/MS fragmentation patterns[a] of kinetin and the ions at [M+H]=216 generated in the different model systems presented below and in figure 8.3.

Kinetin	Deoxyadenosine	Adenine/ribose/furanmethanol
136.0617 (0.1)	136.0612 (0.2)	136.0614 (0.3)
148.0614[b] (1.0)	148.0609 (0.1)	148.0592[b](1.0)
173.0688 (0.1)	173.0685[b](1.0)	173.0700[b] (1.0)
188.0920 (0.2)	188.0912 (0.1)	188.0915(0.2)

[a] The MS/MS fragmentation done at 20ev.

[b] Base peak. The numbers in the parenthesis represent the relative peak heights of the MS/MS fragments relative to their base peaks.

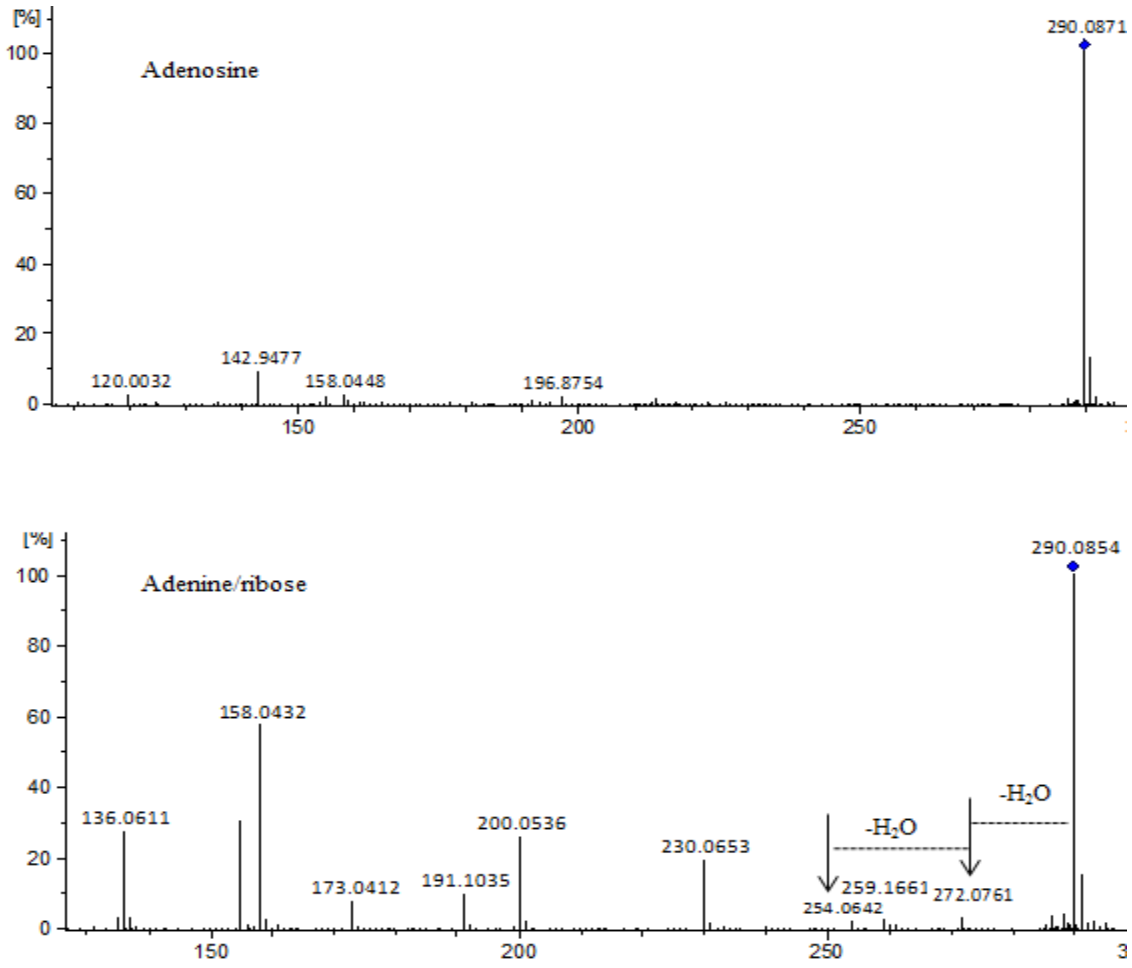

Supplementary Figure S8.1. Comparison of MS/MS fragmentation profiles of adenosine and ribosylated adenine at [M+Na]=290 generated in the adenine/ribose reaction mixture. The m/z 290 represents the sodiated adducts of both compounds.

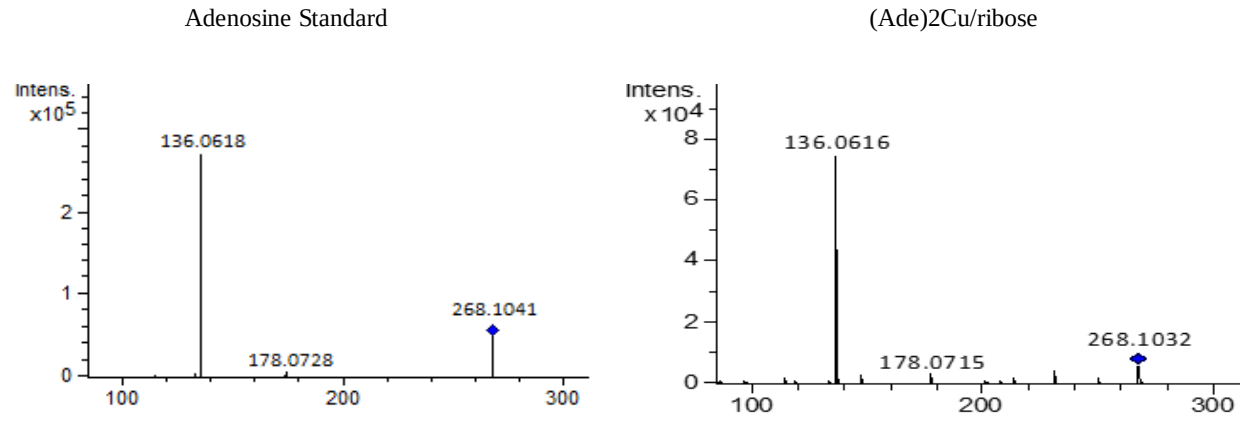

Supplementary Figure S8.2. Comparison of the MS/MS fragmentation patterns of the monoglycated adenine adduct at [M+H]=268 generated in the (Ade)2Cu/ribose model system and adenosine standard.

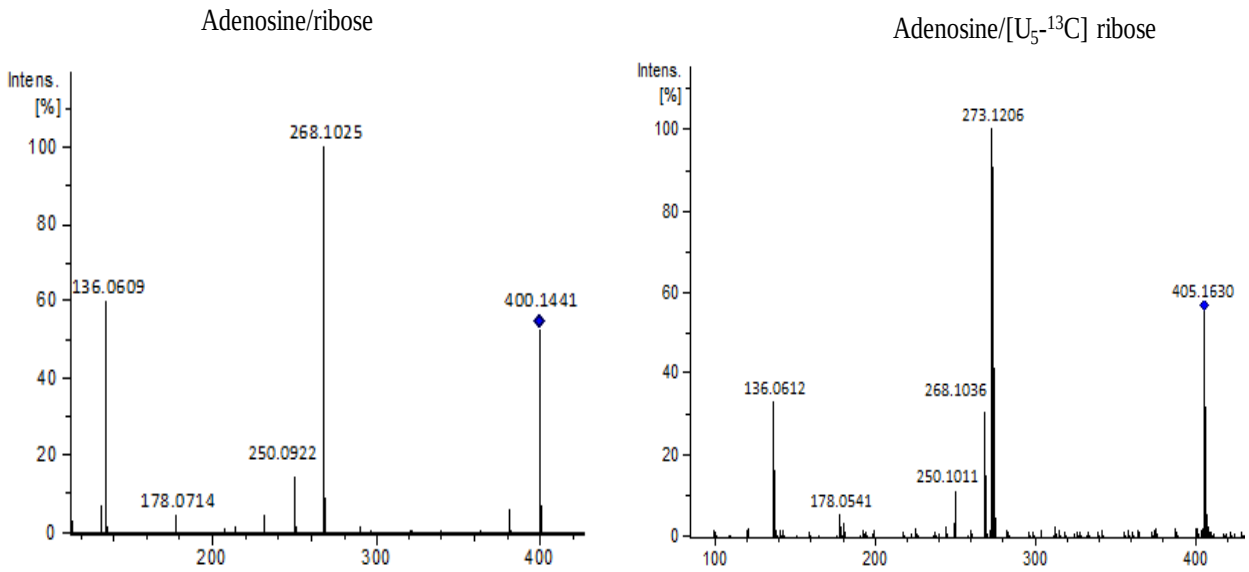

Supplementary Figure S8.3. The MS/MS fragmentation patterns of the adduct at [M+H]=400 generated in the adenosine/ribose model system and it's [U_5-^{13}C] labeled counterpart at [M+H]=405 in adenosine//[U_5-^{13}C] ribose model system.

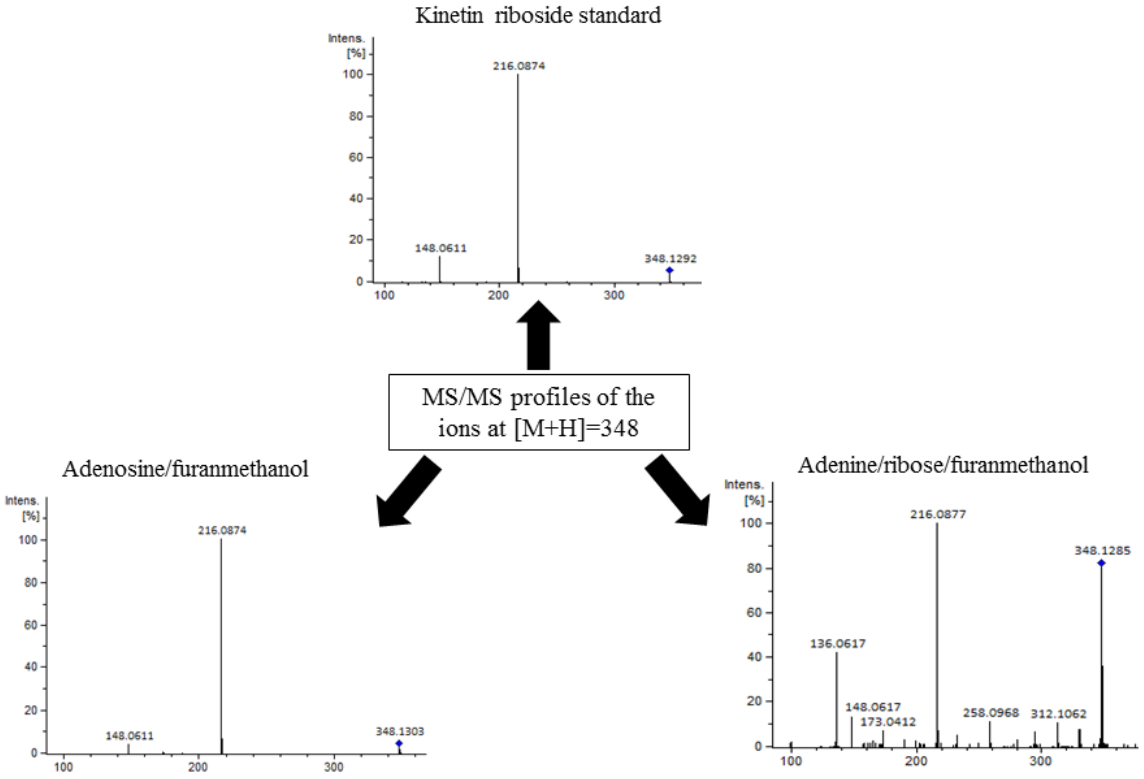

Supplementary Figure S8.4. Comparison of MS/MS profiles of the ions at [M+H]=348 generated in the adenosine/furanmethanol and adenine/ribose/furanmethanol and the commercial kinetin riboside.

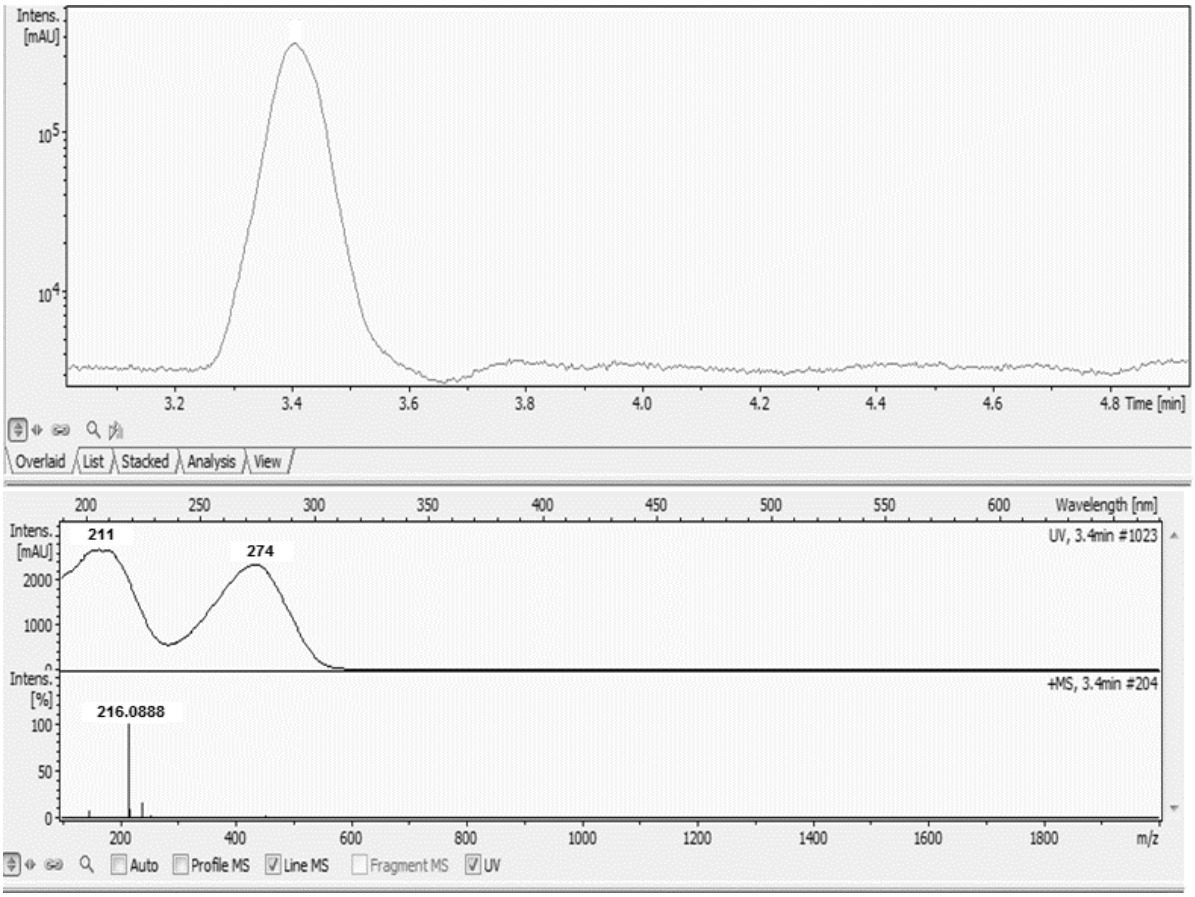

Supplementary Figure S8.5. UHPLC-DAD spectra of commercial kinetin standard.

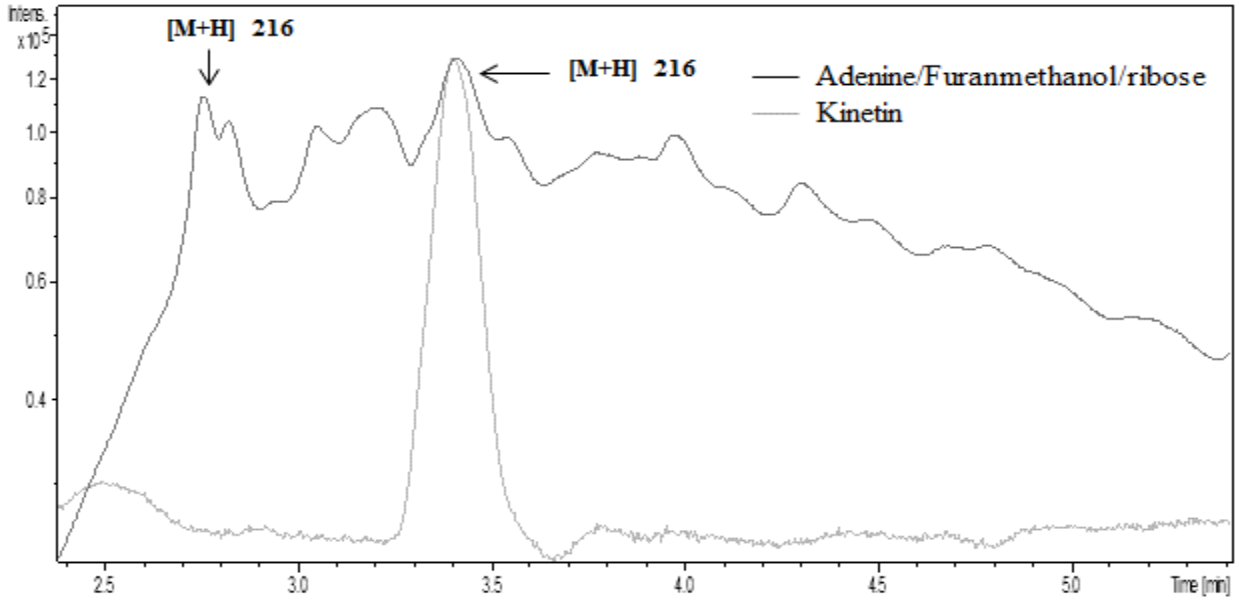

Supplementary Figure S8.6. UHPLC-DAD spectra of furanmethanol/ribose/adenine and commercial kinetin standard.

CHAPTER 9

GENERAL CONCLUSIONS, CONTRIBUTION TO KNOWLEDGE AND FUTURE RESEARCH RECOMMENDATIONS

9.1 General Conclusions

The affinity of divalent metal ions to form coordinated binary complexes with organic molecules such as amino acids or purine bases was used to investigate possible modifications in their chemical reactivity during the Maillard reaction. This study generated and presented for the first time important mechanistic information on the multifunctional role of added metal complexes or those generated *in situ* in modulating the Maillard reaction and its pathways, and their ability to enhance the formation of specific products with different molecular diversities and chemical properties (See Figure 9.1). The amino acid-metal complexes were found to influence the Maillard reaction through their ability to promote the oxidative decarboxylation of free and sugar conjugated amino-acid metal complexes and generate under specific conditions important Maillard reaction intermediates and products, such as Strecker aldehydes, Amadori products, fructosamines or glucosamines. Moreover, in the presence of added Strecker aldehydes, amino-acid metal complexes were able to activate the transformation of α-amino acids into their β-hydroxymethyl derivatives through the Akabori reaction via Schiff base intermediates. While in the presence of sugars, complexes of amino acid sugar conjugates were formed through covalent attachment as Schiff bases and then rearranged into more stable Amadori products. The sugar conjugated amino acid-metal complexes served as molecular scaffolds for the sustained production and release of important aroma precursors, the Amadori products, over time controlling the color and aroma generated during heating. On the other hand, some amino acid-metal salts such as sodium glycinate due to their inability to form binary complexes, function as acid/base modifiers of reaction medium under pyrolytic conditions and are able to play a dual role in inducing base catalyzed sugar fragmentations and formation of reactive carbonyl intermediates and in catalyzing the various enolization reactions required for the generation of Maillard reaction products such as the formation of 2,5-dimethyl-4-hydroxy-tetrahydrofuran-3-one (reduced form of Furaneol®) from the dimerization of acetol with lactaldehyde. Finally, it was demonstrated that coordination of purine bases with metals also enhances their reactivity towards sugars by activating multiple nitrogen atoms in the purine ring to form di-glycated adducts while furanmethanol reaction through its reactive furylium ion generated kinetin and its various derivatives.

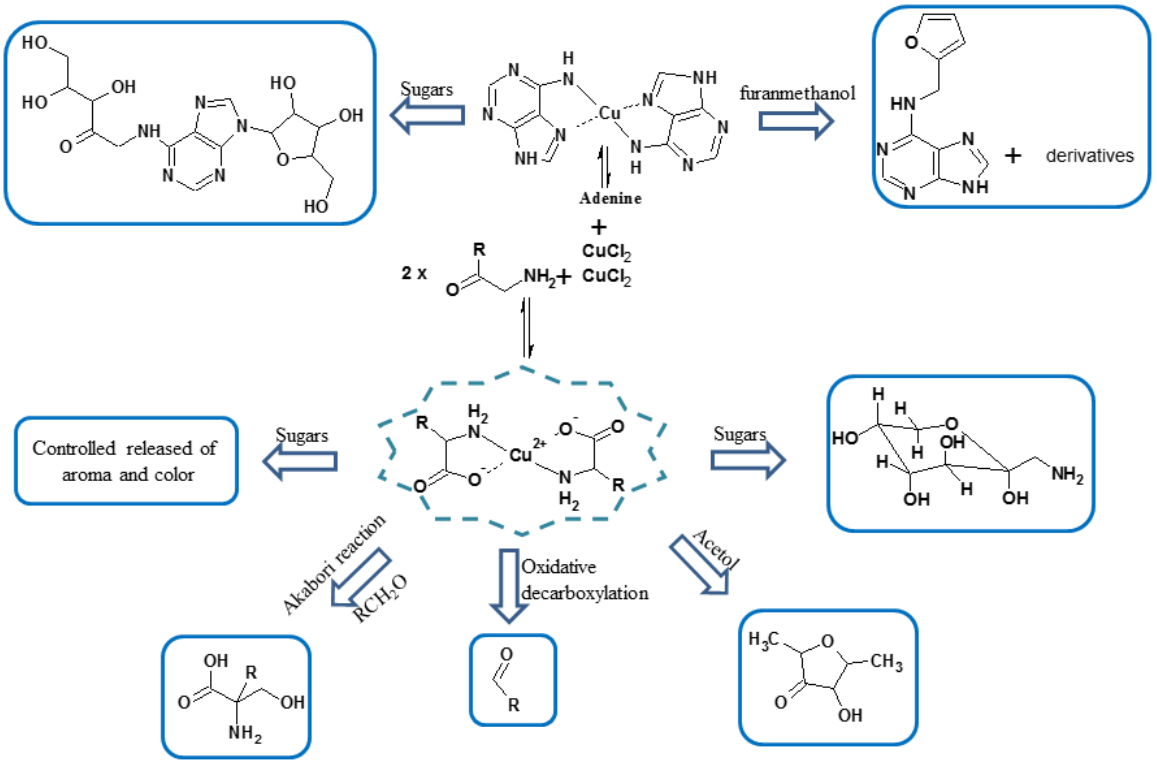

Figure 9.1. Summary of the role of metal ions in controlling the Maillard reaction

9.2 CONTRIBUTIONS TO KNOWLEDGE

The work presented in this thesis provided for the first time evidence for:

1. The identification of a new pathway to generate Strecker aldehydes in the absence of sugars through the thermal degradation of amino acid-metal complexes.

2. Demonstration of the occurrence of Akabori transformation during the Maillard reaction and presentation of mass spectrometric evidence for the detailed mechanism of Akabori transformation of α-amino acids into their β-hydroxymethyl counterparts, through the formation of Schiff base adducts.

3. Demonstration of the formation of sugar conjugated amino acid-metal complexes that can serve as molecular scaffolds to accumulate important aroma precursor Amadori products and release them over time, thus controlling color and aroma generation during the Maillard reaction.

4. Identification of a new pathway for the *in situ* formation of aldose and ketose specific amino sugars during the Maillard reaction through the thermal degradation of sugar conjugated amino acid-metal complexes.

5. The identification of the 2,5-dimethyl-4-hydroxy-tetrahydrofuran-3-one (reduced furaneol) during the Maillard reaction and presentation of the pathway of its formation through amino acid-metal salt catalyzed sugar fragmentations into reactive carbonyl intermediates and/or their subsequent dimerization and cyclisation into the new furanone.

6. The identification of the pathways of formation of $N^{6,9}$ di-ribosylated adenine adducts through the thermal reaction of adenine copper complexes with ribose and the formation mechanism of kinetin and its derivatives during the reaction of adenine with furanmethanol.

9.3 FUTURE RESEARCH

The significant findings of this study based on the use of selected precursors lay the foundation of future research directions not only in the use of new and related precursors but also research into their practical applications. Some proposed future research directions include:

1. Further investigation of the interaction of glycine-copper complexes with other carbonyl electrophiles such as dicarbonyls or reducing disaccharides.

2. Exploration of the chemistry of other amino acid-copper complexes particularly those that can generate important degradation products such as asparagine-copper and histidine-copper complexes, and their further interactions with sugars.

3. Evaluation of the role of other food components that can also complex with copper such as fatty acids and/or their degradation products.

4. Assessment of the role of other transition and non-transition metal ions on the chemistry of the Maillard reaction.

5. Exploration of the full sensorial properties of the identified 2,5-dimethyl-4-hydroxy-tetrahydrofuran-3-one (reduced furaneol®).

6. Formulation of flavor precursors with slow release properties.

REFERENCES

Ajandouz, E. H., & Puigserver, A. (1999). Nonenzymatic Browning Reaction of Essential Amino Acids: Effect of pH on Caramelization and Maillard Reaction Kinetics. *Journal of Agricultural and Food Chemistry, 47*(5), 1786-1793.

Ajandouz, E. H., Tchiakpe, L. S., Ore, F. D., Benajiba, A., & Puigserver, A. (2001). Effects of pH on Caramelization and Maillard Reaction Kinetics in Fructose-Lysine Model Systems. *Journal of Food Science, 66*(7), 926-931.

Ajandouz, E. H., Desseaux, V., Tazi, S., & Puigserver, A. (2008). Effects of temperature and pH on the kinetics of caramelisation, protein cross-linking and Maillard reactions in aqueous model systems. *Food Chemistry, 107*(3), 1244-1252.

Akabori, S., Otani, T. T., Marshall, R., Winitz, M., & Greenstein, J. P. (1959). A synthesis and resolution of DL-serine. *Archives of Biochemistry and Biophysics, 83*(1), 1-9.

Amasino, R. (2005). 1955: Kinetin Arrives. The 50th Anniversary of a New Plant Hormone. *Plant Physiology, 138*, 1177-1184.

Ames, J. M. (1990). Control of the Maillard reaction in food systems. *Trends in Food Science & Technology, 1*, 150-154.

Ames, J. M., Defaye, A. B., Bailey, R. G., & Bates, L. (1998). Analysis of the non-volatile Maillard reaction products formed in an extrusion-cooked model food system. *Food Chemistry, 61*, 521-524.

Ames, J. M. (2005). Application of semiquantitative proteomics techniques to the Maillard reaction. *Annals of the New York Academy of Sciences,1043*(1), 225-235.

Aune, J. P.; Maldonado, P.; Larcheres, G.; Pierrot, M. (1970). The crystal and molecular structure of copper(II) bis-2,5-dimethyloxazolidine-4-carboxylate dihydrate. Relation between the structure of the complex and the synthesis of DL-threonine. *Journal of the Chemical Society D: Chemical Communications*, 1351-1352.

Baltes, W. (1982). Chemical changes in food by the maillard reaction. *Food Chemistry, 9*(1–2), 59-73.

Bandwar, R. P., Sastry, M. D., Kadam, R. M., & Rao, C. P. (1997). Transition-metal saccharide chemistry: synthesis and characterization of d-glucose, d-fructose, d-galactose, d-xylose, d-ribose, and maltose complexes of Co (II). *Carbohydrate research, 297*(4), 333-339.

Banerjee, S., & Mazumdar, S. (2012). Electrospray ionization mass spectrometry: a technique to access the information beyond the molecular weight of the analyte. *International journal of analytical chemistry, 2012*, 1-40.

Bassama, J., Brat, P., Bohuon, P., Hocine, B., Boulanger, R., & Günata, Z. (2011). Acrylamide kinetic in plantain during heating process: precursors and effect of water activity. *Food Research International, 44(*5), 1452-1458.

Bastos, D. H. M., & Gugliucci, A. (2015). Contemporary and controversial aspects of the Maillard reaction products. *Current Opinion in Food Science,1*, 13-20.

Beacham, H. H., & Dull, M. F. (1951). Some Observations on The Browning Reactions. *Journal of Food Science, 16*, 439-445.

Beck, W. (2009). Metal Complexes of Biologically Important Ligands, CLXXII [1]. Metal Ions and Metal Complexes as Protective Groups of Amino Acids and Peptides – Reactions at Coordinated Amino Acids. *Zeitschrift für Naturforschung A, 64b*, 1221-1245.

Beck, W. (2011). Metal complexes of biologically important ligands, CLXXVI.[1] Formation of peptides within the coordination sphere of metal ions and of classical and organometallic complexes and some aspects of prebiotic chemistry. *Zeitschrift für Anorganische und Allgemeine Chemie, 637*, 1647-1672.

Belikov, V. M.; Vitt, S. V.; Kuznetsova, N. I.; Bezrukov, M. G.; Saporovskaya, M. B. (1969). Reaction of the copper complex of L-alanine with acetaldehyde and the mechanism of the Akabori reaction. *Russian Chemical Bulletin, 18*, 2371-2375.

Bishop, K. C. (1976). Transition metal catalyzed rearrangements of small ring organic molecules. *Chemical Reviews, 76*, 461-486.

Blank, I., & Fay, L. B. (1996). Formation of 4-Hydroxy-2,5-dimethyl-3(2H)-furanone and 4-Hydroxy-2(or 5)-ethyl-5(or 2)-methyl-3(2H)-furanone through Maillard Reaction Based on Pentose Sugars. *Journal of Agricultural and Food Chemistry, 44*(2), 531-536.

Blank, I., Devaud, S., & Fay, L. B. (1996). New aspects of the formation of 3(2H)-furanones through the Maillard reaction. In Mottram A. J. T. S. (Ed.), *Flavour Science* (pp. 188-193): Woodhead Publishing.

Bouvarda V., Loomisa D., Guytona K., Grossea Y., Ghissassia F., Benbrahim-Tallaaa L., Guhaa N., Mattocka H., Straifa K. (2015). Carcinogenicity of consumption of red and processed meat. *The Lancet Oncology 16*,1599–1600.

Bugella-Altamirano, E., Choquesillo-Lazarte, D., González-Pérez, J. M., Sánchez-Moreno, M. J., Marın-Sánchez, R., Martın-Ramos, J. D., Niclós-Gutiérrez, J. (2002). Three new modes of adenine-copper (II) coordination: interligand interactions controlling the selective N3-, N7- and bridging μ-N3, N7 metal-bonding of adenine to different N-substituted iminodiacetato-copper (II) chelates. *Inorganica Chimica Acta, 339*, 160-170.

Cambero, M. I., Pereira-Lima, C. I., Ordoñez, J. A., & García de Fernando, G. D. (2000). Beef broth flavour: relation of components with the flavour developed at different cooking temperatures. *Journal of the Science of Food and Agriculture, 80*, 1519-1528.

Cammerer, B., Chodakowski, K., Gienapp, C., Wohak, L., Hartwig, A., & Kroh, L. W. (2012). Pro-oxidative effects of melanoidin–copper complexes on isolated and cellular DNA. *European Food Research and Technology, 234*(4), 663-670.

Cerchiaro, G., Sant'Ana, A. C., Temperini, M. L. A., & da Costa Ferreira, A. M. (2005). Investigations of different carbohydrate anomers in copper (II) complexes with D-glucose, D-fructose, and D-galactose by Raman and EPR spectroscopy. *Carbohydrate research, 340*(15), 2352-2359.

Cerny, C., & Davidek, T. (2003). Formation of Aroma Compounds from Ribose and Cysteine during the Maillard Reaction. *Journal of Agricultural and Food Chemistry, 51*, 2714-2721.

Chen, J., & Ho, C.-T. (1998). Volatile Compounds Formed from Thermal Degradation of Glucosamine in a Dry System. *Journal of Agricultural and Food Chemistry, 46*, 1971-1974.

Chen, Y., Chin, C.-K., & Ho, C.-T. (2004). Influence Of DNA On Volatile Generation From Maillard Reaction Of Cysteine And Ribose. In Shahidi, F., Spanier, A. M., Ho, C.-T. &Braggins T. (Eds.), *Quality of Fresh and Processed Foods* (pp. 327-340). Boston, MA: Springer US.

Cheng, R.; Kawakishi, S. (1994). Novel decomposition of Amadori compound catalyzed by copper ion. *Journal of Agriculture and Food Chemistry, 42*, 700-703.

Cheng Y. L., Da Z. Z., Rong Z., Qi H.D., Ai N. Y., Yang, X. H. (2012). Effect of Metal Ions (Cu^{2+}/Fe^{2+}) on the Antioxidant Activity of L-Ascorbic Acid-Glycine Model System. *Advanced Materials Research,* 396, 28-31.

Choudhary, V.; Mushrif, S. H.; Ho, C.; Anderko, A.; Nikolakis, V.; Marinkovic, N. S.; Frenkel, A. I.; Sandler, S. I.; Vlachos, D. G. (2013). Insights into the Interplay of Lewis and Brønsted Acid Catalysts in Glucose and Fructose Conversion to 5-(Hydroxymethyl)furfural and Levulinic Acid in Aqueous Media. *Journal of American Chemical Society, 135*, 3997-4006.

Chung, Y., Tsai, C., & Li, C. (2006) Preparation and characterization of water-soluble chitosan produced by Maillard reaction. *Fisheries Science, 72*, 1096-1103.

Chuyen, N. V. (1998). Maillard reaction and food processing. Aplication aspects'. *Advances in Experimental Medicine and Biology, 434*, 213-235.

Clarke, R. E., Dordevic, A. L., Tan, S. M., Ryan, L., & Coughlan, M. T. (2016). Dietary Advanced Glycation End Products and Risk Factors for Chronic Disease: A Systematic Review of Randomised Controlled Trials. *Nutrients, 8*(3), 125.

Coghe, S., Gheeraert, B., Michiels, A., & Delvaux, F. R. (2006). Development of maillard reaction related characteristics during malt roasting. *Journal of the Institute of Brewing, 112*(2), 148-156.

Concentration of Contaminants & Other Chemicals in Food Composites. (2003-2007). Retrieved from http://www.hc-sc.gc.ca/fn-an/surveill/total-diet/concentration/index-eng.php#a10.

Crugeiras, J.; Rios, A.; Riveiros, E.; Richard, J. P. (2011). Substituent Effects on Electrophilic Catalysis by the Carbonyl Group: Anatomy of the Rate Acceleration for PLP-Catalyzed Deprotonation of Glycine. *Journal of American Chemical Society, 133*, 3173-3183.

Delgado-Andrade, C., Seiquer, I., & Navarro, M. P. (2002). Copper metabolism in rats fed diets containing Maillard reaction products. *Journal of Food Science, 67*(2), 855-860.

Delgado-Andrade, C., Seiquer, I., Nieto, R., & Navarro, M. P. (2004). Effects of heated glucose–lysine and glucose–methionine model-systems on mineral solubility. *Food Chemistry, 87*(3), 329-337.

Delgado-Andrade, C., Roncero-Ramos, I., Haro, A., Pastoriza, S., & Navarro, M. P. (2015). Do bread-crust-derived Maillard reaction products affect the retention and tissue distribution of trace elements?. *European Journal of Nutrition*, 1-9.

Doob, H., A. Willmann. & P.F. Sharp. (1942). Influence of moisture on browning of dried whey and skim milk. *Industrial & Engineering Chemistry, 34*, 1460–1468.

Dumesic, J. A., Pagán-Torres, Y. J., Wang, T., & Shanks, B. H. (2014). U.S. Patent No. 8,642,791. Washington, DC: U.S. Patent and Trademark Office.

Dutta, U., Cohenford, M. A., & Dain, J. A. (2005). Nonenzymatic glycation of DNA nucleosides with reducing sugars. *Analytical Biochemistry, 345*, 171-180.

Dutta, U., Cohenford, M. A., Guha, M., & Dain, J. A. (2006). In vitro nonenzymatic glycation of DNA nucleobases: an evaluation of advanced glycation end products under alkaline pH. *Analytical and Bioanalytical Chemistry, 386*, 1633–1640.

Echavarria, A. P., Pagán, J., & Ibarz, A. (2012). Melanoidins Formed by Maillard Reaction in Food and Their Biological Activity. *Food Engineering Reviews, 4*(4), 203-223.

Einarsson, H. (1987). The effect of pH and temperature on the antibacterial effect of Maillard reaction products. *Food Science & Technology, 20*(2), 56.

Elder, V.A., Fulcher, J.G., Leung, H., Topor, M.G. (2004). Method for reducing acrylamide in thermally processed foods. *Patent US20040058045*.

Fallico, B., & Ames, J. M. (1999). Effect of hexanal and iron on color development in a glucose/phenylalanine model system. *Journal of Agricultural and Food Chemistry, 47*(6), 2255-2261.

Finot, P. A. (2005). Historical perspective of the Maillard reaction in food science. *Annals of the New York Academy of Sciences, 1043*(1), 1-8.

Fiore, A., Troise, A. D., Ataç Mogol, B., Roullier, V., Gourdon, A., El Mafadi Jian, S., Fogliano, V. (2012). Controlling the Maillard reaction by reactant encapsulation: Sodium chloride in cookies. *Journal of Agricultural and Food Chemistry, 60*(43), 10808-10814.

Fischer, E. (1886). Ueber Isoglucosamin. *Berichte der deutschen chemischen Gesellschaft, 19*(2), 1920-1924.

Fitzpatrick, J. H.; Hopgood, D. (1974). Metal ion catalyzed decarboxylation. Kinetics and mechanism of the oxidative decarboxylation of copper (II) complexes of aminomalonic acid in aqueous solution. *Inorganic Chemistry, 13*, 568-574.

Fogliano, V., Maria Monti, S., Musella, T., Randazzo, G., & Ritieni, A. (1999). Formation of coloured Maillard reaction products in a gluten-glucose model system. *Food Chemistry, 66*, 293-299.

Friedman, L., & Kline, O. L. (1950). The amino acidsugar reaction. *Journal of Biological Chemistry, 184*, 599-606.

Friedman, M. (1996). Food Browning and Its Prevention: An Overview. *Journal of Agricultural and Food Chemistry, 44*, 631-653.

Friedman, M. (1996). Nutritional Value of Proteins from Different Food Sources. A Review. *Journal Agriculture and Food Chemistry, 44*, 6-29.

Frolov, A.; Schmidt, R.; Spiller, S.; Greifenhagen, U.; Hoffmann, R. (2014). Arginine-Derived Advanced Glycation End Products Generated in Peptide–Glucose Mixtures During Boiling. *Journal of Agriculture and Food Chemistry, 62*, 3626-3635.

Fuller, W. D., Sanchez, R. A., & Orgel, L. E. (1972). Studies in prebiotic synthesis: VI. Synthesis of purine nucleosides. *Journal of Molecular Biology, 67*, 25-33.

Gao, H. Y., Yaylayan, V. A., & Yeboah, F. (2010). Oxalic Acid-Induced Modifications of Postglycation Activity of Lysozyme and Its Glycoforms. *Journal of Agricultural and Food Chemistry, 58*, 6219-6225.

García, M. M., Seiquer, I., Delgado-Andrade, C., Galdó, G., & Navarro, M. P. (2009). Intake of Maillard reaction products reduces iron bioavailability in male adolescents. *Molecular Nutrition & Food Research, 53*(12), 1551-1560.

Geetha, K., Raghavan, M. S., Kulshreshtha, S. K., Sasikala, R., & Rao, C. P. (1995). Transition-metal saccharide chemistry: synthesis, spectroscopy, electrochemistry and magnetic susceptibility studies of iron (III) complexes of mono-and disaccharides. *Carbohydrate Research, 271*(2), 163-175.

Gerrard, J. A. (2006). The Maillard reaction in food: Progress made, challenges ahead—Conference Report from the Eighth International Symposium on the Maillard Reaction. *Trends in Food Science & Technology, 17*(6), 324-330.

Girnth-Weller, M., & Beck, W. (1982). Stereoselective aldol reactions on mixed α-aminoacidato copper complexes Cu (L-aaO)(GlyO). *Inorganica Chimica Acta, 57*, 107-110.

Gokmen, V., & Şenyuva, H. Z. (2007a). Acrylamide formation is prevented by divalent cations during the Maillard reaction. *Food Chemistry, 103*(1), 196-203.

Gokmen, V., & Şenyuva, H. (2007b). Effects of some cations on the formation of acrylamide and furfurals in glucose–asparagine model system. *European Food Research and Technology, 225*(5), 815-820.

Goldberg, T., Cai, W., Peppa, M., Dardaine, V., Baliga, B. S., Uribarri, J., & Vlassara, H. (2004). Advanced glycoxidation end products in commonly consumed foods. *Journal of the American Dietetic Association, 104*(8), 1287-1291.

Granvogl, M., & Schieberle, P. (2006). Thermally generated 3-aminopropionamide as a transient intermediate in the formation of acrylamide. *Journal of Agricultural and Food Chemistry, 54*(16), 5933-5938.

Guerra P. V.; Yaylayan, V. A. (2010). Dimerization of azomethine ylides: An alternate route to pyrazine formation in the Maillard reaction. *Journal of Agricultural and Food Chemistry, 58*(23), 12523-12529.

Gupta, R. K., Gupta, K., Sharma, A., Das, M., Ansari, I. A., & Dwivedi, P. D. (2016). Maillard reaction in food allergy: Pros and Cons. *Critical Reviews in Food Science and Nutrition*, (just-accepted), 00-00.

Gupta, A., & Uribarri, J. (2016). Dietary Advanced Glycation End Products and Their Potential Role in Cardiometabolic Disease in Children. *Hormone Research in Paediatrics, 85*(5), 291-300.

Gyurcsik, B.; Gajda, T.; Nagy, L.; Burger, K.; Rockenbauer, A.; Korecz Jr. L. (1993). Proton, copper(II) and nickel(II) complexes of some Amadori rearrangement products of D-glucose and amino acids. *Inoranica Chimica Acta, 214*, 57-66.

Gyurcsik, B., & Nagy, L. (2000). Carbohydrates as ligands: coordination equilibria and structure of the metal complexes. *Coordination Chemistry Reviews, 203*(1), 81-149

Harkins, T. R., & Freiser, H. (1958). Adenine-Metal Complexes1,2. *Journal of the American Chemical Society, 80*, 1132-1135.

Hayase, F., Usui, T., & Watanabe, H. (2006). Chemistry and some biological effects of model melanoidins and pigments as Maillard intermediates. *Molecular Nutrition & Food Research, 50*(12), 1171-1179.

Hayase, F., Shibuya, T., Sato, J., & Yamamoto, M. (1996). Effects of Oxygen and Transition Metals on the Advanced Maillard Reaction of Proteins with Glucose. *Bioscience, Biotechnology, and Biochemistry, 60*(11), 1820-1825.

Hellwig, M., & Henle, T. (2014). Baking, ageing, diabetes: a short history of the Maillard reaction. *Angewandte Chemie International Edition, 53*(39), 10316-10329.

Heyns, K., & Koch, W. Z. (1952) .Über die bildung eines aminozuckers ausd-fruktose und ammoniak. *Zeitschrift für Naturforschung B, 7*B, 486-488

Herrero, M., Simó, C., García-Cañas, V., Ibáñez, E., & Cifuentes, A. (2012). Foodomics: MS-based strategies in modern food science and nutrition. *Mass Spectrometry Reviews, 31*, 49-69.

Ho, C. T. (1996). Thermal generation of Maillard aromas. In Ikan, R. (Ed.), *The Maillard reaction: consequences for the chemical and life sciences* (pp. 27-53): Hoboken, NJ, USA: Wiley.

Hodge, J. E. (1953). Dehydrated Foods, Chemistry of Browning Reactions in Model Systems. *Journal of Agricultural and Food Chemistry, 1*, 928-943.

Hodge J. (1967). Origin of flavor in foods, nonenzymatic browning reactions. In H.W. Schultz (Ed). *Symposium on foods: The chemistry and physiology of flavors* (pp. 465-491): AVI publishing company, Inc.

Hofmann, T., & Schieberle, P. (2000). Formation of Aroma-Active Strecker-Aldehydes by a Direct Oxidative Degradation of Amadori Compounds. *Journal of Agricultural and Food Chemistry, 48*(9), 4301-4305.

Horikawa, H.; Okada, M.; Nakamura, Y.; Sato, A.; Iwamoto, N. (2002). Production of hydroxyl radicals and α-dicarbonyl compounds associated with Amadori compound–Cu^{2+} complex degradation. *Free Radical Research, 36*, 1059– 1065.

Hricovíniová, Z. (2015). Transition-Metal-Catalyzed Transformation of Monosaccharides and Polysaccharides. Polysaccharides: Bioactivity and Biotechnology, 1319-1371.

Hrynets, Y., Ndagijimana, M., & Betti, M. (2013). Non-enzymatic glycation of natural actomyosin (NAM) with glucosamine in a liquid system at moderate temperatures. *Food Chemistry, 139*, 1062-1072.

Hrynets, Y., Ndagijimana, M., & Betti, M. (2015) Studies on the Formation of Maillard and Caramelization Products from Glucosamine Incubated at 37°C. *Journal of Agricultural and Food Chemistry, 63*, 6249-6261.

Hwang, I. G., Kim, H. Y., Woo, K. S., Lee, J., & Jeong, H. S. (2011). Biological activities of Maillard reaction products (MRPs) in a sugar–amino acid model system. *Food Chemistry, 126*, 221-227.

Ibáñez, C., Valdés, A., García-Cañas, V., Simó, C., Celebier, M., Rocamora-Reverte, L., Gómez-Martínez, Á.,Herrero, M., Castro-Puyana, M., Segura-Carretero, A.,Ibáñez, E., Ferragut, J. A., Cifuentes, A. (2012). Global Foodomics strategy to investigate the health benefits of dietary constituents. *Journal of Chromatography A, 1248*, 139-153.

Ichikawa, T.; Maeda, S.; Araki, Y.; Ishido, Y. (1970). Synthetic studies of amino acids by the use of the copper complex. I. Syntheses of beta-hydroxy DL-amino acids by the use of the complex of copper (II) with the Schiff base derived from glycine and pyruvic acid. *Journal of American Chemical Society, 92*, 5514-5516.

Ikutani, Y.; Okuda, T.; Sato, M.; Akabori, S. (1959). The Reaction of Glycine Cobalt Complex with Acetaldehyde. *Bulletin of the Chemical Society of Japan. 32*, 203-204.

Ilavarasi, R., Rao, M. N. S., & Udupa, M. R. (1997). Synthesis and characterization of copper (II) complexes of adenine and aminoacids. In *Proceedings of the Indian Academy of Sciences-Chemical Sciences* (pp. 79-87). Springer India.

Isbell, H. S.; Frush, H. L. (1958). Mutarotation, hydrolysis, and rearrangement reactions of glycosylamines. *Journal of Organic Chemistry, 23*, 1309-1319.

Jaeger, H., Janositz, A., & Knorr, D. (2010). The Maillard reaction and its control during food processing. The potential of emerging technologies.Pathologie Biologie, 58(3), 207-213.

Jahirul, M., Rasul, M., Chowdhury, A., & Ashwath, N. (2012). Biofuels Production through Biomass Pyrolysis —A Technological Review. *Energies, 5*(12), 4952-5001.

Jiao, L., Stolzenberg-Solomon, R., Zimmerman, T. P., Duan, Z., Chen, L., Kahle, L., Risch, A., Subar, A.F., Cross, A.J., Hollenbeck, A., Vlassara, H. (2015). Dietary consumption of advanced glycation end products and pancreatic cancer in the prospective NIH-AARP Diet and Health Study. *The American journal of clinical nutrition, 101*(1), 126-134.

Johnson P, E., Lykken, G., Mahalko, J., Milne, D., Inman, L., Sandstead H, H., Inglett G, E. (1983). Effect of Browned and Unbrowned Corn Products on Absorption of Zinc, Iron, and Copper in Humans. In *The Maillard Reaction in Foods and Nutrition* (pp. 349-360): American Chemical Society.

Jun, M., Shao, Y., Ho, C.-T., Koetter, U., & Lech, S. (2003). Structural Identification of Nonvolatile Dimerization Products of Glucosamine by Gas Chromatography−Mass Spectrometry, Liquid Chromatography−Mass Spectrometry, and Nuclear Magnetic Resonance Analysis. *Journal of Agricultural and Food Chemistry, 51*, 6340-6346.

Keramat, J., LeBail, A., Prost, C., & Jafari, M. (2011). Acrylamide in Baking Products: A Review Article. *Food and Bioprocess Technology, 4*(4), 530-543.

Knerr, T., & Severin, T. (1993). Investigation of the glucose/propylamine reaction by HPLC. *Zeitschrift für Lebensmittel-Untersuchung und Forschung,196*(4), 366-369.

Knerr, T., Ochs, S., & Severin, T. (1994). Reaction of guanosine, 2′-deoxyguanosine and guanosine-5′-monophosphate with glucose. *Carbohydrate Research, 256*, 177-183.

Kobayashi, S., & Manabe, K. (2002). Development of novel Lewis acid catalysts for selective organic reactions in aqueous media. Accounts of chemical research, 35(4), 209-217.

Kokkinidou, S., & Peterson, D. G. (2013). Response surface methodology as optimization strategy for reduction of reactive carbonyl species in foods by means of phenolic chemistry. *Food & Function, 4*(7), 1093-1104.

Kraehenbuehl, K., Davidek, T., Devaud, S., & Mauroux, O. (2008). Basic and acidic sugars as flavour precursors in Maillard reaction. In I. Blank, M. Wust, & C. Yeretzian (Eds.),

Expression of multidisciplinary flavour science (pp. 267–271): Proceedings to 12th Weurman symposium.

Kusch, P., (2012). Pyrolysis-Gas Chromatography/Mass Spectrometry of Polymeric Materials. In Advanced Gas Chromatography - Progress in Agricultural, Biomedical and Industrial Applications, Dr. Mustafa Ali Mohd (Ed.), In Tech open science, pp. 343-362.

Kwak, E. J., & Lim, S. I. (2004). The effect of sugar, amino acid, metal ion, and NaCl on model Maillard reaction under pH control. *Amino Acids, 27*, 85-90.

Laroque, D., Inisan, C., Berger, C., Vouland, É., Dufossé, L., & Guérard, F. (2008). Kinetic study on the Maillard reaction. Consideration of sugar reactivity. *Food Chemistry, 111*, 1032-1042.

Levine, R. A., & Ryan, S. M. (2009). Determining the Effect of Calcium Cations on Acrylamide Formation in Cooked Wheat Products Using a Model System. *Journal of Agricultural and Food Chemistry, 57*(15), 6823-6829.

Lingnert, H., Grivas, S., Jägerstad, M., Skog, K., Törnqvist, M., & Åman, P. (2002). Acrylamide in food: mechanism of formation and influencing factors during heating of foods. *Scandinavian Journal of Nutrition, 46*(4), 159-172.

Limacher, A., Kerler, J., Davidek, T., Schmalzried, F., & Blank, I. (2008). Formation of Furan and Methylfuran by Maillard-Type Reactions in Model Systems and Food. *Journal of Agricultural and Food Chemistry, 56*, 3639-3647.

Linek, K.; Alföldi, J.; Defaye, J. (1993). Structure of glycosylamines and diglycosylamines in the arabinose, mannose, and rhamnose series. *Carbohydrate Research, 247*, 329-335.

Lippert, B. (2000). Multiplicity of metal ion binding patterns to nucleobases. *Coordination Chemistry Reviews*, 200–202, 487-516.

Luevano-Contreras, C., & Chapman-Novakofski, K. (2010). Dietary Advanced Glycation End Products and Aging. *Nutrients, 2*, 1247-1265.

Marshall J. (1980). Mechanisms of saccharide polymerization and depolymerisation (pp. 428-430), New York, USA: Academic press.

Martins, S. I., & Van Boekel, M. A. (2005a). Kinetics of the glucose/glycine Maillard reaction pathways: influences of pH and reactant initial concentrations. *Food Chemistry, 92*(3), 437-448.

Martins, S. I. F. S., & Van Boekel, M. A. J. S. (2005b). A kinetic model for the glucose/glycine Maillard reaction pathways. *Food Chemistry, 90*(1–2), 257-269.

Maurel, M.C., & Convert, O. (1990). Chemical structure of a prebiotic analog of adenosine. *Origins of Life and Evolution of the Biosphere, 20*, 43-48.

Mehta, B. M., and Hilton C. D. (2016). Blocked Lysine in Dairy Products: Formation, Occurrence, Analysis, and Nutritional Implications. *Comprehensive Reviews in Food Science and Food Safety 15*(1), 206-218.

Mesías, M., Seiquer, I., & Navarro, M. P. (2009). Influence of diets rich in Maillard reaction products on calcium bioavailability. Assays in male adolescents and in Caco-2 cells. *Journal of Agricultural and Food Chemistry,57*(20), 9532-9538.

Mestdagh, F., Maertens, J., Cucu, T., Delporte, K., Van Peteghem, C., & De Meulenaer, B. (2008). Impact of additives to lower the formation of acrylamide in a potato model system through pH reduction and other mechanisms. *Food Chemistry, 107*(1), 26-31.

Meurillon, M., & Engel, E. (2016). Mitigation strategies to reduce the impact of heterocyclic aromatic amines in proteinaceous foods. *Trends in Food Science & Technology, 50,* 70–84.

Meynier, A., & Mottram, D. S. (1995). The effect of pH on the formation of volatile compounds in meat-related model systems. *Food Chemistry, 52*, 361-366.

Micera, G., Deiana, S., Dessi, A., Decock, P., Dubois, B., & Kozłowski, H. (1985). Copper (II) complexation by D-glucosamine. Spectroscopic and potentiometric studies. *Inorganica Chimica Acta, 107*(1), 45-48.

Mishra, A. K., Purohit, C. S., & Verma, S. (2008). Contrasting crystallographic signatures of Ag(I)- and Cu(II)-N6, N6'-bisadenine complexes: extended vs. foldback geometries. *CrystEngComm, 10*, 1296-1298.

Migo, V. P., Matsumura, M., Rosario, E. J. d., & Kataoka, H. (1993). The effect of pH and calcium ions on the destabilization of melanoidin. *Journal of Fermentation and Bioengineering 76,* 29-32.

Moldoveanu, S. C. (2010) Pyrolysis of Organic Molecules with Applications to Health and Environmental Issues. In Serban, C. M., (Ed.) *Techniques and Instrumentation in Analytical Chemistry* (pp. 527-578), Amstersdam, Netherlands: Elsevier

Monnier, V. M. (1990). Nonenzymatic Glycosylation, the Maillard Reaction and the Aging Process. *Journal of Gerontology, 45*, 105-111.

Monti, S. M., Borrelli, R. C., Ritieni, A., & Fogliano, V. (2000). A Comparison of Color Formation and Maillard Reaction Products of a Lactose−Lysine and Lactose−Nα-Acetyllysine Model System. *Journal of Agricultural and Food Chemistry, 48*, 1041-1046.

Morales, F. J., & van Boekel, M. A. J. S. (1998). A Study on Advanced Maillard Reaction in Heated Casein/Sugar Solutions: Colour Formation. *International Dairy Journal, 8*, 907-915.

Mossine, V. V., Glinsky, G. V., & Feather, M. S. (1994). The preparation and characterization of some Amadori compounds (1-amino-1-deoxy-d-fructose derivatives) derived from a series of aliphatic ω-amino acids. *Carbohydrate Research, 262*, 257-270.

Mossine, V. V., Barnes, C. L., & Mawhinney, T. P. (2009). Structure of D-Fructosamine Hydrochloride and D-Fructosamine Hydroacetate. *Journal of Carbohydrate Chemistry, 28*, 245-263.

Mossine, V. V., & Mawhinney, T. P. (2010). 1-Amino-1-deoxy-d-fructose ("Fructosamine") and its Derivatives. In H. Derek (Ed.), *Advances in Carbohydrate Chemistry and Biochemistry* (pp. 291-402): Academic Press.

Mottram, D. S. (2007). The Maillard reaction: source of flavour in thermally processed foods. *In Flavours and Fragrances* (pp. 269-283). Berlin Heidelberg: Springer.

Mottram, D. S., & Taylor, A. J.(Eds) (2010). Controlling Maillard pathways to generate flavors. Washington, DC: American Chemical Society.

Mustapha, W. A. W., Hill, S. E., Blanshard, J. M. V., & Derbyshire, W. (1998). Maillard reactions: do the properties of liquid matrices matter. *Food Chemistry, 62*(4), 441-449.

Nabrzyski M. (2007). Functional Role of Some Minerals in Foods Mineral Components in Foods. In Szefer, P., & Nriagu, J. O.(Eds.), *Mineral Components in Foods* (pp. 123 -161). Boca Raton: CRC Press/Taylor & Francis.

Nashalian, O., & Yaylayan, V. A. (2014). Thermally Induced Oxidative Decarboxylation of Copper Complexes of Amino Acids and Formation of Strecker Aldehyde. *Journal of Agricultural and Food Chemistry, 62*(33), 8518-8523.

Nashalian, O and Yaylayan, V. (2015a). De novo synthesis of amino acids during the Maillard reaction: qTOF/ESI mass spectrometric evidence for the mechanism of Akabori transformation. *Journal of Agricultural and Food Chemistry, 63*(1), 328-334.

Nashalian, O., & Yaylayan, V. A. (2015b). Sugar-Conjugated Bis(glycinato)copper(II) Complexes and Their Modulating Influence on the Maillard Reaction. *Journal of Agricultural and Food Chemistry, 63*(17), 4353-4360.

Nashalian, O., & Yaylayan, V. A. (2016). In situ formation of the amino sugars 1-amino-1-deoxy-fructose and 2-amino-2-deoxy-glucose under Maillard reaction conditions in the absence of ammonia. *Food Chemistry, 197*, Part A, 489-495.

Newton, A. E., Fairbanks J. Antony , Golding Matt, Andrewes Paul, & Gerrard, J. A. (2012). The role of the Maillard reaction in the formation of flavour compounds in dairy products – not only a deleterious reaction but also a rich source of flavour compounds. *Food and Fucntion, 3* , 1231-1241.

Nikolov, P. Y. & Yaylayan, V. A. (2012). Role of the Ribose-Specific Marker Furfuryl-amine in the Formation of Aroma Active 1-(Furan-2-ylmethyl)-1H-pyrrole (or Furfurylpyrrole) Derivatives. *Journal of Agriculture and Food Chemistry, 60,* 10155−10161.

Nissl, J., Ochs, S., & Severin, T. (1996). Reaction of guanosine with glucose, ribose, and glucose 6-phosphate. *Carbohydrate Research, 289,* 55-65.

Novotny, O., Cejpek, K., & Velisek, J. (2007). Formation of α-hydroxycarbonyl and α-dicarbonyl compounds during degradation of monosaccharides. *Czech Journal of Food Sciences, 25*, 119– 130.

Nursten, H.E. (2005). The Chemistry of Non Enzymatic Browning. In *Maillard Reaction - Chemistry, Biochemistry and Implications* (pp. 5-29), Cambridge, UK: Royal Society of Chemistry.

Nursten, H. E. (1981). Recent developments in studies of the maillard reaction. *Food Chemistry, 6*(3), 263-277.

O'Brien, J., & Morrissey, P. A. (1989). Nutritional and toxicological aspects of the Maillard browning reaction in foods. *Critical Reviews in Food Science and Nutrition, 28*, 211-248.

O'Brien, J., & Morrissey, P. A. (1997). Metal ion complexation by products of the Maillard reaction. *Food Chemistry, 58,* 17-27.

Otani, T. T.; Winitz, M. (1960). Studies on hydroxyamino acids. I. Synthesis of some α-alkylated serines. *Archives of Biochemistry and Biophysics, 90*, 254-259.

Perez Locas, C., & Yaylayan, V. A. (2004). Origin and Mechanistic Pathways of Formation of the Parent Furan. A Food Toxicant. *Journal of Agricultural and Food Chemistry, 52*, 6830-6836.

Pearson, R. G.; Lanier, R. D. (1964). Rates of Rapid Ligand Exchange Reactions by Nuclear Magnetic Resonance Line Broadening Studies. *Journal of American Chemical Society, 86*, 765-771.

Perrone, L., & Grant, W. B. (2015). Observational and ecological studies of dietary advanced glycation end products in national diets and Alzheimer's disease incidence and prevalence. *Journal of Alzheimer's Disease, 45*(3), 965-979.

Pischetsrieder, M., & Baeuerlein, R. (2009). Proteome research in food science. *Chemical Society Reviews, 38*(9), 2600-2608.

Poisson, L., Schmalzried, F., Davidek, T., Blank, I., & Kerler, J. (2009). Study on the role of precursors in coffee flavor formation using in-bean experiments. *Journal of Agricultural and Food Chemistry, 57*(21), 9923-9931.

Poulsen, M. W., Hedegaard, R. V., Andersen, J. M., de Courten, B., Bügel, S., Nielsen, J., Skibsted L.H., Dragsted, L. O. (2013). Advanced glycation endproducts in food and their effects on health. *Food and Chemical Toxicology, 60*, 10-37.

Prashanth, L., Kattapagari, K. K., Chitturi, R. T., Baddam, V. R. R., & Prasad, L. K. (2015). A review on role of essential trace elements in health and disease. *Journal of Dr. NTR University of Health Sciences, 4*(2), 75.

Ramonaityte, D. T., Keršienė, M., Adams, A., Tehrani, K. A., & Kimpe, N. D. (2009). The interaction of metal ions with Maillard reaction products in a lactose–glycine model system. *Food Research International, 42*, 331-336.

Rao, H. S. P.; Rao, A. V. B. (2015). Copper-Catalyzed C(sp3)–OH cleavage with concomitant C–C coupling: synthesis of 3-substituted isoindolinones. *Journal of Organic Chemistry, 80*, 1506–1516.

Rendleman Jr, J. A., & Inglett, G. E. (1990). The influence of Cu2+ in the Maillard reaction. *Carbohydrate Research, 201*, 311-326.

Rizzi, G. P. (1997). Chemical structure of colored maillard reaction products. *Food Reviews International, 13*, 1-28.

Rizzi, G. P. (2008). Effects of cationic species on visual color formation in model maillard reactions of pentose sugars and amino acids. *Journal of Agricultural and Food Chemistry, 56*(16), 7160-7164.

Roncero-Ramos, I., Pastoriza, S., Navarro, M. P., & Delgado-Andrade, C. (2016). Assessing the effects of model Maillard compound intake on iron, copper and zinc retention and tissue delivery in adult rats. *Food & Function,7*(1), 164-170.

Ross Karl-Heinz, M., Christian Dudeck, L., Walter Himmele, W. R., Lebkuecher, L., & Wolfgang Sauer, M. (1981). *U.S. patent No 4,290,960*. Washington, DC: U.S. Patent and Trademark Office.

Sadd, P. A., Hamlet, C. G., & Liang, L. (2008). Effectiveness of Methods for Reducing Acrylamide in Bakery Products. *Journal of Agricultural and Food Chemistry, 56*(15), 6154-6161.

Sato, M.; Okawa, K.; Akabori, S. (1957). A New Synthesis of Threonine. *The Bulletin of the Chemical Society of Japan, 30*, 937-938.

Schieberle, P. (1992). Formation of furaneol in heat-processed foods. USA: ACS symposium series.

Schiff, H. (1866). Eine neue Reihe organischer Diamine. *Annalen der Chemie und Pharmacie, 140*, 92–137.

Schonberg, A., & Moubacher, R. (1952). The Strecker Degradation of α-Amino Acids. *Chemical Reviews, 50*(2), 261-277.

Schwab, W. (2013). Natural 4-Hydroxy-2,5-dimethyl-3(2H)-furanone (Furaneol®). *Molecules, 18*(6), 6936.

Seiquer, I., Ruiz-Roca, B., Mesias, M., oz-Hoyos, A. M., Galdo´, G., and, J. J. O., & Navarro, M. P. (2008). The antioxidant effect of a diet rich in Maillard reaction products is attenuated after consumption by healthy male adolescents. In vitro and in vivo comparative study. *Journal of the Science of Food and Agriculture, 88*, 1245–1252 .

Shelkovnikov, V. V., & Yeroshkin, V. I. (1985). Two-Stagedness of Thermal Decomposition of Copper Glycinate. Izvestiya Sibirskogo Otdeleniya Akademii Nauk SSSR, *Seriya Kimicheskikh Nauk, 11*, 86-93.

Shilton, N. (2003). Drying: Chemical Changes. In Eds: Benjamin (Ed.), *Encyclopedia of Food Sciences and Nutrition (Second Edition)* (pp. 1947-1950). Oxford: Academic Press.

Shimazaki, Y., Takani, M., & Yamauchi, O. (2009). Metal complexes of amino acids and amino acid side chain groups. Structures and Properties. *Dalton Transactions*, 38, 7854-7869.

Shu, C.-K. (1998). Degradation Products Formed from Glucosamine in Water. *Journal of Agricultural and Food Chemistry, 46*(3), 1129-1131.

Shu, C.-K. (1999). Pyrazine Formation from Serine and Threonine. Journal of Agriculture and *Food Chemistry, 47*, 4332-4335.

Sigel, H. (1993). Interactions of metal ions with nucleotides and nucleic acids and their constituents. *Chemical Society Reviews, 22*(4), 255-267.

Slaughter, J. C. (1999). The naturally occurring furanones: formation and function from pheromone to food. *Biological Reviews, 74*(3), 259-276.

Srikanth, V., Maczurek, A., Phan, T., Steele, M., Westcott, B., Juskiw, D., & Münch, G. (2011). Advanced glycation endproducts and their receptor RAGE in Alzheimer's disease. *Neurobiology of Aging, 32*, 763-777.

Stadler, R. H., Blank, I., Varga, N., Robert, F., Hau, J., Guy, P. A., Riediker, S. (2002). Food chemistry: Acrylamide from Maillard reaction products. *Nature, 419*(6906), 449-450.

Tareke, E., Rydberg, P., Karlsson, P., Eriksson, S., & Törnqvist, M. (2002). Analysis of Acrylamide, a Carcinogen Formed in Heated Foodstuffs. *Journal of Agricultural and Food Chemistry, 50*(17), 4998-5006.

Taylor, A. J., & Mottram, D. S. (Eds.) (1996). Flavour in Science. Recent developments. Cambridge, U.K.: Royal Society of Chemistry.

Teo, S.-B.; O'Connor, M. J. (1984). A polarimetric study of the reaction of bis(L-serinato)copper (II) with formaldehyde. *Inorganica Chimica Acta, 92*, 57-60.

Tessier, F. J., & Birlouez-Aragon, I. (2012). Health effects of dietary Maillard reaction products: the results of ICARE and other studies. *Amino acids,42*(4), 1119-1131.

Thornalley, P. J. (1998). Cell activation by glycated proteins. AGE receptors, receptor recognition factors and functional classification of AGEs. *Cellular and molecular biology (Noisy-le-Grand, France), 44*(7), 1013-1023.

Tomita, H.; Mitusaki, S.; Tamaki, E. (1964). Chemical studies on ninhydrin-positive compounds in cured tobacco leaves. *Agriculture and Biological Chemistry, 28*, 451-455.

Tonkovicc, M.; Jakas, A.; Horvat, S. (1997). Preparation and properties of an Fe(III)-complex with an Amadori compound derived from L-tyrosine. *Biometals, 10*, 55-59.

Troise, A. D., & Fogliano, V. (2013) Reactants encapsulation and Maillard Reaction. *Trends in Food Science & Technology*, 1-12.

Troise, A. D., Vitiello, D., Tsang, C., & Fiore, A. (2016). Encapsulation of ascorbic acid promotes the reduction of Maillard reaction products in UHT milk. *Food & Function. doi: 10.1039/c6fo00151c*

Tsuchida, H., Komoto, M., Kato, H., & Fujimaki, M. (1973). Formation ol Deoxy-fructosazme and Its 6-Isomer on the Browning Reaction between Glucose and Ammonia in Weak Acidic Medium. *Agricultural and Biological Chemistry, 37*(11), 2571-2578

Tsuchida, H., Tachibana, S., Kitamura, K., & Komoto, M. (1976). Formation of Deoxyfructosazine and Its 6-Isomer by the Browning Reaction between Fructose and Ammonium Formate. *Agricultural and Biological Chemistry, 40*(5), 921-925.

Ulrich, P., & Cerami, A. (2001). Protein Glycation, Diabetes, and Aging. *Recent Progress in Hormone Research*, 56, 1-22.

Uribarri, J., Woodruff, S., Goodman, S., Cai, W., Chen, X., Pyzik, R., Striker.G, Vlassara, H. (2010). Advanced Glycation End Products in Foods and a Practical Guide to Their Reduction in the Diet. *Journal of the American Dietetic Association, 110*(6), 911-916.

Vadlamani, K. R., & Seib, P. A. (1999). Effect of Zinc and Aluminum Ions in Breadmaking 1. *Cereal Chemistry, 76*(3), 355-360.

Van Boekel, M. A. J. S. (1998). Effect of heating on Maillard reactions in milk. *Food Chemistry, 62*(4), 403-414.

Van Boekel, M.A.J.S. (2006). Formation of flavour compounds in the Maillard reaction. *Biotechnology Advances, 24* (2), 230–23.

Voller, J.; Zatloukal, M.; Lenobel, R.; Doležal, K.; Béreš, T.; Kryštof, V.; Spíchal, L.; Niemann, P.; Džubák, P.; Hajdúch, M.; Strnad, M. (2010). Anticancer activity of natural cytokinins: A structure–activity relationship study. *Phytochemistry, 71,* 1350-1359.

Wang, J., Guan, Y.-G., Yu, S.-J., Zeng, X.-A., Liu, Y.-Y., Yuan, S., & Xu, R. (2011). Study on the Maillard reaction enhanced by pulsed electric field in a glycin–glucose model system. *Food and Bioprocess Technology, 4*(3), 469-474.

Wang X. (2014) Investigation of the role of glycine/sugar ratio, sodium and hydrochloride salts of glycine, glucose or fructose on the profile of the Maillard reaction products (Master's thesis). McGill University, Montreal, Canada.

Weiser, J. R., Ricapito, N. G., Yueh, A., Weiser, E. L., & Putnam, D. (2012). A mechanistic analysis of the quantitation of α-hydroxy ketones by the bicinchoninic acid assay. *Analytical Biochemistry, 430,* 116-122.

Wen, C., Shi, X., Wang, Z., Gao, W., Jiang, L., Xiao, Q., Deng, F. (2016). Effects of metal ions on formation of acrylamide and 5-hydroxymethylfurfural in asparagine–glucose model system. *International Journal of Food Science & Technology, 51*(2), 279-285.

Weenen, H. (1998). Reactive intermediates and carbohydrate fragmentation in Maillard chemistry. *Food Chemistry, 62*(4), 393-401.

Whitfield, D. M., Stojkovski, S., & Sarkar, B. (1993). Metal coordination to carbohydrates. Structures and function. *Coordination Chemistry Reviews,122*(1), 171-225.

Williams, D. H.; Busch, D. H. (1965). Selective Labilizing of α-Hydrogen Atoms by Chelation of α-Aminocarboxylic Acids. *Journal of American Chemical Society, 87,* 4644-4645.

Wolff, S. P. (1993). Diabetes mellitus and free radicals. *British Medical Bulletin, 49,* 642-652.

Wondrak, G. T., Tressl, R., & Rewicki, D. (1997). Maillard Reaction of Free and Nucleic Acid-Bound 2-Deoxy-d-ribose and d-Ribose with ω-Amino Acids. *Journal of Agricultural and Food Chemistry, 45*, 321-327.

Wong, K. H.; Abdul Aziz, S.; Mohamed, S. (2008). Sensory aroma from Maillard reaction of individual and combinations of amino acids with glucose in acidic conditions. International. *Journal of Food Science and Technology, 43,* 1512-1519.

Yablokov, V. A., Smel'tsova, I. L., & Faerman, V. I. (2014). Kinetics of heat-induced transformation of copper complexes with amino acids. *Russian Journal of General Chemistry, 84*(3), 568-570.

Yamaguchi, K., Noumi, Y., Nakajima, K., Nagatsuka, C., Aizawa, H., Nakawaki, R., Mizude E., Otsuka Y., Homma T., Chuyen, N. V. (2009). Effects of salt concentration on the reaction rate of Glc with amino acids, peptides, and proteins. *Bioscience, biotechnology, and biochemistry, 73*(11), 2379-2383.

Yaylayan, V., Perez Locas, C., Wnorowski, A., & O'Brien, J. (2005). Mechanistic Pathways of Formation of Acrylamide from Different Amino Acids. In Friedman M., Mottram D.S., (Eds.), *Chemistry and Safety of Acrylamide in Food* (pp. 191-203), New York: Springer.

Yaylayan, V. A., Huyghues-Despointes, A., & Feather, M. S. (1994). Chemistry of Amadori rearrangement products: Analysis, synthesis, kinetics, reactions, and spectroscopic properties. *Critical Reviews in Food Science and Nutrition, 34*, 321-369.

Yaylayan, V. A.; Keyhani, A. (1999). Origin of 2,3-Pentanedione and 2,3-Butanedione in d-Glucose/l-Alanine Maillard Model Systems. *Journal of Agriculture and Food Chemistry, 47*, 3280-3284.

Yaylayan, V. A., & Keyhani, A. (2000). Origin of Carbohydrate Degradation Products in l-Alanine/D-[^{13}C]Glucose Model Systems. *Journal of Agricultural and Food Chemistry, 48(*6), 2415-2419.

Yaylayan, V. A.; Keyhani, A. (2001). Carbohydrate and Amino Acid Degradation Pathways in l-Methionine/D-[^{13}C] Glucose Model Systems. *Journal of Agriculture and Food Chemistry, 49*, 800-803.

Yaylayan, V. A. (2003) Recent Advances in the Chemistry of Strecker Degradation and Amadori Rearrangement: Implications to Aroma and Color Formation. *Food Science and Technology Research, 9*, 1-6.

Zabetakis, I., Gramshaw, J. W., & Robinson, D. S. (1999). 2, 5-Dimethyl-4-hydroxy-2H-furan-3-one and its derivatives: analysis, synthesis and biosynthesis—a review. *Food Chemistry, 65*(2), 139-151.

Zamora, R., & Hidalgo, F. J. (2011). The Maillard reaction and lipid oxidation. *Lipid Technology, 23*(3), 59-62.

Zeng, Y., Zhang, X., Guan, Y., & Sun, Y. (2011). Characteristics and Antioxidant Activity of Maillard Reaction Products from Psicose-Lysine and Fructose-Lysine Model Systems. *Journal of Food Science, 76*(3), C398-C403.